Analysis of polyhedral domed structures composed of flat plates of sandwich material

Bettess, P.

Analysis of Polyhedral domed structures composed of flat plates of sandwich material

by

P. Bettess

A thesis submitted to satisfy the requirements for the degree of Ph.D

Department of Engineering Science
University of Durham

July 1971

Our torments also may in length of time

Become our elements

Paradise Lost, Book 2, J. Milton

there is a dark

Inscrutable workmanship that reconciles

Discordant elements, and makes them cling together

in one society

The Prelude, Book 1, W. Wordsworth

Summary

The finite element method was used to analyse a number of domed structures. Two new sandwich plate bending elements (rectangular and triangular) were devised. They were used to produce results for comparison with other solution methods. The agreement was excellent. They were also used to produce results for comparison with experimental work on sandwich plates. The agreement varied. To the triangular element was added a plane stress component, together with suitable apparatus for making transformations at plate boundaries. This element was used to solve three tetrahedral domes, a square pyramid, a hexagonal dome, and a 16-faced dome. All these were investigated experimentally. The agreements varied between very good and moderate. A comparison was also made with the only other published results on a sandwich folded plate structure, due to Benjamin. In conclusion some improvements were suggested.

Contents

Summary

1 Introduction

Plantema's definition of sandwich construction (2), will be used: "..... a three layer type of construction, consisting of two thin sheets of high strength material between which a thick layer of low average strength and density is sandwiched. The two thin sheets are called the faces, and the intermediate layer is the core of the sandwich."

A polyhedral dome is defined as a dome in the form of a polyhedron (30).

The origin of sandwich construction is unknown, but, as described by Elliott in a useful and detailed survey of its development (34), dates back at least to 1846, and Robert Stephenson's Brittania bridge over the Menai Straits (40). The recent interest in this extremely efficient type of construction started about 1940. Symptomatic of its resurgence was the Mosquito bomber, in which balsa and plywood were used as sandwich materials. Since then sandwich construction has been used extensively (2, 3, 34, 42, 49, 59, 60).

Domes are of course much older than sandwich structures. They are structurally efficient, and this is largely because under load they usually develop direct stress resultants, as well as bending stress resultants.

The chief drawback of domes and shells is that they are difficult to fabricate. The polyhedral dome has been conceived as a merging of these two structural forms, so as to solve, or at any rate ease, the problems of fabrication. The idea was that polygons of flat sandwich plate could be assembled to form a polyhedral dome. It was hoped that the flexural properties of sandwich plates, and the efficiency of domes would together produce a new economical structural form. This thesis is

concerned with the analysis of such structures.

There have been few attempts at the analysis of polyhedral domes, or indeed any folded plate structures, composed of sandwich elements, although folded plate structures with ordinary plate elements have been widely discussed. (see, for example, 8, 37, 41, 63, 66). Such attempts as have been made are largely approximate. Benjamin (3, 18, 20) postulated separation of the bending behaviour of an individual face, from the action of the structure as a whole, so as to simplify his analysis. His treatment of the behaviour of the component parts, and the whole of the structure is fairly crude, but gives good agreement with experiment.

In some respects the structural action of a polyhedral dome can be considered as a super-position of sandwich plate bending and membrane actions. On both of these problems much work has been done. It was decided to attempt to analyse the domes on this basis. If only small displacements (up to about half the plate thickness), are developed, then it is reasonable to suppose that the interaction between plate bending, and membrane action will only occur on the folds at plate boundaries. The analysis which follows proceeds on the basis of this assumption. It is also restricted entirely to linear elastic material behaviour. At the risk of tediousness, some of the numerous effects which are thereby neglected are catalogued below.

1 Large deflection bending behaviour.

1.1 Invalidity of bending equations for large slopes.

1.2 Development of membrane actions.

2 Membrane forces bending action, instability and stiffening.

3 Stability.

3.1 Wrinkling of faces.

3.2 Core buckling.

3.3 Plate buckling.

3.4 Overall buckling.

4 All time-dependent behaviour, reaction to live loading, and all creep phenomena.

5 Non-linear material properties.

The feature thought to be most desirable in any scheme of analysis was generality. To this end it was resolved to use a numerical method, as any analytical solution must be constrained in respect of geometry, material properties and boundary conditions. Again in considering the generality of numerical methods, the most suited one was that of finite elements. The use of a Variational Principle makes the application of boundary conditions at once general and straightforward. The finite element method also admits of great variation in the problem geometry and material properties. These advantageous facets of the method have been expounded at length by several authors (10, 25). The penalty usually paid for these useful features, is a larger computer program than that used for more direct methods (for example, finite differences, dynamic relaxation, fourier series, numerical integration). However, after consideration of the other possibilities, the finite element method was chosen as being the most promising scheme. Given the assumption of membrane and flexure independence within each plate, the problem resolved into developing an element of suitably general geometry which could represent separately membrane and bending actions. In the event a number of elements were devised.

2 Sandwich Plate Bending

2.1 History

A detailed and useful account of the various theories available for plate bending problems, both accounting for, and neglecting, the shear problem, is given by Sander (73). The various assumptions that can be made are summarized in a table. Classical plate theory [see, for example, (75)], neglects the shear deformation of the plate. It was shown by Kirchhoff (55) that this causes redundancy of one of the three boundary conditions originally specified by Poisson (64). The position regarding this neglect of one boundary condition is fully explained by Thomson and Tait (74). Usually the two boundary conditions, dealing with the twisting moment and the shear force of an edge, are merged into one, as suggested by Kirchhoff (55).

Reissner, in a series of papers which, together with the comments upon them, have become classical (67, 68, 69, 44, 32), showed that the lack of a third boundary condition was due to the neglect of the shear strain energy of the plate, and put forward a new theory, which included the shear strain energy, and used all three boundary conditions. Reissner's plate bending theory takes into account the shear deformation and shear stress in the plate. His starting point is an assumption about the variation of the shear stress across the plate thickness. For ordinary plates Reissner assumes a quadratic distribution of shear stress. However, in (69) as a special case he deals with the deformation of a sandwich plate, and as is commonly justified [see, for example (2)], he assumes that the shear stress is constant across the core of the plate. An alternative to the assumption of a stress distribution, is a kinematical

assumption (15, 73). This alternative approach seems to have been pursued independently for plates in which the shear is taken into account, by Hencky (47) and Libove and Batdorf (15). The original classical plate theory was based on the kinematic assumption of Kirchhoff (55).

The Libove and Batdorf theory considered the small deflection of sandwich plates. Alwan (7) and Reissner (72) considered large deflections of sandwich plates. Stein and Mayer (61) produced a small deflection theory for curved sandwich plates, and Reissner (70) dealt more generally with shells. More recent extensions of sandwich shell theory have come from Wempner and Baylor (16) and Wempner (76) who extended the theory to large deflections, using tensor notation.

The first finite element which dealt with the shearing deformation of plates in flexure was due to Herrmann (48). He used an unusual variational principle due, not surprisingly perhaps, to Reissner (71). This principle uses a simultaneous variation on the stress and displacement fields. The element was not applied to sandwich plates. More recently Clough and Felippe (29) described a quadrilateral plate flexure element which incorporated a simple description of the shear deformation, identical in effect with that used in the elements shown in this thesis. Clough and Felippe were only concerned with the approximate representation of shearing deformation, in ordinary plates. They advocated the use of static condensation in order to eliminate the shear deformation parameter after completion of the element stiffness matrix. This process is less valid in sandwich plate problems, where the shearing deformations are large. Sander (73) described 2 families of flexural finite elements which account for shearing deformations. In his displacement model the

rotation of the plate and the normal displacements were represented by entirely separate shape functions. The procedure was successful, and Sander gave a number of solutions to sandwich plate problems, all with a relatively high shear stiffness. He also developed equilibrium elements and was able to bound the exact solutions to several problems with his finite element results. Sander reported a loss of accuracy at very high shear stiffnesses, as the model of the sandwich plate approached close to classical plate behaviour. The isoparametric thick shell finite element described by Ahmad, Irons and Zienkiewicz (6) used a kinematic hypothesis almost identical to those used later in this thesis. With small modifications this element would be suitable for the solution of sandwich plate and shell problems, and would be very powerful.

Abel and Popov (5) described the application of finite elements to sandwich beams and axisymmetrical shells. They used a linear kinematic assumption, but also took account of the shearing of the faces of the sandwich. Monforton and Schmit (62) presented a rectangular element for sandwich plate and singly curved shell analysis. This element can deal with unequal face thicknesses. They solved a case of a simply supported rectangular plate under a uniform load. Beisinger and Key (17) described an element for the analysis of thin shells in which the transverse shear strains are accommodated. However, their motive was not to solve problems in which these shear strains are likely to be large, for example in sandwich shells, but to avoid some of the continuity requirements demanded by the Kirchhoff theory.

With the exception of the Sander equilibrium element, and the Herrmann element, all these finite elements are displacement models, which minimise strain energy.

Evans and Rockey (37) used rectangular classical plate bending, and plane stress elements, to solve folded plate structures.

2.2 Fundamental Plate Theory

The notation used is, in the main, that of Green and Zerna (43). Theory is restricted to infinitesimal elastic behaviour.

Essentially the metric tensors of the strained body are assumed identical with those of the unstrained body. For a plate we can express the position vector, $\bar{R}$ of any point in the unstrained body as

$$\bar{R} = \bar{r}(\theta_1, \theta_2) + \theta_3 \bar{a}_3 \tag{2.2.1}$$

where $\bar{a}_3$ is a constant unit vector perpendicular to the plane surface $\theta_3 = 0$. The rectangular axes x_i are chosen such that the origin of the vectors $\bar{R}$ and $\bar{r}$ and the coordinates x_i are identical. Hence the θ_α curves lie in the (x_1 , x_2) plane. The plate is bounded by two plane surfaces

$$\theta_3 = x_3 = \pm h \tag{2.2.2}$$

Consider now the surface θ_1 = constant.

The force acting on an element of this surface is

$$\bar{T}_1 \, d\theta^2 d\theta^3 \tag{2.2.3}$$

where

$$\bar{T}_1 = \sqrt{(g g^{11})}\, \bar{t}_1 = \sqrt{(g)}\, \tau^{1k} \bar{g}_k \tag{2.2.4}$$

and the length of the corresponding line element of the middle plane $x_3 = 0$ is

$$\sqrt{(a_{22})}\, d\theta^2 = \sqrt{(a\, a_{11})}\, d\theta^2 \tag{2.2.5}$$

The stress across the surface θ_1 = constant may therefore be replaced by a physical stress resultant $\bar{n}_1$ and a physical stress couple $\bar{m}_1$, measured per unit length of the middle line of the plane $x_3 = 0$, which is in the surface θ_1 = constant, where

$$\bar{n}_1 = \frac{1}{\sqrt{(a a^{11})}} \int_{-h}^{h} \bar{T}_1 \, dx_3 \tag{2.2.6}$$

and

$$\bar{m}_1 = \frac{1}{\sqrt{(a\,a^{11})}} \int_{-h}^{h} (\bar{a}_3 \times \bar{T}_1) x_3 \, dx_3 \qquad (2.2.7)$$

General formulae for stress resultants and stress couples over the surface ϑ_α = constant, for unit length of the line ϑ_α = constant and $x_3 = 0$ are

$$\bar{n}_\alpha = \frac{\bar{N}_\alpha}{\sqrt{(a\,a^{\alpha\alpha})}} \qquad \bar{m}_\alpha = \frac{\bar{M}_\alpha}{\sqrt{(a\,a^{\alpha\alpha})}} \qquad (2.2.8)$$

where

$$\bar{N}_\alpha = \int_{-h}^{h} \bar{T}_\alpha \, dx_3 \quad \bar{M}_\alpha = \int_{-h}^{h} (\bar{a}_3 \times \bar{T}_\alpha) x_3 \, dx_3 . \qquad (2.2.9)$$

The stress resultant $\bar{n}$ and stress couple $\bar{m}$ per unit length of a line of the middle plane, whose unit normal in the plane is

$$\bar{u} = u_\alpha \bar{a}^\alpha \qquad (2.2.10)$$

are

$$\bar{n} = \sum_{\alpha=1}^{2} u_\alpha \bar{n}_\alpha \sqrt{a^{\alpha\alpha}}, \quad \bar{m} = \sum_{\alpha=1}^{2} u_\alpha \bar{m}_\alpha \sqrt{a^{\alpha\alpha}} \qquad (2.2.11)$$

For changes of the surface coordinates ϑ_α, $\bar{n}_\alpha \sqrt{a^{\alpha\alpha}}$ and $\bar{m}_\alpha \sqrt{a^{\alpha\alpha}}$ follow the contravariant transformation.

$$\bar{T}_i = \sqrt{(a)}\, \tau^{ik} \bar{a}_k \qquad (2.2.12)$$

Substituting this in equations (2.2.9) gives

$$\sqrt{a^{\alpha\alpha}}\, \bar{n}_\alpha = n^{\alpha\rho} \bar{a}_\rho + q^\alpha \bar{a}_3 \qquad (2.2.13)$$

$$\bar{m}_\alpha \sqrt{a^{\alpha\alpha}} = m^{\alpha\rho} \bar{a}_3 \times \bar{a}_\rho \qquad (2.2.14)$$

$$\bar{N}_\alpha = N^{\alpha\rho} \bar{a}_\rho + Q^\alpha \bar{a}_3 \qquad (2.2.15)$$

$$\bar{M}_\alpha = M^{\alpha\rho} \bar{a}_3 \times a_\rho \qquad (2.2.16)$$

where

$$N^{\alpha\rho} = n^{\alpha\rho} \sqrt{a} \quad M^{\alpha\rho} = m^{\alpha\rho} \sqrt{a} \quad Q^\alpha = q^\alpha \sqrt{a}$$

and
$$n^{\alpha\beta} = \int_{-h}^{h} \tau^{\alpha\beta}\, dx_3 \tag{2.2.17}$$

$$m^{\alpha\beta} = \int_{-h}^{h} \tau^{\alpha\beta} x_3\, dx_3 \tag{2.2.18}$$

$$q^{\alpha} = \int_{-h}^{h} \tau^{\alpha 3}\, dx_3 \tag{2.2.19}$$

$n^{\alpha\beta}$ and $m^{\alpha\beta}$ are symmetrical in α and β.

$$\bar{n} = u_\alpha (n^{\alpha\beta}\bar{a}_\beta + q^{\alpha}\bar{a}_3), \quad \bar{m} = u_\alpha m^{\alpha\beta}\bar{a}_3 \times \bar{a}_\beta \tag{2.2.20}$$

These can be changed into

$$\bar{m}_1 = (m^{11}\bar{a}^2 - m^{12}\bar{a}^1)\sqrt{(a/a^{11})}, \quad \bar{M}_1 = (M^{11}\bar{a}^2 - M^{12}\bar{a}^1)\sqrt{a} \tag{2.2.21}$$

$$\bar{m}_2 = (m^{12}\bar{a}^2 - m^{22}\bar{a}^1)\sqrt{(a/a^{22})}, \quad \bar{M}_2 = (M^{12}\bar{a}^2 - M_2^{22}\bar{a}^1)\sqrt{a} \tag{2.2.22}$$

$n^{\alpha\beta}$, $m^{\alpha\beta}$ and q^{α} are all surface tensors. The components of the symmetrical contravariant tensor $n^{\alpha\beta}$ are called stress resultants, those of the symmetrical contravariant tensor $m^{\alpha\beta}$ are called stress couples, and those of the contravariant tensor q^{α} are called shearing forces.

2.3 Stress resultant-displacement relations

Using the known stress-strain relations of the materials of the plate, and making some assumptions, we may derive the relationships between stress-resultants and displacements for a sandwich plate in flexure. These, together with the boundary conditions, will be all that is required for the variational formulation of the finite element problem. The earlier equations applied to any plate, but the introduction of a special geometry and some assumptions make them much more specific.

We consider a sandwich plate having faces of equal thickness f, and a core of thickness c (in the x_3 direction). The middle surface of the plate is still defined by $x_3 = \vartheta_3 = 0$. A displacement W is introduced, which is the displacement of the middle surface of the plate, in the ϑ_3 direction. [Green and Zerna (43), and Reissner (67), take W as a "weighted displacement" i.e. the integral of the displacement V_3 over the thickness of the plate, divided by the plate thickness].

The following assumptions are introduced

1 All V_3 across plate thickness $\equiv W$

2 The following kinematic relationship holds (Fig. 1)

$$V_\alpha = -\left(W|_\alpha - {}_c\gamma_\alpha\right)x_3 \qquad -\frac{c}{2} \leq x_3 \leq \frac{c}{2} \quad (2.3.1)$$

$$V_\alpha = -W|_\alpha x_3 - {}_c\gamma_\alpha c/2 \qquad \frac{c}{2} \leq x_3 \leq \frac{c}{2}+f \quad (2.3.2)$$

$$V_\alpha = -W|_\alpha x_3 + {}_c\gamma_\alpha c/2 \qquad -\frac{c}{2}-f \leq x_3 \leq -\frac{c}{2} \quad (2.3.3)$$

3 $c \gg f$

${}_c\gamma_\alpha$ is another weighted displacement.

The general elastic stress-strain relationships may be written, for cartesian coordinates, as

$$t_{ij} = c^{ij}_{rs}\, e_{rs} \qquad (2.3.4)$$

For symmetry with respect to a plane (Green and Zerna, p.158) the 21 elastic coefficients can be reduced to 13

$$\begin{array}{cccccc} C^{11}_{11} & C^{11}_{22} & C^{11}_{33} & 0 & 0 & C^{11}_{12} \\ & C^{22}_{22} & C^{22}_{33} & 0 & 0 & C^{22}_{12} \\ & & C^{33}_{33} & 0 & 0 & C^{33}_{12} \\ & & & C^{23}_{23} & C^{23}_{13} & 0 \\ \text{symmetrical} & & & & C^{13}_{13} & 0 \\ & & & & & C^{12}_{12} \end{array} \qquad (2.3.5)$$

This applies separately to both core and faces. If we transform to general coordinates in the (x_1 , x_2) plane, while still retaining the third axis $x_3 = \theta_3$, the equations become

$$\tau^{\alpha\beta} = F^{\alpha\beta\mu\lambda}\epsilon_{\mu\lambda} \qquad (2.3.6)$$

(A prefix c on $F^{\alpha\beta\mu\lambda}$ denotes core, and a prefix f denotes face.)

where

$$F^{3\beta\lambda\mu} = F^{\lambda\mu 3\beta} = F^{333\mu} = F^{3\mu 33} = 0 \qquad (2.3.7)$$

and also

$$F^{\alpha\beta\mu\lambda} = F^{\beta\alpha\mu\lambda} = F^{\beta\alpha\lambda\mu} = F^{\alpha\beta\lambda\mu} \qquad (2.3.8)$$

So we can write, for the faces,

$$\tau^{\alpha\beta} = {}_f F^{\alpha\beta\mu\lambda}\epsilon_{\mu\lambda} + {}_f F^{\alpha\beta 33}\epsilon_{33} \qquad (2.3.9)$$

(Now we have that $\alpha, \beta, \mu, \lambda \neq 3$.)

But since $\epsilon_{33} = 0$, from the first assumption, then

$$\tau^{\alpha\beta} = {}_f F^{\alpha\beta\mu\lambda} \epsilon_{\mu\lambda} \tag{2.3.10}$$

In the core the elastic constants are further constrained

$$\begin{aligned} F^{\alpha\beta\mu\lambda} &= F^{\alpha\beta\lambda\mu} = F^{\beta\alpha\mu\lambda} = F^{\beta\alpha\lambda\mu} = 0 \\ F^{\alpha\beta 33} &= F^{\beta\alpha 33} = F^{33\alpha\beta} = F^{33\beta\alpha} = 0 \end{aligned} \tag{2.3.11}$$

We already have an expression for the covariant strain tensor, in terms of displacements,

$$\epsilon_{\alpha\beta} = \frac{1}{2}\left(v_\alpha|_\beta + v_\beta|_\alpha\right) \tag{2.3.12}$$

and we can now relate the contravariant stress tensor to displacements, using equations (2.3.10) and (2.3.12). The expressions for the stress resultants (2.2.17), (2.2.18) and (2.2.19) can each be split into three parts, for example

$$\begin{aligned} n^{\alpha\beta} = {}_f F^{\alpha\beta\mu\lambda} \int_{\frac{c}{2}}^{\frac{c}{2}+f} \epsilon_{\mu\lambda}\, dx_3 + {}_c F^{\alpha\beta\mu\lambda} \int_{-\frac{c}{2}}^{\frac{c}{2}} \epsilon_{\mu\lambda}\, dx_3 \\ + {}_f F^{\alpha\beta\mu\lambda} \int_{-\frac{c}{2}-f}^{-\frac{c}{2}} \epsilon_{\mu\lambda}\, dx_3 \end{aligned} \tag{2.3.13}$$

Hence

$$n^{\alpha\beta} = -\frac{1}{2}\left\{ {}_{f}F^{\alpha\beta\mu\lambda}\int_{\frac{c}{2}}^{\frac{c}{2}+f}\left(V_{\mu}|_{\lambda}+V_{\lambda}|_{\mu}\right)dx_3 \right.$$

$$\left. +{}_{c}F^{\alpha\beta\mu\lambda}\int_{-\frac{c}{2}}^{\frac{c}{2}}\left(V_{\mu}|_{\lambda}+V_{\lambda}|_{\mu}\right)dx_3 + {}_{f}F^{\alpha\beta\lambda\mu}\int_{-\frac{c}{2}-f}^{-\frac{c}{2}}\left(V_{\mu}|_{\lambda}+V_{\lambda}|_{\mu}\right)dx_3 \right\} \qquad (2.3.15)$$

$$n^{\alpha\beta} = 0$$

This result is a consequence of the kinematic assumption. The stress couple $m^{\alpha\beta}$ may be written,

$$m^{\alpha\beta} = -\frac{1}{2}\left\{ {}_{f}F^{\alpha\beta\mu\lambda}\int_{\frac{c}{2}}^{\frac{c}{2}+f}\left(\left(w|_{\mu\lambda}+w|_{\lambda\mu}\right)x_3^2 - \left({}_{c}\gamma_{\mu}|_{\lambda}+{}_{c}\gamma_{\lambda}|_{\mu}\right)\frac{x_3 c}{2}\right)dx_3 \right.$$

$$\left. +{}_{f}F^{\alpha\beta\mu\lambda}\int_{-\frac{c}{2}-f}^{-\frac{c}{2}}\left(\left(w|_{\mu\lambda}+w|_{\lambda\mu}\right)x_3^2 + \left({}_{c}\gamma_{\mu}|_{\lambda}+{}_{c}\gamma_{\lambda}|_{\mu}\right)\frac{x_3 c}{2}\right)dx_3 \right\} \qquad (2.3.16)$$

On integrating we obtain

$$m^{\alpha\beta} = -{}_{f}F^{\alpha\beta\mu\lambda}\left[\left(\frac{c^2 f}{4}+\frac{c f^2}{2}+\frac{f^3}{3}\right)\left(w|_{\mu\lambda}+w|_{\lambda\mu}\right) + \left(\frac{c^2 f}{4}+\frac{c f^2}{4}\right)\left({}_{c}\gamma_{\mu}|_{\lambda}+{}_{c}\gamma_{\lambda}|_{\mu}\right)\right] \qquad (2.3.17)$$

We introduce a new variable, γ_α , where

$$\gamma_\alpha = {}_c\gamma_\alpha\left(\frac{c+f}{c}\right) \tag{2.3.18}$$

Substitution in (2.3.17) yields

$$m^{\alpha\beta} = -{}_f F^{\alpha\beta\mu\lambda}\left[\left(\frac{c^2 f}{4}+\frac{cf^2}{2}+\frac{f^3}{3}\right)\left(w|_{\mu\lambda}+w|_{\lambda\mu}\right)\right.$$
$$\left.-\left(\frac{c^2 f}{4}+\frac{cf^2}{2}+\frac{f^3}{4}\right)\left(\gamma_\mu|_\lambda+\gamma_\lambda|_\mu\right)\right] \tag{2.3.19}$$

The difference of $f^3/12$, in the coefficients of $\left(w|_{\mu\lambda}+w|_{\lambda\mu}\right)$ and $\left(\gamma_\mu|_\lambda+\gamma_\lambda|_\mu\right)$, is due to the effect of bending of the individual faces. If we assume that the faces act as membranes, and there is no bending effect, we can write equation (2.3.19) as

$$m^{\alpha\beta} = {}_f F^{\alpha\beta\mu\lambda}\Phi\left(w|_{\mu\lambda}+w|_{\lambda\mu}-\gamma_\mu|_\lambda-\gamma_\lambda|_\mu\right) \tag{2.3.20}$$

where $\Phi = \frac{c^2 f}{4}+\frac{cf^2}{2}+\frac{f^3}{4}$

This assumption is justified if $c \gg f$.

From equation (2.2.19) we have

$$q^\alpha = \int_{\frac{c}{2}}^{\frac{c}{2}+f}\tau^{\alpha 3}dx_3+\int_{-\frac{c}{2}}^{\frac{c}{2}}\tau^{\alpha 3}dx_3+\int_{-\frac{c}{2}-f}^{-\frac{c}{2}}\tau^{\alpha 3}dx_3 \tag{2.3.21}$$

The contributions from the faces are zero, because of the kinematic assumption. Consider the core contribution

$$\int_{-\frac{c}{2}}^{\frac{c}{2}}\tau^{\alpha 3}dx_3 = \int_{-\frac{c}{2}}^{\frac{c}{2}}{}_c F^{\alpha 3\beta 3}\epsilon_{\beta 3}\,dx_3 . \tag{2.3.22}$$

Now $$\tau^{\alpha 3} = {}_c F^{\alpha 3 \beta 3} \left(v_\beta |_3 + v_3 |_\beta \right) \qquad (2.3.23)$$

On substituting in equation (2.3.21) we find

$$q^\alpha = \frac{1}{2} {}_c F^{\alpha 3 \beta 3} (c+f) \gamma_\beta \qquad (2.3.24)$$

This completes the set of stress-resultant displacement relations.

Another approach is to define these stress-resultant displacement relations as the fundamental properties of the plate. These are then

$$m^{\alpha\beta} = D^{\alpha\beta\lambda\mu} \left(w|_{\lambda\mu} + w|_{\mu\lambda} - \gamma_\mu|_\lambda - \gamma_\lambda|_\mu \right) \qquad (2.3.26)$$

and $$q^\alpha = S^{\alpha\mu} \gamma_\mu \qquad (2.3.27)$$

$$(n^{\alpha\beta} = 0)$$

The properties $D^{\alpha\beta\lambda\mu}$ and $S^{\alpha\mu}$ can be determined experimentally directly.

It is from these equations that the finite element treatment will be developed.

2.4 The Rectangular Finite Element for Sandwich Plates in Flexure

This element has been developed from the rectangular plate bending element described by Cheung and Zienkiewicz (25). We restrict our attention to the rectangular cartesian coordinates (x_1, x_2, x_3). The plate considered is orthotropic in these coordinates, so that the following relationships hold in D.

$$D_{11}^{22} = D_{22}^{11} \; ; \quad D_{11}^{12} = D_{11}^{11} = D_{12}^{12} = D_{22}^{22} = D_{12}^{22} = 0 \qquad (2.4.1)$$

The non zero components of D are D_{11}^{11} D_{22}^{22} D_{11}^{22} and D_{12}^{12} .

The finite element has the same thickness as the plate, and dimensions $2a$ in the x_1 direction and $2b$ in the x_2 direction. Over this rectangular domain the normal displacement W is represented by the polynomial

$$W = \alpha_1 + \alpha_2 x_1 + \alpha_3 x_2 + \alpha_4 x_1^2 + \alpha_5 x_1 x_2 + \alpha_6 x_2^2 + \alpha_7 x_1^3$$
$$+ \alpha_8 x_1^2 x_2 + \alpha_9 x_1 x_2^2 + \alpha_{10} x_2^3 + \alpha_{11} x_1^3 x_2 + \alpha_{12} x_1 x_2^3 \qquad (2.4.1)$$

In addition two polynomials are used to represent γ_μ .

$$\gamma_1 = c_1 + c_2 x_1 + c_3 x_2 + c_4 x_1 x_2 \qquad (2.4.2)$$

$$\gamma_2 = d_1 + d_2 x_1 + d_3 x_2 + d_4 x_1 x_2 \qquad (2.4.3)$$

The degrees of freedom at any node, i, are chosen to be

$$W_i \; , \; W_{,1})_i \; , \; W_{,2})_i \; , \; \gamma_1)_i \; , \; \gamma_2)_i \qquad (2.4.4)$$

The relationship between nodal displacements and polynomial coefficients can be represented in matrix form as follows:

$$\{\delta\}_e = [H]\{\alpha\} \tag{2.4.5}$$

where $\{\alpha\}$ is the set of all 20 polynomial coefficients, and $\{\delta\}_e$ is the set of all 20 nodal degrees of freedom. The matrix $[H]$ is obtained by substituting the coordinates of element nodes into expressions (2.4.1), (2.4.2) and (2.4.3). The curvatures or strains can be expressed in terms of the polynomial coefficients by means of a matrix, $[Q]$,

$$\{\epsilon\} = [Q]\{\alpha\} \ , \tag{2.4.6}$$

where

$$\{\epsilon\} = \left\{ w|_{11} - \gamma_1|_1, w|_{22} - \gamma_2|_2, w|_{12} - \frac{\gamma_1|_2}{2} - \frac{\gamma_2|_1}{2}, \gamma_1, \gamma_2 \right\}^T$$

The stiffness matrix $[K]$ of the element may be expressed as

$$[k] = [H^{-1}]^T \left(\int_0^{2a} \int_0^{2b} ([Q]^T [D][Q]) dx_2 dx_1 \right) [H^{-1}]^T \tag{2.4.7}$$

(Cheung and Zienkiewicz, page 94), where $[D]$ is the "elasticity" matrix for the plate, expanded as

$$[D] = \begin{bmatrix} D_{11}^{11} & D_{22}^{11} & 0 & 0 & 0 \\ D_{21}^{11} & D_{22}^{22} & 0 & 0 & 0 \\ 0 & 0 & D_{12}^{12} & 0 & 0 \\ 0 & 0 & 0 & S_1^1 & 0 \\ 0 & 0 & 0 & 0 & S_2^2 \end{bmatrix} \tag{2.4.8}$$

The stress resultant can be obtained in terms of nodal displacements from

$$\{\sigma\} = [D][Q][H^{-1}]\{\delta\}_e \tag{2.4.9}$$

where

$$\{\sigma\} = \{m^{11}, m^{22}, m^{12}, q^1, q^2\}^T .$$

The element stiffness matrix, $[k]$, and the matrix relating stresses to nodal displacements can be evaluated explicitly, in terms of the stiffnesses, and dimensions of the element. They are given in Appendix I. The stresses may be determined at any point in the element. Here they are calculated at the four corners, which values suffice to determine all stresses uniquely. The symmetries of the element are exploited, and the matrices partitioned for conciseness of presentation.

2.5 The Triangular Finite Element for Sandwich Plates in Flexure

This element has its ancestry in the quadrilateral element of de Veubeke (31, 73). Some of de Veubeke's procedures are retained, but the geometry is different, and the element is directed at sandwich plate theory and not the "classical" plate theory of the original.

The triangular element is divided into three smaller triangles by lines joining its centroid to its verticles. The 3 triangles are numbered I, II and III. The choice of the centroid as a generator is arbitrary, although this function must always be performed by a point within the triangle. The 3 angles at the centroid are designated α, β and γ. l_i are the distances from the centroid to the 3 vertices in triangles I, II and III. These are clearly shown in Fig (2). Obviously, $\alpha + \beta + \gamma = 2\pi$.

In triangle I the displacement, W , is represented by the polynomial (in local oblique coordinates x_1 , and x_2)

$$W = s_1^1 + s_2^1 x_1 + s_3^1 x_2 + s_4^1 x_1^2 + 2 s_5^1 x_1 x_2 + s_6^1 x_2^2$$
$$+ 4\left(s_7^1 x_1^3 + s_8^1 x_1^2 x_2 + s_9^1 x_1 x_2^2 + s_{10}^1 x_2^3\right) \qquad (2.5.1)$$

and the displacements γ_α , by the polynomials

$$\gamma_1 = s_1^2 + s_2^2 x_1 + s_3^2 x_2 \qquad (2.5.2)$$

$$\gamma_2 = s_1^3 + s_2^3 x_1 + s_3^3 x_2 \qquad (2.5.3)$$

In triangles II and III, polynomials u^i_j and v^i_j are used. As depicted in Fig 2 , the 4 nodes are numbered. In each sub-element triangle the displacement W , and the slopes $W_{,1}$ and $W_{,2}$ are used as nodal displacements at each of the 3 nodes. The slope $W_{,1}$ at the midpoint of the external edge completes the set of 10 nodal displacements required to determine uniquely all the polynomial coefficients $s^1_{j,j}$ = 1 to 10. In addition γ_1 and γ_2 are used at each node; these suffice to determine the remaining polynomial coefficients.

A summary of the formulation of the element stiffness matrix follows. Element stiffness matrices are generated for the 3 sub-elements, using the procedures described by de Veubeke. Those of triangles II and III are transformed to the oblique coordinates of triangle I, and the element stiffness matrix assembled. A set of constraints which ensure internal continuity of displacements and slopes is used to condense this stiffness matrix, causing several of the degrees of freedom at the central node to disappear. The stiffness matrix is finally transformed into the global cartesian coordinates in which the geometry of the element was defined.

The choice of all displacement polynomials satisfy the criteria of Dunne (33). They are complete, and hence have no preferred directions, and it is shown that inter-element continuity is ensured.

The set of 16 nodal displacements, q_1 , in triangle I is

$$q_1 = w_4, \varphi_4, \vartheta_4, \gamma_{14}, \gamma_{24}, w_1, \varphi_1, \vartheta_1, \gamma_{11}, \gamma_{21}, w_2, \varphi_2, \vartheta_2, \gamma_{12}, \gamma_{22}, \varphi_{12}$$

where

$$\varphi = w|_1 = w_{,1} \tag{2.5.5}$$

$$\vartheta = w|_2 = w_{,2} \tag{2.5.6}$$

and φ_{12} is the slope $w|_1$ at the middle of side 1-2.

As before the matrix relating the set of nodal displacements to polynomial coefficients can be written

$$\{q\} = [H]\{\alpha\}. \tag{2.5.7}$$

The matrix $[H]$ can be inverted to give

$$\{\alpha\} = [H^{-1}]\{q\}. \tag{2.5.8}$$

The plate is supposed to be elastically orthotropic in some cartesian coordinate system, randomly oriented with respect to the triangular element. For each sub-element the elasticity matrix must be obtained, in local oblique coordinates. The contravariant tensor D^{ijrs} , representing the properties of the plate in flexure (equation 2.3.26) is readily transformed

$$D^{\alpha\beta\lambda\mu} = D^{ijrs} \frac{\partial\theta^\alpha}{\partial x^i} \frac{\partial\theta^\beta}{\partial x^j} \frac{\partial\theta^\lambda}{\partial x^r} \frac{\partial\theta^\mu}{\partial x^s} \tag{2.5.9}$$

Similarly, the shear properties may be transformed

$$S^{\alpha\beta} = S^{ij} \frac{\partial\theta^\alpha}{\partial x^i} \frac{\partial\theta^\beta}{\partial x^j} \tag{2.5.10}$$

The strain matrix $\{\epsilon\}$ may be written

$$\{w|_{11}-\gamma_1|_1,\ w|_{12}-\gamma_1|_2,\ w|_{21}-\gamma_2|_1,\ w|_{22}-\gamma_2|_2,\ \gamma_1,\ \gamma_2\}^T \tag{2.5.11}$$

The relationship between the strains and the polynomial coefficients,

$$\{\epsilon\} = [Q]\{\alpha\} \tag{2.5.12}$$

is obtained from (2.5.1), (2.5.2) and (2.5.3).

On substituting (2.5.8) in (2.5.12) we further obtain

$$\{\varepsilon\} = [R]\{q\} \tag{2.5.13}$$

where

$$[R] = [Q][H^{-1}] \tag{2.5.14}$$

The matrix $[R]$ can be split into 3 other matrices, $[W]$, $[W_x]$ and $[W_y]$ which are independent of x_1 and x_2 where

$$[R] = \left(\frac{1}{l_1^2 l_2^2}[W] + \frac{2x_1}{l_1^3 l_2^2}[W_x] + \frac{2x_2}{l_1^2 l_2^3}[W_y] \right) \tag{2.5.15}$$

de Veubeke shows that the sub-element stiffness matrix $[k]$ can be written

$$[k] = \frac{1}{6l_1^3 l_2^3}\left\{[A]^T[D][A]+[B]^T[D][B]+[C]^T[D][C]\right\} \tag{2.5.16}$$

where

$$[A] = [W]+[W_x],\quad [B] = [W]+[W_y]$$

$$[C] = [W]+[W_x]+[W_y] \tag{2.5.17}$$

These matrices, $[A]$, $[B]$ and $[C]$, are shown in Fig 3. Since the de Veubeke element deals solely with "classical" plate theory, no terms relating to shearing deformations, γ, appear in the original matrices.

The stiffness matrices from triangles II and III must be transformed to the oblique coordinates of triangle I. The displacement, W, is the same in all triangles. The slopes and shears follow a covariant transformation

$$W|_\alpha = \frac{\partial \theta^\beta}{\partial \theta^\alpha} W|_\beta \qquad (2.5.18)$$

$$\gamma_\alpha = \frac{\partial \theta^\beta}{\partial \theta^\alpha} \gamma_\beta$$

The overall stiffness matrix is formed by simple addition. The complete set of nodal displacements, $\{r\}$ is now

$$\{w_4, \varphi_4, \theta_4, \gamma_{14}, \gamma_{24}, w_1, \varphi_1, \theta_1, \gamma_{11}, \gamma_{21}, w_2, \varphi_2, \theta_2, \gamma_{12}, \gamma_{22},$$

$$w_3, \varphi_3, \theta_3, \gamma_{13}, \gamma_{23}, \varphi_{12}, \varphi_{23}, \varphi_{31}\}^T$$

On the internal sub-element interfaces, the displacements do not necessarily conform. On any internal edge, the displacement W can be written as a cubic polynomial, and the two slopes $W|_\alpha$, as quadratics. Since complete continuity of normal displacements and slopes is wanted, we equate these polynomials on the 3 interfaces, term by term. This gives a total of 30 equations. Not all of these are independent. Moreover some of the equations are pre-empted by the identity of nodal displacements at the ends of interfaces. There remain only 3 independent equations, which may be written as

$$s_5' = \frac{\sin(\alpha+\beta)}{\sin\beta} u_4' - \frac{\sin\alpha}{\sin\beta} u_5' \qquad (2.5.19)$$

$$s_5^1 = \frac{\sin\alpha}{\sin(\alpha+\beta)} v_5^1 + \frac{\sin\beta}{\sin(\alpha+\beta)} v_6^1 \qquad (2.5.20)$$

$$u_5^1 = \frac{\sin\alpha}{\sin(\alpha+\beta)} v_4^1 + \frac{\sin\beta}{\sin(\alpha+\beta)} v_5^1 \qquad (2.5.21)$$

By substituting from equations (2.5.8) the polynomial coefficients can be eliminated, in favour of the nodal displacements, and equations, (2.5.19), (2.5.20) and (2.5.21) can be written

$$\{0\} = [\ E\ ]\{r\} \qquad (2.5.22)$$

or, more usefully

$$[F]\begin{Bmatrix} w_4 \\ \varphi_4 \\ \vartheta_4 \end{Bmatrix} = [G]\{p\}$$

where $\{p\}$ is the set of nodal displacements, $\{r\}$, with the first three deleted. The matrix $[F]$ can be inverted, so that

$$\begin{Bmatrix} w_4 \\ \varphi_4 \\ \vartheta_4 \end{Bmatrix} = [F^{-1}][G]\{p\} = [M]\{p\} \qquad (2.5.23)$$

We now form a condensation matrix, $[N]$, by adding to $[M]$ a unit diagonal matrix, thus

$$\{r\} = \begin{bmatrix} M \\ I \end{bmatrix}\{p\} = [N]\{p\} \qquad (2.5.24)$$

The matrix $[N]$ is used to "condense" the element stiffness matrix, eliminating W_4, φ_4 and θ_4.

$$[k'] = [N]^T[k][N] \qquad (2.5.25)$$

Along each external edge of the triangle the displacement varies cubically. (It is fully determined by the end displacements and slopes. This implies continuity of W between adjacent elements). It is therefore possible to calculate the mid-side slope, along the edge, purely in terms of these end displacements and slopes. At this mid-point the slope $W\big|_1$ is also known. These two slope components, determine fully any and all slope components at this point, and in particular the slope normal to the edge. The normal slope at the vertices can also be calculated, so that on each edge of the element we know 3 values of the slope normal to the edge. Since the normal slope varies quadratically along the edge, it is fully determined by these 3 values, and therefore there is slope continuity between adjacent elements. The element is fully conforming. In use the slope in the middle of each edge is conveniently transformed into a normal slope. The slope φ_{12}, in local oblique coordinates, is expressed in terms of the outward normal slope, η_{12}, and the other nodal displacements.

$$\varphi_{12} = \frac{3\cos(\alpha-\alpha')}{2\,d_1}(w_1-w_2) + \frac{\cos(\alpha-\alpha')}{4}(u_{12}h_{11}+u_{22}h_{21})(\vartheta_1+\vartheta_2) + \frac{\cos(\alpha-\alpha')}{4}(u_{11}h_{11}+u_{21}h_{21})(\varphi_1+\varphi_2) + \eta_{12}\sin(\alpha-\alpha') \qquad (2.5.26)$$

where

$$u_{11} = (x_2^1 - x_2^4)/l_1$$
$$u_{12} = (x_1^1 - x_1^4)/l_1$$
$$u_{21} = (x_1^2 - x_2^4)/l_2$$
$$u_{22} = (x_1^2 - x_1^4)/l_2 \quad , \qquad (2.5.27)$$

$$b_1^1 = \alpha'-\alpha \qquad b_2^1 = \alpha'-\beta$$
$$b_1^2 = \beta'-\alpha \qquad b_2^2 = \beta'-\beta$$
$$b_1^3 = \gamma'-\gamma \qquad b_2^3 = \gamma'-\beta \qquad (2.5.28)$$

$$h_{j1} = \sin b_2^j / \sin(b_2^j - b_1^j)$$
$$h_{j2} = \sin b_1^j / \sin(b_1^j - b_2^j) \qquad (2.5.29)$$

(u, b and h are not tensors)

Similar formulae apply to φ_{23} and φ_{31}.

$$\varphi_{23} = \frac{3\cos(\beta-\beta')}{2d_2}(w_2-w_3) + \frac{\cos(\beta-\beta')}{4}(u_{12}h_{12}+u_{22}h_{22})(\vartheta_2+\vartheta_3) + \frac{\cos(\beta-\beta')}{4}(u_{11}h_{12}+u_{21}h_{22})(\varphi_2+\varphi_3) + \sin(\beta-\beta')\,n_{23}\,, \tag{2.5.30}$$

$$\varphi_{31} = \frac{3\cos(\gamma-\gamma')}{2d_3}(w_3-w_1) + \cos(\gamma-\gamma')(u_{12}h_{31}+v_{22}h_{32})(\vartheta_3+\vartheta_1) + \cos(\gamma-\gamma')(u_{11}h_{31}+v_{21}h_{32})(\varphi_3+\varphi_1) + \sin(\gamma-\gamma')\,n_{31} \tag{2.5.31}$$

These together with transformations of the form of equations (2.5.18) enable the production of a matrix $[P]$, which transforms vertex displacements into "global" cartesian coordinates, and mid-side slopes into normal slopes. This gives the final "ready-to-use" stiffness matrix

$$[K] = [P]^T[K'][P] \tag{2.3.32}$$

3. Plane Stress

3.1 Fundamental Theory

We retain the geometrical concept of a sandwich plate, as defined in 2.2., and again make use of the equations (2.2.17),(2.2.18) and (2.2.19). This time however the kinematical assumption is different. We now choose that

$$V_\alpha = V_\alpha(\theta_1, \theta_2) \qquad -\tfrac{c}{2}-f \leqslant x_3 \leqslant \tfrac{c}{2}+f \tag{3.1.1}$$

$$V_3 \equiv 0$$

That is, all displacements in the (θ_1, θ_2) plane are constant across the thickness of the plate. It is now readily seen that

$$\epsilon_{\alpha 3} = \epsilon_{3\alpha} = \tfrac{1}{2}(V_\alpha|_3 + V_3|_\alpha) = 0 \tag{3.1.2}$$

and so

$$q^\alpha = \int_{-\frac{c}{2}-f}^{\frac{c}{2}+f} \tau^{\alpha 3}\, dx_3 \quad = 0 \tag{3.1.3}$$

Also we see that

$$m^{\alpha\beta} = 0 \tag{3.1.4}$$

(from 2.2.18)

We may re-write here (2.3.6) and (2.3.12)

$$\tau^{\alpha\beta} = F^{\alpha\beta\mu\lambda}\epsilon_{\mu\lambda}$$

and

$$\epsilon_{\alpha\beta} = \tfrac{1}{2}(V_\alpha|_\beta + V_\beta|_\alpha)$$

Consider the direct stress resultant $n^{\alpha\beta}$

$$n^{\alpha\beta}=\int_{\frac{c}{2}}^{\frac{c}{2}+f}\tau^{\alpha\beta}dx_3+\int_{-\frac{c}{2}}^{\frac{c}{2}}\tau^{\alpha\beta}dx_3+\int_{-\frac{c}{2}-f}^{-\frac{c}{2}}\tau^{\alpha\beta}dx_3 \tag{3.1.5}$$

The central term, which is the direct stress contribution of the core, may be neglected, because the core is usually very flexible. (This assumption is implicit in the earlier kinematic assumptions for flexure). After eliminating this term, and substituting from (2.3.6) we obtain

$$n^{\alpha\beta}=\int_{\frac{c}{2}}^{\frac{c}{2}+f}{}_fF^{\alpha\beta\lambda\mu}\epsilon_{\lambda\mu}+\int_{-\frac{c}{2}-f}^{-\frac{c}{2}}{}_fF^{\alpha\beta\lambda\mu}\epsilon_{\lambda\mu}\ , \tag{3.1.6}$$

which on the introduction of (2.3.12) yields

$$n^{\alpha\beta}=2f\,{}_fF^{\alpha\beta\lambda\mu}(v_{\lambda|\mu}+v_{\mu|\lambda}) \tag{3.1.7}$$

These are the stress resultant-displacement equations used in the development of a plane stress element. It is sometimes more convenient to cast them in the form

$$n^{\alpha\beta}=E^{\alpha\beta\lambda\mu}\,(v_{\lambda|\mu}+v_{\mu|\lambda}) \tag{3.1.8}$$

where

$$E^{\alpha\beta\lambda\mu}=2f\,{}_fF^{\alpha\beta\lambda\mu}$$

3.2 The Triangular Plane Stress Finite Element

This simple, triangular, constant stress element was one of the first finite elements ever developed (27, 28), and has been frequently described (25), and used, effectively, to solve many problems, (28, 35). It will only be briefly described here.

The "in-plane" displacements, V_i , in some rectangular cartesian coordinate system, are represented by linear polynomials, in the domain of the triangle of plate, which the element comprises. (The triangle can of course be of any configuration.) These polynomials are

$$V_1 = \zeta_1 + \zeta_2 x_1 + \zeta x_2$$

and (3.2.1)

$$V_2 = \eta_1 + \eta_2 x_1 + \eta_3 x_2$$

Now the 3 polynomial coefficients ζ_i $i = 1$ to 3, are related to the nodal displacements, $V_1^i, i = 1$ to 3, by

$$\begin{Bmatrix} \zeta_1 \\ \zeta_2 \\ \zeta_3 \end{Bmatrix} = \frac{1}{2\Delta} \begin{bmatrix} p_1 & p_2 & p_3 \\ q_1 & q_2 & q_3 \\ r_1 & r_2 & r_3 \end{bmatrix} \begin{Bmatrix} V_1^1 \\ V_1^2 \\ V_1^3 \end{Bmatrix} \qquad (3.2.2)$$

(the upper suffices on V denote the vertex or node number)

where
$$p_i = x_1^j x_2^k - x_1^k x_2^j$$
$$q_i = x_2^j - x_2^k \qquad (3.2.3)$$
and
$$r_i = x_1^k - x_1^j$$

and i , j , k are anti-clockwise cylic nodal numbers for the triangle. Δ is the area of the triangle. The relations between v_ℓ^i and $\eta_{\ell i}$ are identical to (3.2.2), so the relations between strains and displacements can be explicitly stated in matrix form as

$$\{\varepsilon\} = [R]\{\delta\}_e \tag{3.2.4}$$

where

$$\{\varepsilon\} = \{\varepsilon_{11}, \varepsilon_{12}, \varepsilon_{21}, \varepsilon_{22}\}^T \tag{3.2.5}$$

$$\{\delta\} = \{v_1^1, v_2^1, v_1^2, v_2^2, v_1^3, v_2^3\}^T \tag{3.2.6}$$

and $[R]$ is

$$\frac{1}{2}\begin{bmatrix} 2q_i, & 0, & 2q_j, & 0, & 2q_k, & 0 \\ r_i, & q_i, & r_j, & q_j, & r_k, & q_k \\ r_i, & q_i, & r_j, & q_j, & r_k, & q_k \\ 0, & 2r_i, & 0, & 2r_j, & 0, & 2r_k \end{bmatrix} \tag{3.2.7}$$

The "stress-strain" relations in the original cartesian coordinate system (2.3.6) may be written in matrix form as

$$\begin{Bmatrix} \eta^{11} \\ \eta^{12} \\ \eta^{21} \\ \eta^{22} \end{Bmatrix} = \begin{bmatrix} E^{1111}, & E^{1112}, & E^{1121}, & E^{1122} \\ E^{1211}, & E^{1212}, & E^{1221}, & E^{1222} \\ E^{2111}, & E^{2112}, & E^{2121}, & E^{2122} \\ E^{2211}, & E^{2212}, & E^{2221}, & E^{2222} \end{bmatrix} \begin{Bmatrix} \varepsilon^{11} \\ \varepsilon^{12} \\ \varepsilon^{21} \\ \varepsilon^{22} \end{Bmatrix} \tag{3.2.8}$$

This comprises the " $[D]$ " matrix for the element.

The stiffness matrix is readily formed from

$$[k] = \int [R]^T [D][R] \, d(\text{area}) \tag{3.2.9}$$

the integrations being especially easy since all terms are constants, so that

$$[k] = \Delta\, [R]^T [D][R] \,. \tag{3.2.10}$$

4 Application of bending elements to bending problems

4.1 Boundary Conditions

It was mentioned earlier that there are 3 boundary conditions on each edge of a sandwich plate in flexure (2.1). These take the form of constraints upon stress resultants or displacements. Consider the edge θ^1 = constant.

The boundary conditions are :-

1 either m^{11} or $(w|_1 - \gamma_1)$ is constrained

and 2 either m^{12} or γ_2 is constrained

and 3 either q^1 or w is constrained.

The boundary conditions upon the stress resultants, will be supplied automatically, in the absence of a constraint upon the corresponding displacement. (This is a consequence of the Variational Formulation of the finite element. 56).

For each boundary condition, the two extreme cases are that the displacement or the force should be fixed. Alternatively, the displacement can be limited by a spring of specific stiffness. There can also be cross linking between the displacements as occurs for instance with an edge beam. Three boundary conditions will always be applied on an edge. If cross linked displacements and edge springs are ignored we have 2^3 possible boundary conditions, obtained by fixing or freeing each displacement (Fig. 4). The number assigned to each boundary condition will be used later, as they are concise. If we assume that displacements are to be fixed only at zero, we have the above set of 8 possibilities for each edge.

4.2 Available Results

There are few analytical solutions to sandwich plate flexure problems. The case of a circular plate with simply supported edges under circularly symmetric loading has been solved (2) and it is also possible to obtain exact answers for rectangular plates with simply supported edges, and double sine wave distributed loading. These cases aside, all other results appear to be either series solutions (2, 23, 45, 65), or solution by some numerical method.• Reissner seems to have been the first to point out the separability of bending and shearing effects, in plates with simply supported edges, under a uniform loading. Plantema (2) shows results obtained using this simplification. He added to the results obtained by classical plate theory (75), the effects of the finite shear stiffness. An interesting feature of these solutions is the independence of the shear stiffnesses and the bending moments. Other series solutions for rectangular plates with pinned edges under uniform and concentrated loadings are given by Raville (65) and Gunturkun et al. (45). Lockwood-Taylor (57) gave a series solution for the case of a square plate with clamped edges under a uniform load. More recently research at Imperial College by Chapman and Williams (24) and Basu and Dawson (14) has produced a large number of solutions for cases of rectangular sandwich plates in flexure. Chapman and Williams used a finite difference program to produce a very large number of results, with various stiffness parameters and edge restraints. Basu and Dawson using a dynamic relaxation program, investigated the effect of various boundary conditions, and also considered the behaviour of box girder structures, which behave in a very similar manner to sandwich plates.

4.3 Comparisons with available theoretical and numerical results

The finite elements were used to solve a large number of flexural problems, to which other solutions had been given.

4.3.1 Series solutions for rectangular isotropic sandwich plate, under a uniform load, boundary condition 3

For this class of problem, the increase in deflection over those of "classical" plate theory, is proportional to the inverse of the shear stiffness of the plate. This prompted Basu and Dawson to plot central deflection against the inverse of the shear stiffness for a range of the plates (14). A similar presentation is shown in Figs. 5, 6, 7, which show a wide range of results. The agreement between the series solution values for the central deflection, due to Plantema (2), and those obtained with the rectangular finite element is excellent. The stress resultants also agree well, and as expected, are independent of the shear stiffness of the plate. The agreement with the dynamic relaxation results which for clarity are not shown, is also good. The results plotted were all for a 6 by 6 mesh of elements, applied to a quarter of the plate. Fig. 8. shows the convergence of the central displacement, obtained by finite elements, towards the series solution value, for a particular plate size and stiffness, with an increasing number of elements.

4.3.2 Dynamic Relaxation solution for a rectangular isotropic sandwich plate, under uniform loading, boundary condition 7

The effect of the extra boundary condition, is to modify the distribution of shear force across the plate boundary, the bending moments, and the central deflection. The two sets of results (with

and without an edge stiffener) are shown in Figs. 9, 10, 11, together with solutions obtained by dynamic relaxation. The agreement between the two methods is very good. The influence of this third boundary condition is marked, in its modification of both displacements and stresses.

4.3.3 Series, and Dynamic Relaxation Solutions for a clamped plate with boundary conditions 1 and 4

The series results due to Lockwood Taylor (57) for the case of clamped plate (boundary condition 4), are shown in Fig. 12. Results for the same problem, obtained by dynamic relaxation (14) and with finite elements for both clamped boundary conditions (1 and 4) are also shown. Again a 6 by 6 mesh of elements was used. The agreement between the dynamic relaxation and finite element results is excellent. Dawson suggests that the slight difference between his results and those of Lockwood Taylor, is due to Lockwood Taylor's premature truncation of a series. The close agreement of the present results with those of Dawson, lends weight tothis hypothesis. The difference is still very small.

4.3.4 Series, and dynamic relaxation solutions for a rectangular sandwich plate, with isotropic faces and an orthotropic core, boundary condition 3

The table in Fig. 13 shows results obtained by Raville (65) using a series method, and Basu and Dawson using dynamic relaxation, compared with results obtained using finite elements. The agreement is uniformly excellent, despite as Dawson remarks, Raville's completely different formulation.

4.3.4 Chapman and Williams' Results

Chapman and Williams (24) produced many results, of which two have been chosen for comparison. These were a clamped plate under a uniform transverse load, with varying shear stiffness, and a simply supported plate under uniform transverse load, with varying orthotropic flexural properties. Figures 14 to 16 are the authors Figs. 3 to 5, with finite element results superposed. For each case the mesh of elements was varied from 1 by 1 to 6 by 6. The agreement between the Chapman and Williams results (obtained by a finite difference method), and the finite element results is excellent.

4.3.5 Sander's skew plate results

Sander (73) gives moments and shearing forces obtained by the finite element method, for the case of a 30° skew plate, under a uniformly distributed load, with both types of pinned edges (3, 7). He solves the problem for a fairly high value of shear stiffness ($S_1' = S_2^2 = 2|8.4\, D_{11}'' / a^2$). Fig. 17 shows the displacements obtained by analysing $\frac{1}{4}$ of the plate with a regular mesh of 36 of the triangular elements described in section 2.5, (for boundary condition 3). Figs 18 and 19 show shear forces and moments, compared with those obtained by Sander, for the case of the stiffened edges. The agreement of moments and shear forces is quite tolerable. An unusual feature of Sander's results is the non-zero shear force at the oblique corner, which is unexpected (cf equations 2.3.24). Away from this corner, the agreement of shear forces is good.

4.4 Comparison with experiment

Figs 20 to 30 show displacements obtained by the finite element program, with experimental results superposed. Seven different plates were used as described in 8.6. In each case $\frac{1}{4}$ of the plate was analysed, using meshes of elements from 1 by 1 up to 6 by 6. As can be seen the agreement between experiment and theory is varied. The closest agreement is for the aluminium plate, 7, for which the experimental and theoretical results are practically identical. The thicker plywood and fibreglass plates (1 and 4), also show very good agreement of displacements. The largest differences, of up to about 25%, occur with the thinner fibreglass and plywood plates. In general it seems that the larger the ratio c/f, the better the agreement between theory and experiment. This was also noted by Elliott (34), and it is entirely consistent with the assumptions made in deriving the theory for sandwich plates in flexure (section 2.3). Stress resultants m^{11} and q^{1}, obtained for a quarter of each plate are shown for plates 7 and 8. Some experimental results are also shown. The values of the moments m^{11}, calculated from strain gauge readings are plotted. The agreement with the theory is not good for the aluminium plate. For the hardboard plate the one experimental value of m^{11} agrees very well with the finite element value.

4.5 Conclusions from plate bending results

The finite element is at two removes from the reality which it is supposed to represent. It is based on a mathematical model of the real plate, and it introduces approximations into the treatment of this model. The second step, that from model to finite element was tested by the comparisons in section 4.3. These show conclusively that the finite elements described are a feasible, accurate and powerful method of solving the sandwich plate equations, in numerous situations. The results of section 4.4 demonstrate the solution of real problems. These problems are more stringent. First, the accuracy of the mathematical model chosen to describe the plate, is tested. Second, it happens that the particular problems chosen, plates with corner supports and point loads, are a more searching test of the finite elements themselves than those in section 4.3. In the neighbourhood of the point supports and the point load, the kinematic modelling of the element has to accommodate large displacement and stress gradients. In particular at the centre of the plate, there is a conflict between the requirements of symmetry (that $\gamma_1 = \gamma_2 = 0$) and those of equilibrium (that the shear forces should balance the load). However, even classical plate theory collapses beneath point loads. Just at the point support, the equations demand that $q_1 = q_2 \to \infty$. This is not possible either in reality, because the support is not really a point, or in the element, because of the chosen representation for γ_1 and γ_2 (equations (2.4.2, 3) and (2.5.2, 3)). As can be seen in Figs 28 and 30, there are large peaks in q_1 and q_2 at the point support. The displacement finite element achieves equilibrium by a variation on the displacements. In general the worse the representation of the displacements the greater the lack of equilibrium.

Even in the stringent tests the finite element results show that the boundary conditions, of no shear forces or moments, across plate edges, are closely approached (Figs 27 to 30). The agreement between experimental and theoretical displacements is very good for some of the plates, and even the errors with the thinner plates are not surprising. They show that if used judiciously the elements will give a very good representation of the behaviour of a real plate.

5. The dome elements

No attempt was made to make a rectangular sandwich dome element. The two dome elements used were triangular. Both derived from the triangular flexural element described in 2.3, in combination with three of the membrane elements described in 3.2. The simpler of the two dome elements consisted merely of the sum of these elements. It had a stiffness matrix of order 28. The ordering of the nodal degrees of freedom was

i	1	2	3				
	1	8	15	v_1^i	22	φ_{12}	
	2	9	16	v_2^i	23	φ_{23}	
	3	10	17	v_3^i	24	φ_{31}	$[v_3 \equiv w]$
	4	11	18	$-\theta_i \; -\frac{\partial w}{\partial y}$	25	v_1^4	
	5	12	19	$\varphi_i \; +\frac{\partial w}{\partial x}$	26	v_2^4	
	6	13	20	$-\gamma_{2i}$	27	$-\gamma_{24}$	
	7	14	21	γ_{1i}	28	γ_{14}	

The set of displacements v_i, at each vertex, is complete, and is capable of transformation. The set of rotations however is not complete, since there is no rotation about the axis normal to the element. To complete the set of rotations it would be necessary to introduce this rotation into the plane stress element. Although this has been suggested by Cheung and Zienkiewicz (25), it is accompanied by difficulties in algebra and in compatibility, and no displacement element of this form appears to have been reported. It is possible that it would produce poor conditioning of the resulting equilibrium equations since the stiffness corresponding to rotations about the normal axis would be much greater than that due to rotations about the in plane axes. For

these reasons, this rotation has always been discarded. In this respect we follow the procedure of Cheung and Zienkiewicz (25).

In the second element the four degrees of freedom at the centre node were eliminated by static condensation. This process has been described in, for example (25). It will be briefly repeated here. The nodal degrees of freedom are divided into two sets, those which are to be retained, and those which are to be eliminated. The element stiffness matrix may then be partitioned, so that

$$\{F_1\} = [K_{11}]\{\delta_1\} + [K_{12}]\{\delta_2\} \qquad (5.1)$$

and

$$\{F_2\} = [K_{21}]\{\delta_1\} + [K_{22}]\{\delta_2\} \qquad (5.2)$$

On premultiplying 5.2. by $[K_{21}][K_{22}^{-1}]$ and subtracting from 5.1. we obtain

$$(\{F_1\}-[K_{12}][K_{22}^{-1}]\{F_2\})=([K_{11}]-[K_{12}][K_{22}^{-1}][K_{21}])\{\delta_1\}. \qquad (5.3)$$

The unwanted displacements may also be eliminated from the stress matrices, so that if originally

$$\{\sigma\} = [Q_1]\{\delta_1\} + [Q_2]\{\delta_2\} \qquad (5.4)$$

then after condensation

$$(\{\sigma\}-[Q_2][K_{22}^{-1}]\{F_2\})=([Q_1]-[Q_2][K_{22}^{-1}][K_{21}])\{\delta_1\}. \qquad (5.5)$$

After the elimination of the 4 degrees of freedom at the centre node, the element has 24 degrees of freedom. The slopes of the middle surface of the plate φ and θ in the first element, are replaced by total rotations at each of the nodes, in the second element.

Two further options are available within the element. They are for use,

1 for edges of intersecting plates,

and 2 for nodes at the intersection of more than 2 plates.

In both cases the displacements V_i are transformed to global coordinates. In the first option the total rotations are transformed into coordinates defined by a given edge of the element, and the vertical plane through it. The shear angles about this edge are then condensed out. (There is no requirement of continuity of this shear angle). In the second option, the two shear angles at the node are condensed out, and the rotations are transformed into global coordinates.

6. Programs

All programs used in this work were written in FORTRAN IV, and were run on the NUMAC I.B.M. 360/67 computer.

Initially, when the finite element programs were being developed, and even later, for medium size programs, it was feasible to store the entire program and its working store, in the fast store of the computer. The "core" storage of the 360 was 512 K bytes*. Approximately 330 K bytes of this storage was available for users, and with 4 bytes to a word large stiffness matrices with up to about 50,000 non zero terms within the half band, could be stored. The early programs were written on an ad hoc basis for each element, and had the following features.

1. The assembly routine was written specially for each element.
2. Simple constraints were applied by eliminating a row and column from the stiffness matrix, replacing with zeros, and putting a unit on the diagonal.
3. Half the stiffness matrix, within the band was stored as a vector.
4. Solution was by the Choleski method. (38).

For large problems it was evidently no longer possible to store everything in "core", particularly as double precision words would be needed.

Fortunately, at about this time descriptions of the frontal solution method, and even program listings were published (13,52,53,54).

---

* 64 bits ≡ 8 bytes ≡ 2 words ≡ 1 double precision word
K = 1024

The Mark VI Irons frontal solution program (54), was modified so as to suit my needs. The main innovations were

1 A scheme to allow the assembly of any type of element.

2 A Lagrange Multiplier package for applying constraints.

Irons (53) advocates the use of Lagrange Multipliers for applying constraints. There is no doubt that they are the most general, powerful and elegant method available (56,51,53,52,26).

In operation on the NUMAC I.B.M. 360/67, the Irons frontal solution program uses 3 disc data sets as backing store. The limits on the size of problem have not yet been encountered in operation. The "front" of active degrees of freedom must contain less than 241 degrees of freedom, in the present version of the program. The program is available in two forms, one for use on the time sharing system, and one for use on the batch system.

7. Results from dome elements

The dome elements were applied to the following structures.

1. Three tetrahedral domes (Fig. 31) composed of plates 1, 2 and 3. (guide to numbers in Appendix II.)
2. A square pyramid (Fig. 32) composed of plates 7.
3. A hexagonal pyramid (Fig. 33) composed of plates 9.
4. A barrel vault (Fig. 35) described by Benjamin (3, 19, 20).
5. A dome with 16 faces (Fig. 34) composed of plates 3.

Some description of the various domes is given in 8.6.

7.1 Tetrahedral dome results

These are shown in Figs. 43 to 59. Each of the 3 domes was analysed under 2 loadings. These were a unit vertical load at the centroid of each face and at the centroid of one face. This gave a total of 6 load cases. Attention has been concentrated upon the loaded faces. Deflections and stresses in other faces were relatively small. The 6 displacement profiles for loaded faces are in Figs. 43 to 47. The experimental results obtained for these domes will be discussed later by Mr. Parton. The experimental displacements which were measured at the load and at the midpoint of the lower edge of each face were larger than the theoretical ones. The horizontal displacements of the plate folds are shown for some load cases in Figs. 49 to 52. Fig. 53 shows normal displacements over half the tetrahedral dome made of plates 1. Stress resultants are shown in Figs. 54 to 58. The results are all for a 6 x 6 mesh of 36 elements on each face. For the dome made of plates 1 under 3 loads the convergence was closely investigated. A plot of an important displacement varying with the mesh size is given in Fig. 59. For the smaller meshes the convergence is not monotonic, but this is probably

due to load lumping, and from the 4 x 4 mesh onwards to 10 x 10 the convergence is smoothly monotonic. The results generally appear to be consistent and plausible. Bending displacements of the loaded face dominate the dome behaviour. The in plane displacements are very much smaller typically only a tenth of the bending displacement. Also the carry over of bending effects to adjacent panels seems from Fig. 53 to be relatively small. The effect of a plate fold on bending is very similar to that of a spring support in a continuous beam. The downward deflection of one face under load is matched by a much smaller upward deflection of adjacent faces.

7.2 Square pyramid results

These results are shown in Figs. 60 to 72. The horizontal displacements in Figs. 60 and 61 display the symmetries that are expected for the cases with the same load on each face or with just one loaded face. Again Figs. 62 to 65 show the normal displacements of individual faces for the two load cases. These figures also show experimental results. The agreement between theory and experiment is quite good. The differences are systematic as though the shear stiffnesses were slightly wrong. The normal displacements over the square pyramid with a point load on one face are shown in Fig. 66. The effect of continuity over the plate fold noted in the tetrahedral dome is seen again. The few strain gauge readings have been used to calculate stresses. The agreement of the moments m_{11} and m_{22} with theory is excellent (Figs. 67 and 68). The agreement is much better than that seen in the plate bending experiments, and it corresponds to a change to a better strain gauge adhesive in the experiments. The representation of the direct stresses n_{11} and n_{22} is clumsy because of the nature of the

finite element. Since the plane stress component of the finite element is constant any stress representation obtained from it must be discontinuous.

7.3 Hexagonal dome results

The hexagonal dome results are shown in Figs. 73 to 79. No stresses are plotted since no experimental strain measurements were made. Figs. 73 and 74 show the horizontal displacements of the dome for the two load cases of one face loaded and all faces loaded. The normal displacements over half the dome with one face loaded are shown in Fig. 75. They are more complicated than the corresponding displacements for the tetrahedron and the square pyramid. The deflected profiles in Figs. 76 to 79 show a very good agreement between theory and experiment particularly for the case of one face loaded. In these results and those of the tetrahedral domes and the square pyramid the excess of the experimental deflections over theoretical ones may be due to the panel joints not being rigid.

7.4 Benjamin Barrel Vault results

Benjamin analysed his barrel vault as an arch using a weighted mean of the second moment of area of the changing section which the folded plates form. His approximate centroidal line is shown in all the Figs.80 to 85. His experimental and theoretical deflections agree very well. Unfortunately Benjamin does not say exactly where on the structure he measured the deflections. He also refers to the displacements shown in Figs. 80 to 85 variously as displacements and vertical displacements. It is not clear whether the horizontal displacement component is included or not.

The first attempt at finite element analysis used 81 elements and each face of an "arch rib" was divided into 9 elements. The deflections were much smaller than those found by Benjamin (Fig. 80). A more intense

investigation was then started. Attention was restricted to the 5 plates of a half arch rib. A 5 x 5 mesh using a total of 125 elements was used (Fig. 82) and when the results from this were not satisfactory 4 x 4 and 6 x 6 meshes (Figs. 81 and 83) were used. Finally an 8 x 8 element mesh comprising 320 elements was used. Of all problems attempted this had the largest number of unknown displacements. Even so the answer does not agree exactly with Benjamin's theory or experiment.

In most of the figures the displacements of the outer fold line of the barrel vault have been plotted as it was thought that this displacement would compare most precisely with Benjamin's centroid displacement. For the 8 x 8 mesh the displacements along the centre line of the arch rib have also been plotted. However these will be affected by the bending and shearing deformation of individual plates which Benjamin neglected in his overall analysis but which are important especially under the load. The study of the convergence (Fig. 86) indicates that the finite element solutions have not converged to the final answer even with a relatively fine mesh. It does however make it possible to put reasonably confident bounds on the final displacement. Benjamin's mathematical model of the vault supposes that it acts as an arch and this seems to work very well. The bending action of the arch is being represented by the in plate action of the finite elements. The constant stress plane stress finite elements are notoriously slow to converge in bending situations, and probably these results are another manifestation of this disadvantage. They also show the importance of ensuring that the finite element solution has converged.

7.5 16 faced dome results

One eighth of the total dome was analysed using a 10 x 10 mesh of 200 elements in all. Only a symmetrical load pattern could be applied.

A study of the convergence was not made. The inner of the two faces was subjected to a 1 N vertical load at the centroid. This corresponds to a 1 N vertical load at each of the inner face centroids in the complete dome. The displacements are shown in various parts of the dome in Figs. 87 to 89. As was noted in the other domes bending effects in the loaded plate appear to dominate the structural behaviour. A fuller discussion of these results and comparison with experiment is to be produced by Mr. Parton.

8. Experimental Work

The tests applied to the materials were orthodox and widely accepted. The results obtained for material properties, and in beam tests were broadly similar to those reported by other testers (3, 11, 34, 42, 49).

8.1 Materials

The following materials were used

for faces	birch marine plywood hardboard aluminium fibreglass
for core	expanded polyurethane expanded polyvinyl chloride

The sizes and properties of these materials are shown in Appendix II. Details of foamed materials are given in (21, 22, 50).

8.2 Testing of Materials

An earlier programme of work by Elliott (34) had established the properties of some of the materials used, and even more helpfully, had bequeathed a number of proven experimental techniques.

Tensile tests were carried out on an "E" type tensometer, as described by Elliott. Extensions were measured using strain gauges and a Hounsfield Extensometer. Torsional tests on materials were performed on a Tecmatic torsion testing machine. Elliott's equipment for shear tests, based on the ASTM method (9), was also used. The properties obtained by this testing programme (some due to Elliott) are shown in Appendix II.

8.3 Plate and beam construction

All the plywood/expanded polyurethane plates were glued up using "Mouldrite" UF 232, a urea formaldehyde synthetic resin in the manner described by Elliott. The fibreglass/expanded PVC and the aluminium/expanded PVC plates were supplied ready made. The hardboard/expanded polyurethane plates were made using "purlboard". This is an I.C.I. product, which consists of plates of expanded polyurethane of 1 inch nominal thickness, bonded to hardboard. The thick sandwich plates, 8, were formed by glueing two of these plates together, at the polyurethane side, using mouldrite. The thin sandwich plates, 9, were formed by glueing a sheet of hardboard directly to the exposed polyurethane, again using mouldrite.

The fibreglass/expanded PVC plates were not marked by a distinct core/face boundary. The expanded PVC and fibreglass overlapped, so that it was impossible to define the core thickness and the face thickness. It was not possible therefore to derive the properties of the plate, from those of its components. The reinforcing of the fibreglass was randomly oriented chopped strands.

8.4 Beam Tests

These tests were designed to find the flexural and shearing stiffnesses of the materials as they were to be used in the plates. The values obtained in these tests were compared with those obtained by substituting the elastic properties and dimensions of the plate into equations (2.3.20) and (2.3.24). The tests were of two sorts: three point, and four point bending.

The first was used to determine the shearing stiffness of the beam and the second to determine its bending stiffness. Some tests were carried out as described by Elliott, using two simple roller supports and hangers and weights. Also a 100 kN Denison Universal Testing machine was used. Later a special bending rig was constructed to fit the Tensometer Ltd., "E" type tensometer, and a large number of tests were performed on that. This rig could deal with both the tests mentioned above. Curvatures were measured by a dial gauge reading to .001 mm. Other displacements were measured directly by the tensometer. All the flexural and shearing stiffnesses are shown in Appendix II. The inplane stiffnesses of the plate [in equations (3.1.9)] were derived directly from the earlier elastic properties.

8.5 Plate Tests

All the plates tested were square, with sides of .5m or 1m. Loads were applied at the centre of the plate by means of a hanger. This was a piece of prestressing wire, which was passed through a hole in the centre of each plate, and fixed with a prestressing cone. Deflections under load were measured by means of an array of dial gauges, reading to 0.01 mm, which covered a triangle of 1/8th of the plate area. The whole apparatus is shown in Fig. 36. Tests were performed on all the plates listed except 9. Plates 7 and 8 were 1m square, and the rest were .5m square. The plates were supported at all four corners on point supports, consisting of ball bearings. The plate edges were unstiffened. The compression of the plates over supports was measured by a dial gauge reading to .002 mm . Plates 7 and 9 were also instrumented with a number of strain gauges. The two aluminium plates each had 16 strain gauges fixed to them, and the hardboard plates had

2 strain gauges fixed to them. Fig. 37 shows the location of these gauges. The strain gauges used were Tokyo Sokki Kenyujo RR 200 and RR.5,120 ohm rosette wire gauges, and Tinsley type LSG8/4/CN/E, 120 ohm linear foil gauges. Gauges factors were 2.08 and 2.14 respectively. Loads up to 60 kilogramf were applied to each plate. All the plates behaved linearly, and the deformations were all recovered upon unloading. Plots of typical dial and strain gauge readings under loading, are shown in Figs. 38, 39.

The plate bending results are shown in Figs. 20 to 26. In each case profiles of the deflected shape are shown for $\frac{1}{4}$ of each plate, in metres, under a central load of 1 N. All these tests were repeated several times, and most were performed on more than one specimen. The results were consistent. Those shown are means.

8.6 Dome Testing

Much of the dome testing was performed by Mr. Parton of Durham University as part of this same programme of research. The first tests by Mr. Parton were on a set of 3 externally statically determinate tetrahedral domes, composed of plates 1, 2 and 3, (Fig. 31). Later Mr. Parton went on to test a set of much larger and more complicated domes (Fig. 34). These were again composed of the plywood/expanded polyurethane plates 1, 2 and 3.

A Hexagonal dome, was constructed from plates 9. It was supported on 6 feet, and was thus 3^{o} indeterminate. Three components of horizontal constraint were applied, so that the horizontal reactions were determinate. Provision was made for vertical loading at the centroid of each of the 6 faces, by means of hangers. The dome was instrumented in two different ways. The purpose of the first set of tests was to establish whether the

dome behaved linearly and elastically. Dial gauges were placed as shown in Fig. 40. In the second set of tests, largely as a result of the first set, attention was directed towards the behaviour of an individual panel, and dial gauges were positioned as shown in Fig.41.

A "square" dome with 4 faces was constructed from sections of aluminium plate 7. The dome had a base of .85m, and a central rise of .26m. This gave a base to rise ratio of roughly π . Again the supports were arranged so that horizontal reactions would be determinate. The vertical reactions were 1^{o} indeterminate. The instrumentation was again by dial gauges, and this time, in addition, strain gauges were used. Loads were applied vertically at the centroid of each face.

9. Conclusions

The sandwich plate bending finite element results are convincing. The plane stress component of the dome element is well tried and reliable. The finite element results for the square pyramid and the hexagonal dome compare well with experimental results. The finite element results for the tetrahedral domes and the 16-faced dome appear reasonable. Those for the Benjamin barrel vault are not the same as the experimental and simple theoretical ones. The claim that a finer mesh of elements would give a closer agreement is justifiable. The triangular sandwich dome element has proved fairly successful in these applications. The barrel vault behaviour is dominated by the arch bending action. This is represented by the plane stress action of the element. The slow convergence leads to two conclusions. First the bending part of the element is probably "wasted" away from the load. Again in this and in many other folded plate structures the in plane bending is important and it would probably be better to use an element which could represent this exactly. For instance a quadratic variation of the in plane displacements and therefore a linear stress distribution would probably be more accurate. It would represent exactly simple bending but at the expense of 6 extra degrees of freedom per element. The more general case raised by this sort of structure seems to be this. Close to the places where the loads are applied the plate bending effect is dominant. Well away, perhaps two folds away, only the in plane effect is really important. It might therefore be advantageous to use different kinds of elements, which concentrated on bending or on the in plane action. Far from the loading it might be feasible to delete the bending action entirely. Presumably the usual criterion of convergence with finer

meshes could be used to test this hypothesis in action. Even with large and powerful computers the size of 3 dimensional problems like these domes is formidable and any saving obtained by a grading of element type which matched element function to the behaviour of the structure would be worthwhile. This would of course require more judgement and understanding of the structure on the part of the user.

Some itemised ideas for a new element are proffered in the light of experience. Most are not original but they do not appear to have been applied previously to the present type of structure.

1. Use numerical integration and lagrange interpolation for shape functions. This has the advantage of simplicity and leads to an open ended family of elements.

2. For nodal displacements choose the three displacements and the two face rotations. This is the best set for application of boundary conditions and inter element continuity.

3. For interpolation use the two shear angles. This ensures that as the shear stiffness increases the behaviour tends towards classical plate theory and the equations do not become poorly conditioned. [This difficulty was reported by Ahmad, Irons and Zienkiewicz (6) and Sander (73)].

4. Have the element basically rectangular in form, with facilities for different orders of shape function in the two directions and with a parametric representation to accommodate curved and irregular boundaries.

A study of the results from the elements shows that generally they are of little use unless accompanied by some indication of their accuracy. Either bounds put on the results by anotber method as done by Sander (73) or some convergence study are needed. To paraphrase

Lord Hewart; the correct answer should not only be found, but should be manifestly and undoubtedly be seen to be found.

The system of using a family of similar elements affords a potentially cheap method of investigating convergence. The same mesh can be used with various order elements and convergence with higher order element instead of finer mesh should occur. This could be useful in irregular problems when mesh generation routines are not feasible and data preparation devours time and money.

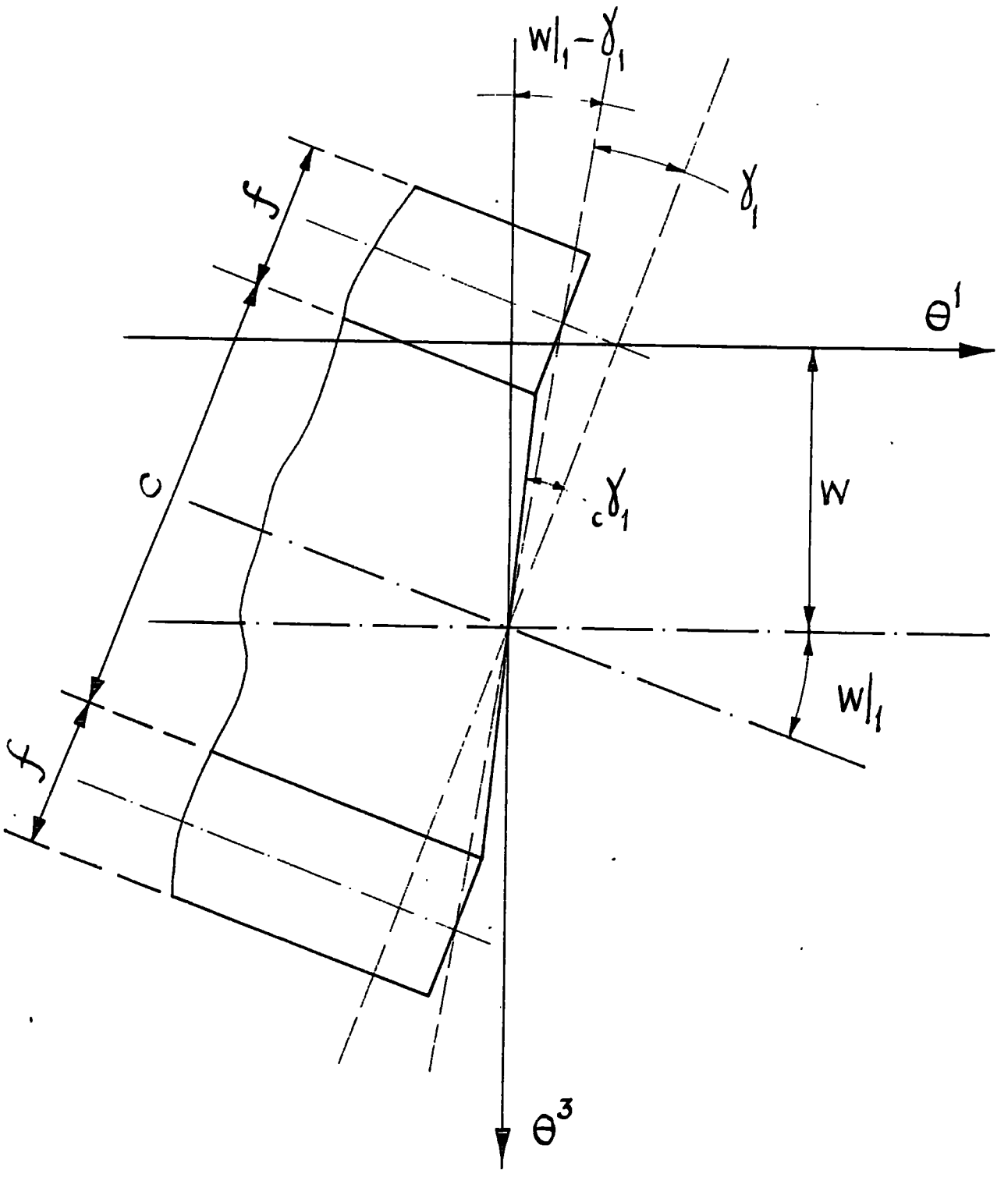

FIG. 1 SANDWICH PLATE KINEMATICS

x^i global and local oblique coordinates

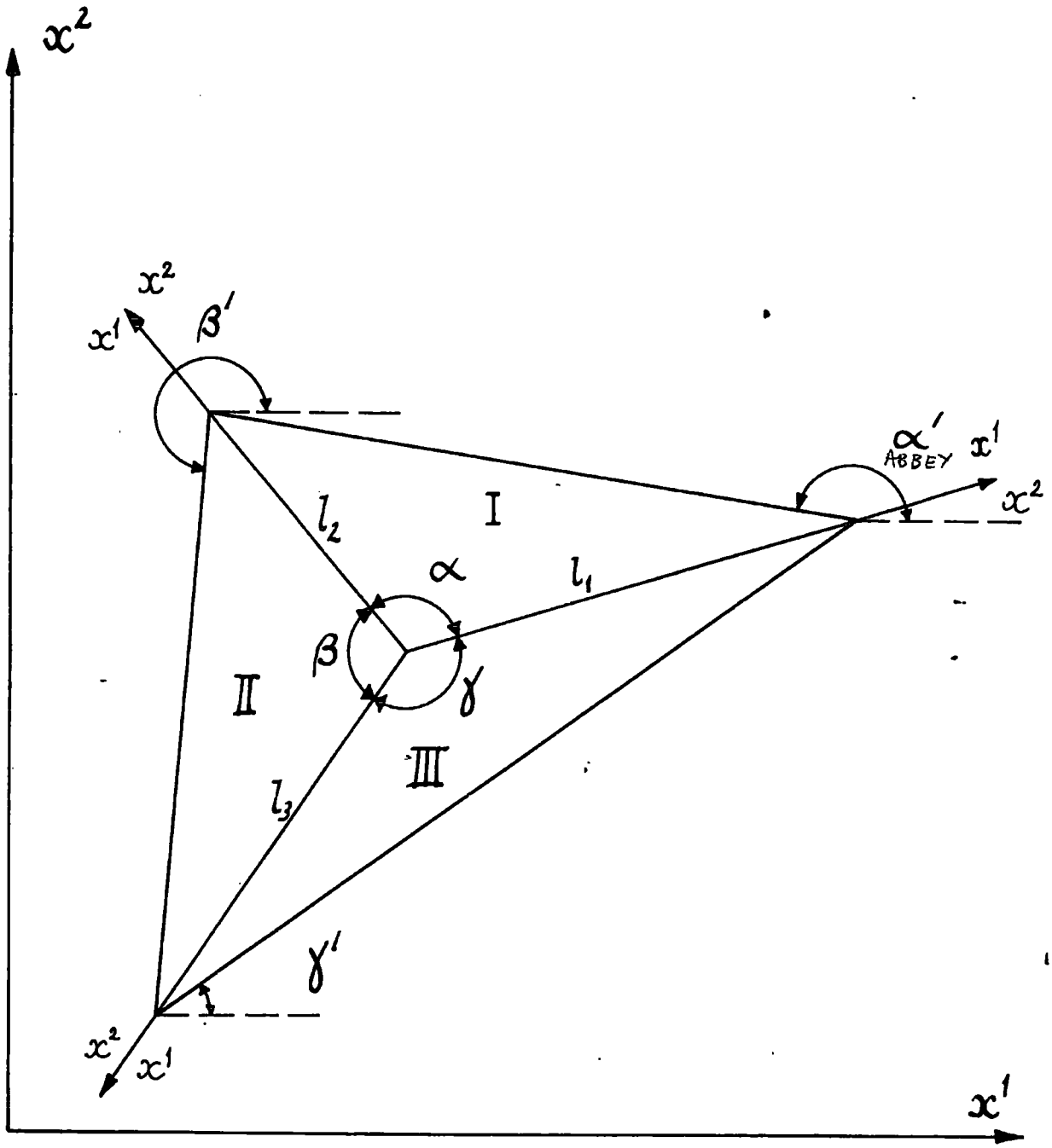

FIG. 2 TRIANGULAR ELEMENT GEOMETRY

FIG. 3 COMPONENT MATRICES

TRIANGULAR PLATE BENDING ELEMENT

A

0	$-l_2^2 l_1$	0	0	$l_2^2 l_1$	0	0	0	0	$l_1 l_2^2$	$-l_1 l_2^2$	0	0
0	0	$-l_1 l_2^2$	0	0	$l_1 l_2^2$	0	0	0	$\frac{1}{2} l_1^2 l_2$	0	$-\frac{1}{2} l_1^2 l_2$	0
0	0	$-l_1^2 l_2$	0	0	$l_1^2 l_2$	0	0	0	$\frac{1}{2} l_1^2 l_2$	0	$-\frac{1}{2} l_1^2 l_2$	0
0	l_1^3	$-2 l_1^2 l_2$	$-6 l_1^2$	l_1^3	$-2 l_1^2 l_2$	$6 l_1^2$	0	$-2 l_1^2 l_2$	$4 l_1^3$	0	0	$-l_1^2 l_2$
0	0	0	0	0	0	0	0	0	0	$\frac{l_1^2 l_2}{2}$	0	0
0	0	0	0	0	0	0	0	0	0	0	$\frac{l_1^2 l_2}{2}$	0

B

0	$-2 l_1 l_2^2$	l_2^3	0	$-l_2^2 l_1$	$-l_2^3$	0	$-l_2^2 l_1$	0	$4 l_1 l_2^2$	$l_1 l_2^2$	$-l_1 l_2^2$	0
0	$-l_1^2 l_2$	0	0	0	0	0	$l_1^2 l_2$	0	0	$\frac{1}{2} l_1^2 l_2$	0	$-\frac{1}{2} l_1^2 l_2$	0
0	$-l_1^2 l_2$	0	0	0	0	0	$l_1^2 l_2$	0	0	$\frac{1}{2} l_1^2 l_2$	0	$-\frac{1}{2} l_1^2 l_2$	0
0	0	$-l_1^2 l_2$	0	0	0	0	0	$l_1^2 l_2$	0	0	$l_1^2 l_2$	0	$-l_1^2 l_2$
0	0	0	0	0	0	0	0	0	$l_1^2 l_2^2$	0	0	0	0
0	0	0	0	0	0	0	0	0	0	0	0	0	$l_1^2 l_2^2$

C

$6l_2^2$	$l_2^2 l_1$	l_2^3	$-6l_2^2$	$2l_1 l_2^2$	$-l_2^3$	0	$-l_2^2 l_1$	0	$4l_1 l_2^2$	$l_1 l_2^2$	$-l_1 l_2^2$	0	0	0	0
$6l_1 l_2$	$l_1^2 l_2$	$l_1 l_2^2$	$-6l_1 l_2$	$l_1^2 l_2$	$-l_1 l_2^2$	0	0	0	$4l_1^2 l_2$	$\frac{1}{2} l_1^2 l_2$	0	$-\frac{1}{2} l_1^2 l_2$	$\frac{1}{2} l_1 l_2^2$	$-\frac{1}{2} l_1 l_2^2$	0
$6l_1 l_2$	$l_1^2 l_2$	$l_1 l_2^2$	$-6l_1 l_2$	$l_1^2 l_2$	$-l_1 l_2^2$	0	0	0	$4l_1^2 l_2$	$\frac{1}{2} l_1^2 l_2$	0	$-\frac{1}{2} l_1^2 l_2$	$\frac{1}{2} l_1 l_2^2$	$-\frac{1}{2} l_1 l_2^2$	0
$6l_1^2$	l_1^3	$l_1^2 l_2$	$-6l_1^3$	$-l_1^3$	$-2l_1^2 l_2$	0	0	$l_1^2 l_2$	$4l_1^3$	0	0	0	$l_1^2 l_2$	0	$-l_1^2 l_2$
0	0	0	0	0	0	0	0	0	0	$-l_1^2 l_2^2$	$l_1^2 l_2^2$	$l_1^2 l_2^2$	0	0	0
0	0	0	0	0	0	0	0	0	0	0	0	0	$-l_1^2 l_2^2$	$l_1^2 l_2^2$	$l_1^2 l_2^2$

Number	w	$w\|_2 - \gamma_2$	γ_1	description
1	0	0	0	clamped, with edge stiffener
2	1	0	0	axis of symmetry
3	0	1	0	pinned edge with stiffener
4	0	0	1	clamped, no edge stiffener
5	1	1	0	free edge with stiffener
6	1	0	1	axis of symmetry
7	0	1	1	pinned edge without stiffener
8	1	1	1	free

1 free 0 fixed

FIG. 4 PLATE BENDING BOUNDARY CONDITIONS

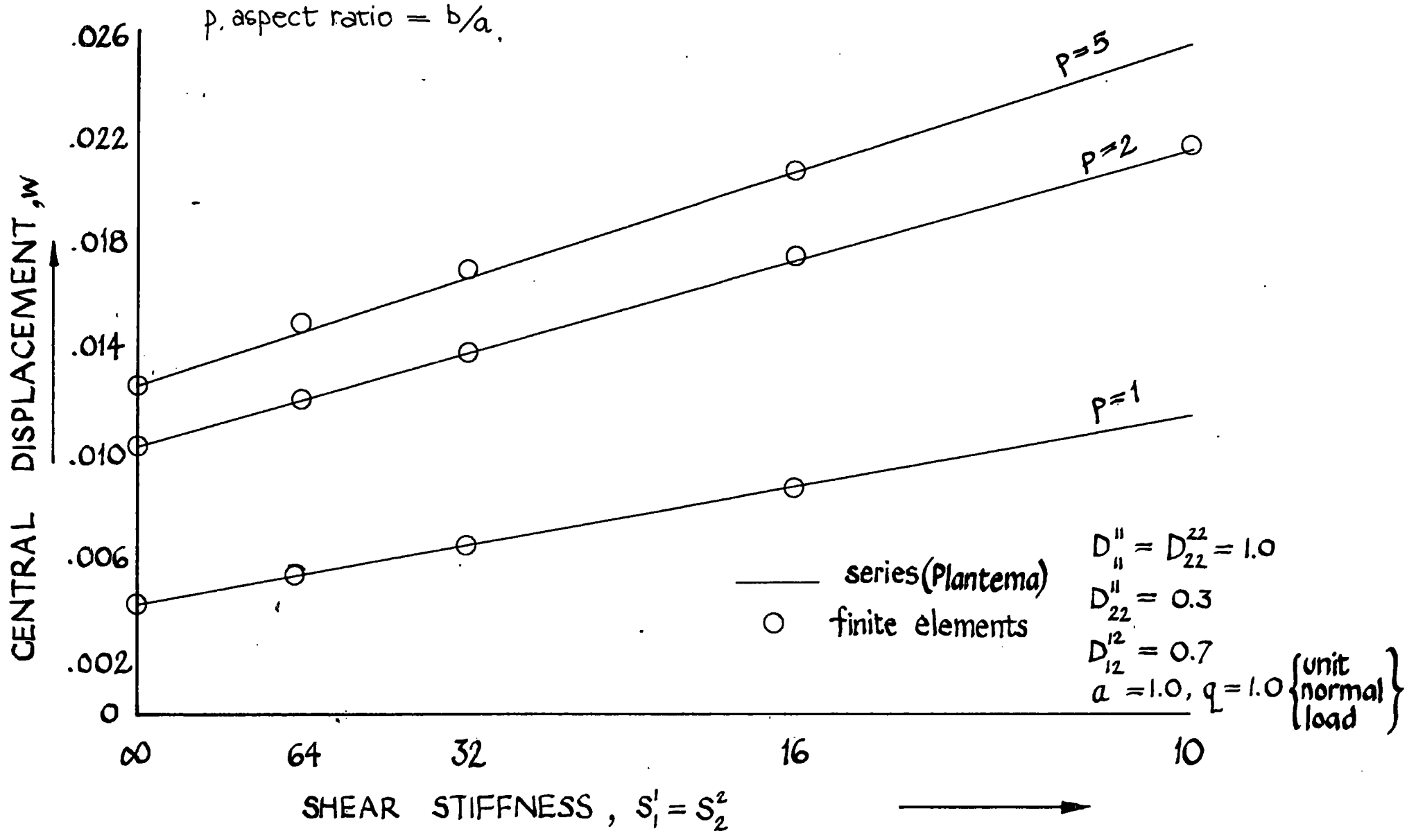

FIG. 5 CENTRAL DEFLECTION AGAINST SHEAR STIFFNESS

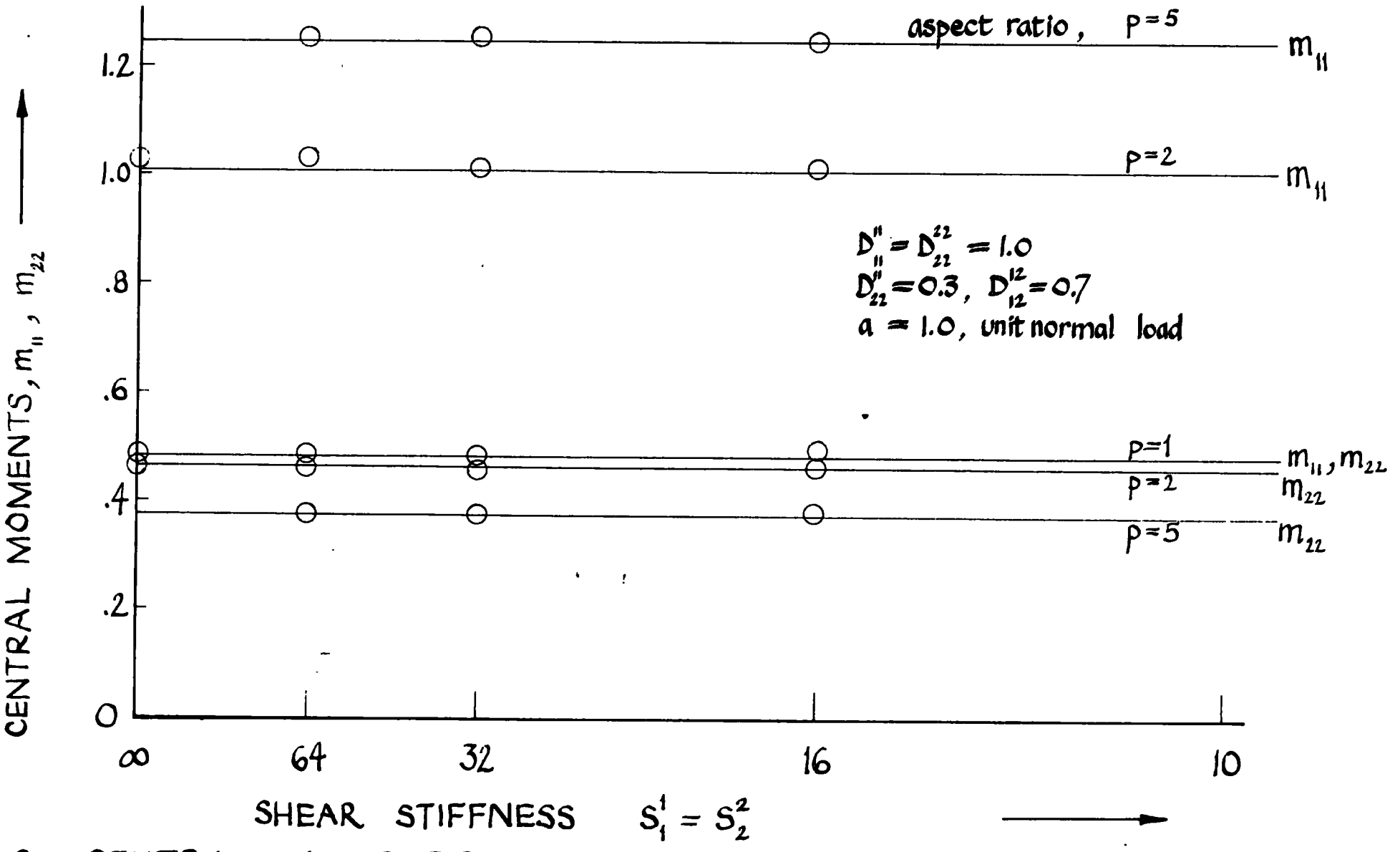

FIG. 6 CENTRAL MOMENTS AGAINST SHEAR STIFFNESS

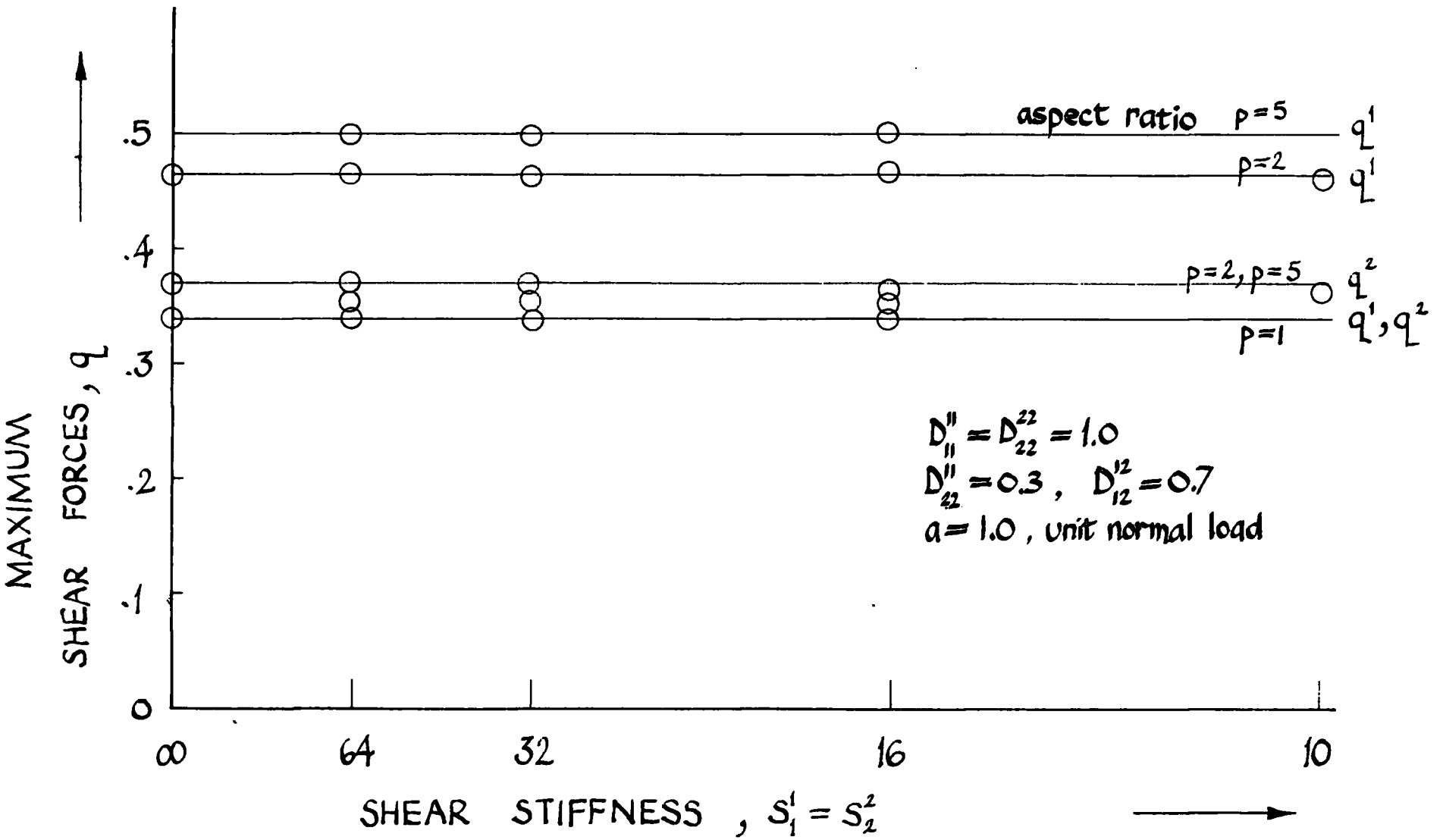

FIG. 7 MAXIMUM SHEAR FORCES AGAINST SHEAR STIFFNESS

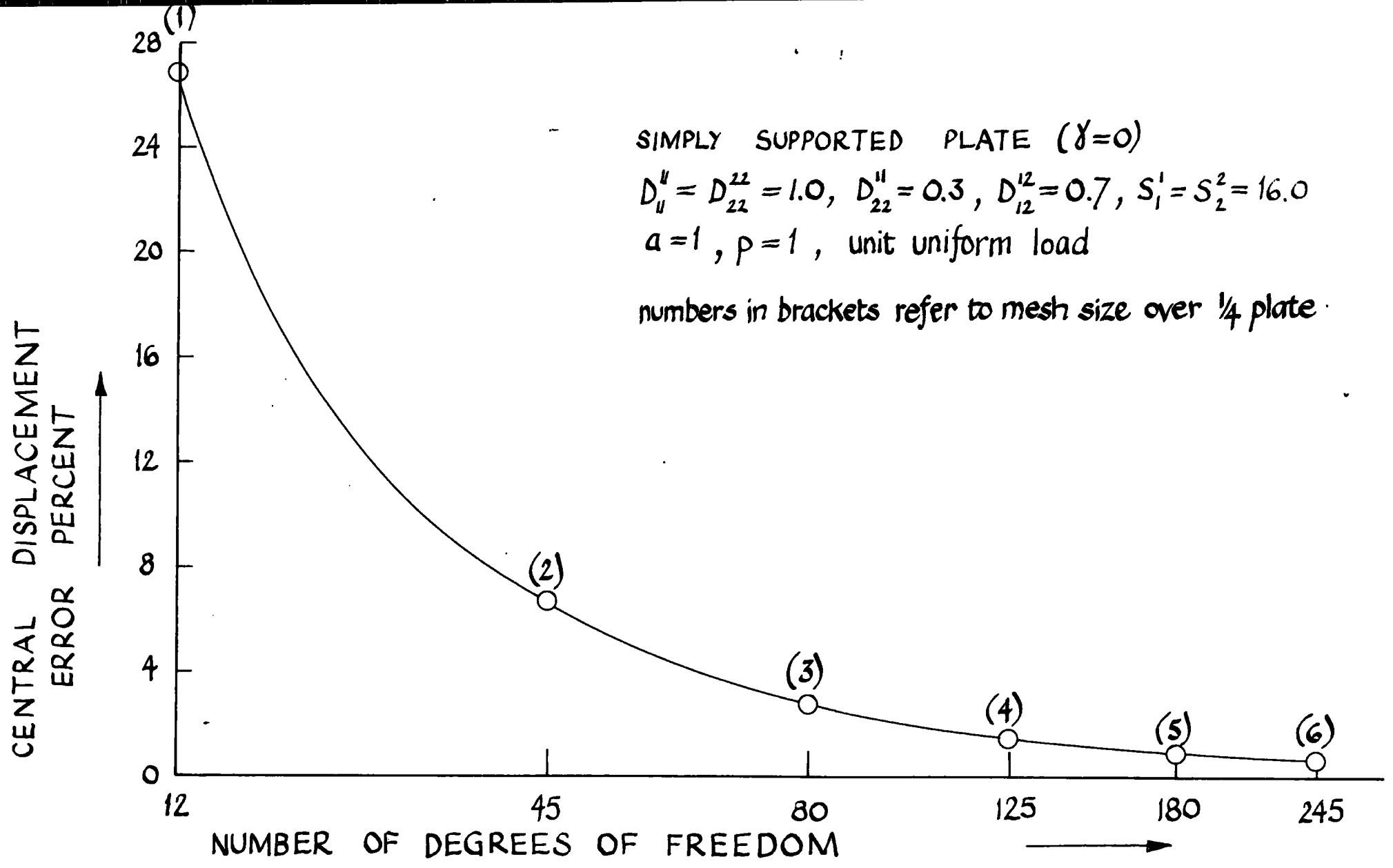

FIG.8 CONVERGENCE TOWARDS SERIES SOLUTION

SIMPLY SUPPORTED SQUARE PLATE UNDER UNIFORM LOAD

$D_{11}^{11} = D_{22}^{22} = 1.0$, $D_{22}^{11} = 0.3$, $D_{12}^{12} = 0.7$, $S_1^1 = S_2^2 = 16.0$, $a = 1.0$.

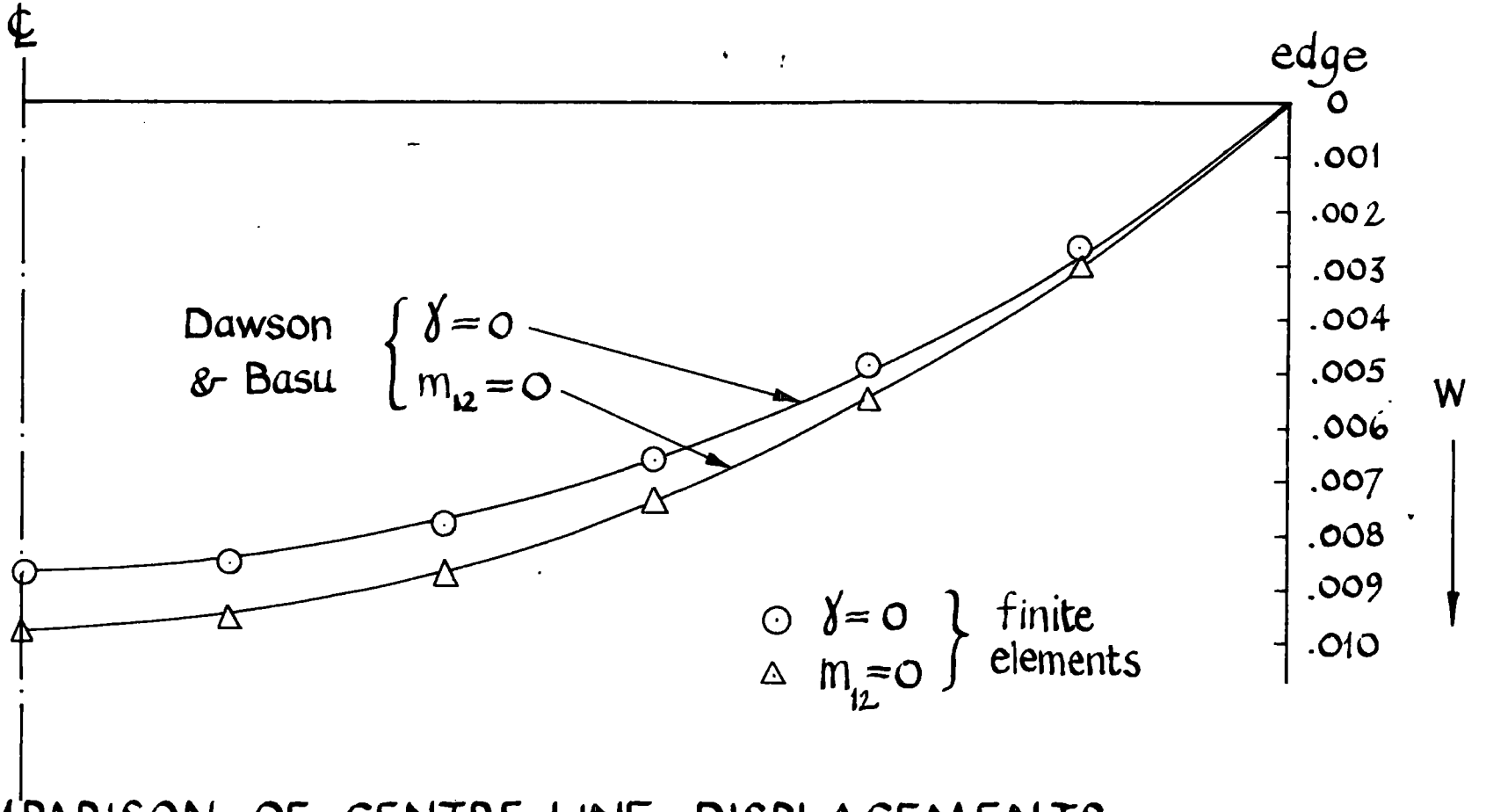

FIG. 9 COMPARISON OF CENTRE LINE DISPLACEMENTS

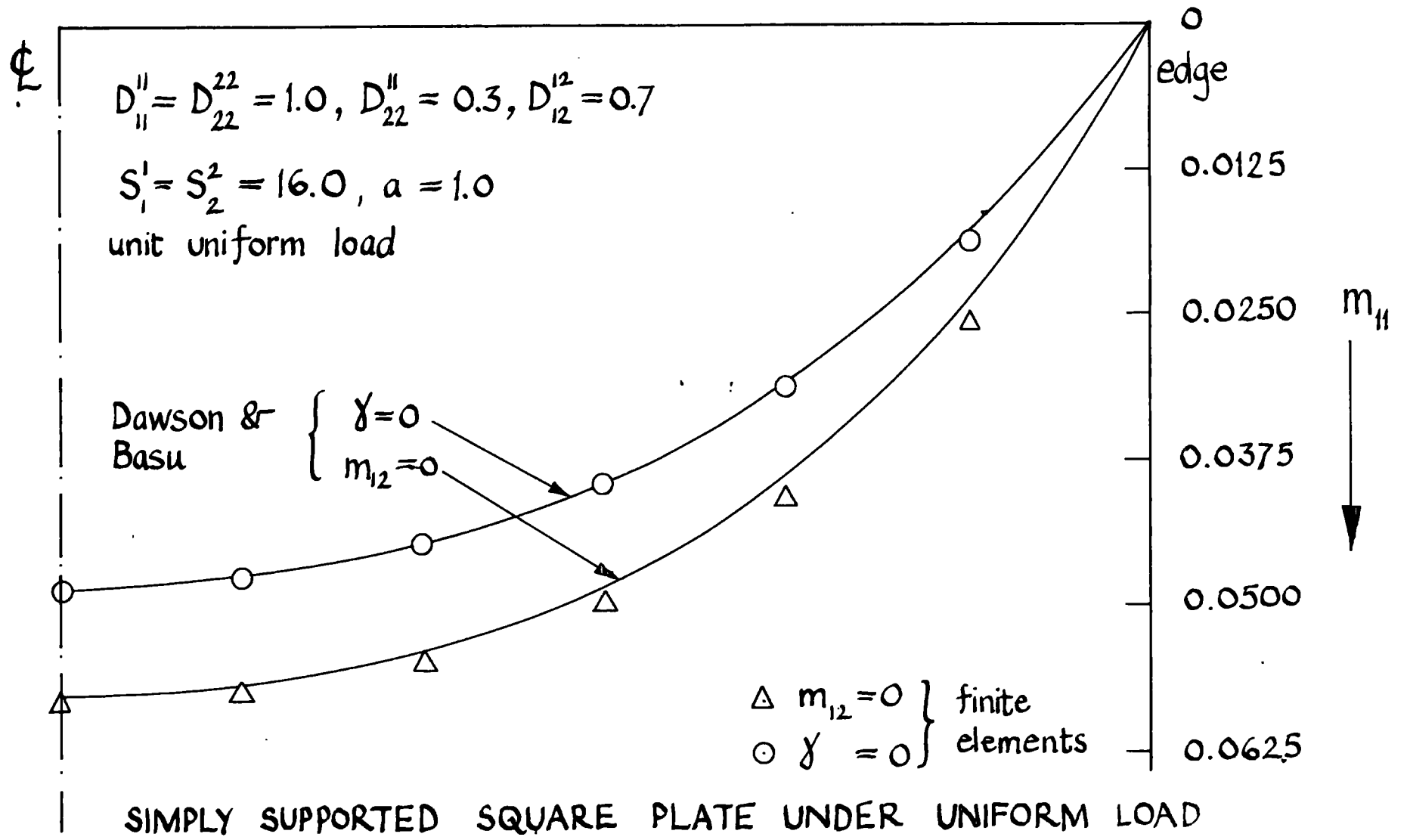

FIG.10 COMPARISON OF CENTRE LINE MOMENTS

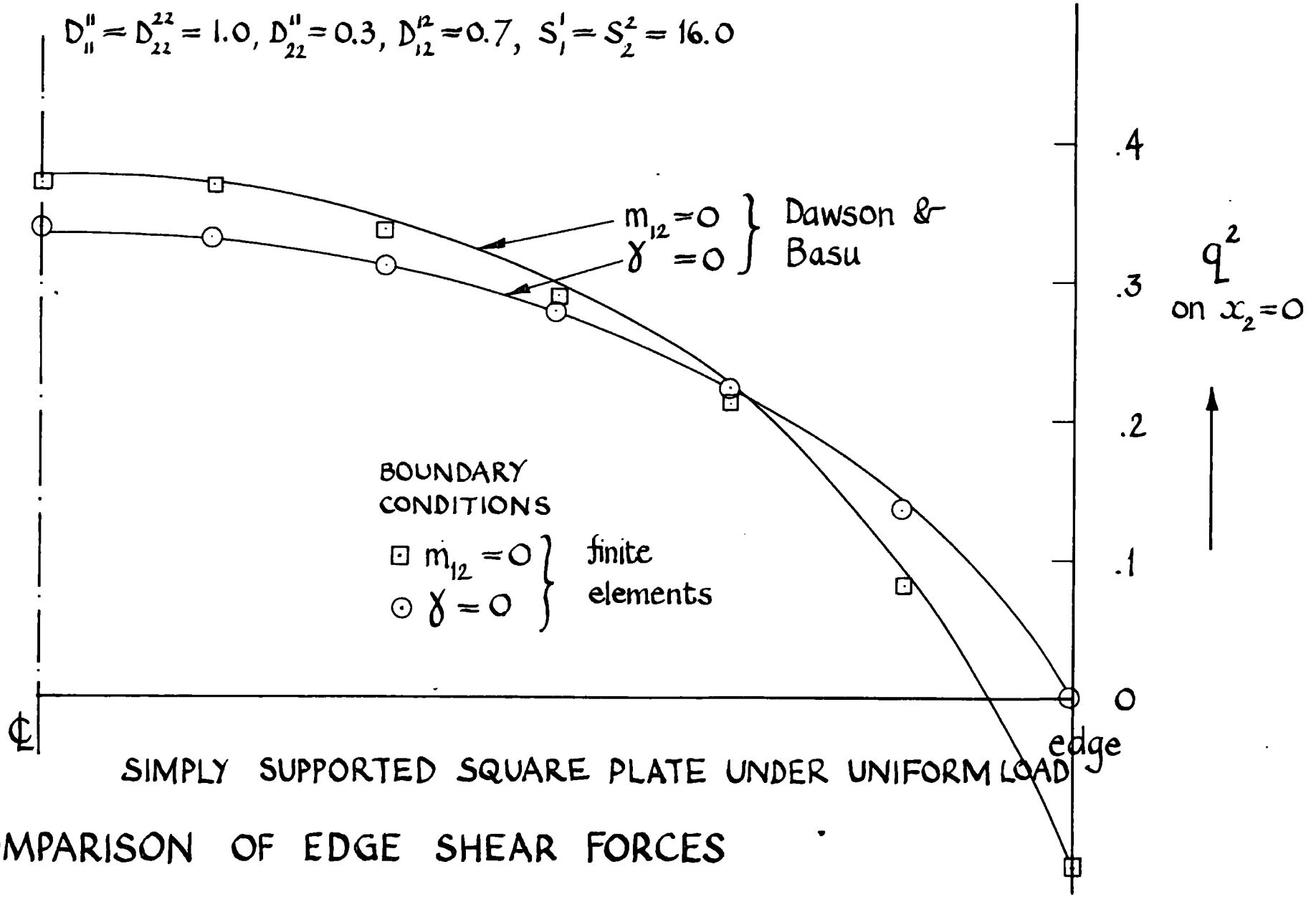

FIG. 11 COMPARISON OF EDGE SHEAR FORCES

CLAMPED SQUARE PLATE UNDER UNIFORM LOAD

Source	dynamic relaxation		finite elements		Lockwood Taylor	Classical Plate
Third b.c.	$m_{12}=0$	$\gamma=0$	$m_{12}=0$	$\gamma=0$	$m_{12}=0$	$S_1^1=S_2^2=\infty$
central deflection w	.00329	.00324	.00331	.00325	.00325	.00126
mid edge moment m_{11}	.0455	.0439	.0459	.0439	.0410	.0513

$D_{11}^{11}=D_{22}^{22}=1.0$, $D_{22}^{11}=0.3$, $D_{12}^{12}=0.7$, $a=1$, $p=1$, $S_1^1=S_2^2=4\pi^2$, unit uniform load.

FIG.12 COMPARISON WITH LOCKWOOD TAYLOR AND DAWSON AND BASU

	$S_1^1 = 2.5\ S_2^2$			$S_1^1 = S_2^2$			$S_1^1 = 0.4\ S_2^2$		
	Raville	D.R.	F.E.	Raville	D.R.	F.E.	Raville	D.R.	F.E.
w (max)	.0147	.0144	.01474	.0209	.0207	.0210	.0325	.0320	.0324
m_{11} (max)	.0842	.0838	.0853	.0713	.0710	.0721	.0473	.0465	.0470
m_{22} (max)	.0375	.0377	.0377	.0502	.0502	.0506	.0745	.0747	.0754
q_1 (max)	.425	.422	.426	.401	.399	.402	.349	.343	.342
q_2 (max)	.302	.304	.305	.358	.353	.354	.434	.431	.432

$D_{11}^{11} = D_{22}^{22} = 1.0$, $D_{22}^{11} = 0.3$, $D_{12}^{12} = 0.7$, $a = 1.0$, $p = 4/3$, $S_2^2 = 2\pi^2/3$, unit uniform load.

SIMPLY SUPPORTED PLATE UNDER UNIFORM LOAD

FIG. 13 COMPARISON WITH RAVILLE AND BASU AND DAWSON

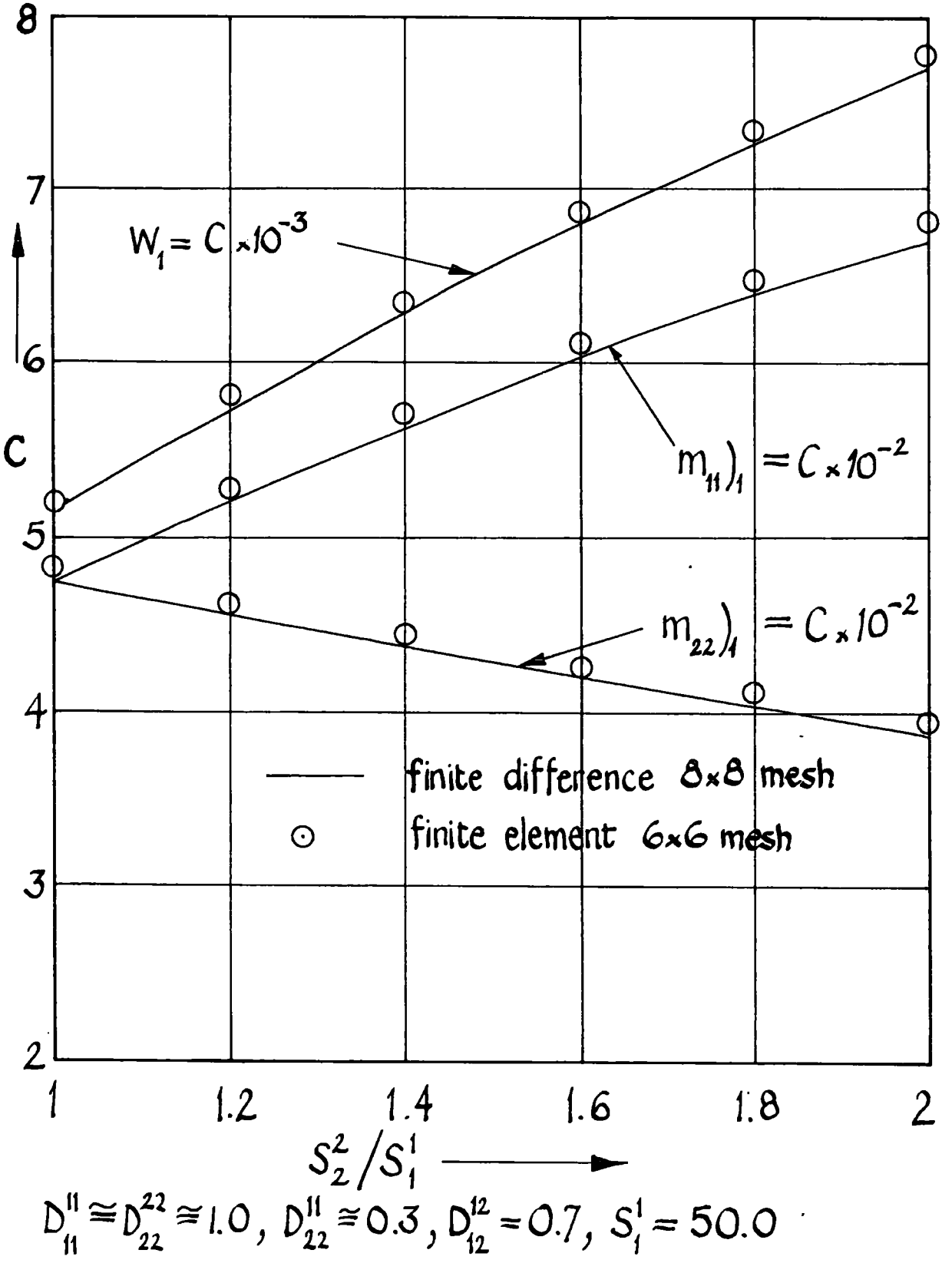

$D_{11}^{11} \cong D_{22}^{22} \cong 1.0$, $D_{22}^{11} \cong 0.3$, $D_{12}^{12} = 0.7$, $S_1^1 = 50.0$

SIMPLY SUPPORTED PLATE, UNIFORM LOAD

FIG. 14 COMPARISON WITH CHAPMAN AND WILLIAMS

CLAMPED PLATE UNDER UNIT UNIFORM LOAD

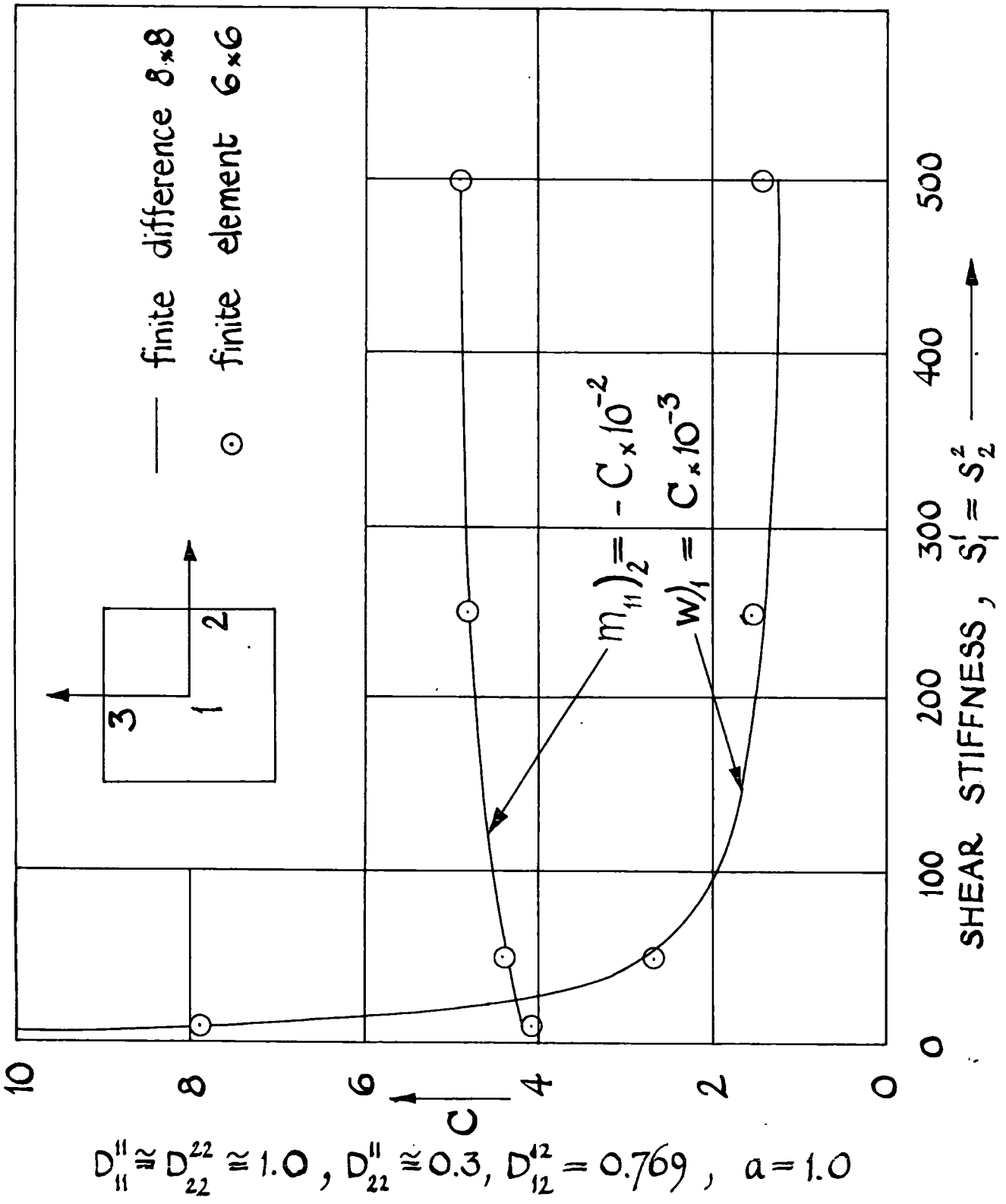

$D_{11}^{11} \cong D_{22}^{22} \cong 1.0$, $D_{22}^{11} \cong 0.3$, $D_{12}^{12} = 0.769$, $a = 1.0$

FIG. 15 COMPARISON WITH CHAPMAN AND WILLIAMS

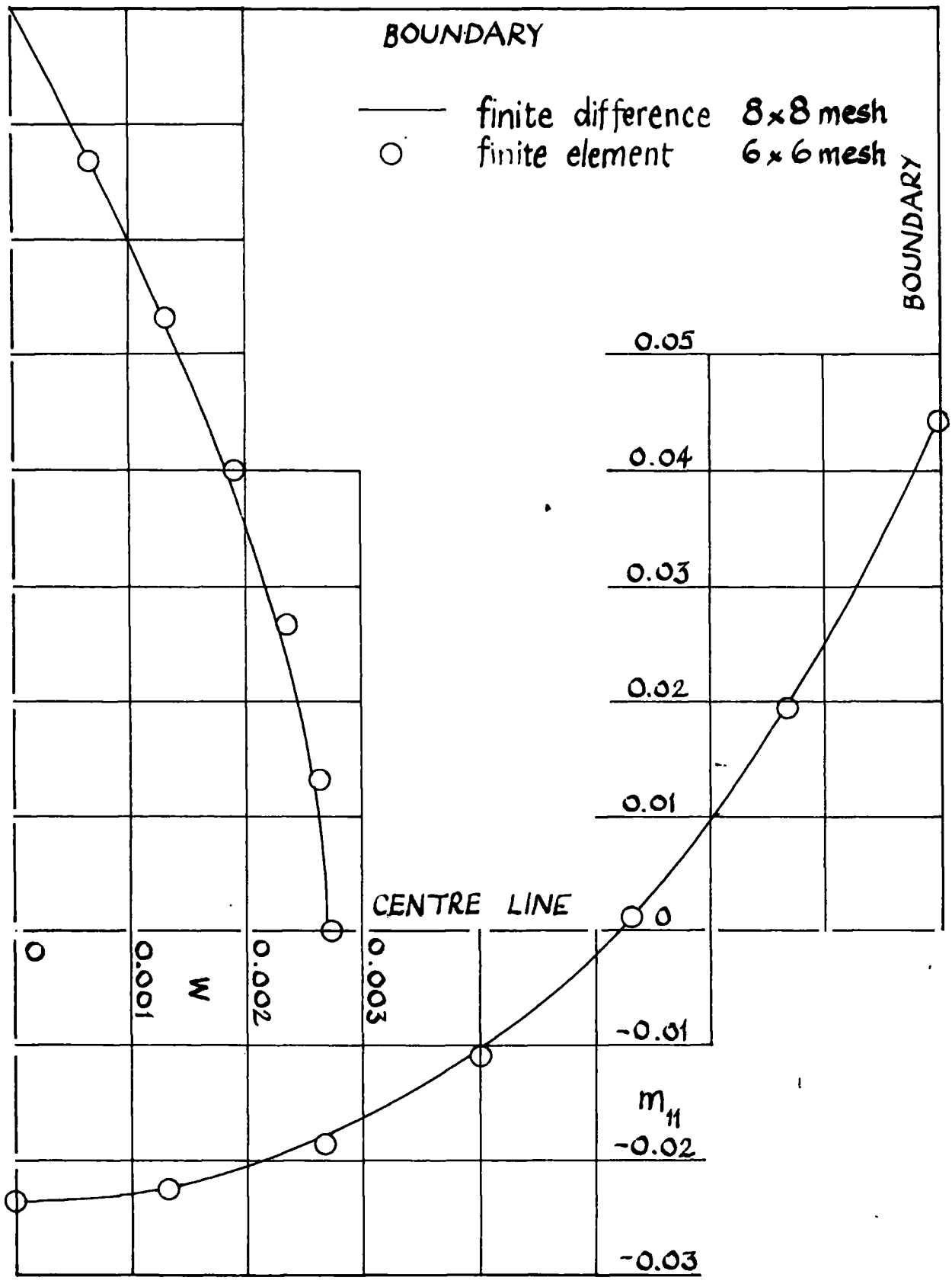

$D_{11}^{11} = D_{22}^{22} = 1.0989$, $D_{22}^{11} = 0.32967$, $D_{12}^{12} = .76852$, $S_1^1 = S_2^2 = 50.0$

CLAMPED PLATE ($\gamma = 0$), UNIT UNIFORM LOAD

FIG. 16 COMPARISON WITH CHAPMAN & WILLIAMS

DISPLACEMENTS OF 1/4 OF A 30° SKEW PLATE UNDER UNIT UNIFORM LOAD

$D_{11}^{11} = D_{22}^{22} = 1.0,\ D_{22}^{11} = 0.3,\ D_{12}^{12} = 0.7,\ S_1^1 = S_2^2 = 218.4.$

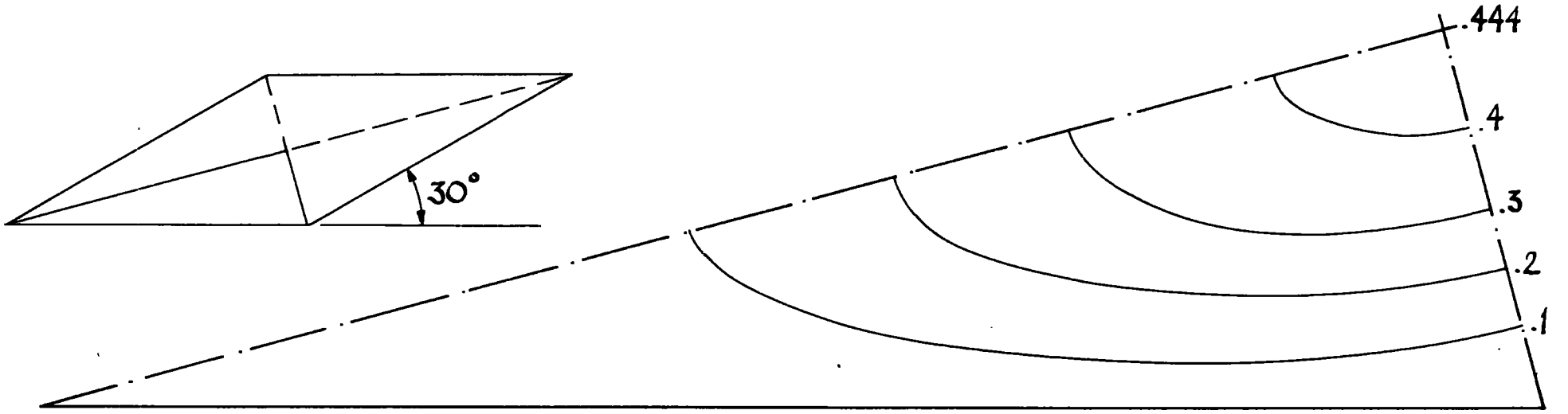

PINNED EDGES, $\gamma = 0$ DISPLACEMENTS $\times 10^3$

FIG. 17 COMPARISON WITH SANDER

PRINCIPAL MOMENTS ON PLATE DIAGONAL

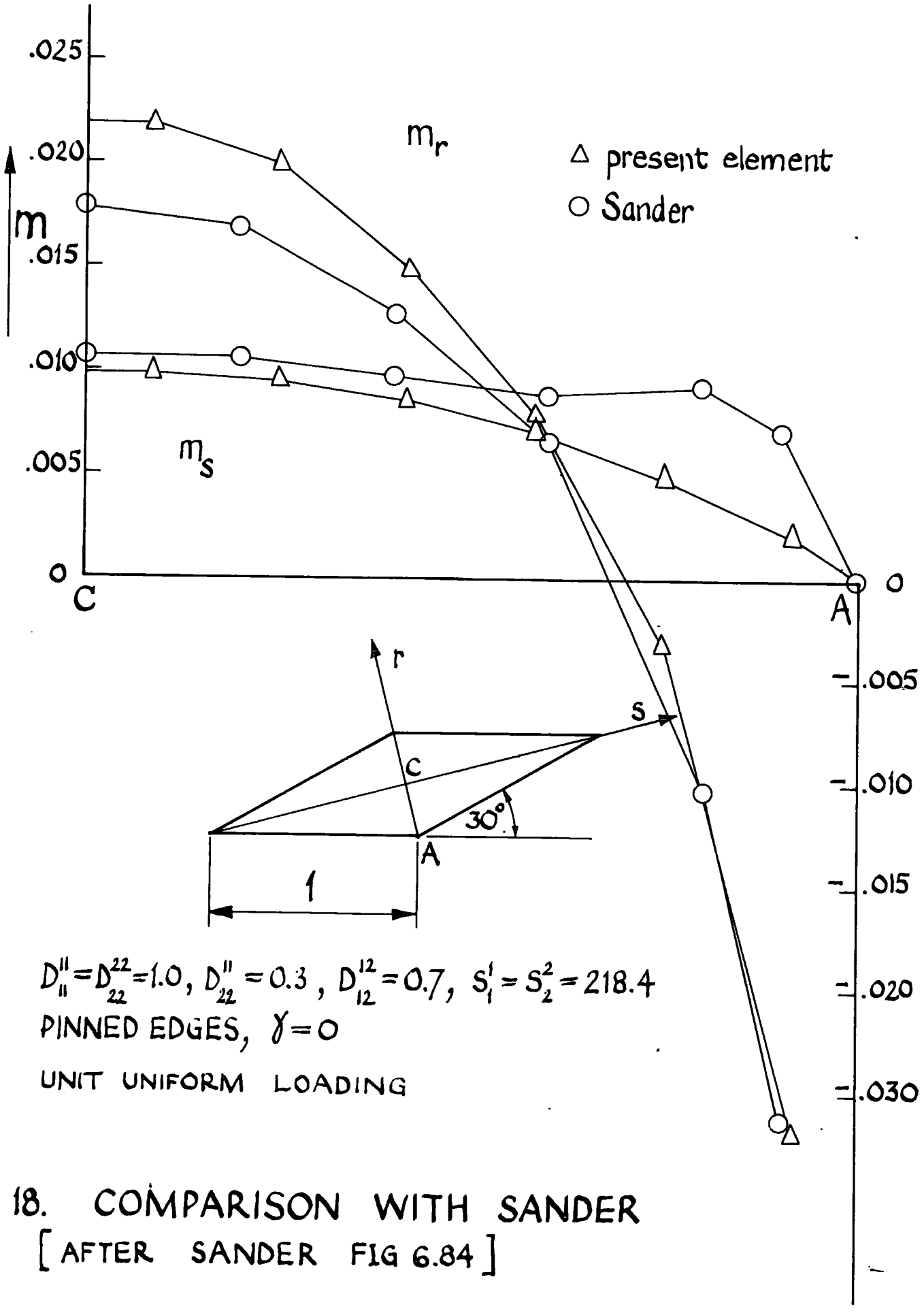

FIG 18. COMPARISON WITH SANDER
[AFTER SANDER FIG 6.84]

SHEARING FORCES ACROSS PLATE BOUNDARY

$D_{11}^{11} = D_{22}^{22} = 1.0,\ D_{22}^{11} = 0.3,\ D_{12}^{12} = 0.7,\ S_1^1 = S_2^2 = 218.4$

PINNED EDGES, $\gamma = 0$

UNIT UNIFORM LOADING

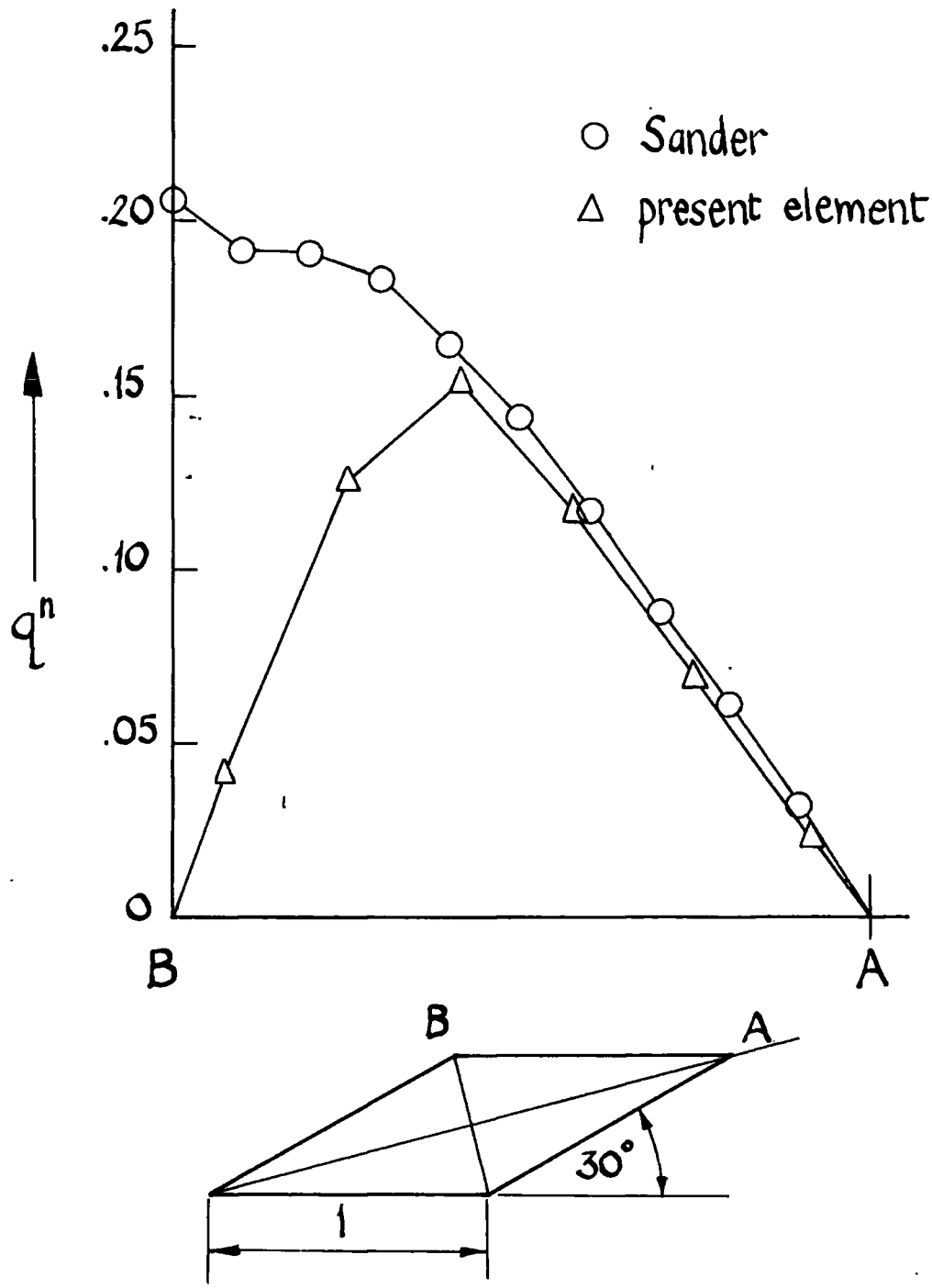

FIG. 19 COMPARISON WITH SANDER

[AFTER SANDER FIG 6.85]

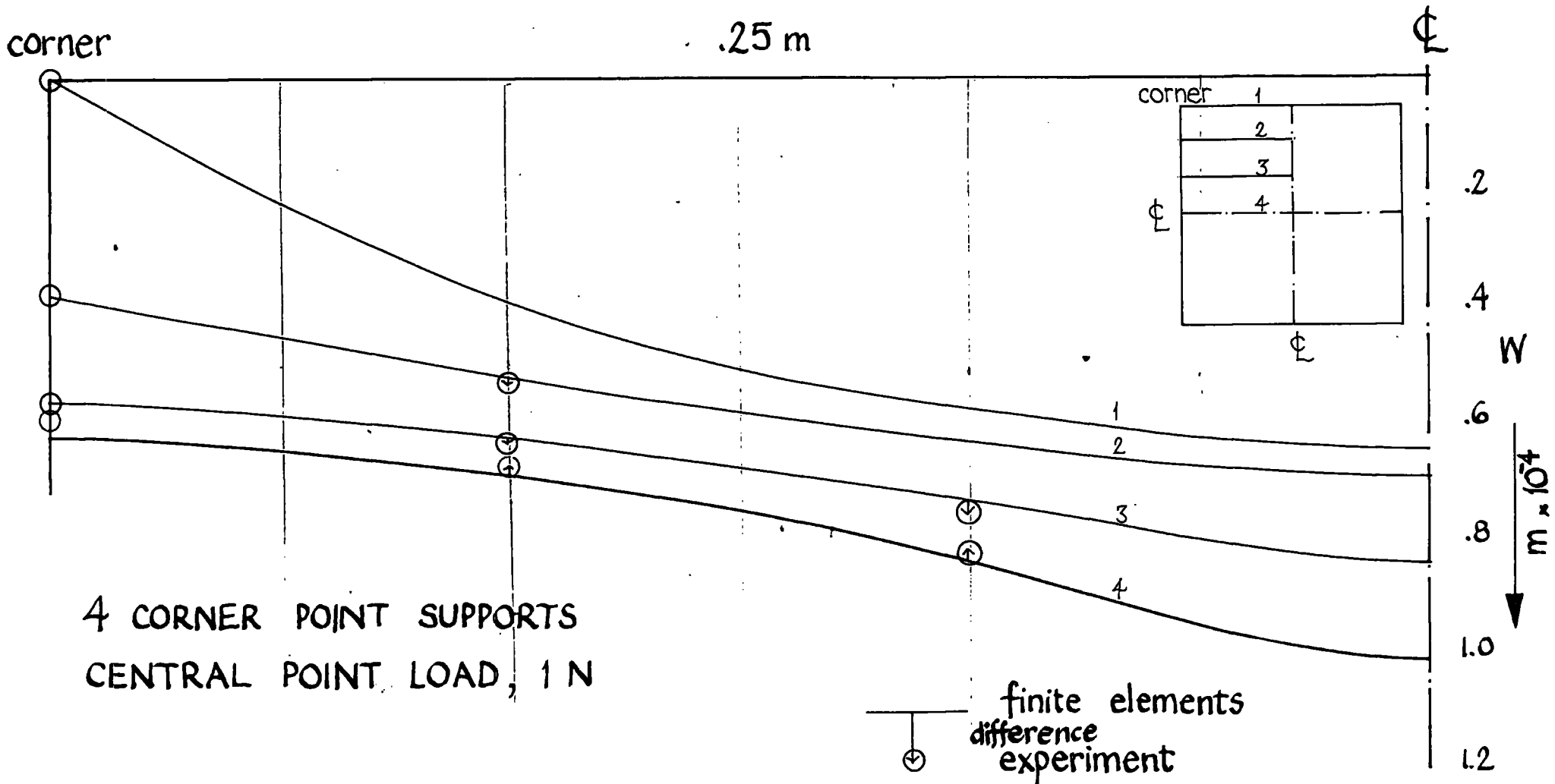

FIG. 20 PLYWOOD PLATE (1), DISPLACEMENTS

$\frac{c}{f} = 15.7$

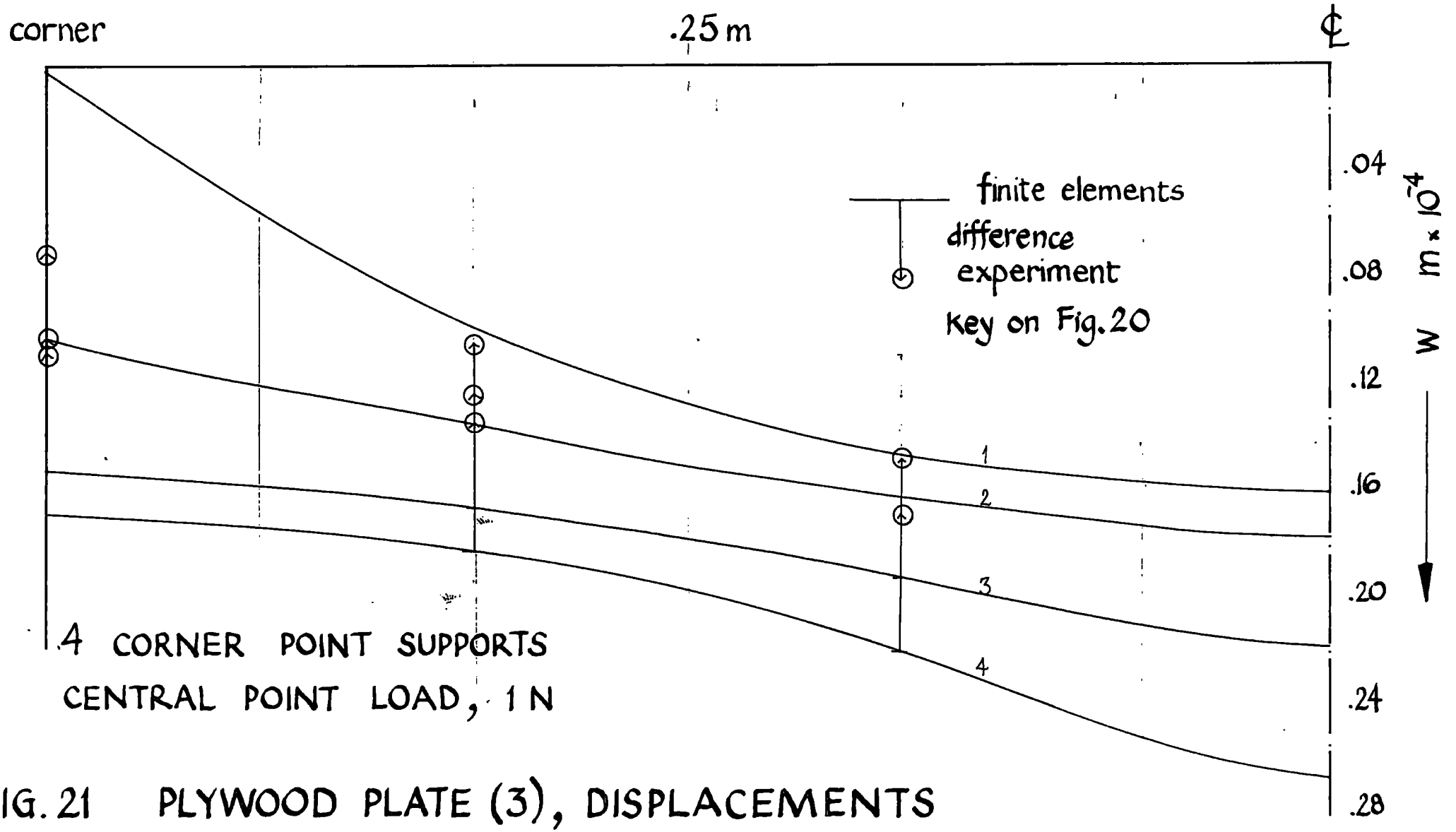

FIG. 21 PLYWOOD PLATE (3), DISPLACEMENTS

$\frac{c}{f} = 7.5$

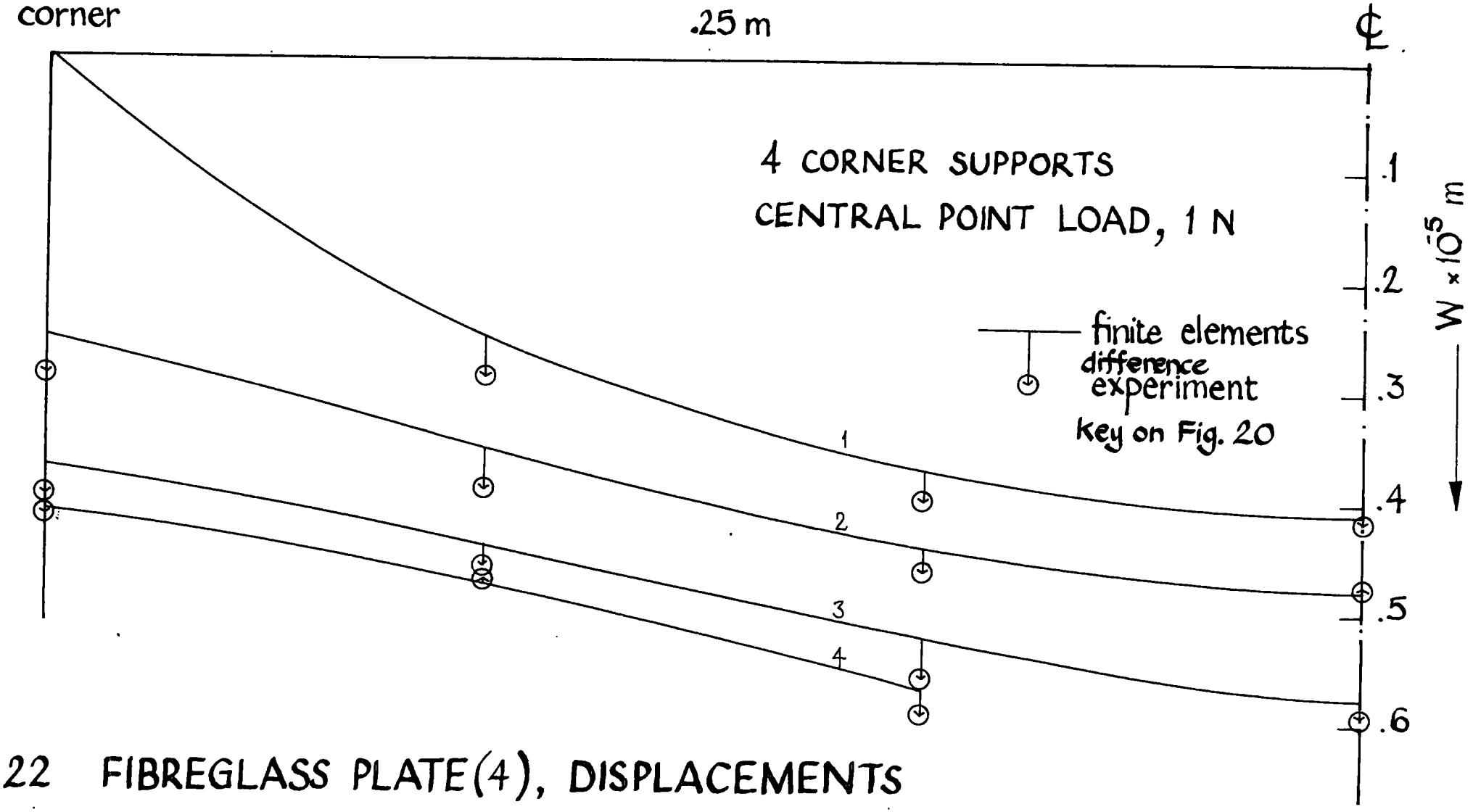

FIG. 22 FIBREGLASS PLATE(4), DISPLACEMENTS

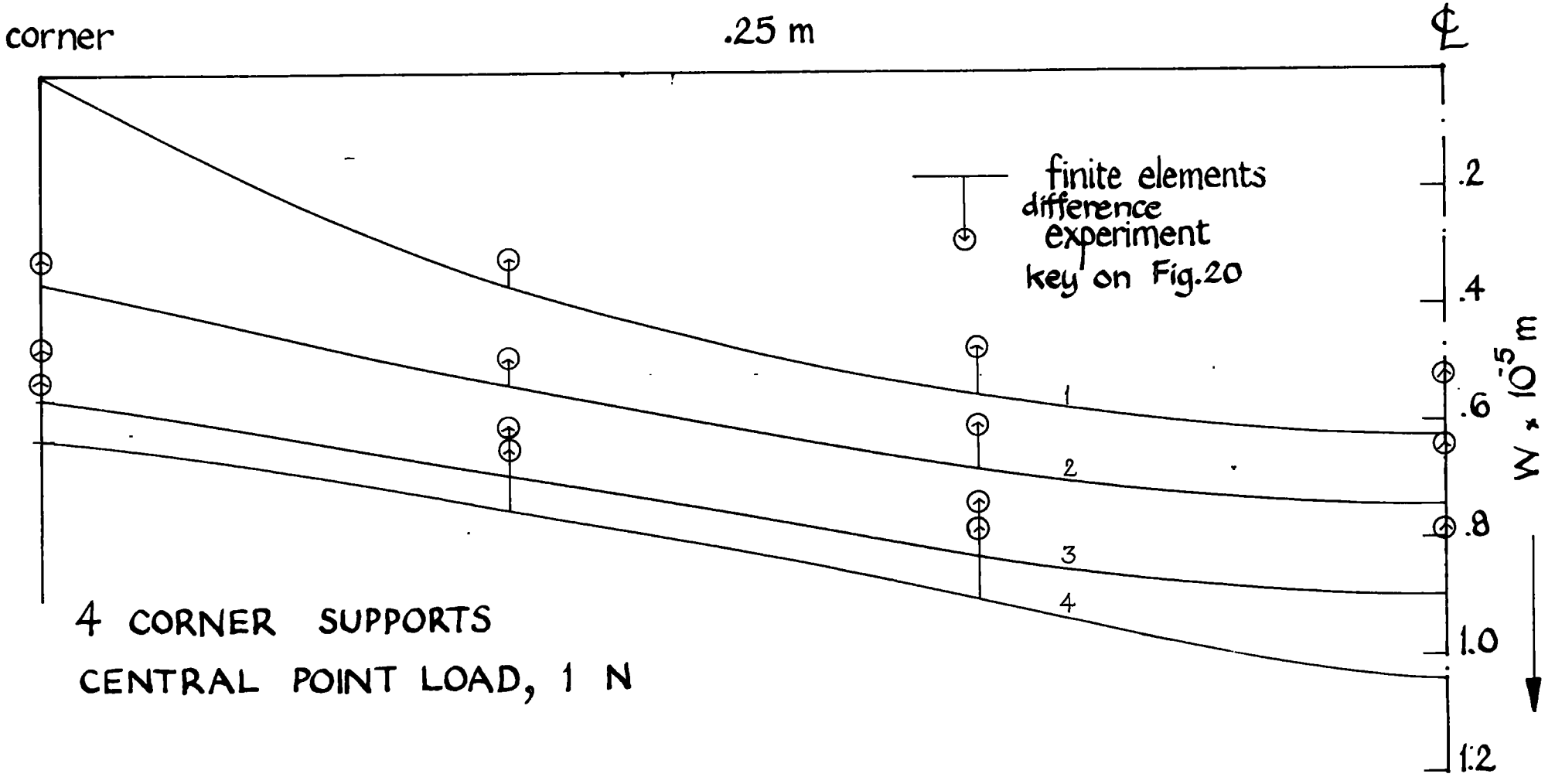

FIG. 23 FIBREGLASS PLATE (5), DISPLACEMENTS

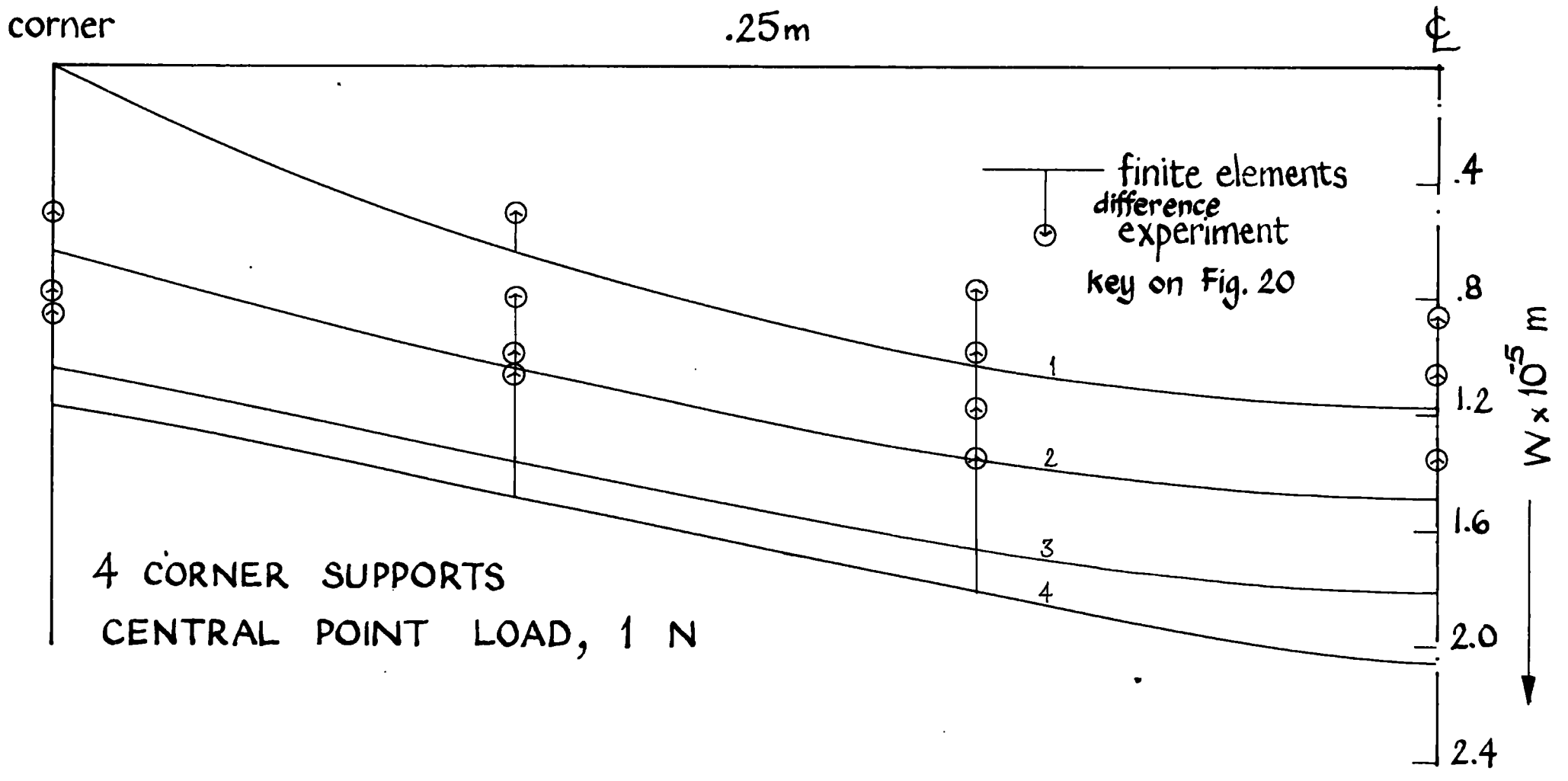

FIG. 24 FIBREGLASS PLATE (6), DISPLACEMENTS

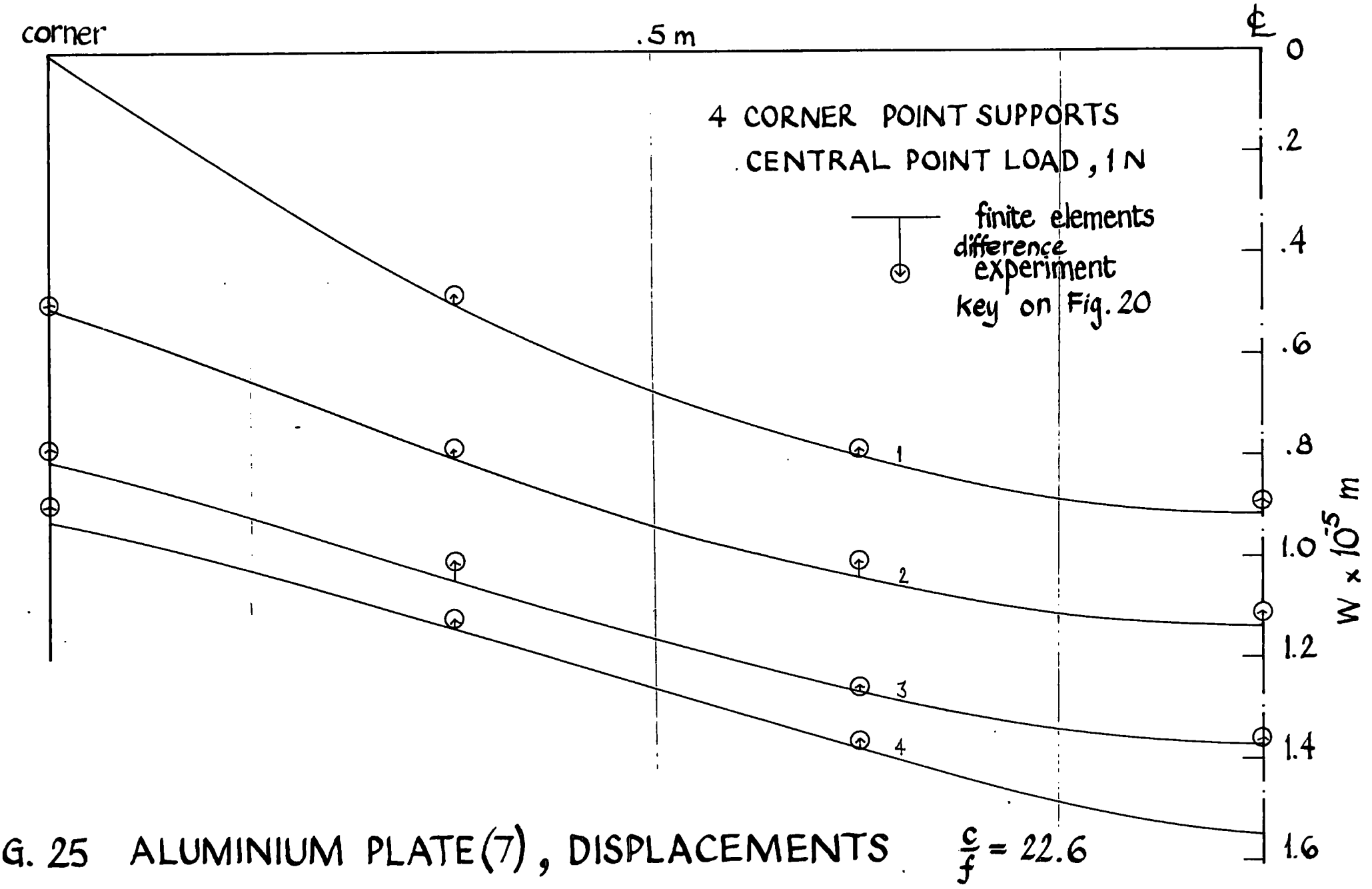

FIG. 25 ALUMINIUM PLATE(7), DISPLACEMENTS $\frac{c}{f} = 22.6$

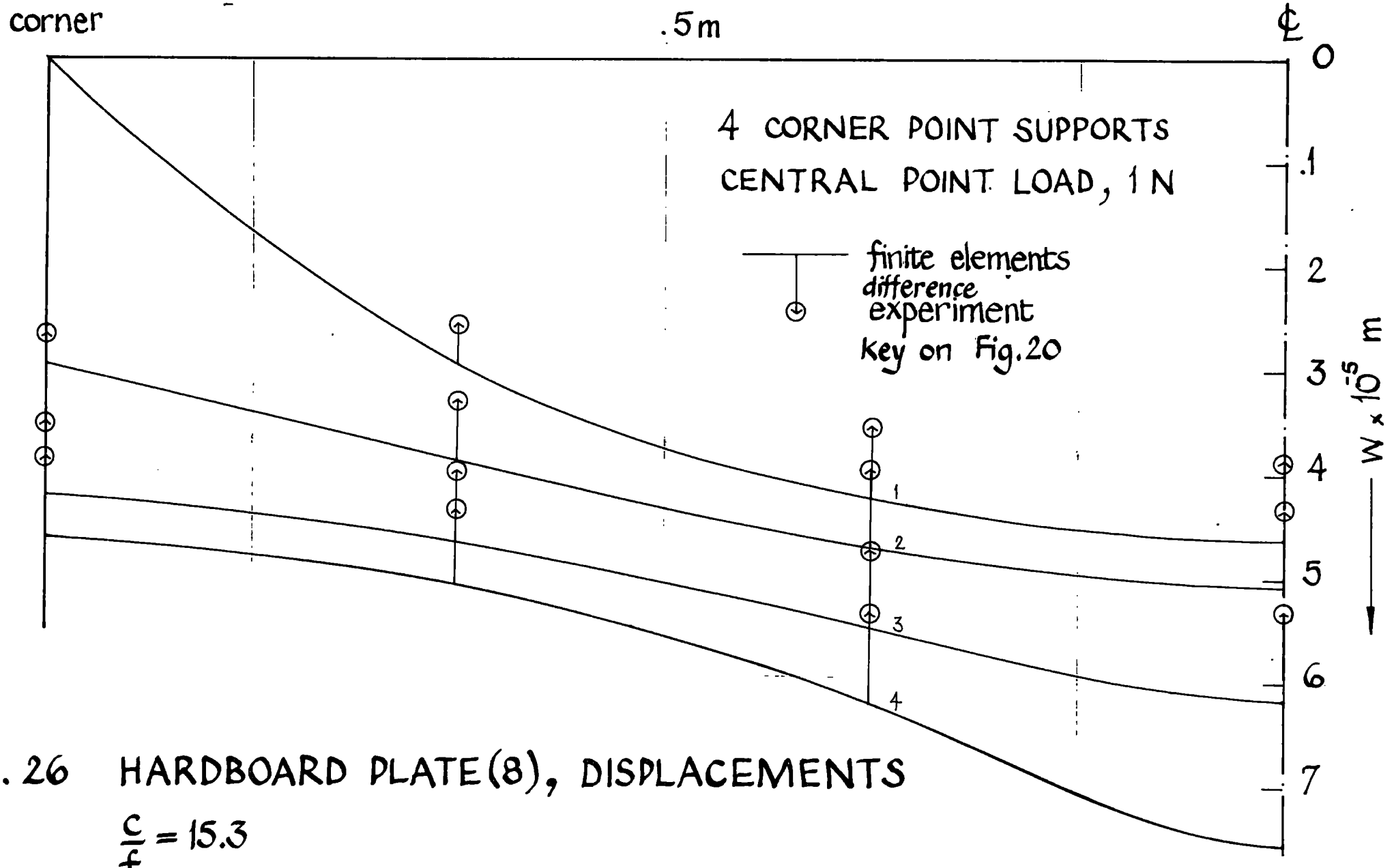

FIG. 26 HARDBOARD PLATE(8), DISPLACEMENTS

$\frac{c}{f} = 15.3$

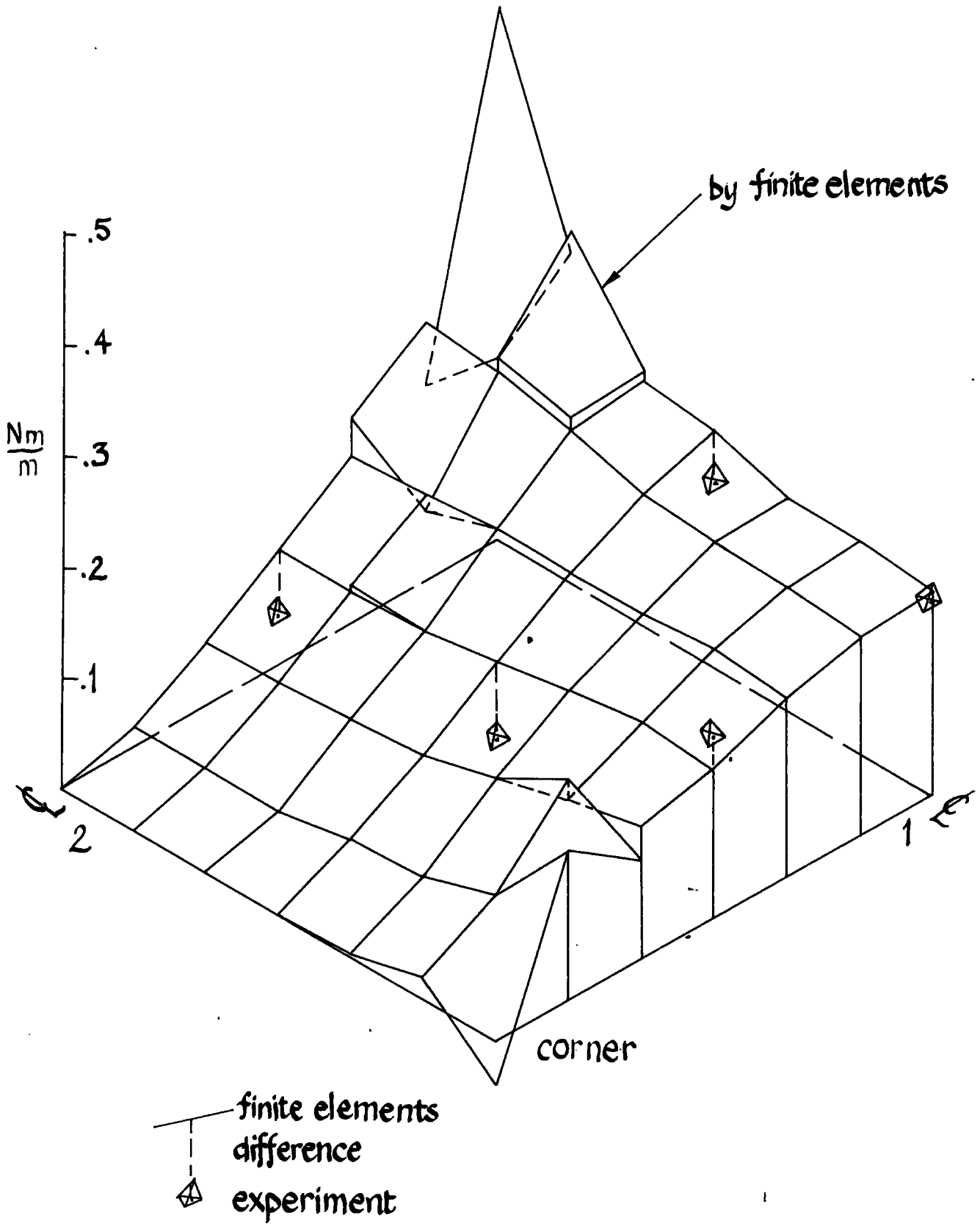

FIG. 27 ALUMINIUM PLATE (7), STRESS COUPLES, m_{11}
by finite elements

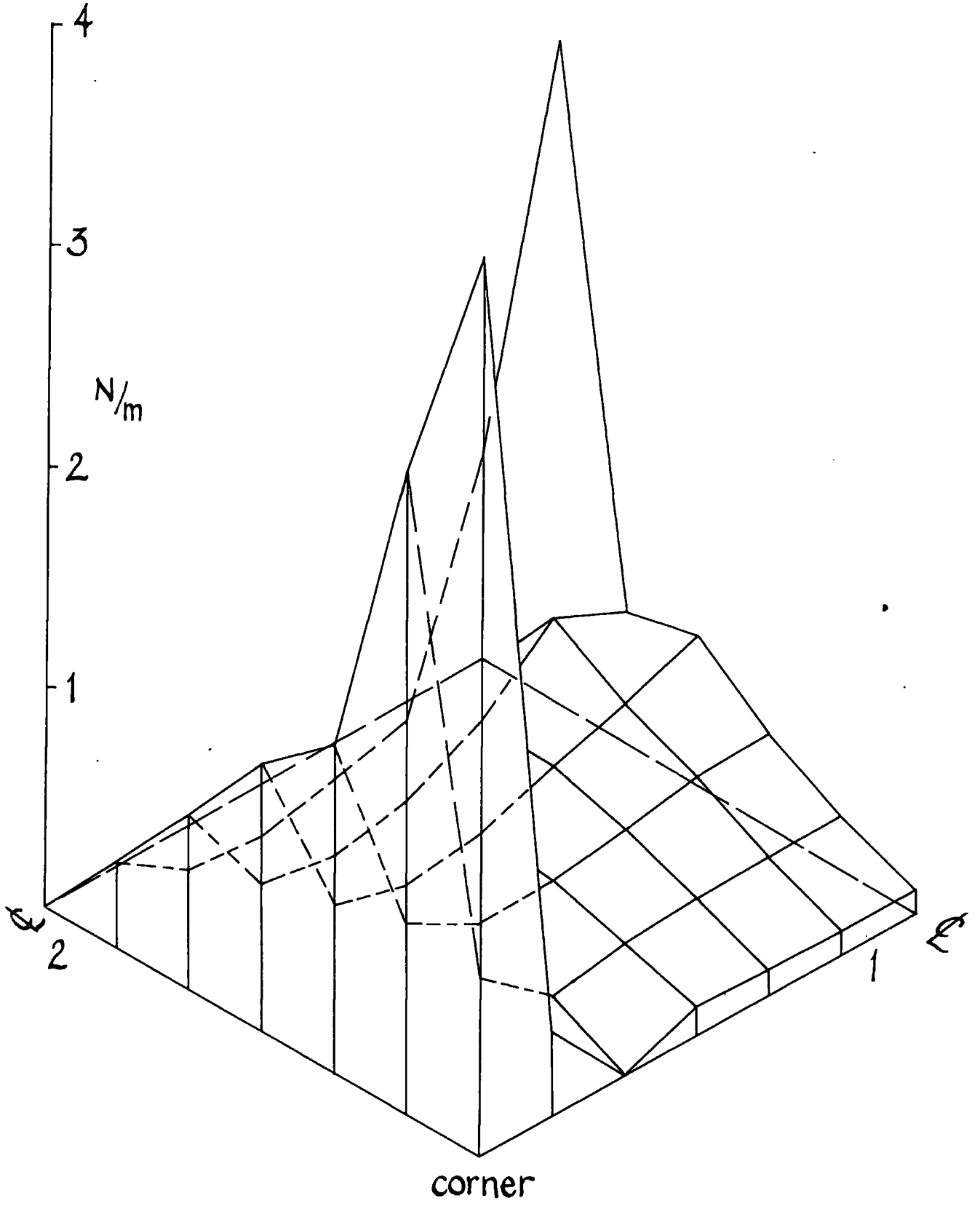

FIG.28 ALUMINIUM PLATE (6), SHEARING FORCE q_2
by finite elements

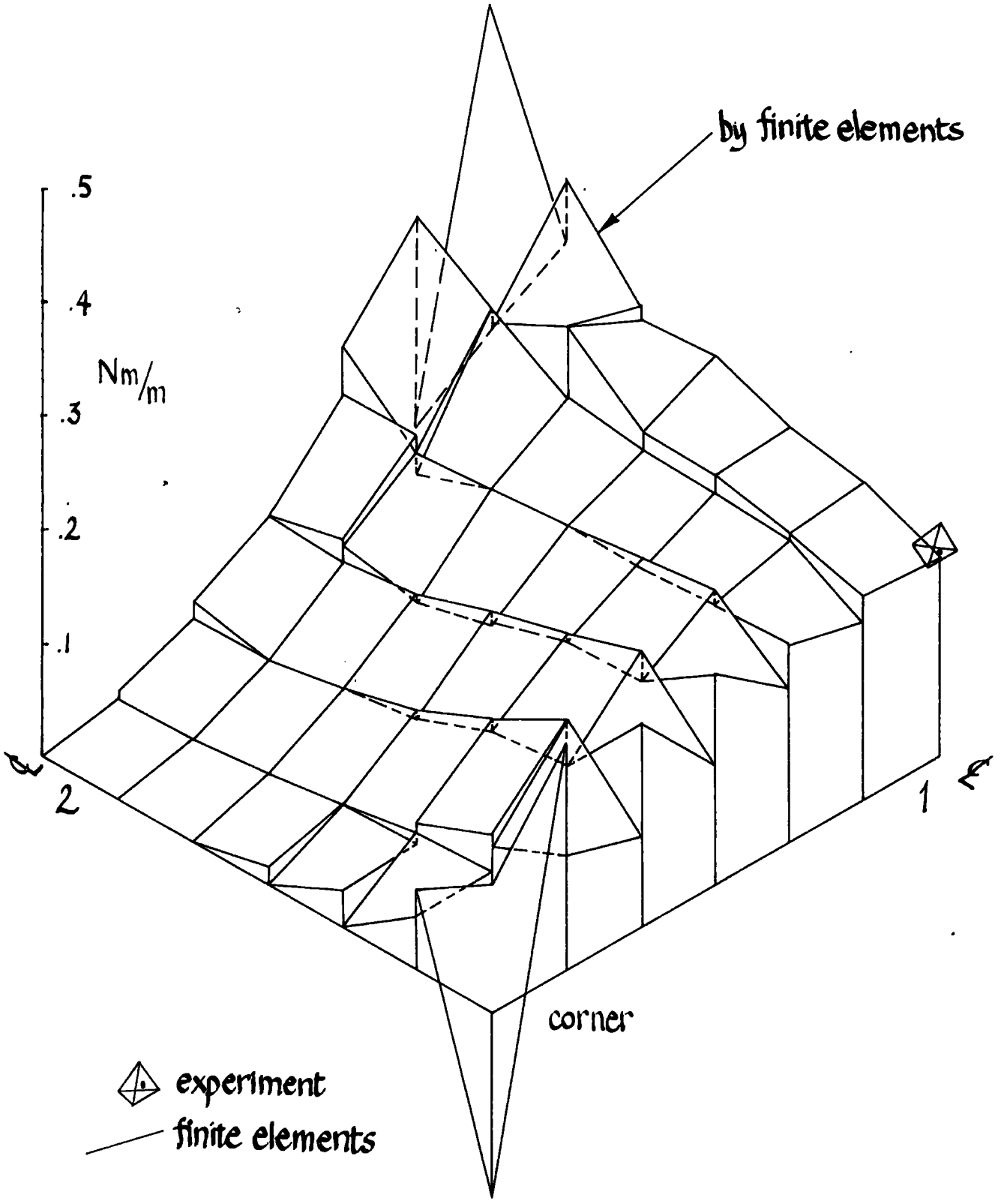

FIG.29 HARDBOARD PLATE (8), STRESS COUPLE m_{11}

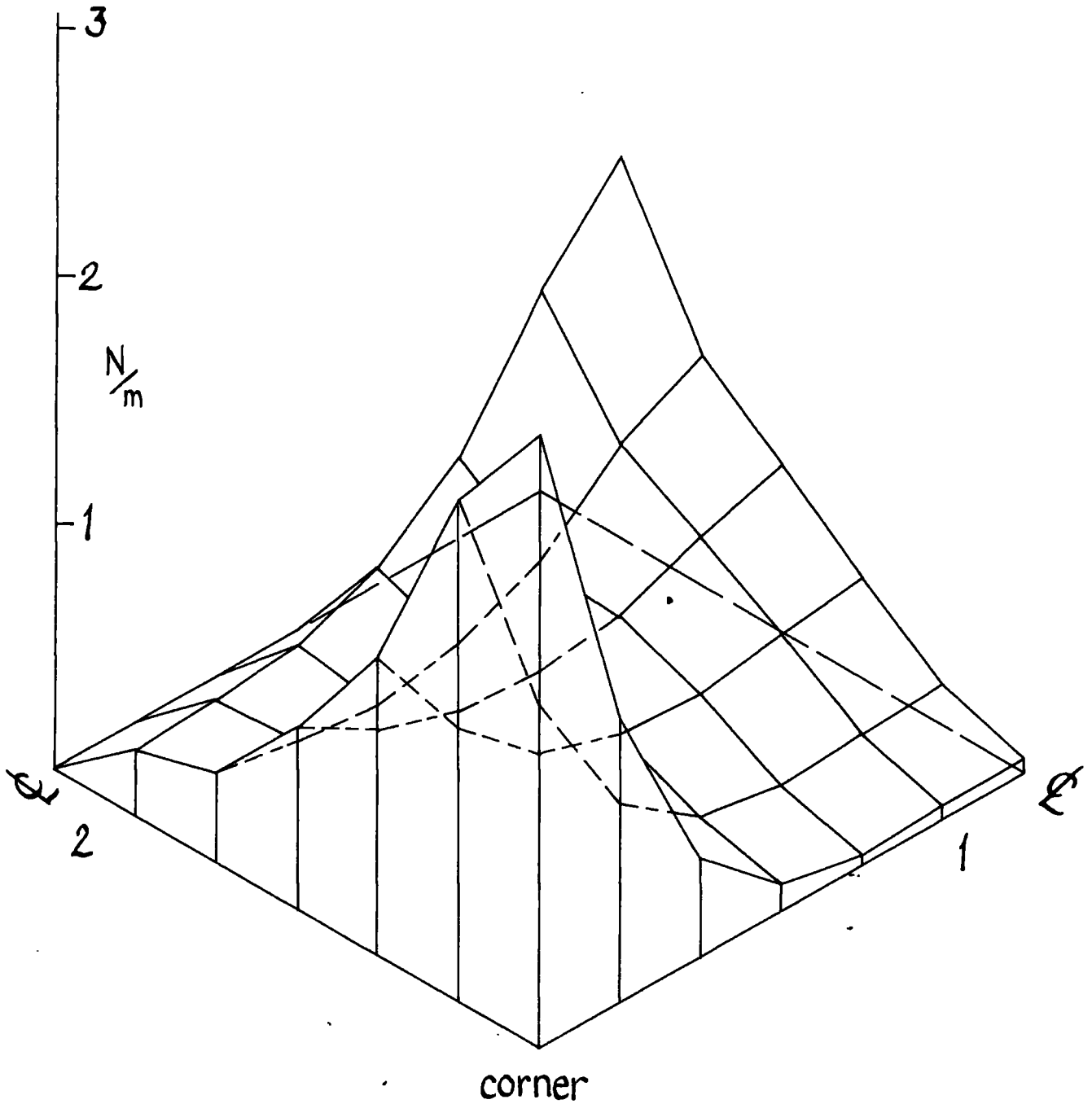

FIG.30 HARDBOARD PLATE(8), SHEARING FORCE, q_2
by finite elements

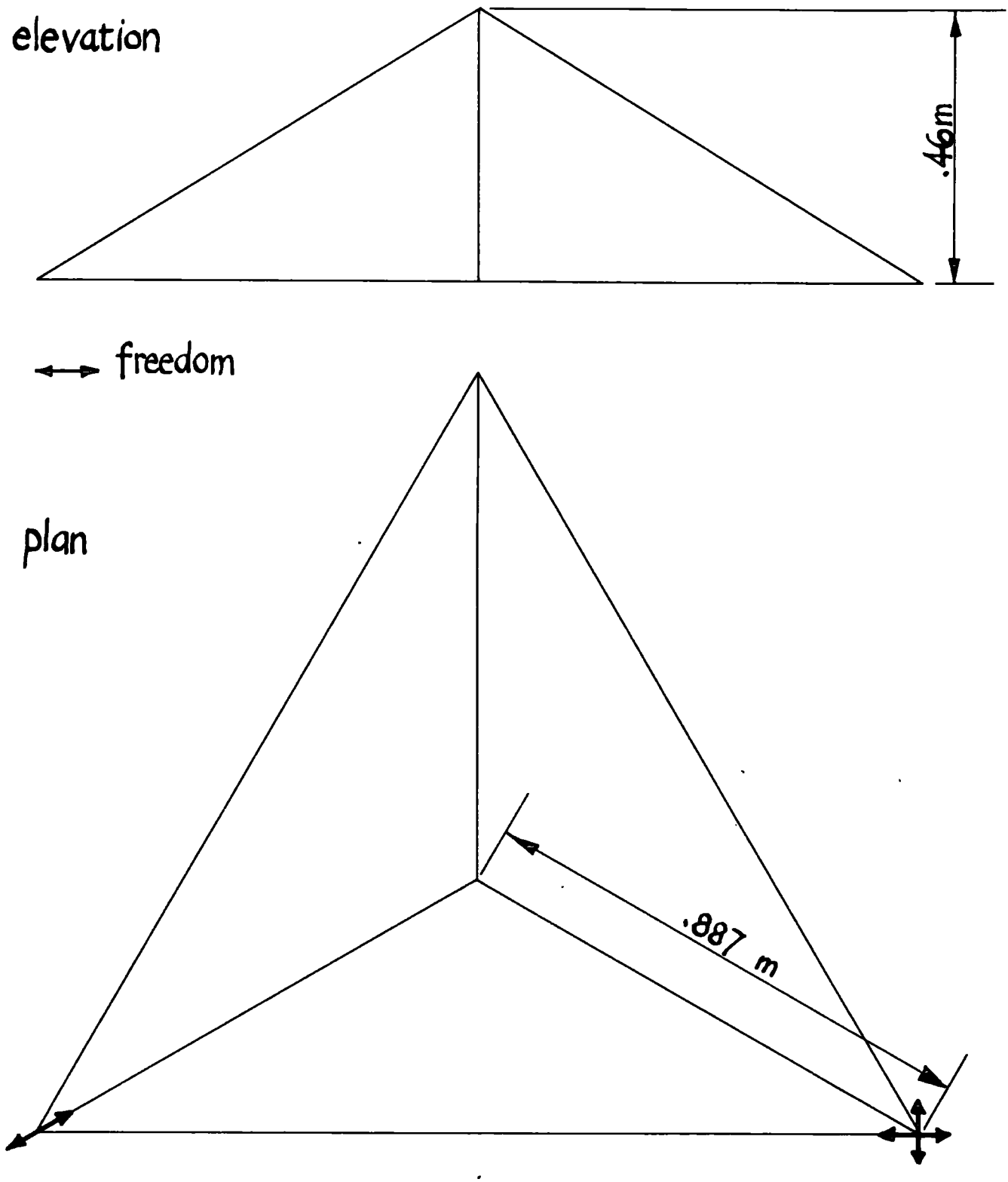

SCALE 1:10

FIG.31 GENERAL ARRANGEMENT OF TETRAHEDRAL DOME

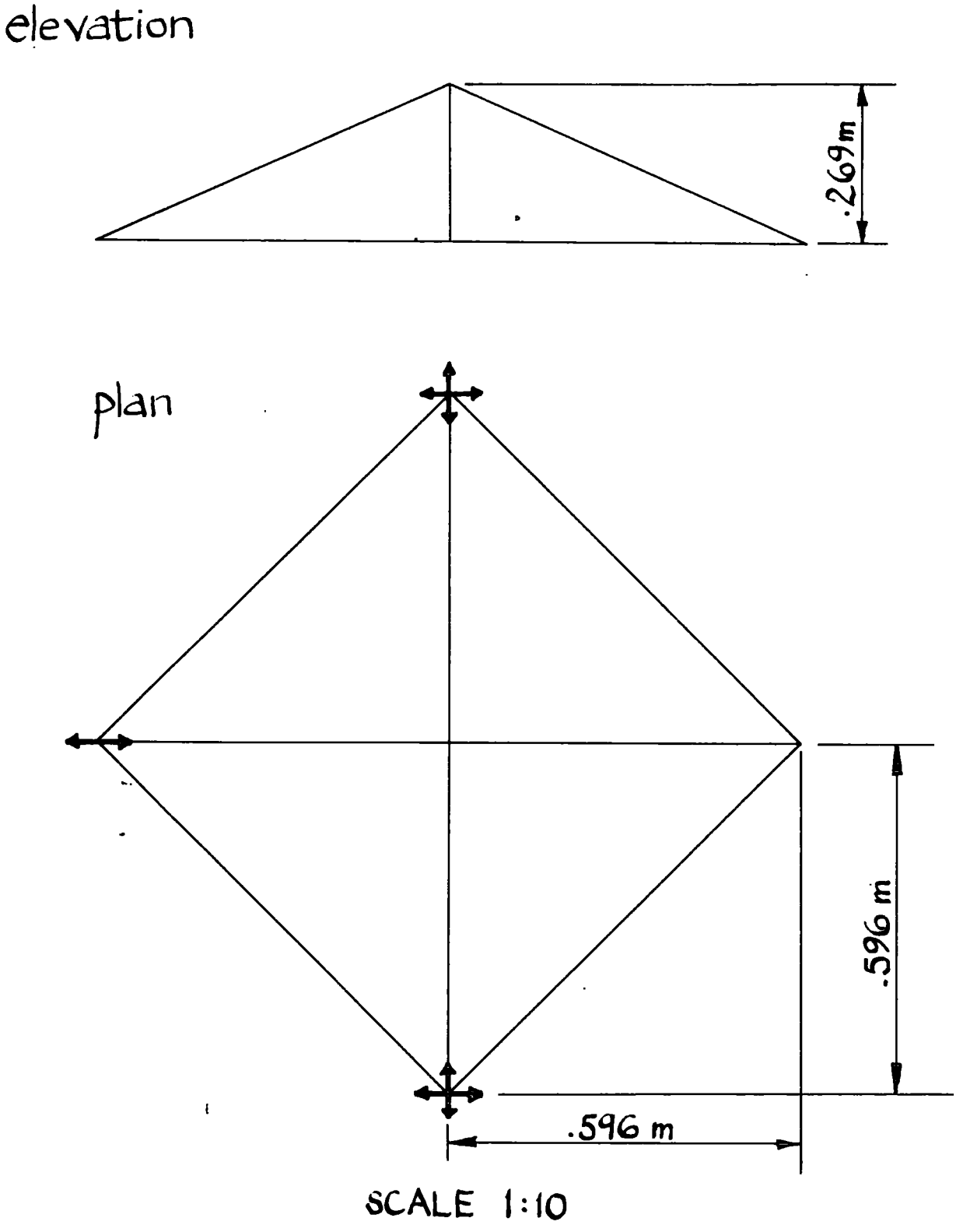

FIG. 32 GENERAL ARRANGEMENT OF SQUARE PYRAMID

elevation

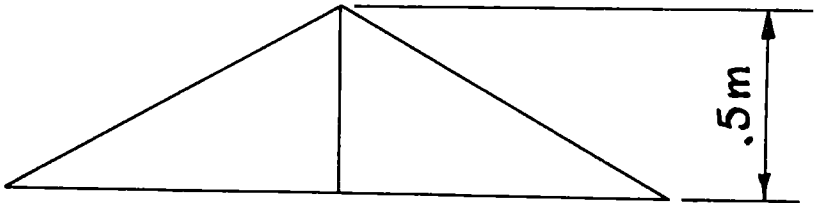

plan

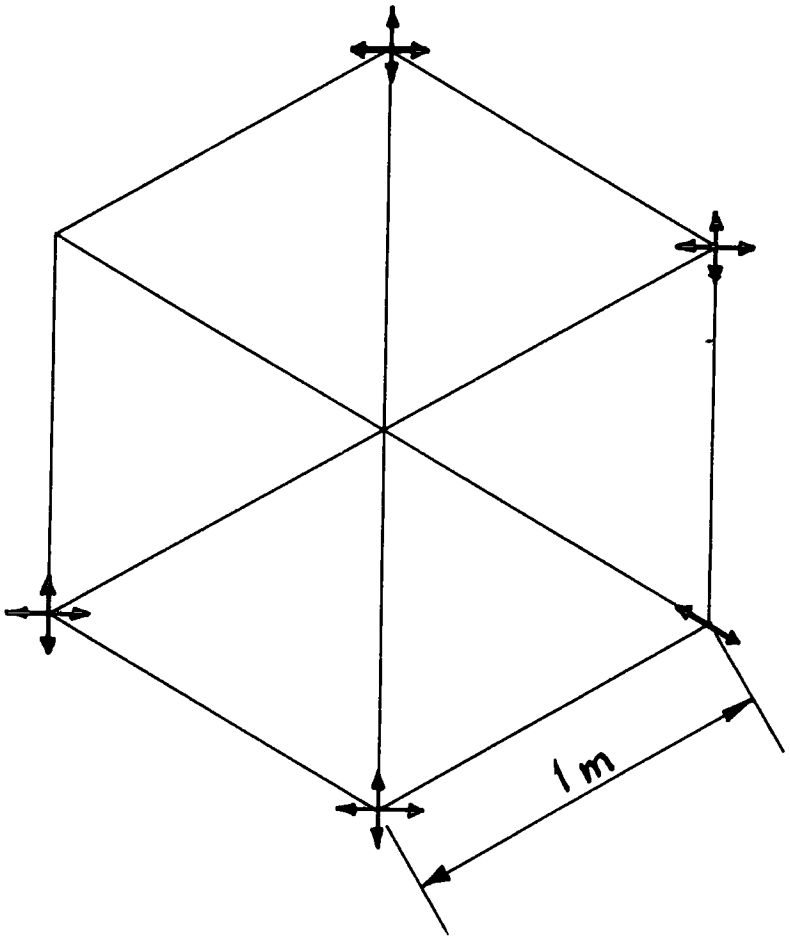

SCALE 1:20

FIG.33 GENERAL ARRANGEMENT OF HEXAGONAL DOME

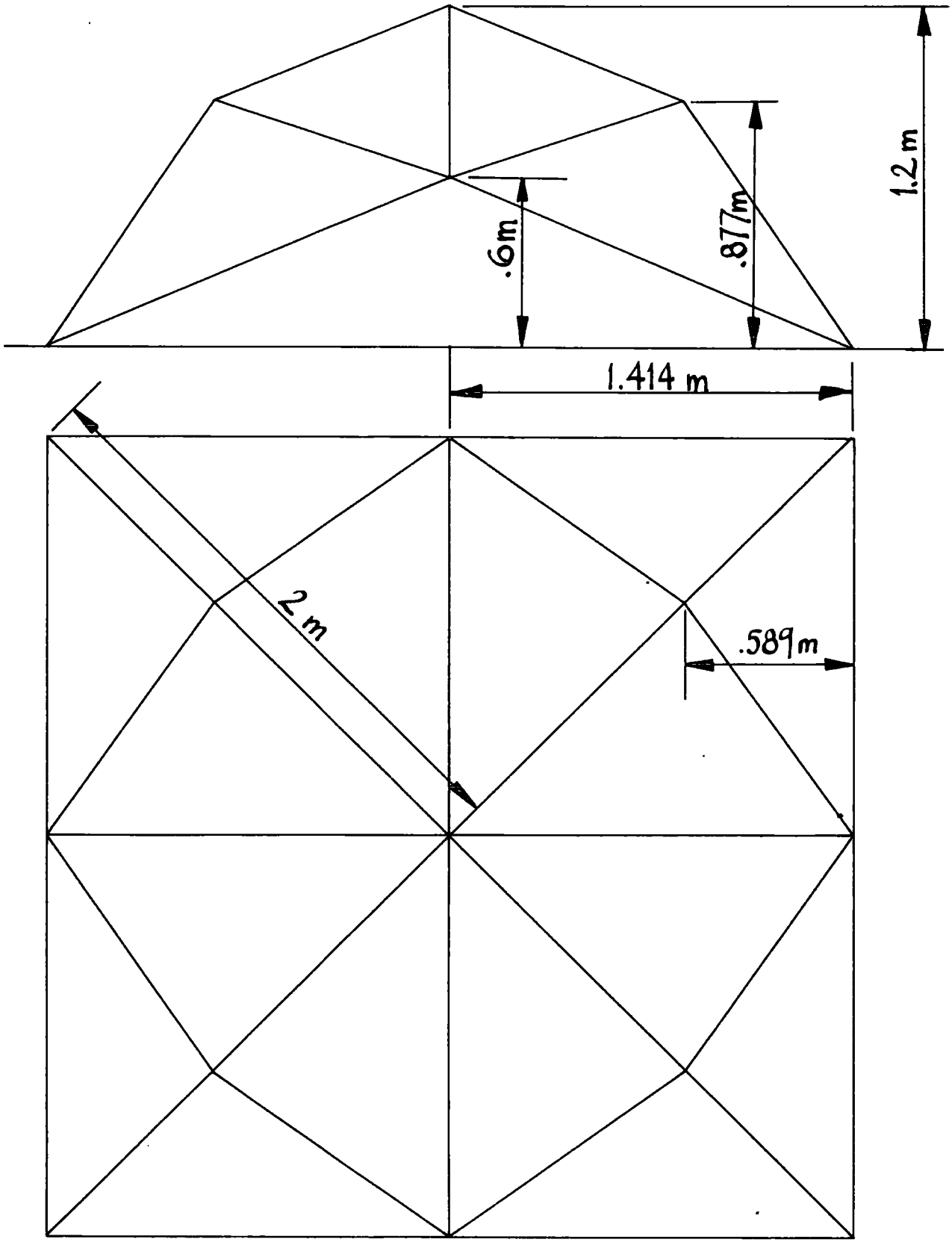

SCALE 1:20

FIG. 34 GENERAL ARRANGEMENT OF 16 FACED DOME

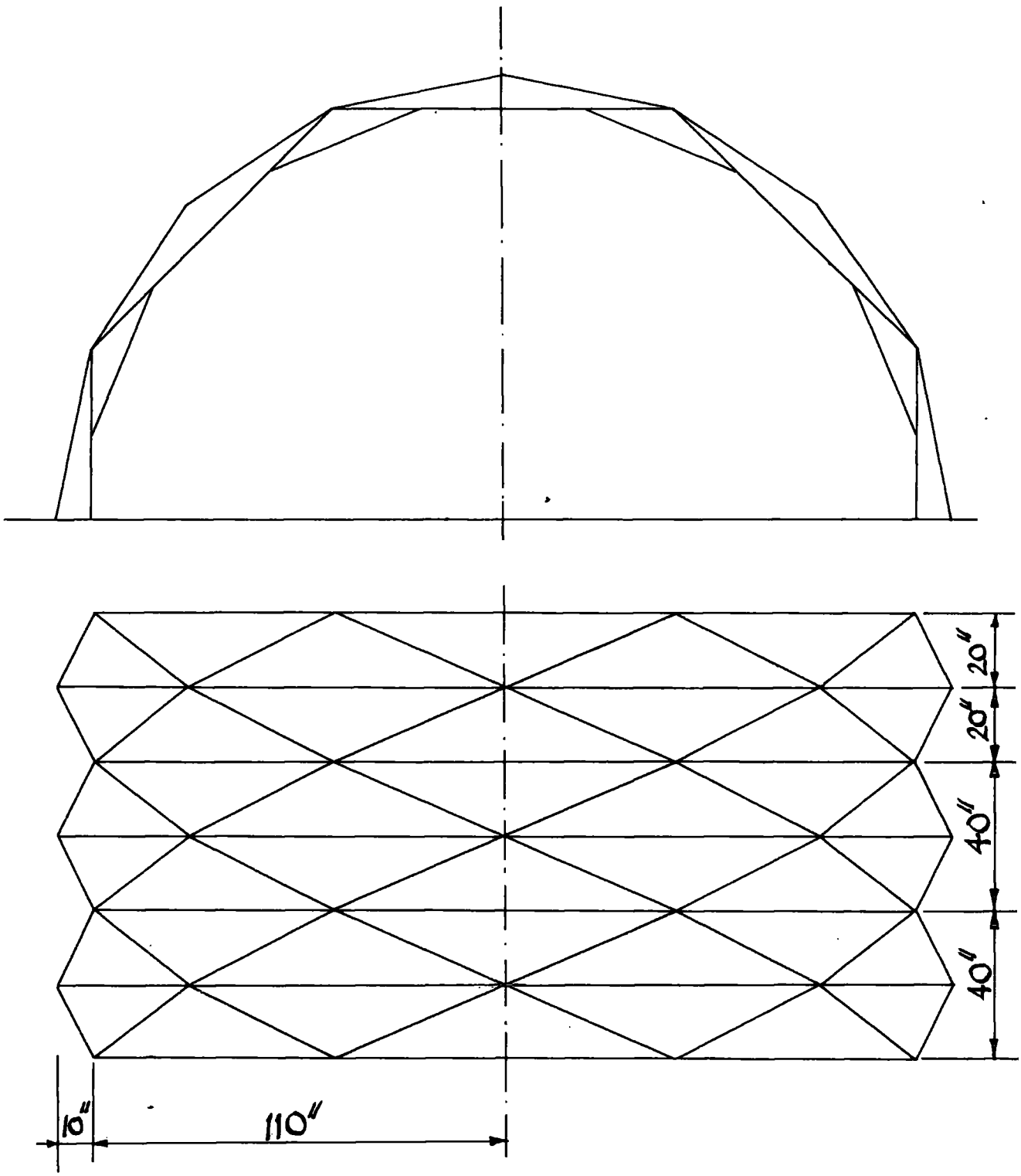

SCALE 1:40

FIG. 35 GENERAL ARRANGEMENT OF BENJAMIN BARREL VAULT

FIG. 36 SKETCH OF PLATE RIG

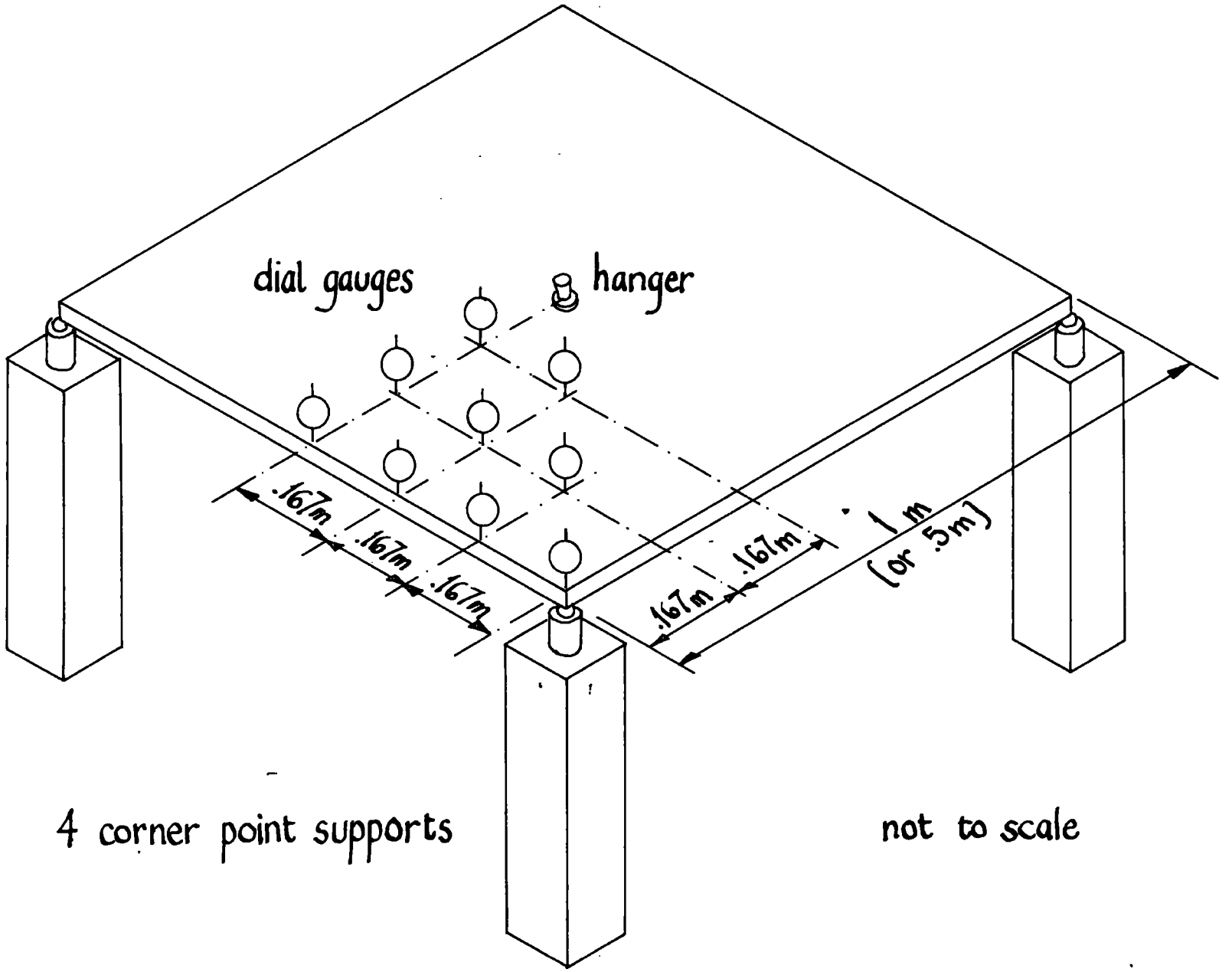

HARDBOARD PLATE (8)

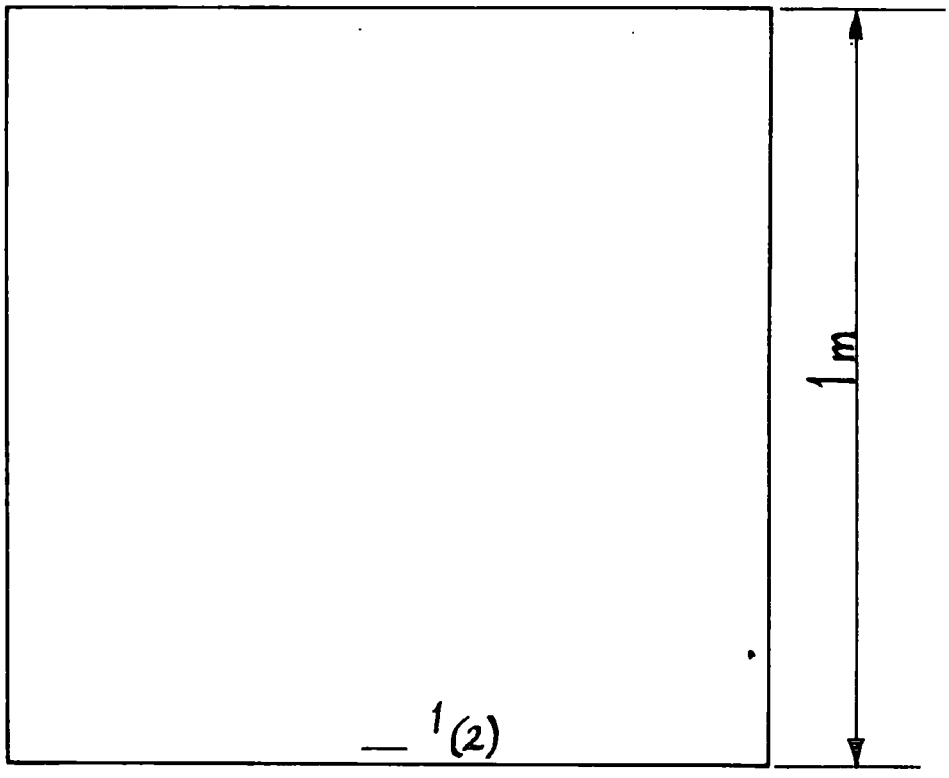

ALUMINIUM PLATE (7)

numbers in brackets indicate gauges on underside

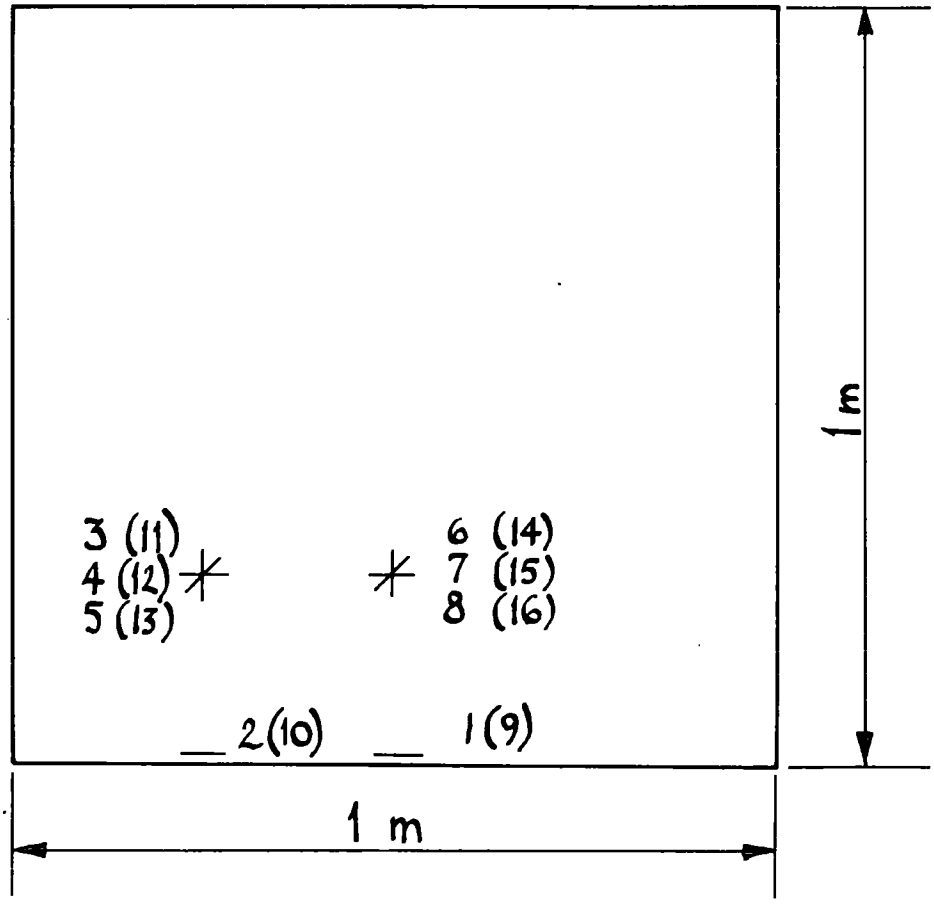

FIG. 37 PLATE STRAIN GAUGE LOCATIONS

SCALE 1 : 10

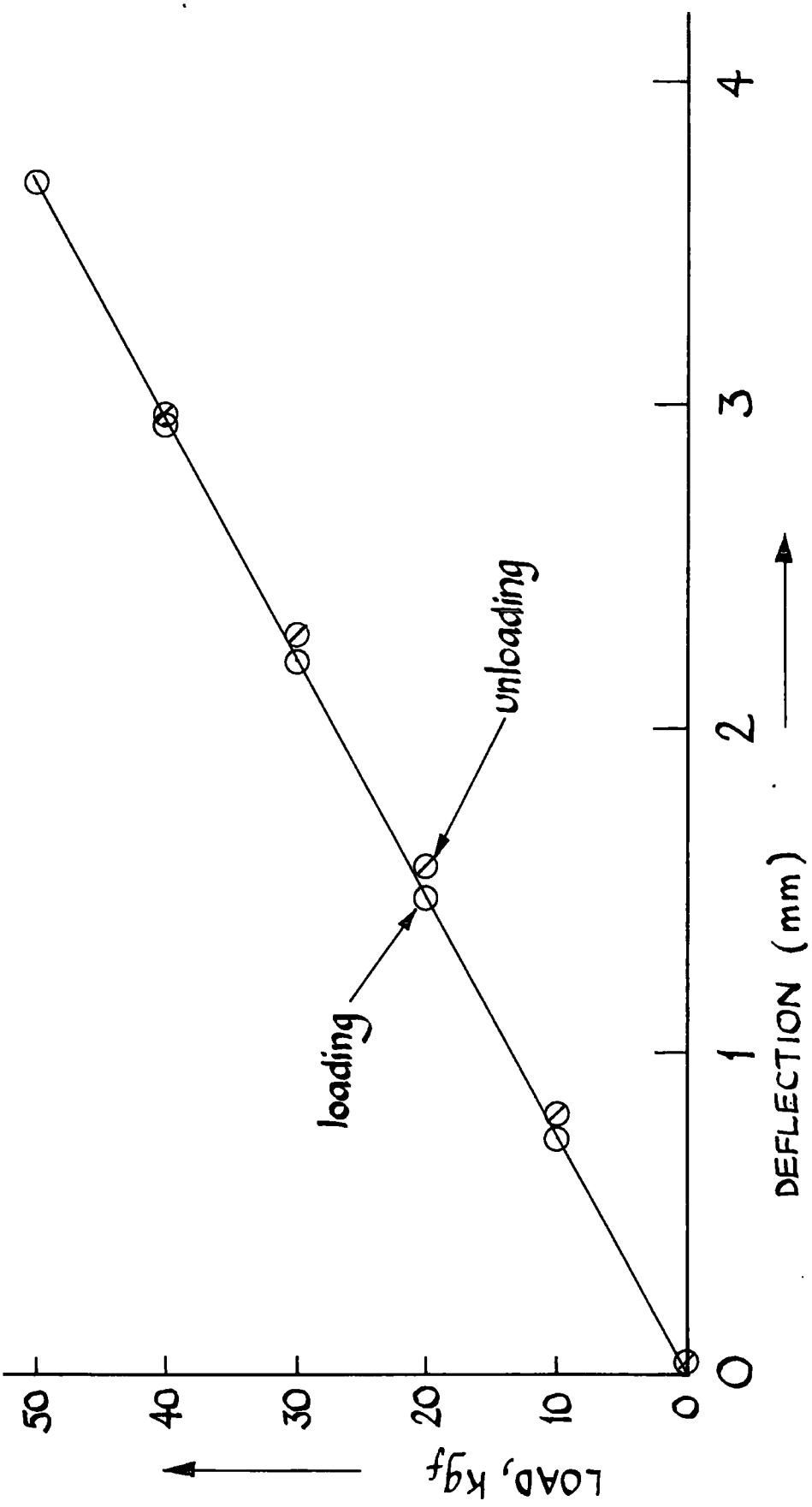

FIG. 38 TYPICAL DIAL GAUGE READINGS
(PLATE 7)

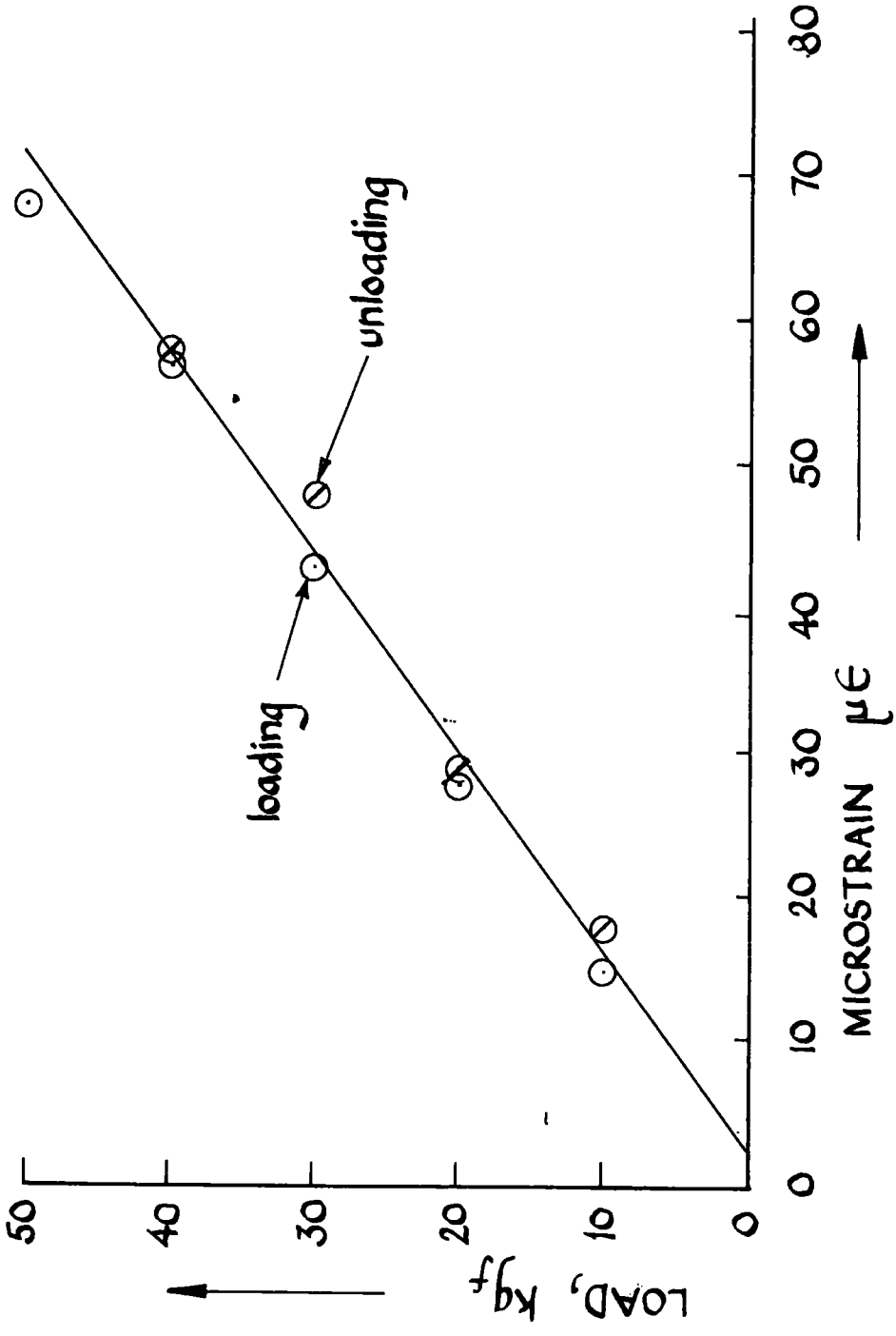

FIG. 39 TYPICAL STRAIN GAUGE READINGS
(PLATE 8)

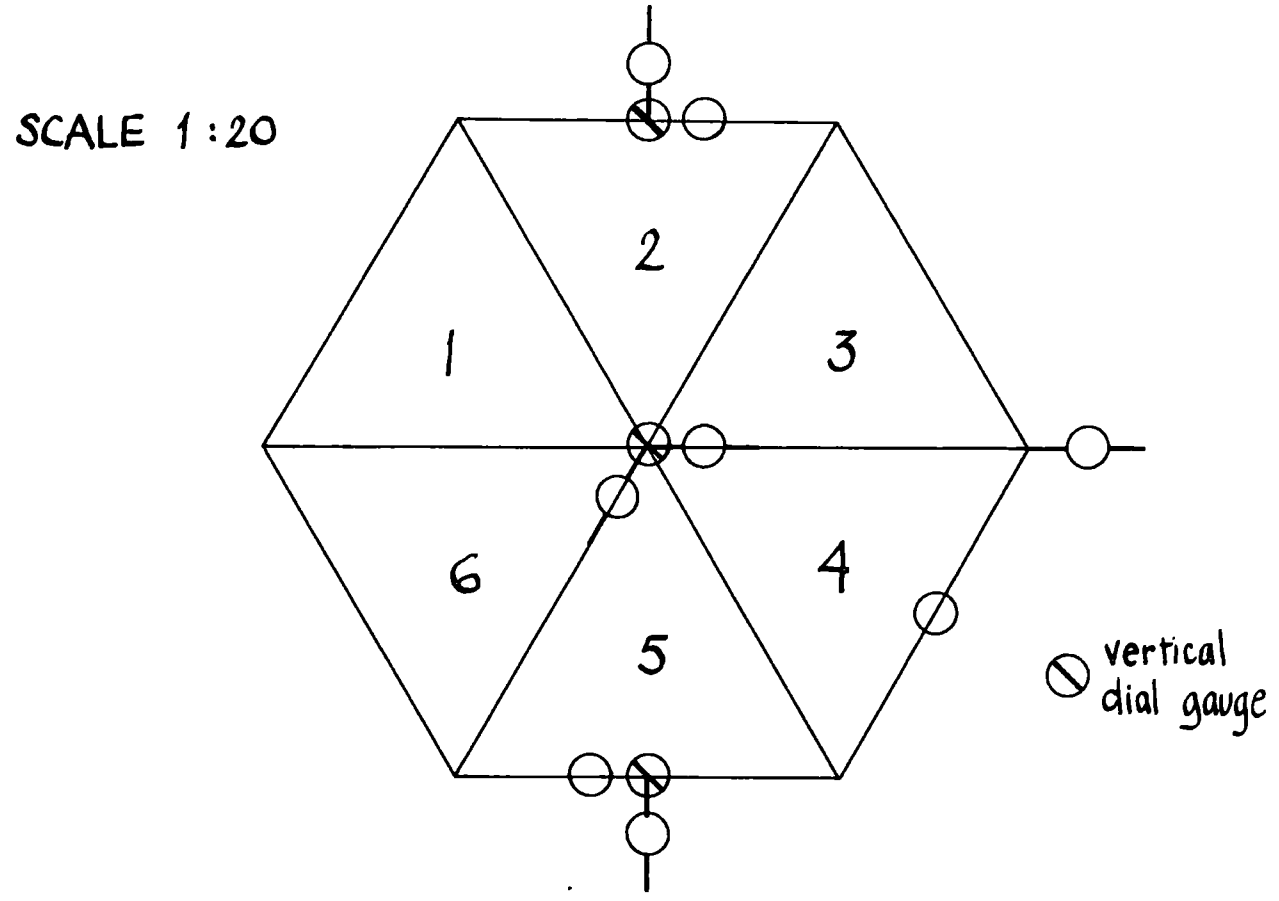

FIG. 40 DIAL GAUGES ON HEXAGONAL DOME (1)

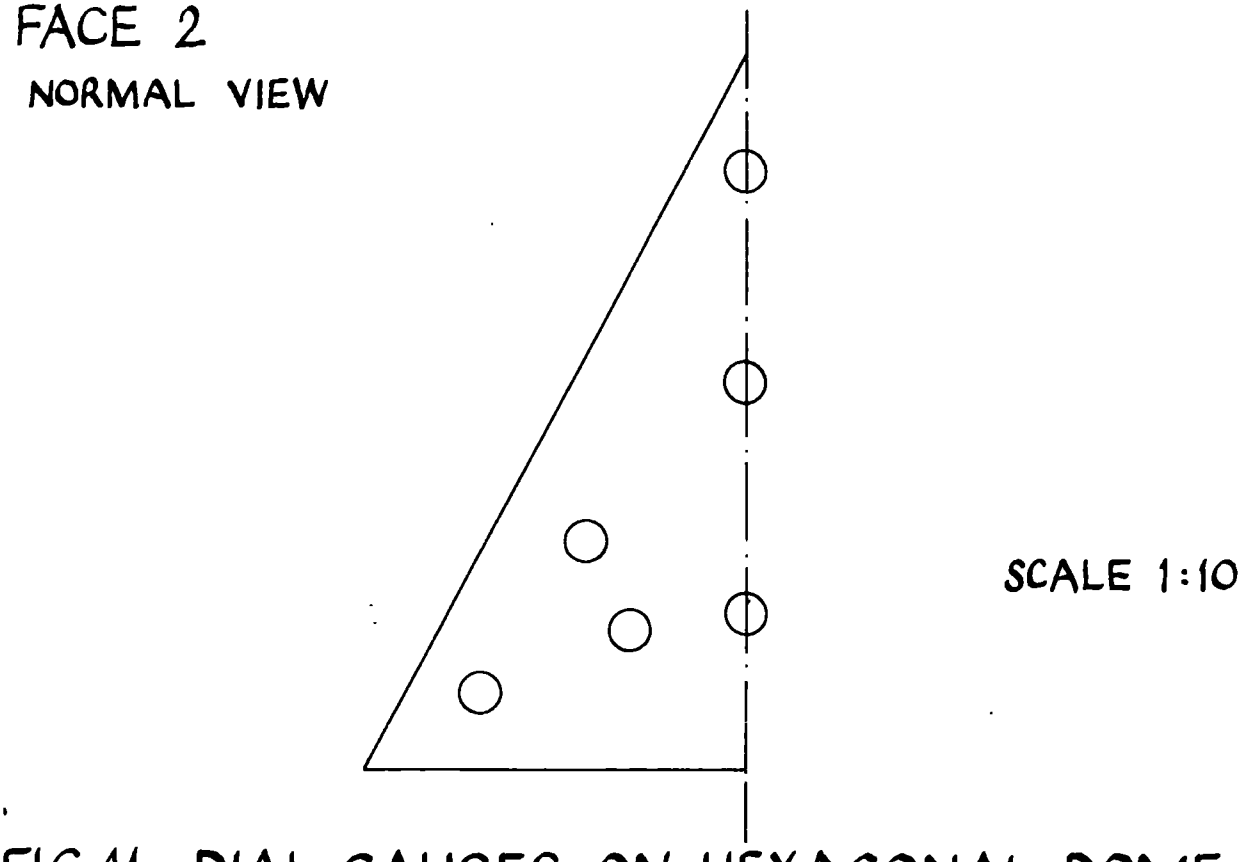

FIG. 41 DIAL GAUGES ON HEXAGONAL DOME (2)

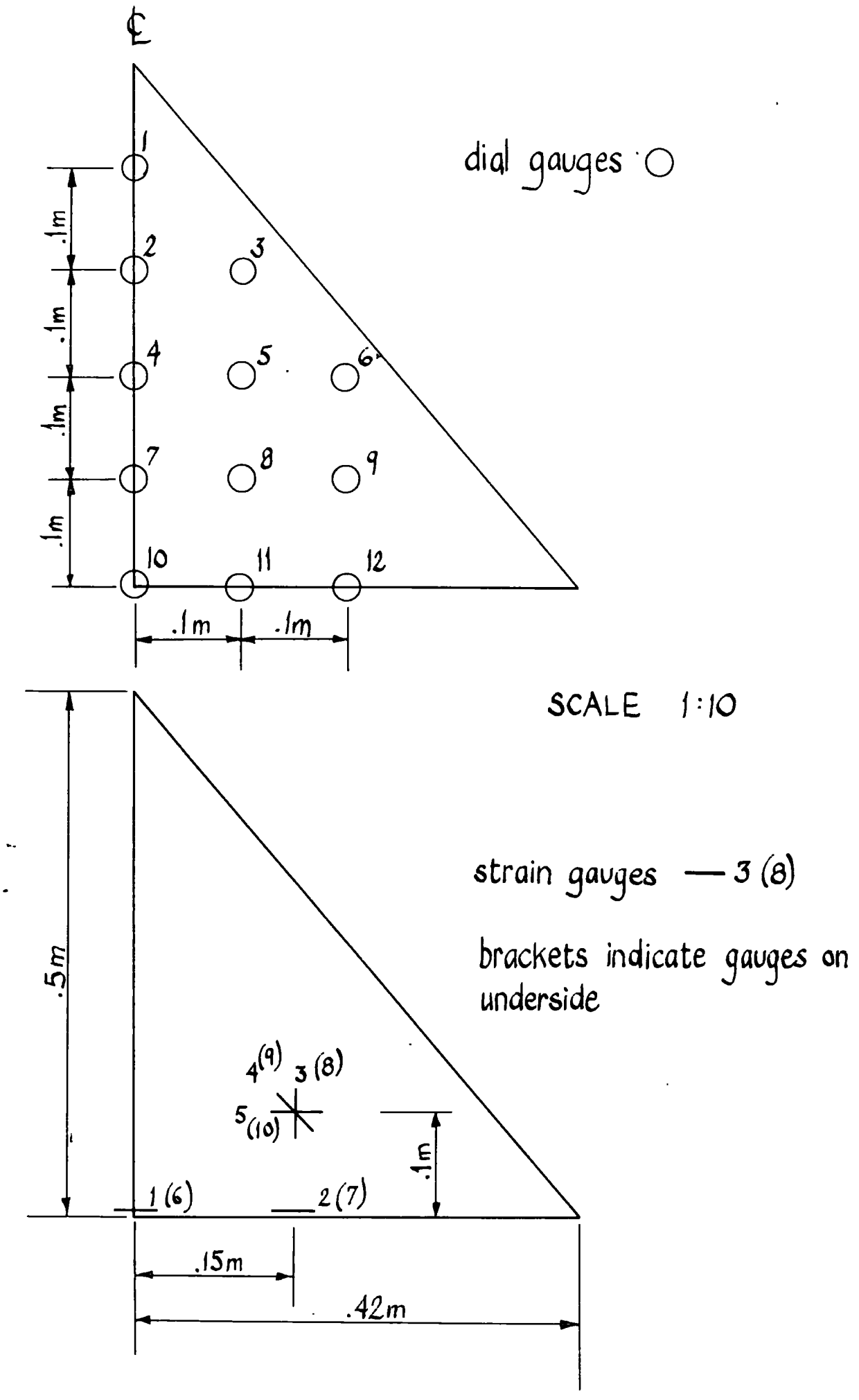

FIG. 42 SQUARE PYRAMID

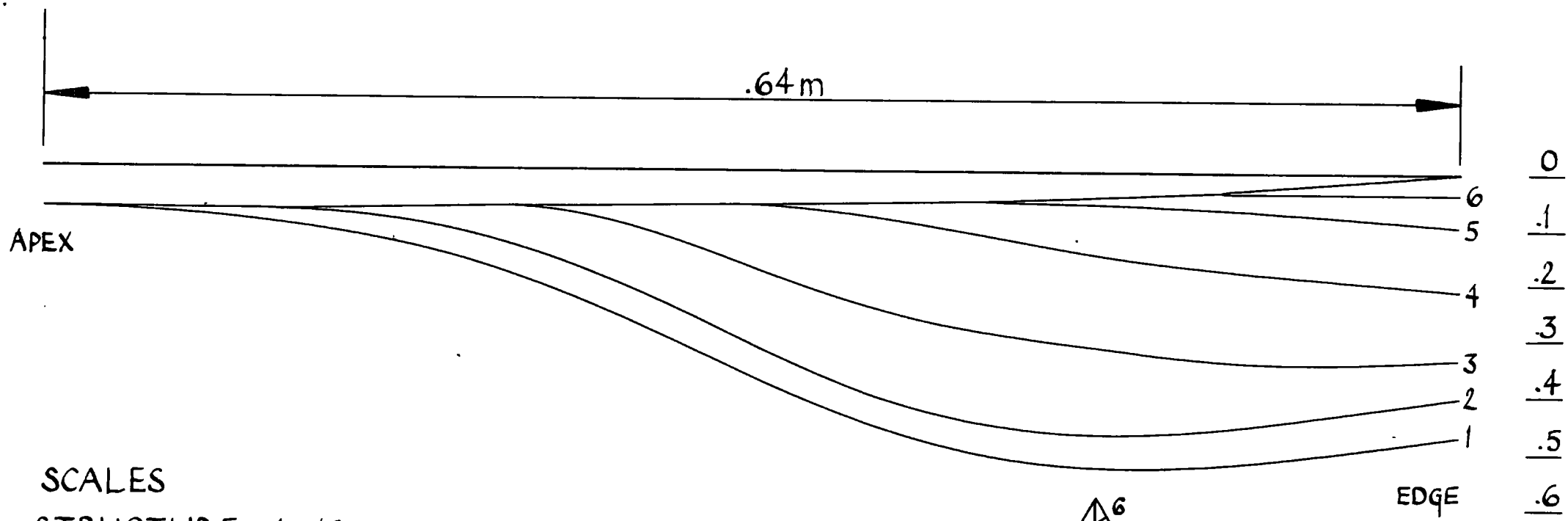

SCALES
STRUCTURE 4:10
DISPLACEMENTS 10^4:1

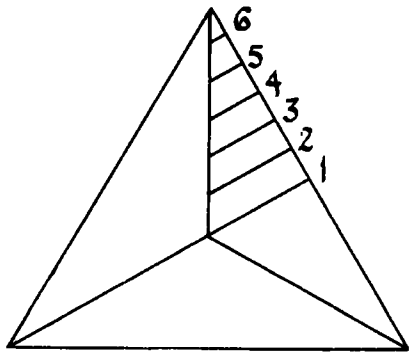

1 N VERTICAL LOAD AT ALL 3 CENTROIDS
NORMAL DISPLACEMENTS OF ONE FACE

FIG. 43 TETRAHEDRAL DOME (PLATES 1)

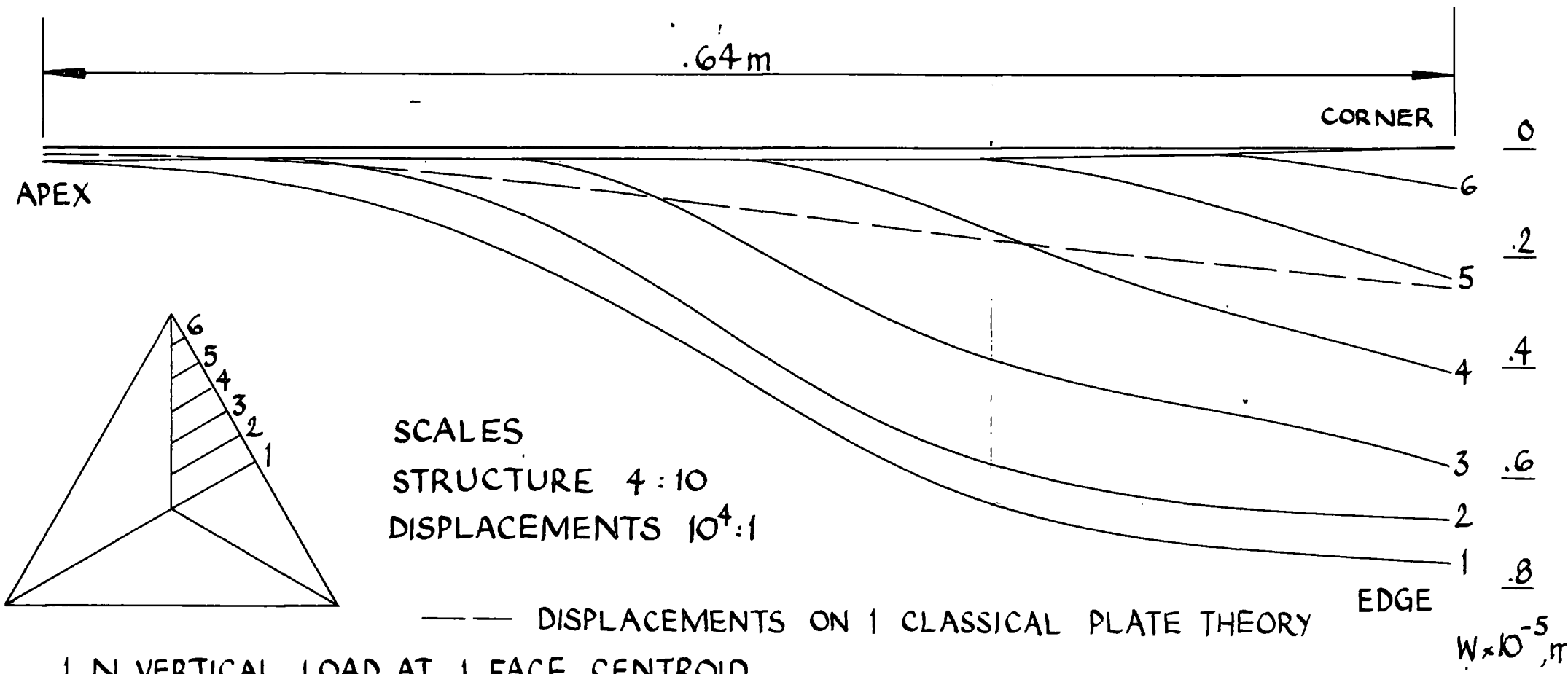

FIG. 44 TETRAHEDRAL DOME (PLATES 1)

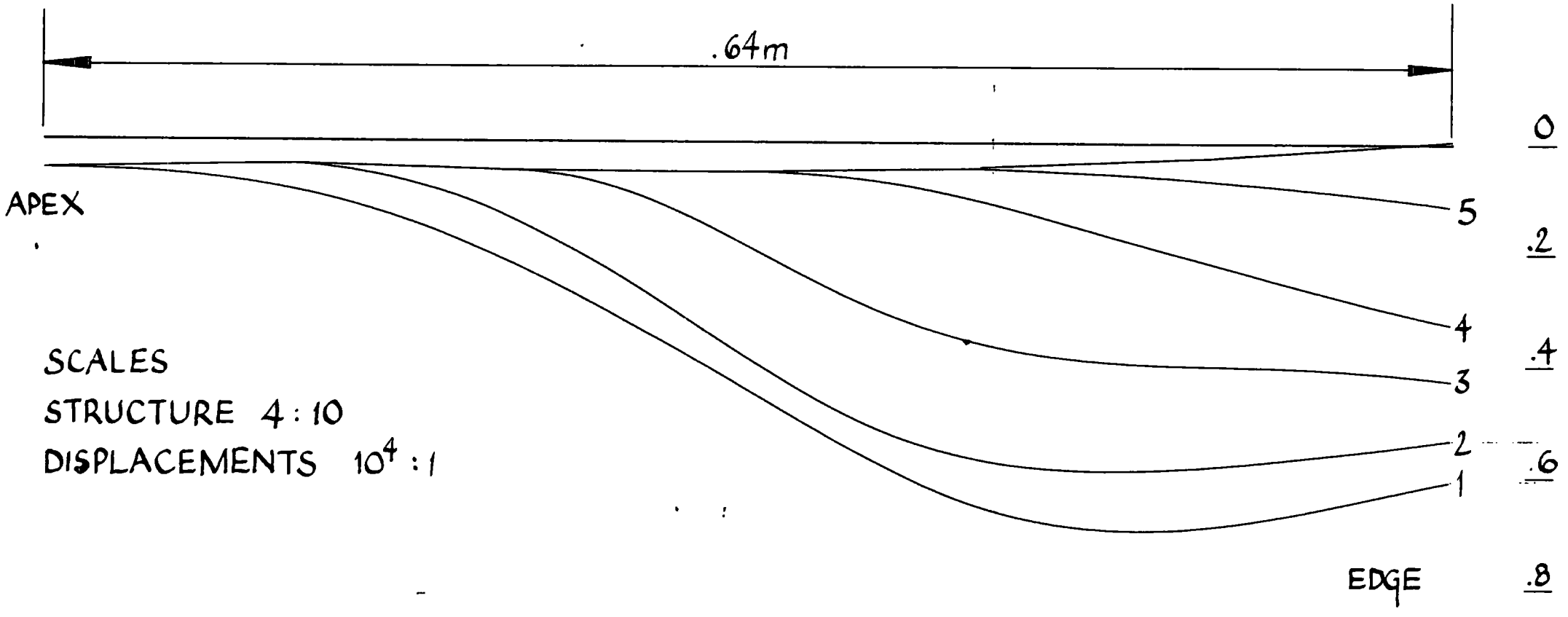

1 N VERTICAL LOAD AT ALL 3 CENTROIDS
NORMAL DISPLACEMENTS OF 1 FACE

FIG. 45 TETRAHEDRAL DOME (PLATES 2)

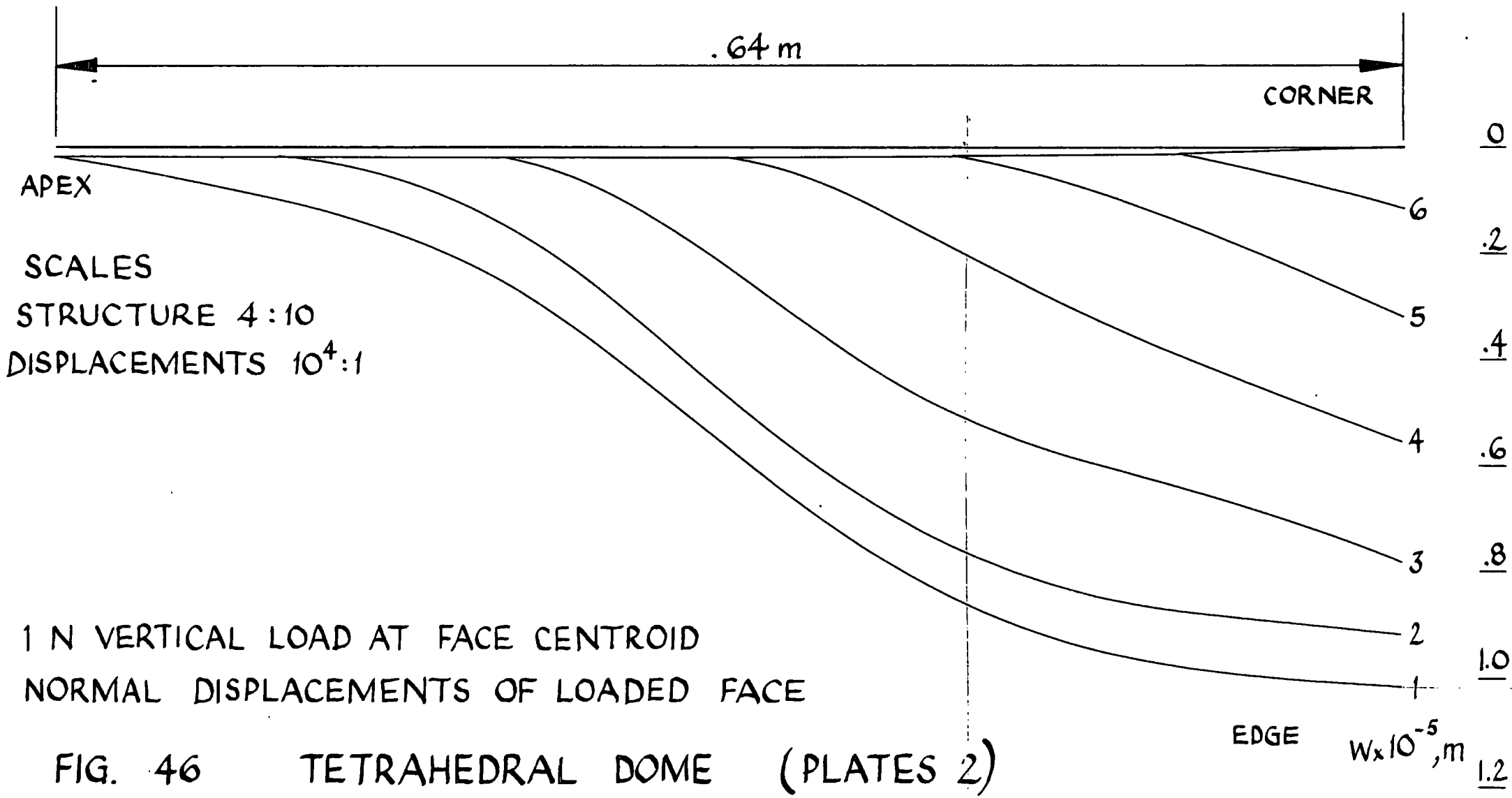

FIG. 46 TETRAHEDRAL DOME (PLATES 2)

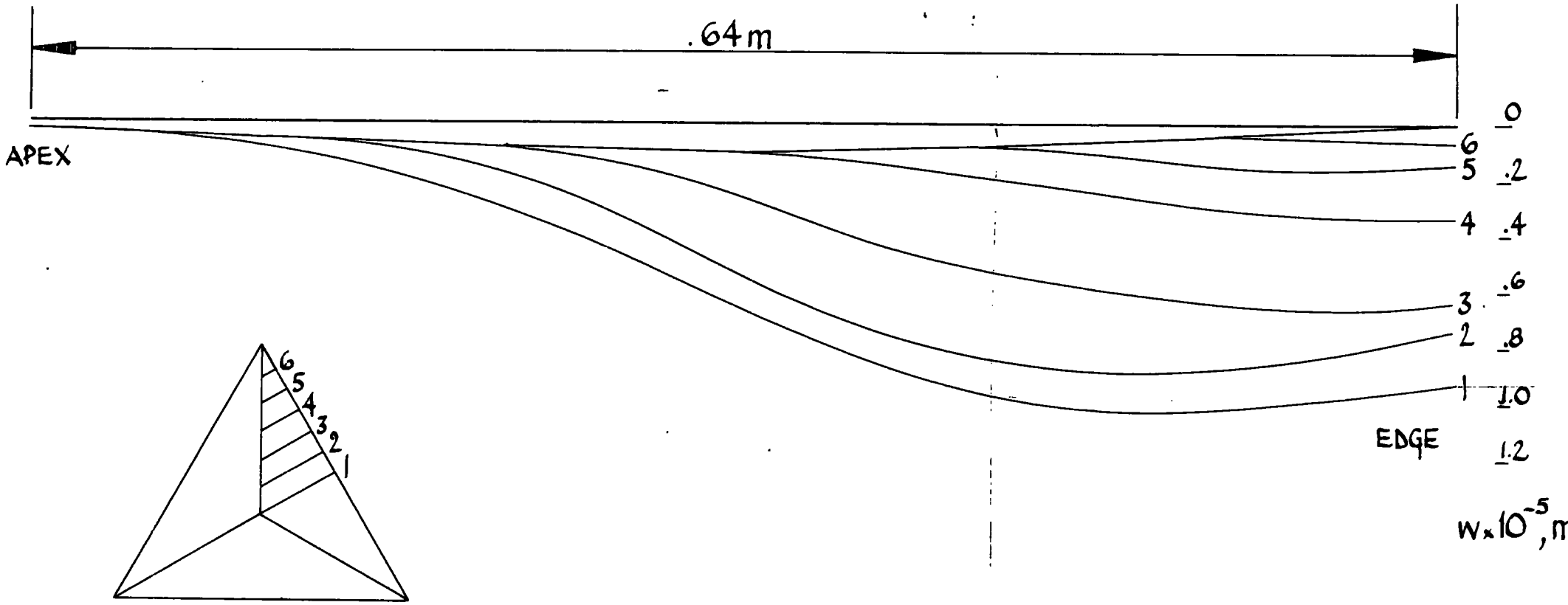

NORMAL DISPLACEMENTS OF FACE
1 N VERTICAL LOAD AT ALL 3 CENTROIDS

SCALES
DISPLACEMENTS 5000 : 1
STRUCTURE 4 : 10

FIG 47 TETRAHEDRAL DOME (PLATES 3)

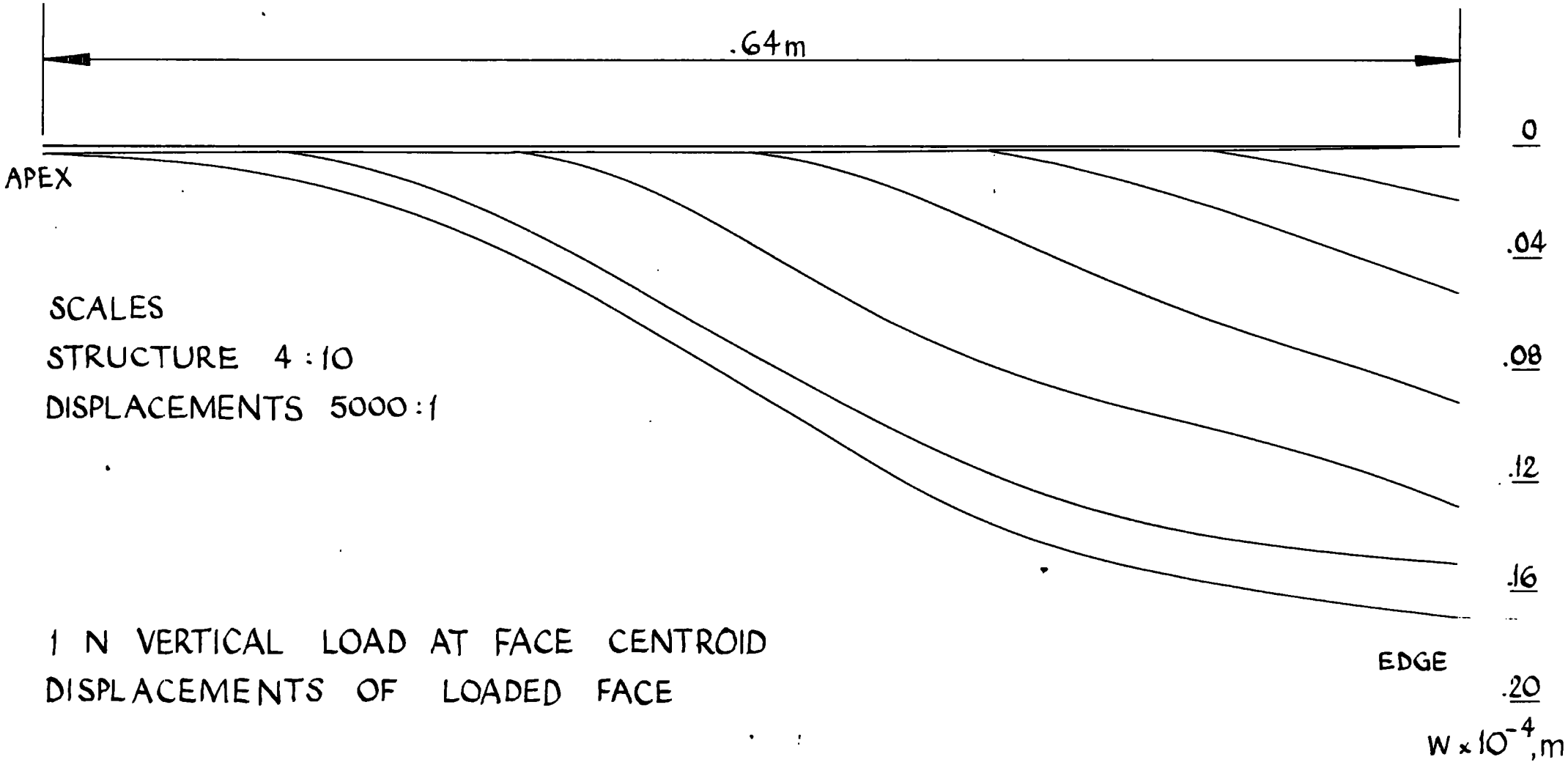

FIG. 48 TETRAHEDRAL DOME (PLATES 3)

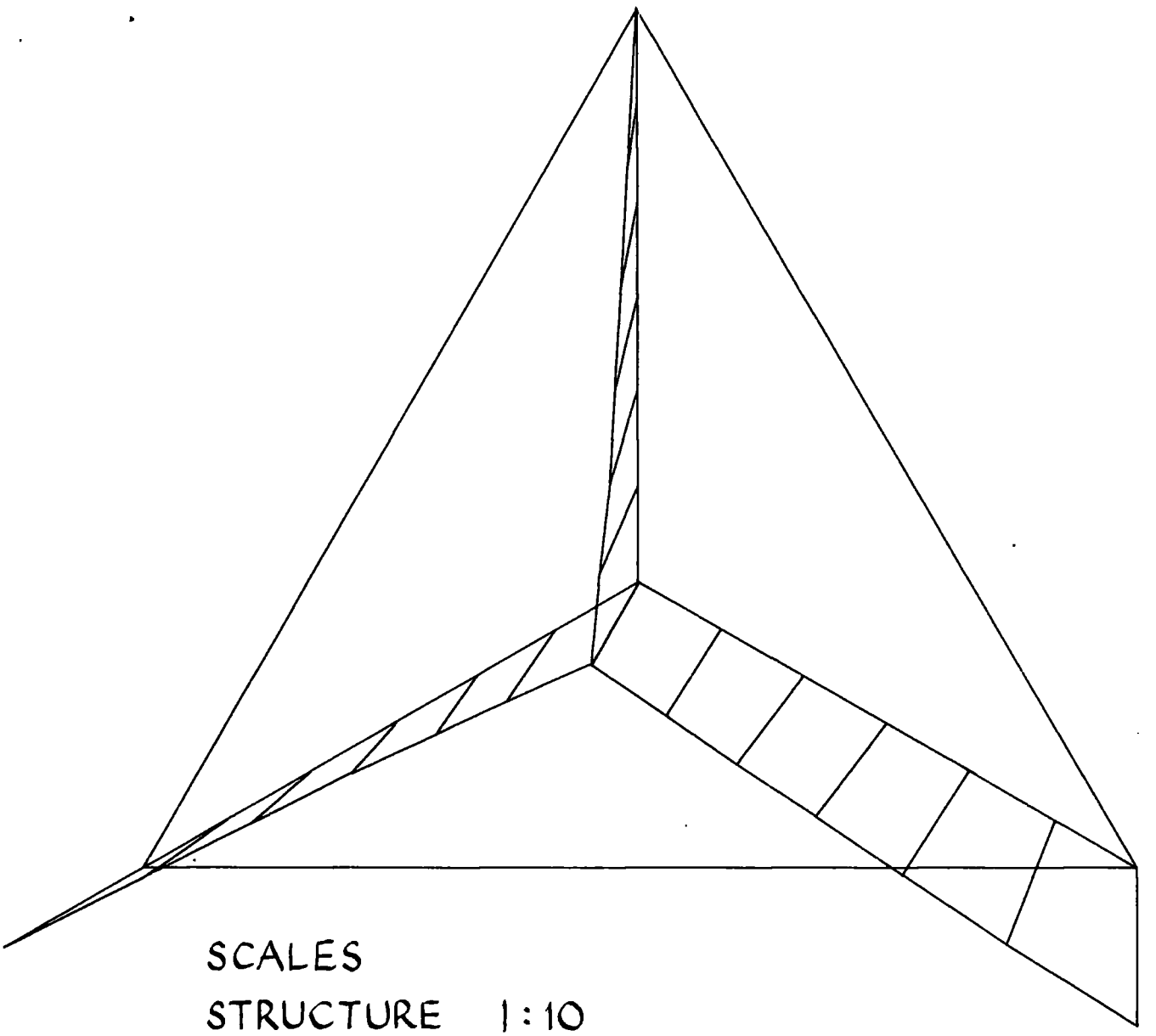

SCALES
STRUCTURE 1:10
DISPLACEMENTS 50000:1

HORIZONTAL DISPLACEMENTS

1 N VERTICAL LOAD AT ALL 3 CENTROIDS

FIG. 49 TETRAHEDRAL DOME (PLATES 1)

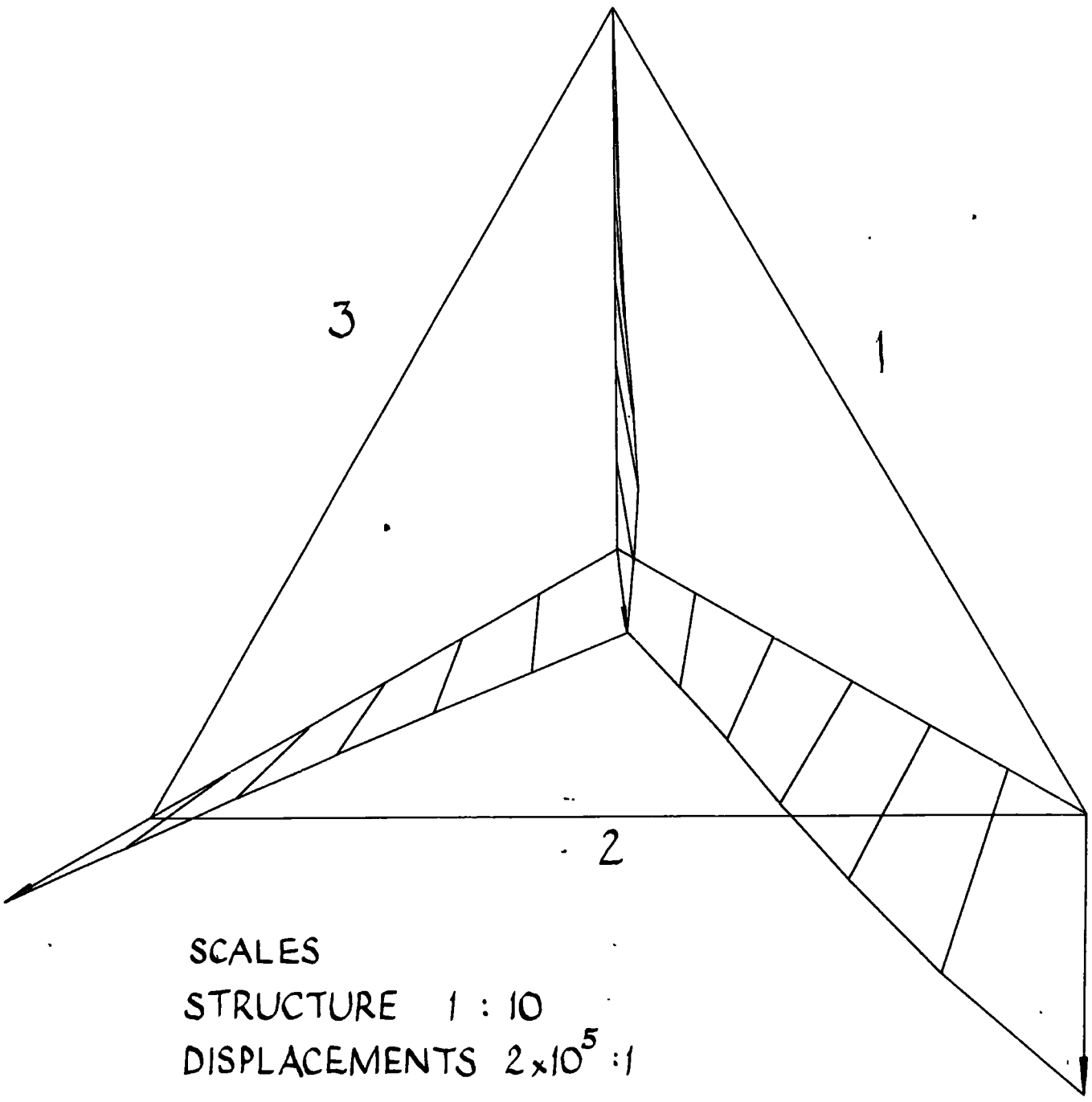

SCALES
STRUCTURE 1 : 10
DISPLACEMENTS 2×10^5 : 1

1 N VERTICAL LOAD AT CENTROID OF FACE 1
HORIZONTAL DISPLACEMENTS

FIG. 50 TETRAHEDRAL DOME (PLATES 1)

SCALES
STRUCTURE 1 : 10
DISPLACEMENTS $2 \times 10^5 : 1$

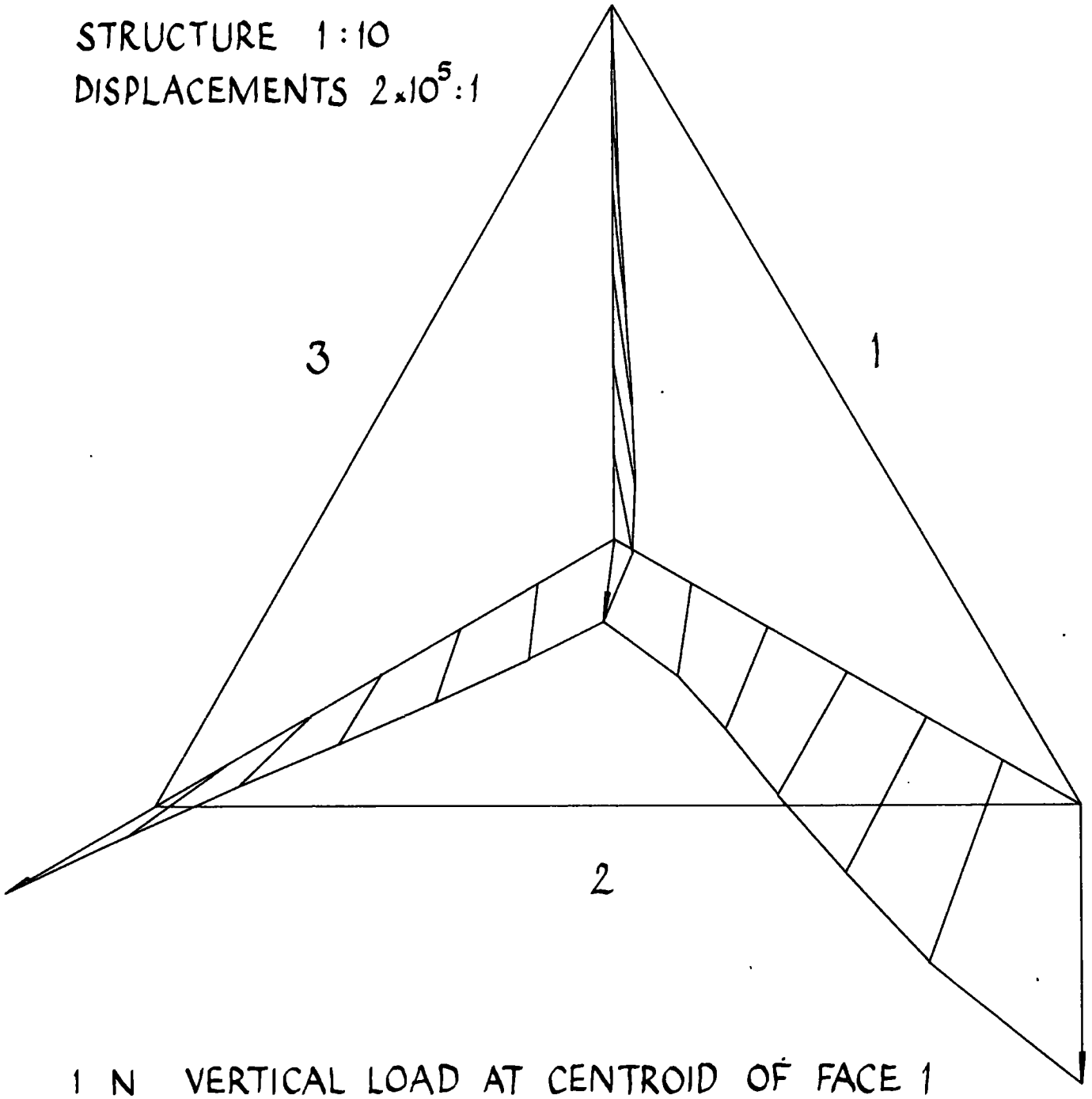

1 N VERTICAL LOAD AT CENTROID OF FACE 1
HORIZONTAL DISPLACEMENTS

FIG 51 TETRAHEDRAL DOME (PLATES 2)

SCALES

STRUCTURE 1 : 10

DISPLACEMENTS $2 \times 10^5 : 1$

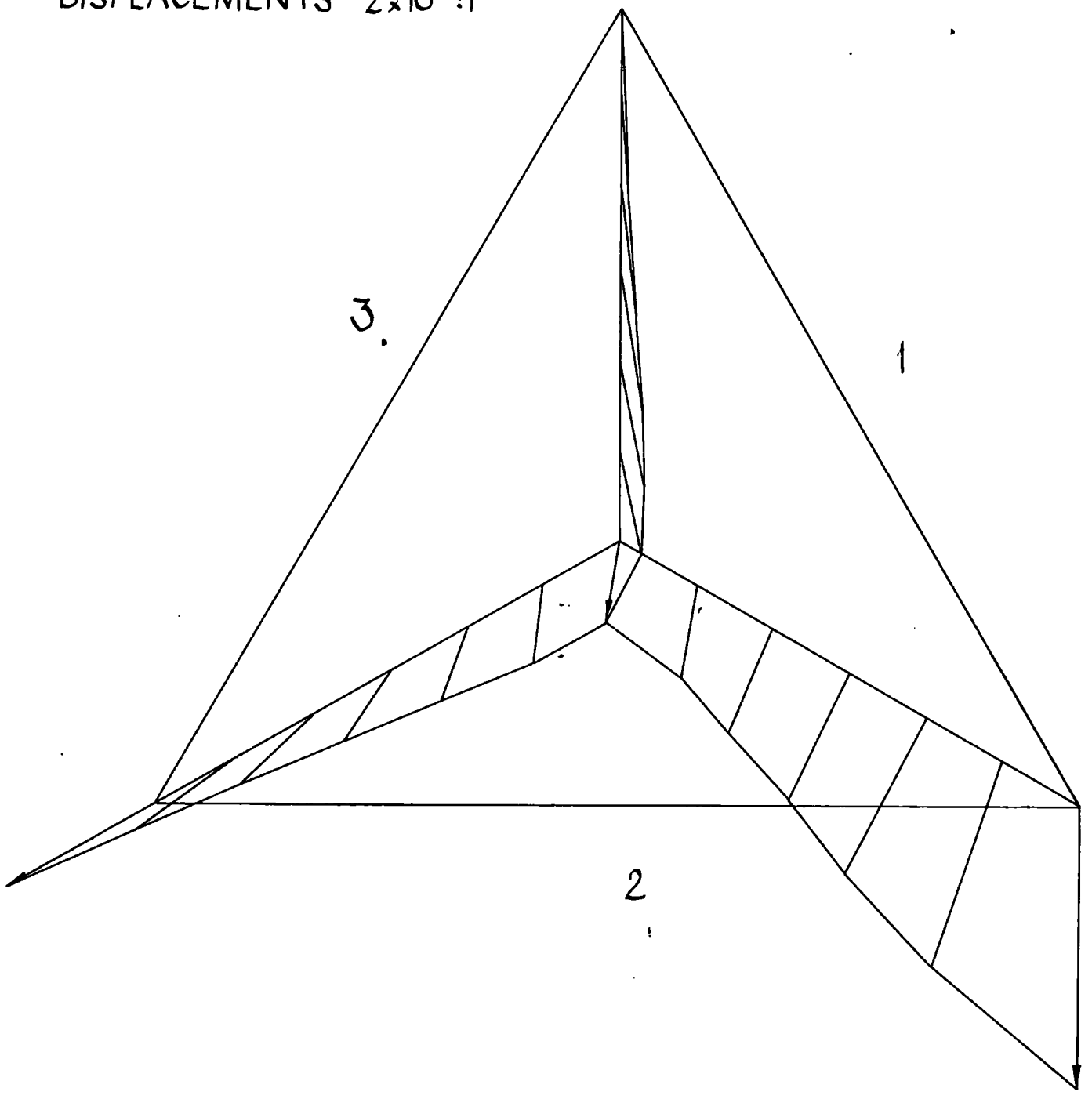

HORIZONTAL DISPLACEMENTS

1 N VERTICAL LOAD, FACE 1 CENTROID

FIG. 52 TETRAHEDRAL DOME (PLATES 3)

FIG. 53 TETRAHEDRAL DOME (PLATES 1)
1 N VERTICAL LOAD AT 1 FACE CENTROID
NORMAL DISPLACEMENTS

$\times 10^{-6}$, m

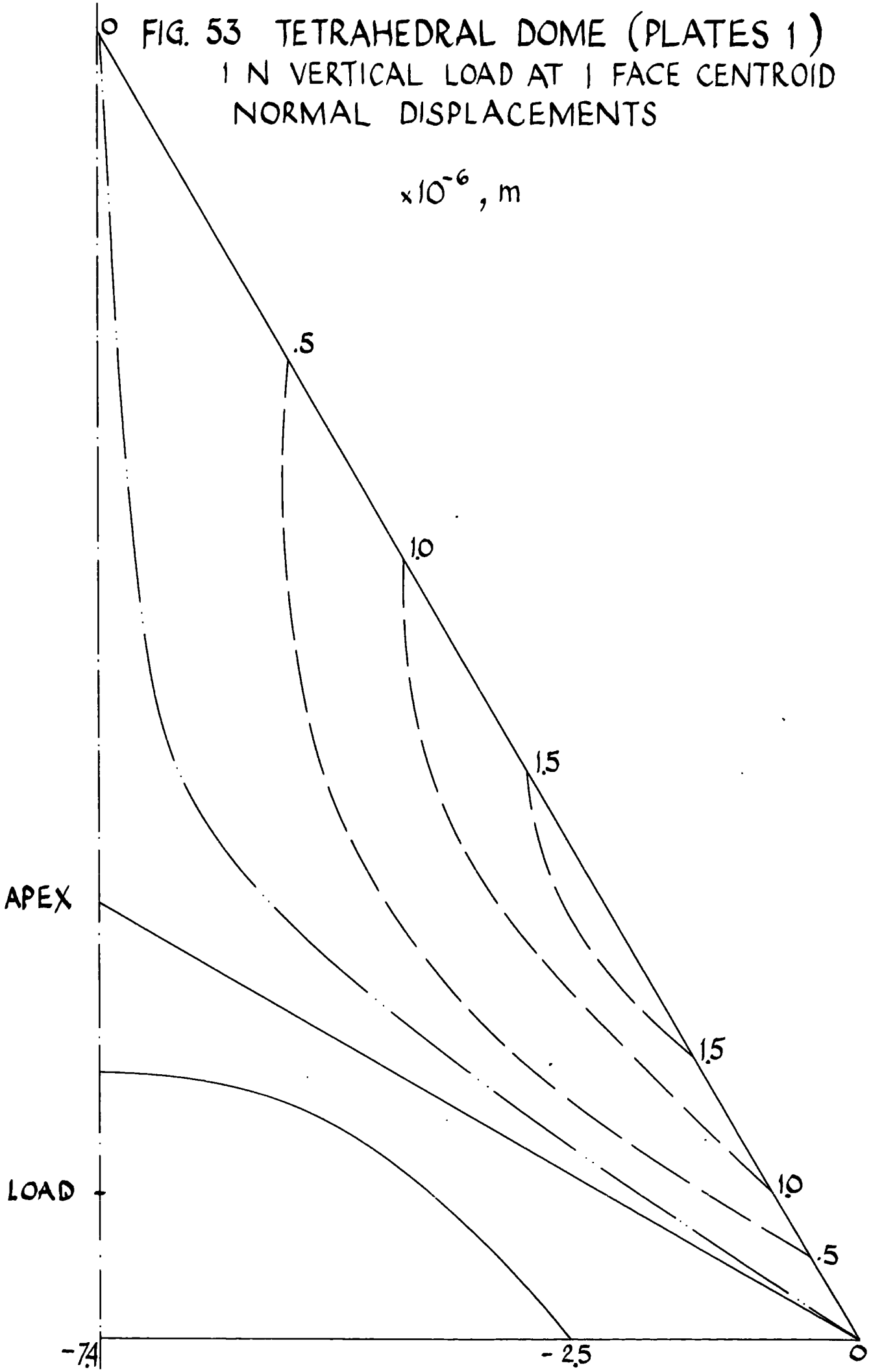

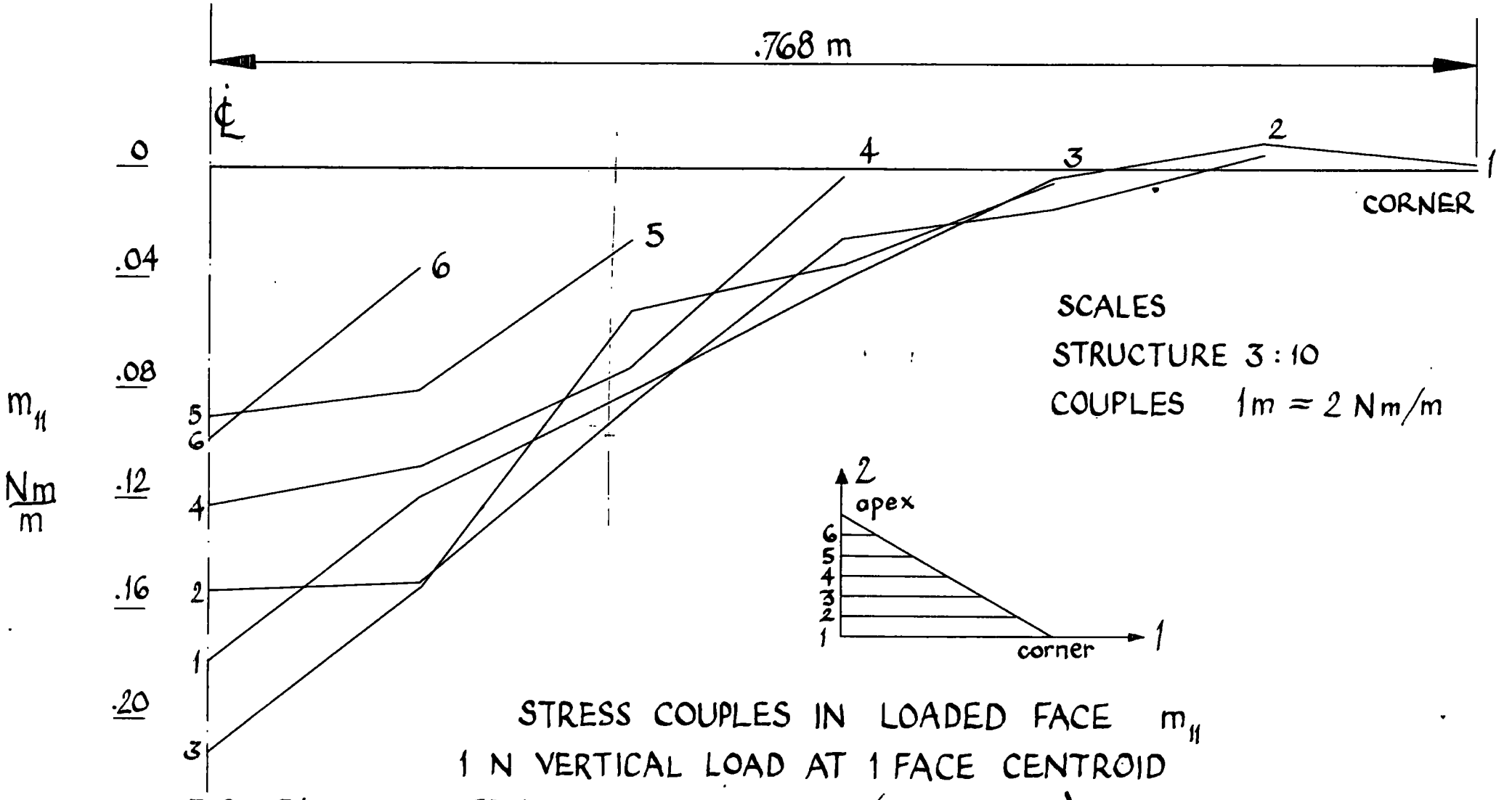

STRESS COUPLES IN LOADED FACE m_{11}

1 N VERTICAL LOAD AT 1 FACE CENTROID

FIG 54 TETRAHEDRAL DOME (PLATES 1)

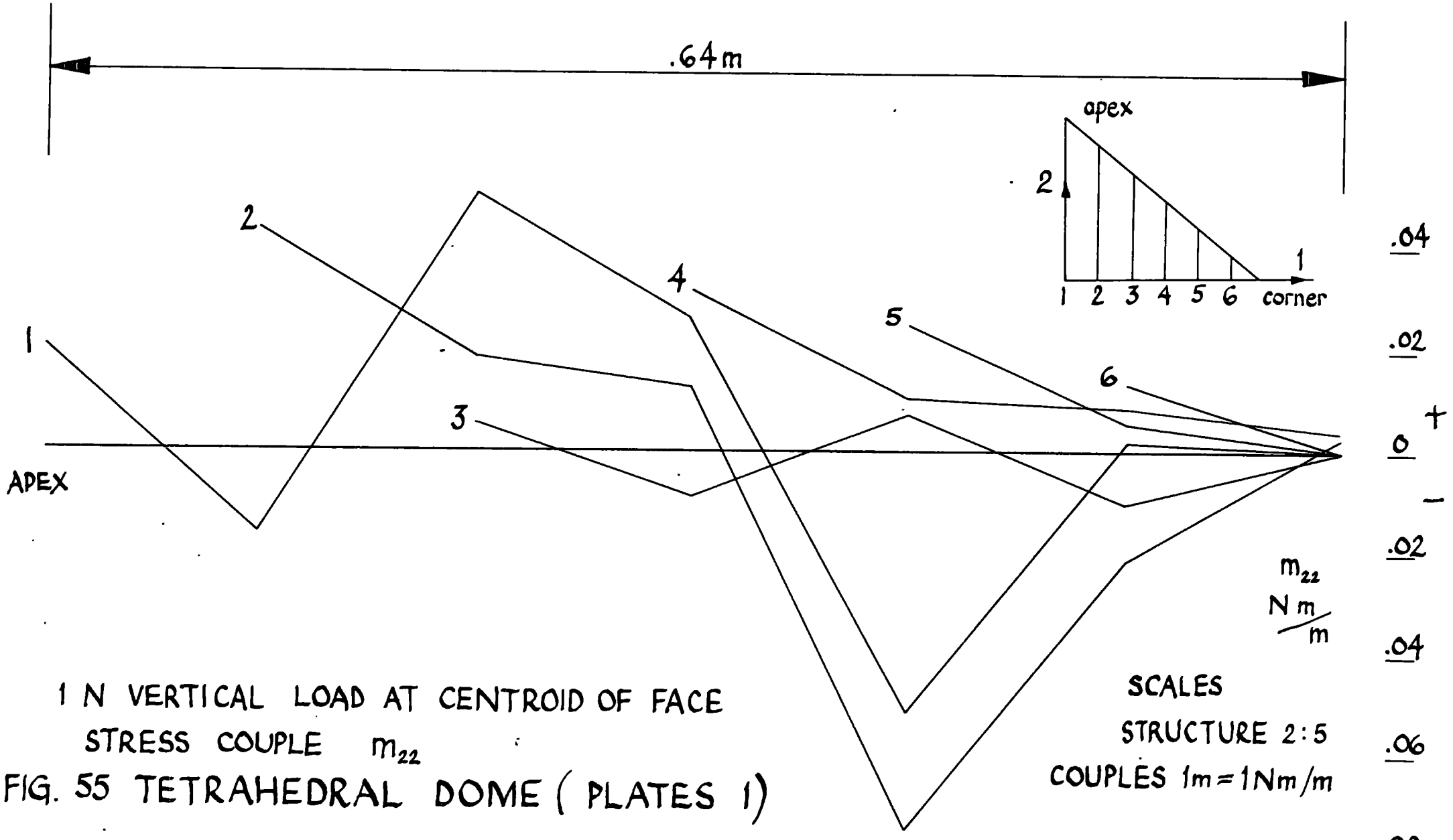

1 N VERTICAL LOAD AT CENTROID OF FACE
STRESS COUPLE m_{22}

FIG. 55 TETRAHEDRAL DOME (PLATES 1)

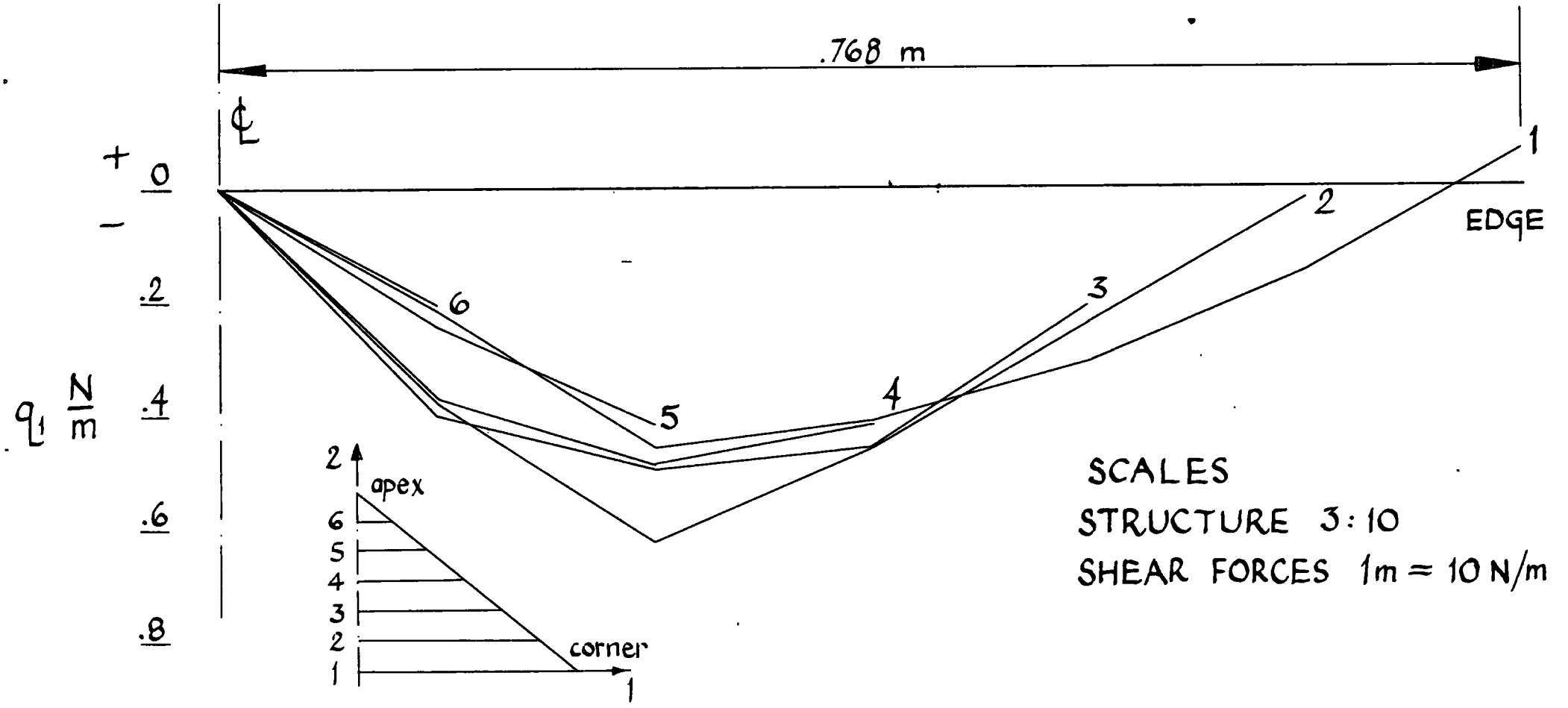

SHEAR FORCE q_1 1 N VERTICAL LOAD AT CENTROID OF FACE

FIG. 56 TETRAHEDRAL DOME (PLATES 1)

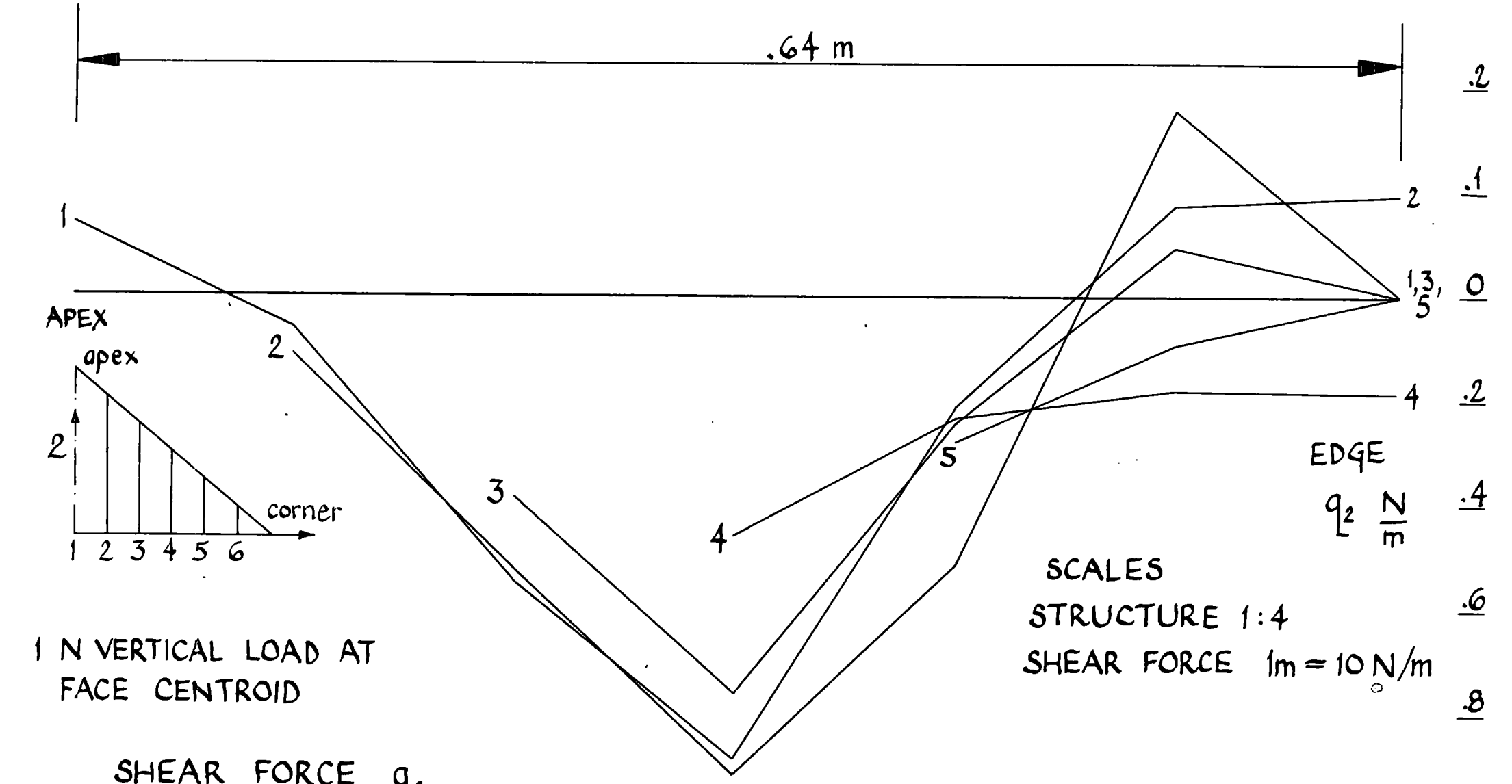

SHEAR FORCE q_2

FIG. 57 TETRAHEDRAL DOME (PLATES 1)

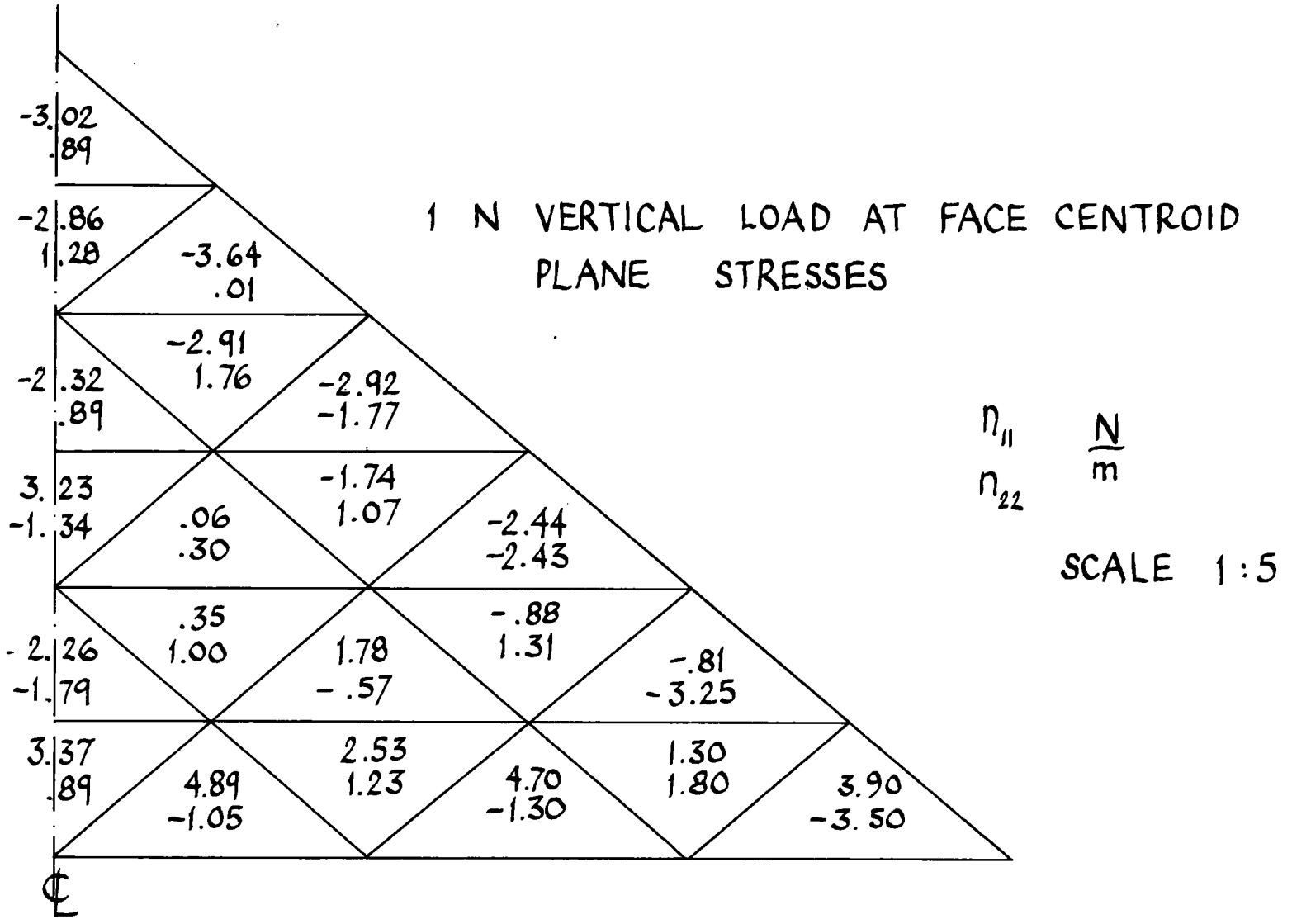

FIG. 58 TETRAHEDRAL DOME (PLATES 1)

1 N VERTICAL LOAD AT ALL 3 FACE CENTROIDS
CONVERGENCE OF MID EDGE DISPLACEMENT

FIG. 59 TETRAHEDRAL DOME (PLATES 1)

1 N VERTICAL LOAD AT 4 FACE CENTROIDS
SCALES
STRUCTURE 3:20
DISPLACEMENTS 10^5:1

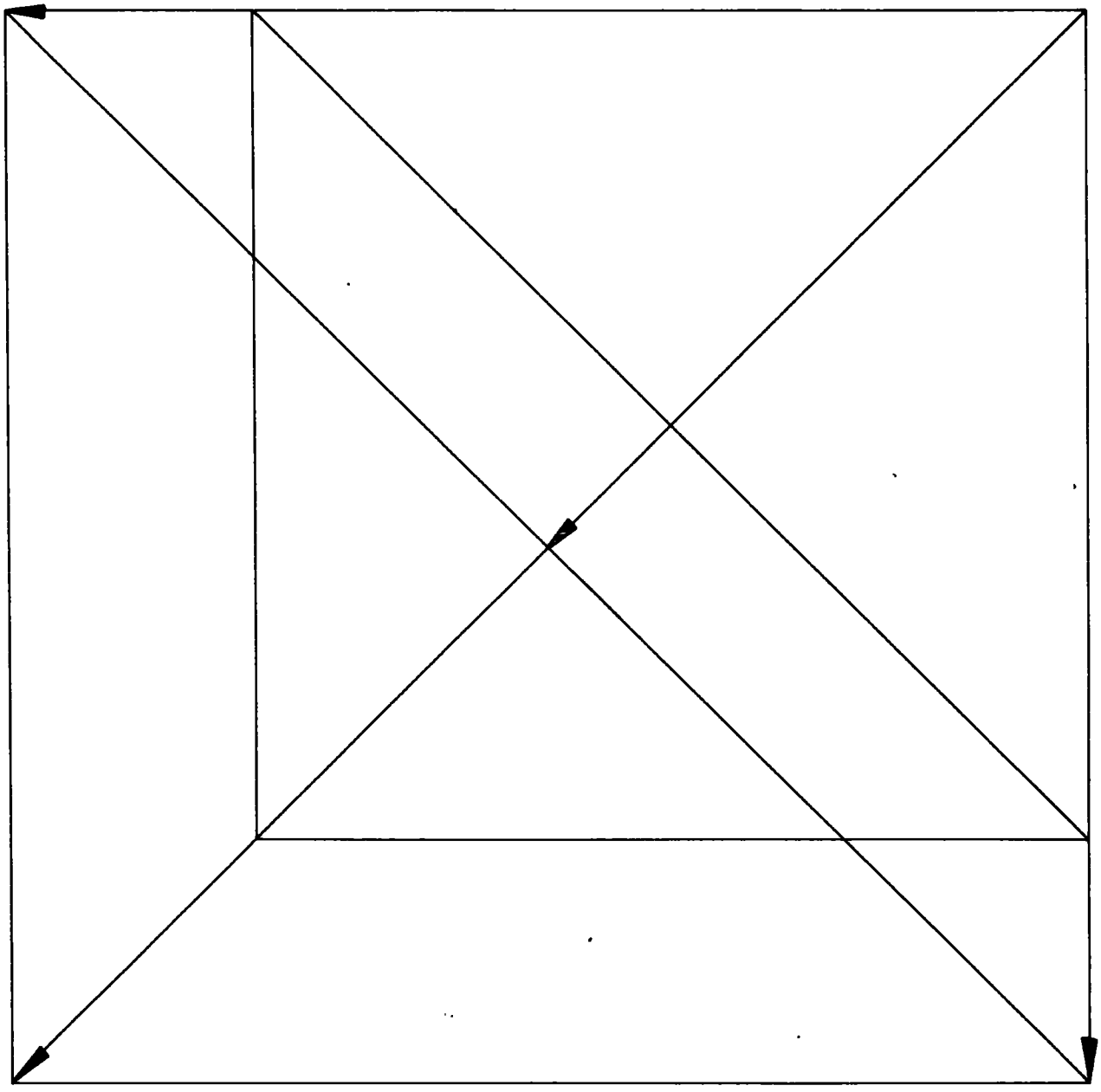

HORIZONTAL DISPLACEMENTS

FIG 60 SQUARE PYRAMID

1 N VERTICAL LOAD AT CENTROID OF FACE 3

SCALES

STRUCTURE 3 : 20

DISPLACEMENTS $2 \times 10^5 : 1$

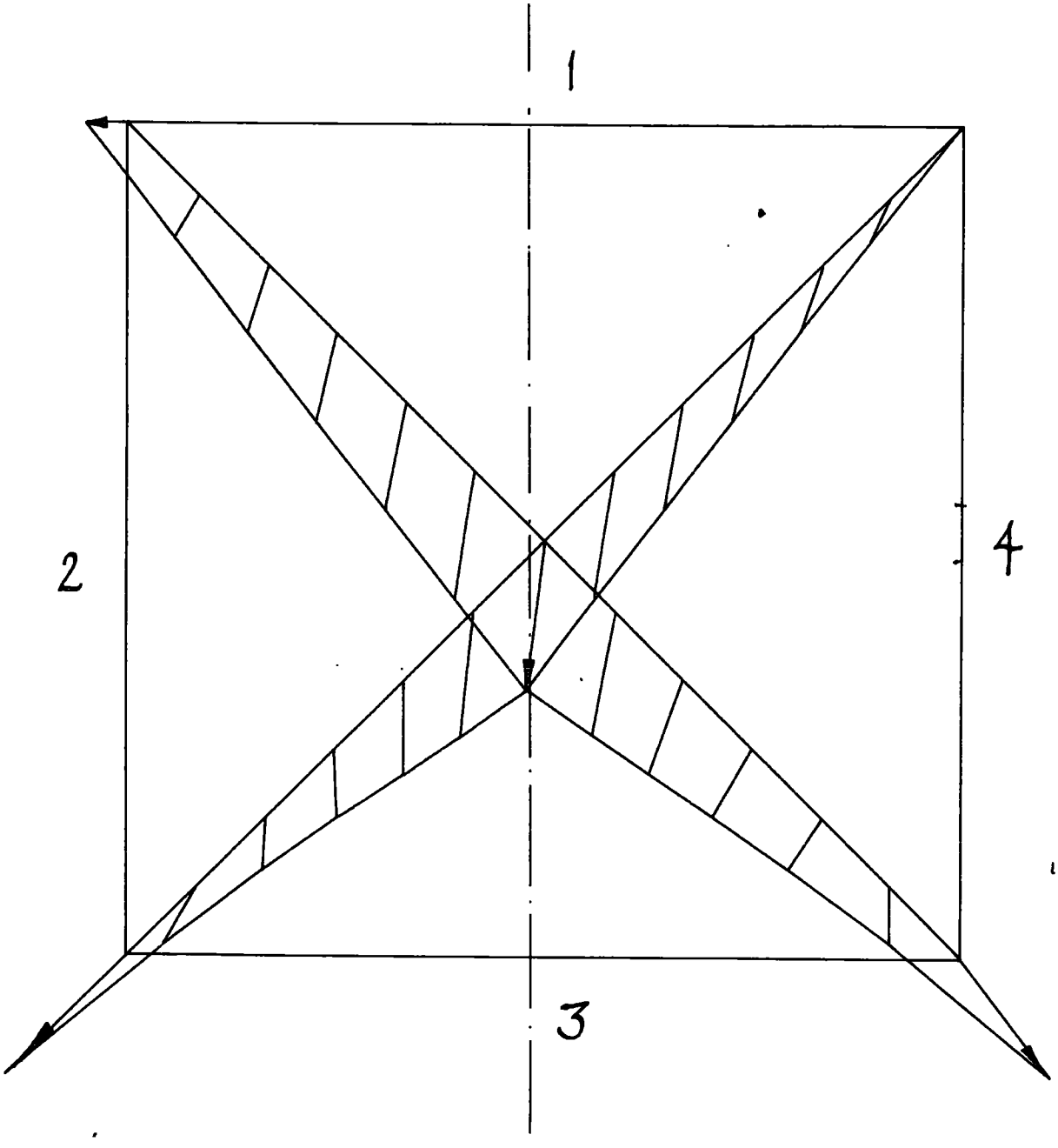

HORIZONTAL DISPLACEMENTS

FIG.61 SQUARE PYRAMID

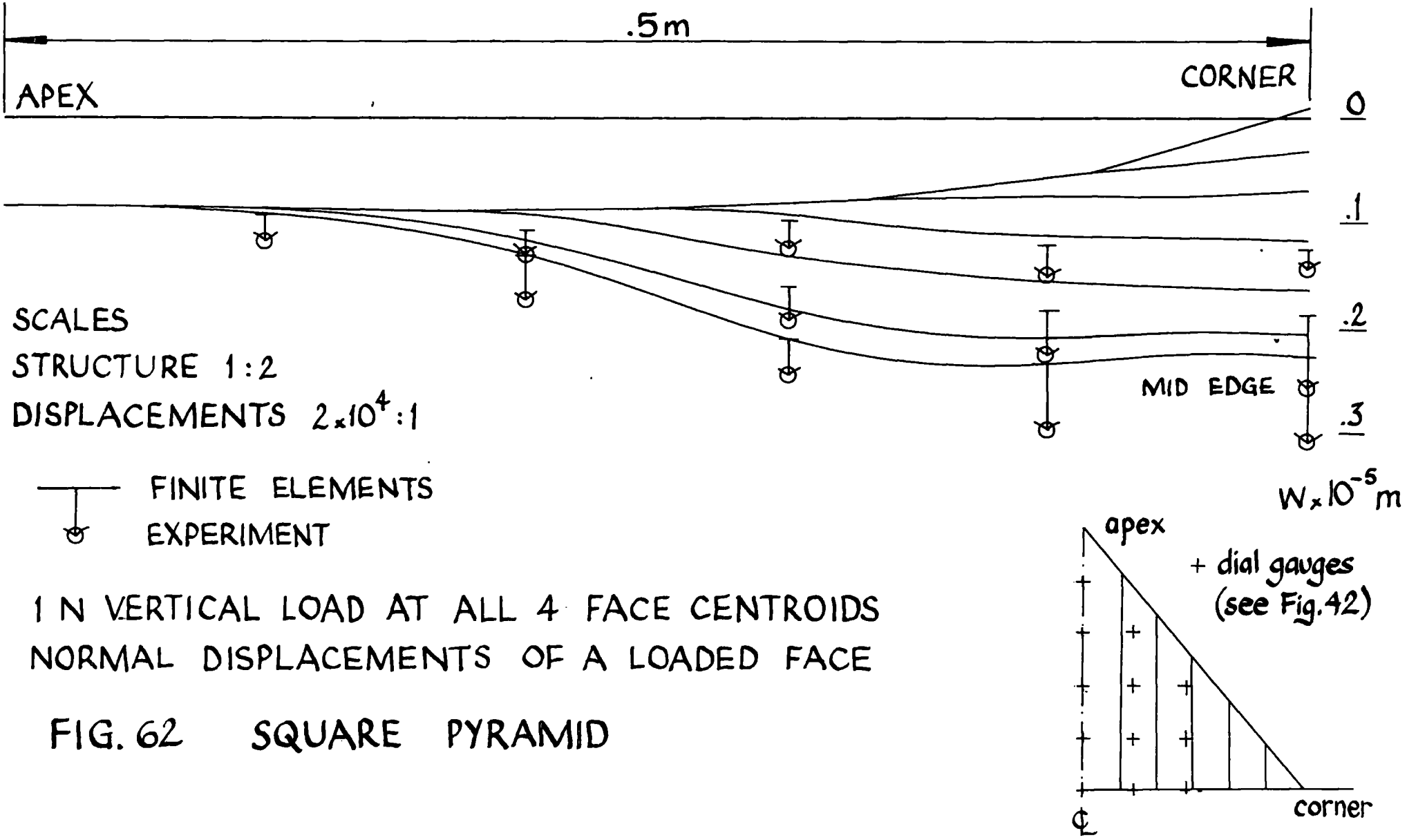

1 N VERTICAL LOAD AT ALL 4 FACE CENTROIDS
NORMAL DISPLACEMENTS OF A LOADED FACE

FIG. 62 SQUARE PYRAMID

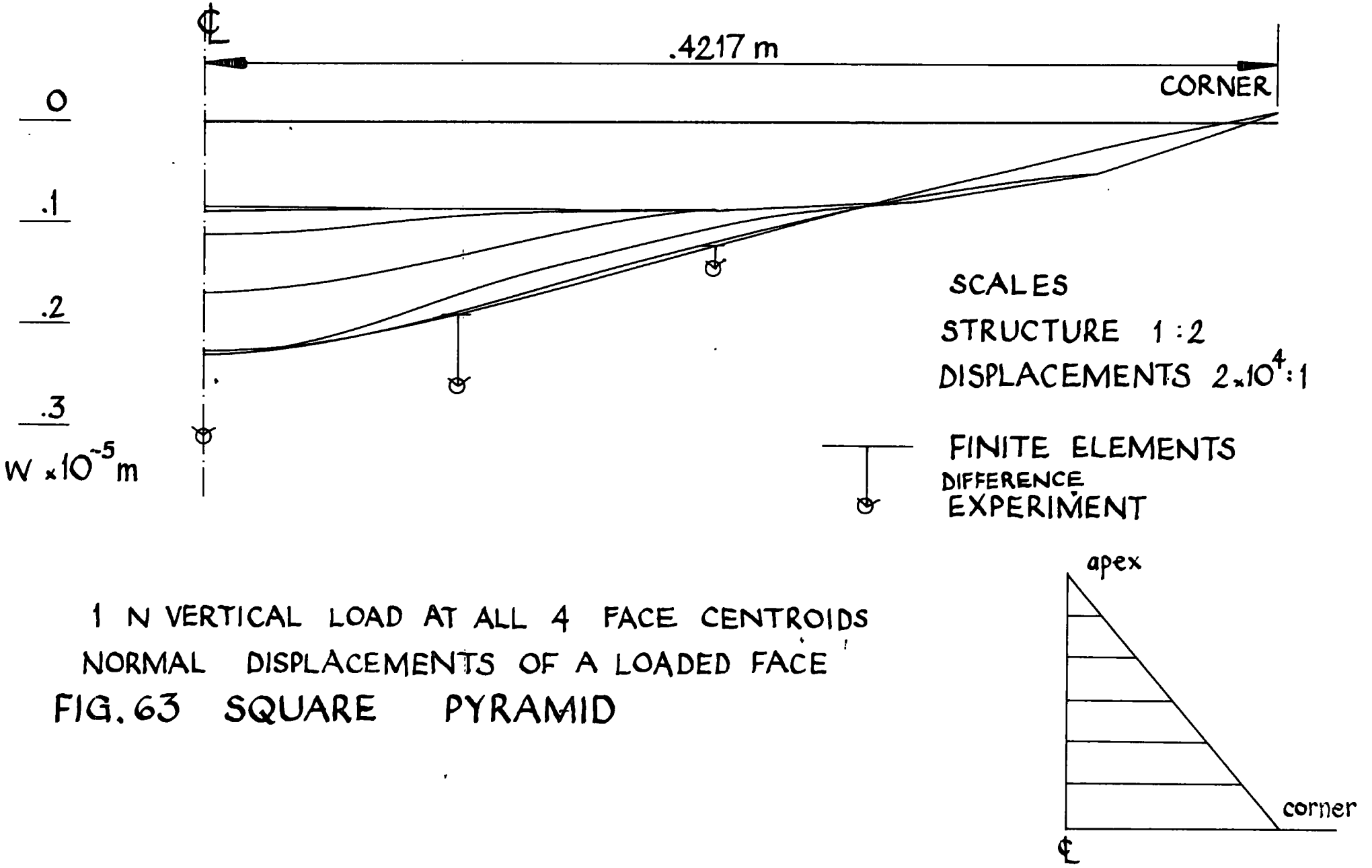

1 N VERTICAL LOAD AT ALL 4 FACE CENTROIDS
NORMAL DISPLACEMENTS OF A LOADED FACE

FIG. 63 SQUARE PYRAMID

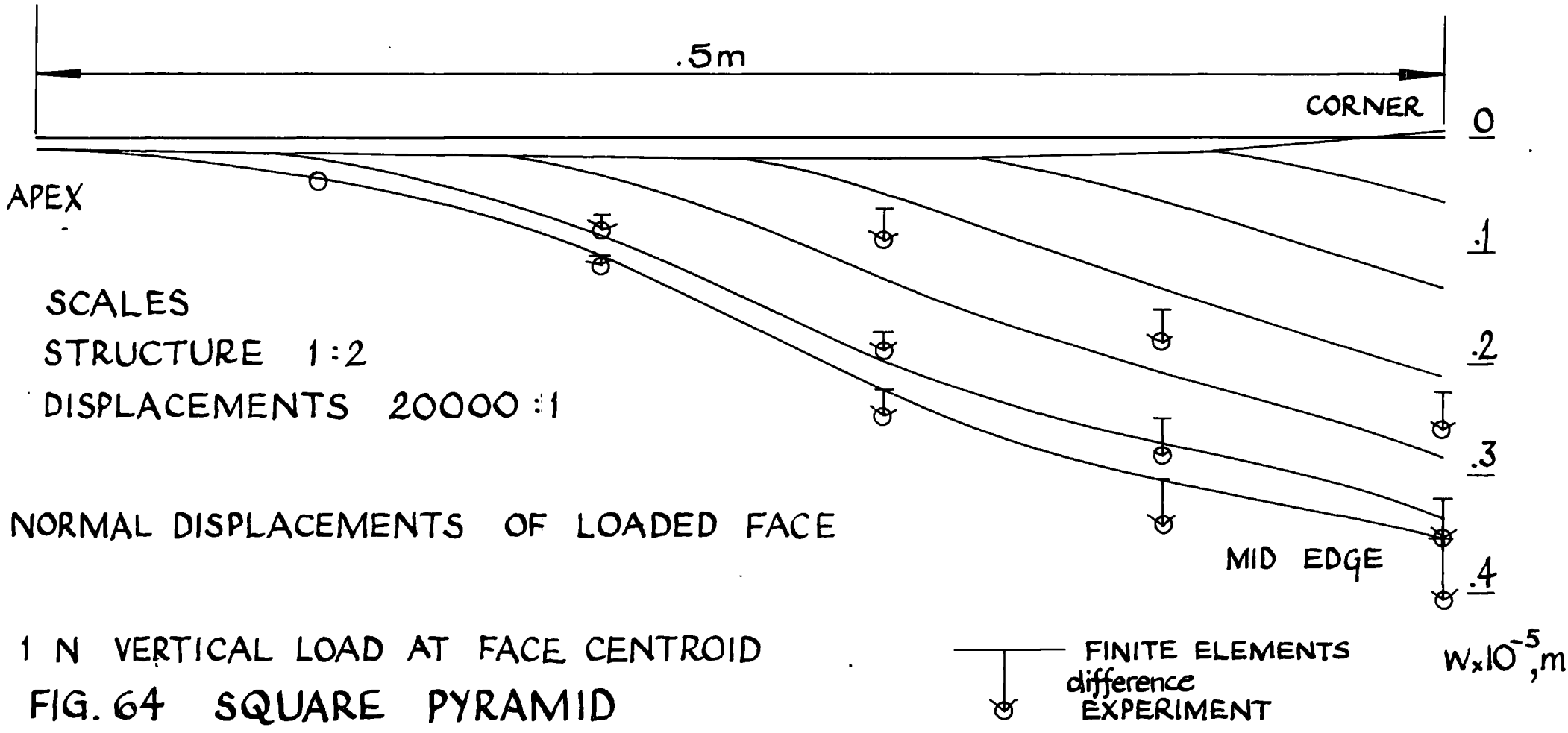

FIG. 64 SQUARE PYRAMID

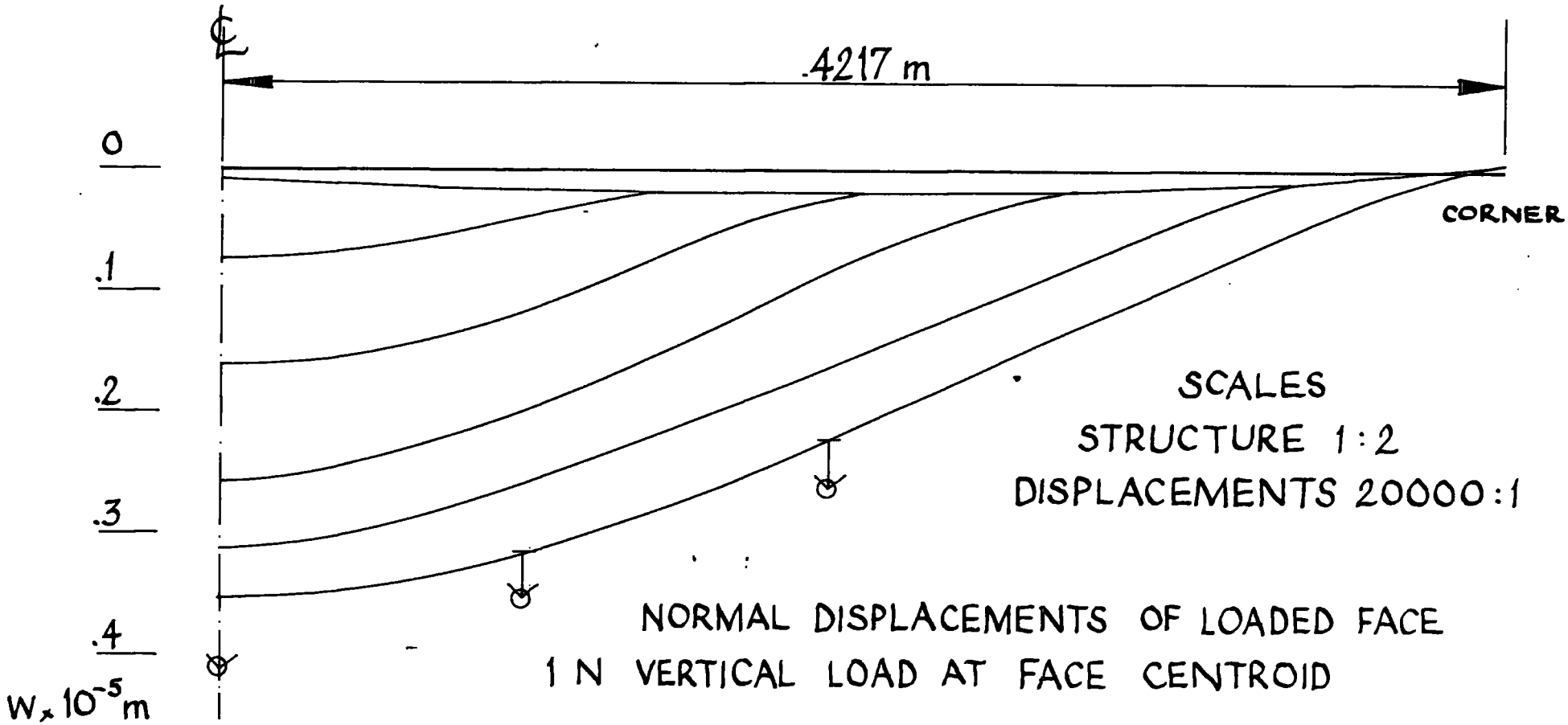

FIG. 65 SQUARE PYRAMID

FINITE ELEMENTS
DIFFERENCE
EXPERIMENT

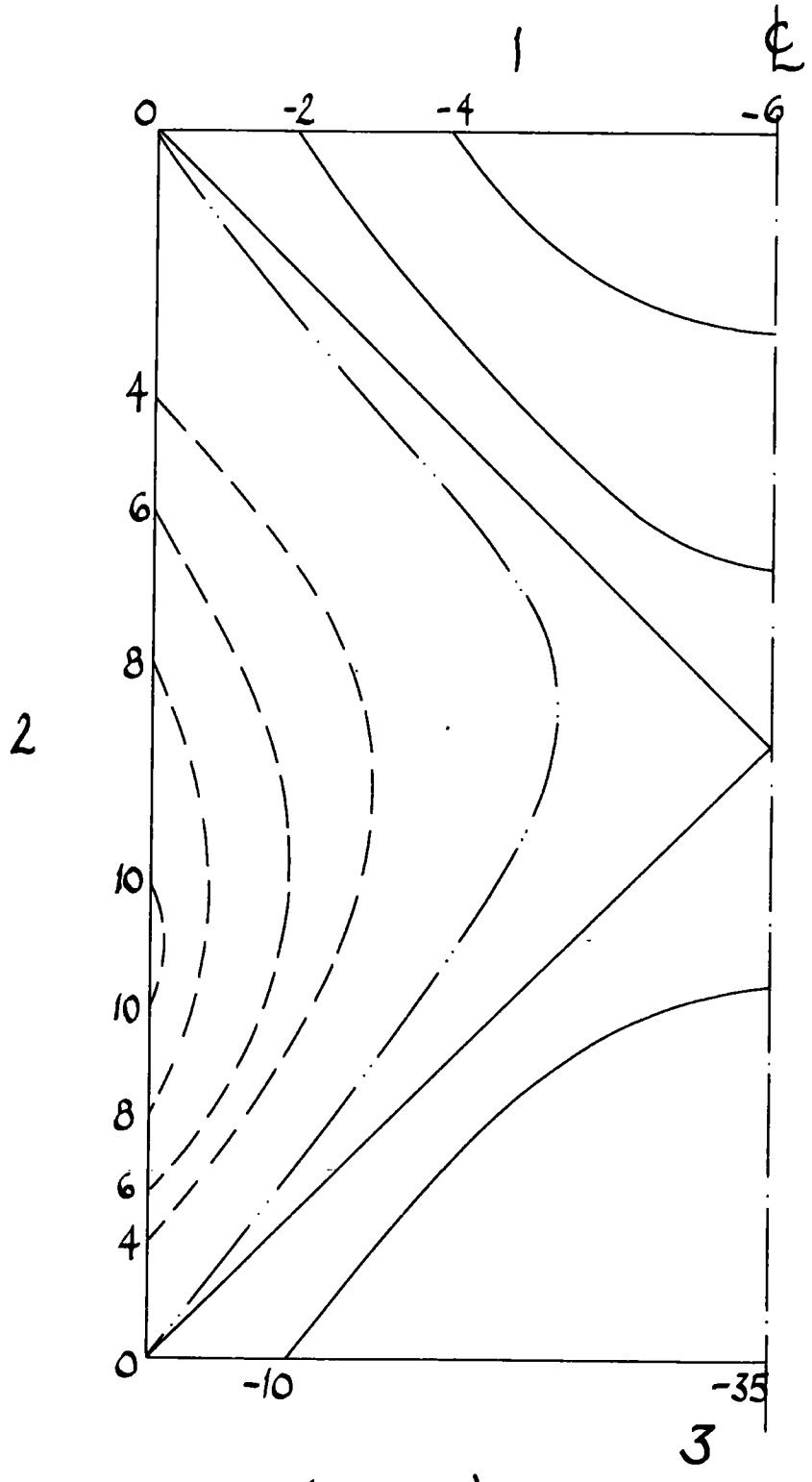

NORMAL DISPLACEMENTS $(m \times 10^{-7})$
SCALE 1 : 5

1 N VERTICAL LOAD AT CENTROID OF FACE 3

FIG. 66 SQUARE PYRAMID

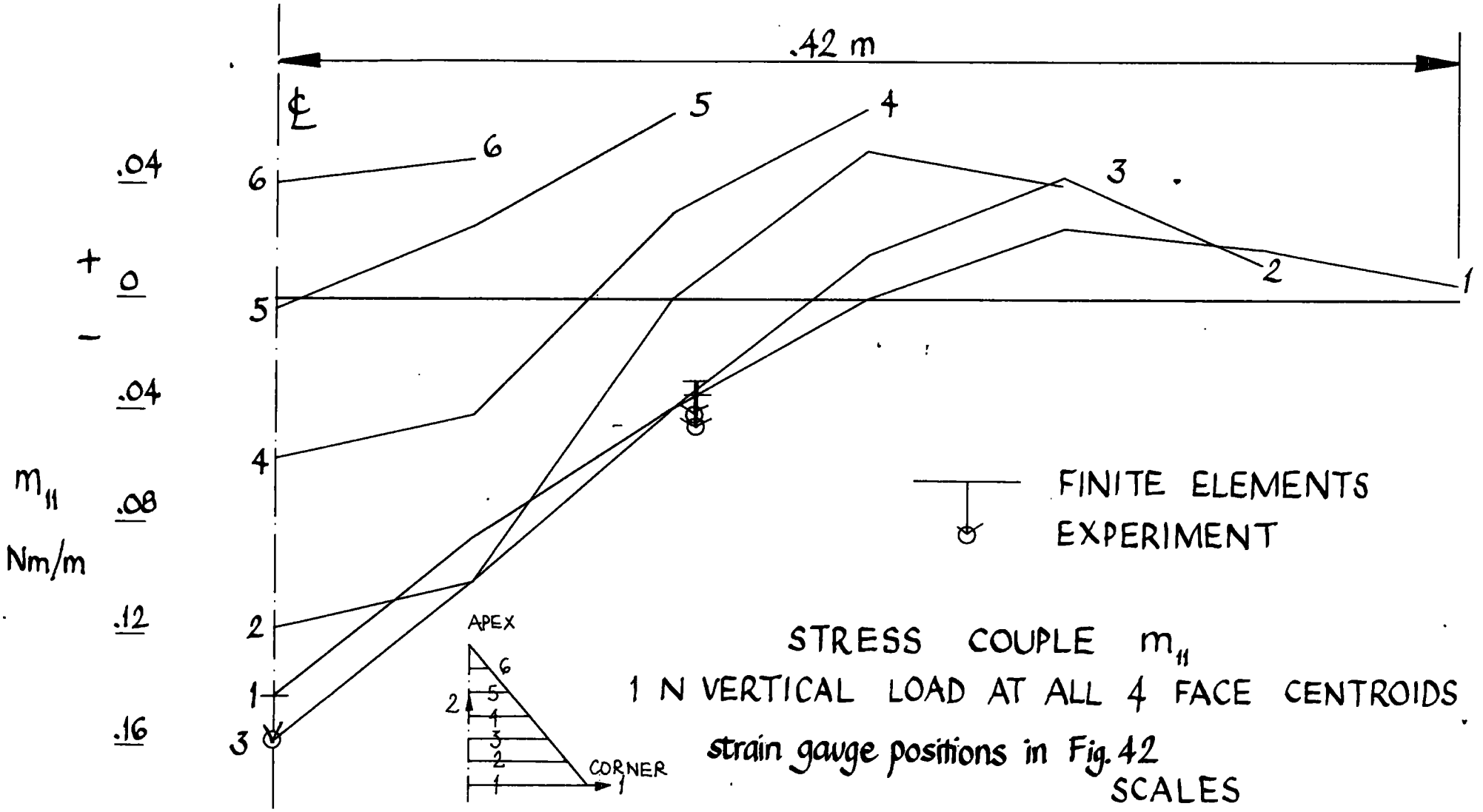

FIG. 67 SQUARE PYRAMID

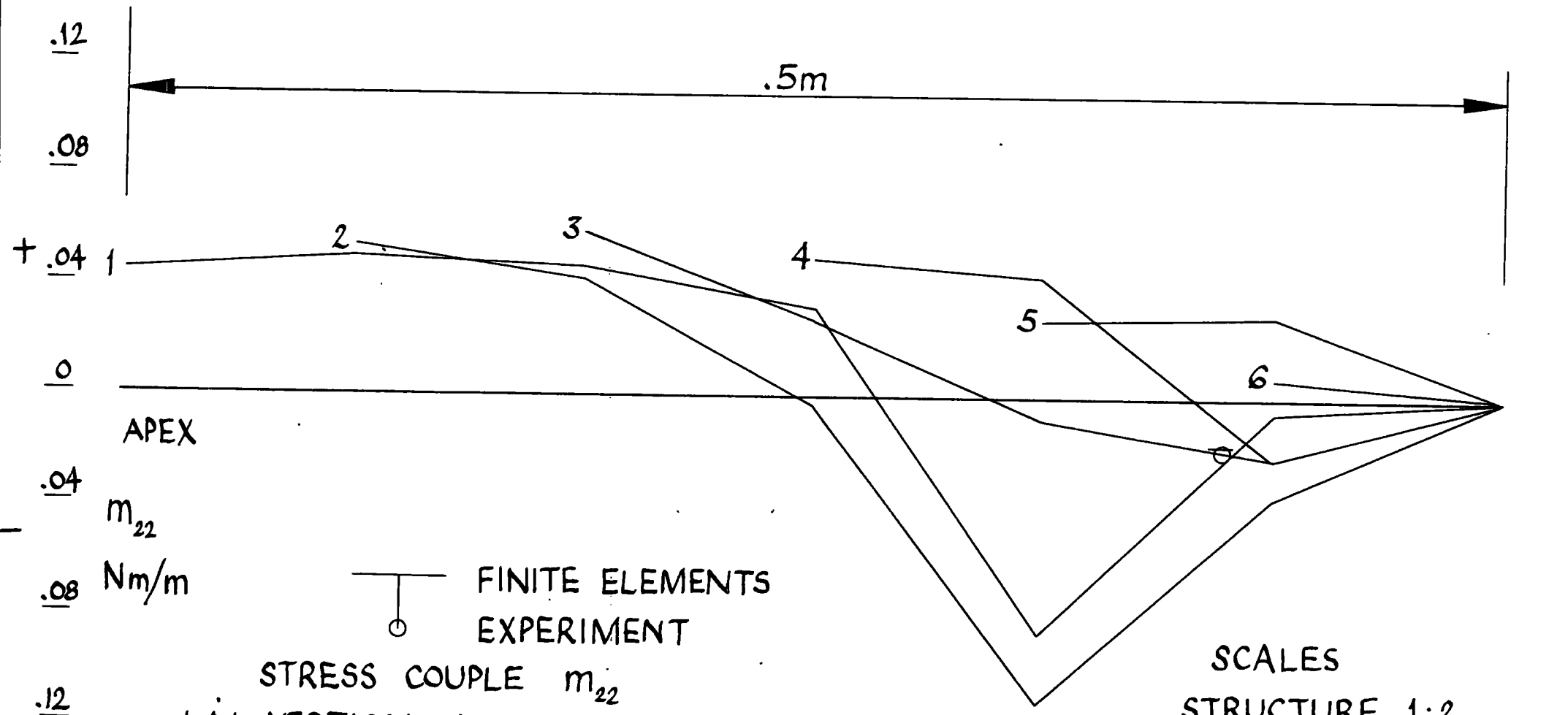

FIG. 68 SQUARE PYRAMID

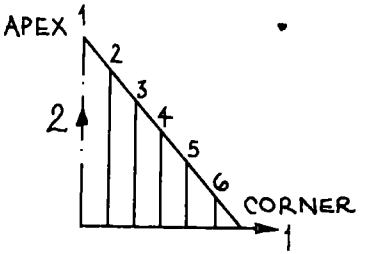

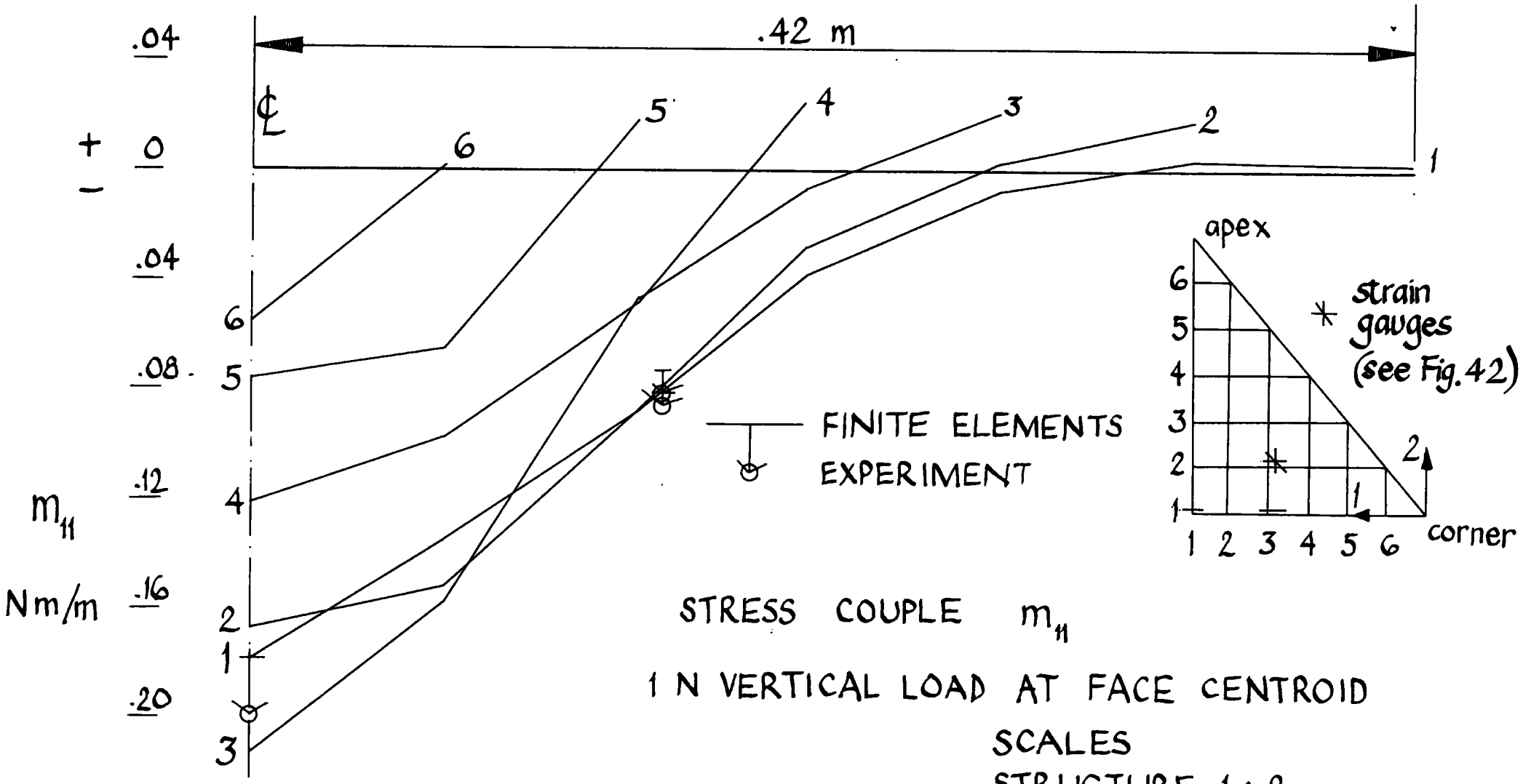

STRESS COUPLE m_{11}

1 N VERTICAL LOAD AT FACE CENTROID

SCALES
STRUCTURE 1 : 2
COUPLES 1 m = 2 Nm/m

FIG. 69 SQUARE PYRAMID

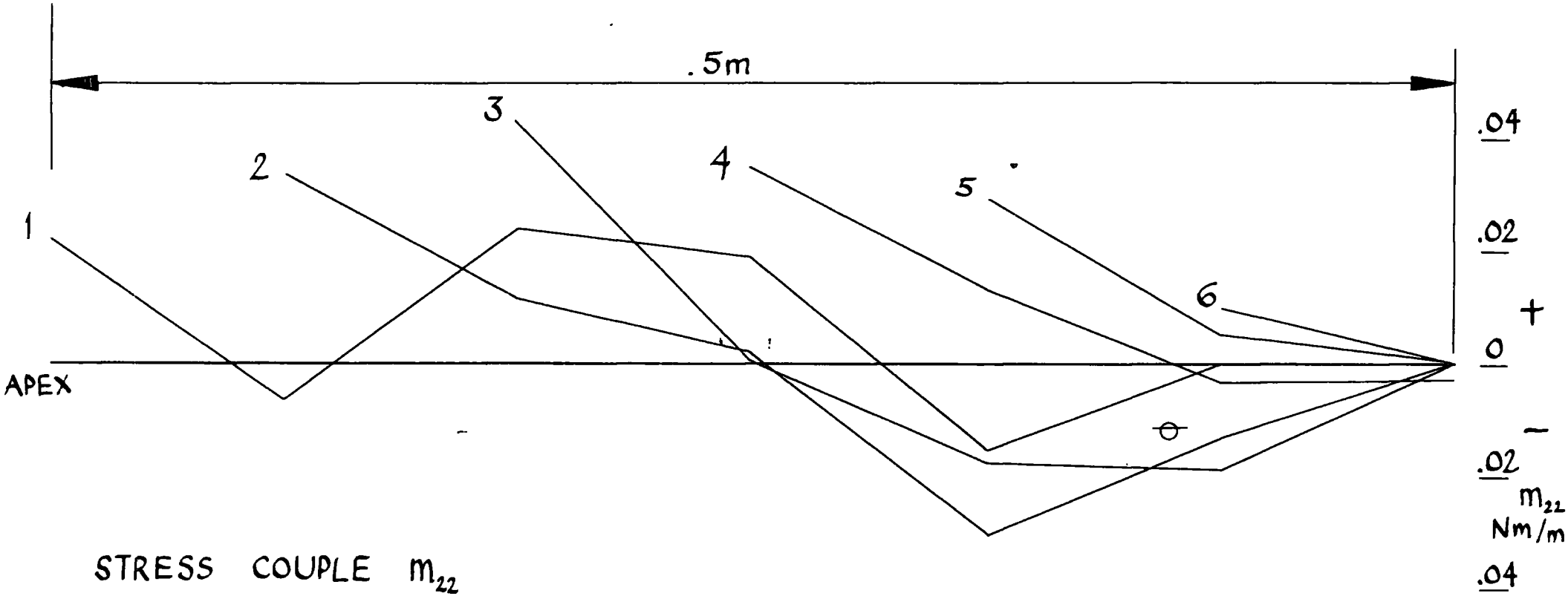

STRESS COUPLE m_{22}
1N VERTICAL LOAD AT FACE CENTROID

FINITE ELEMENTS
EXPERIMENT

SCALES
STRUCTURE 1:2
COUPLES 1m = 2 Nm/m

FIG. 70 SQUARE PYRAMID

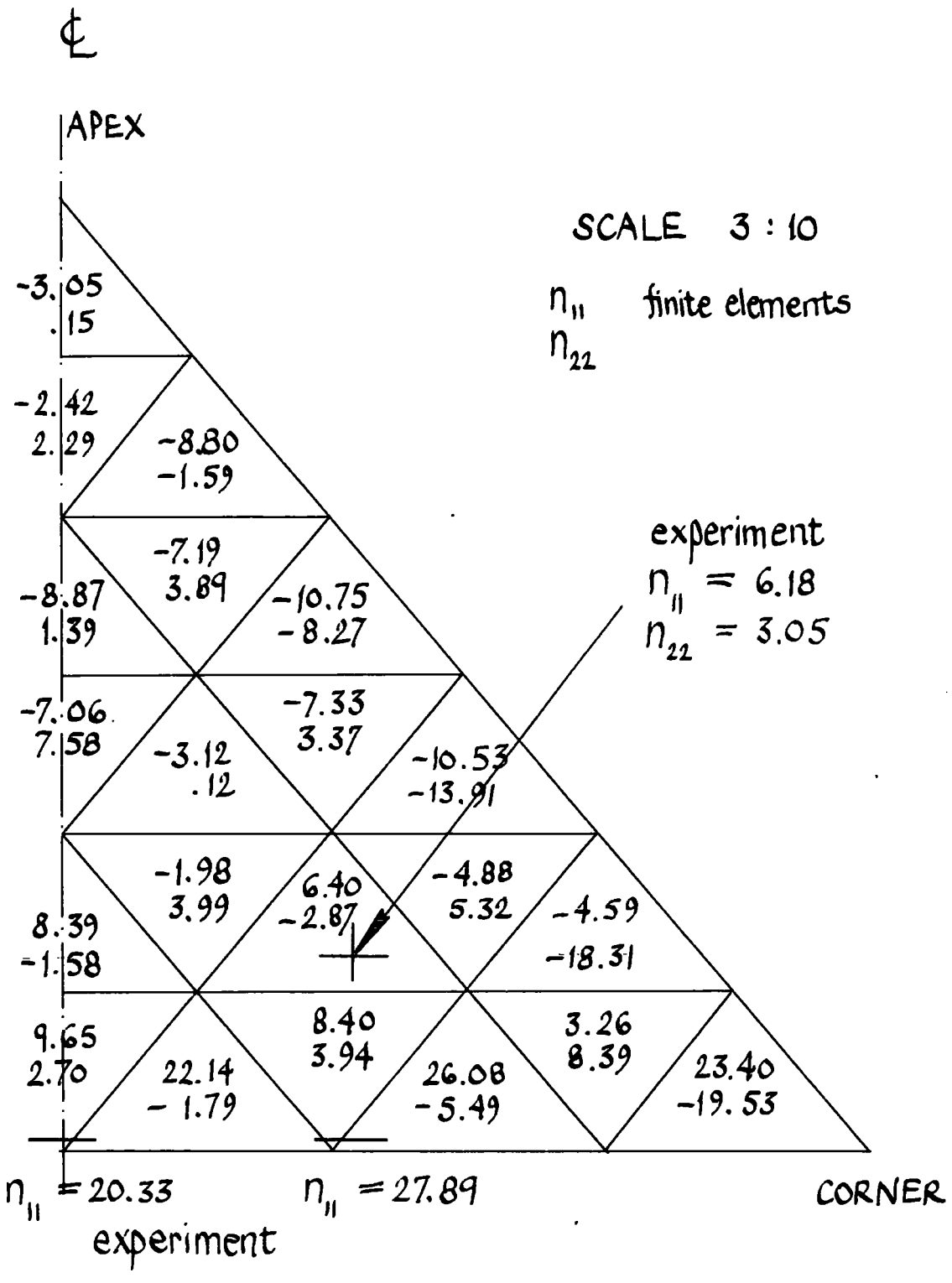

1 N VERTICAL LOAD AT ALL 4 FACE CENTROIDS
DIRECT STRESS RESULTANTS, n_{11} AND n_{22} (N/m)

FIG. 71 SQUARE PYRAMID

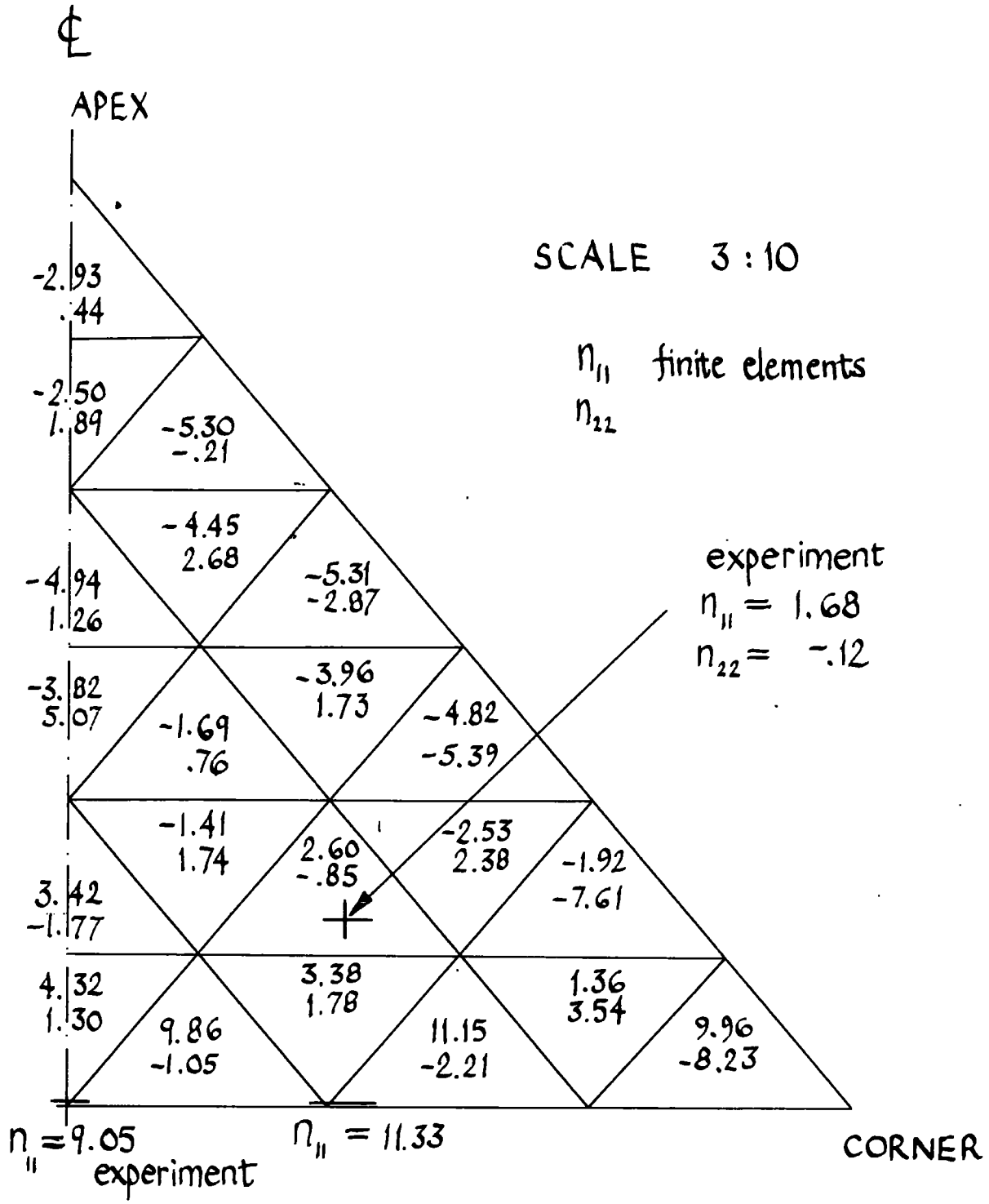

1 N VERTICAL LOAD AT FACE CENTROID
DIRECT STRESS RESULTANTS, n_{11} AND n_{22} (N/m)

FIG. 72 SQUARE PYRAMID

HORIZONTAL DISPLACEMENTS

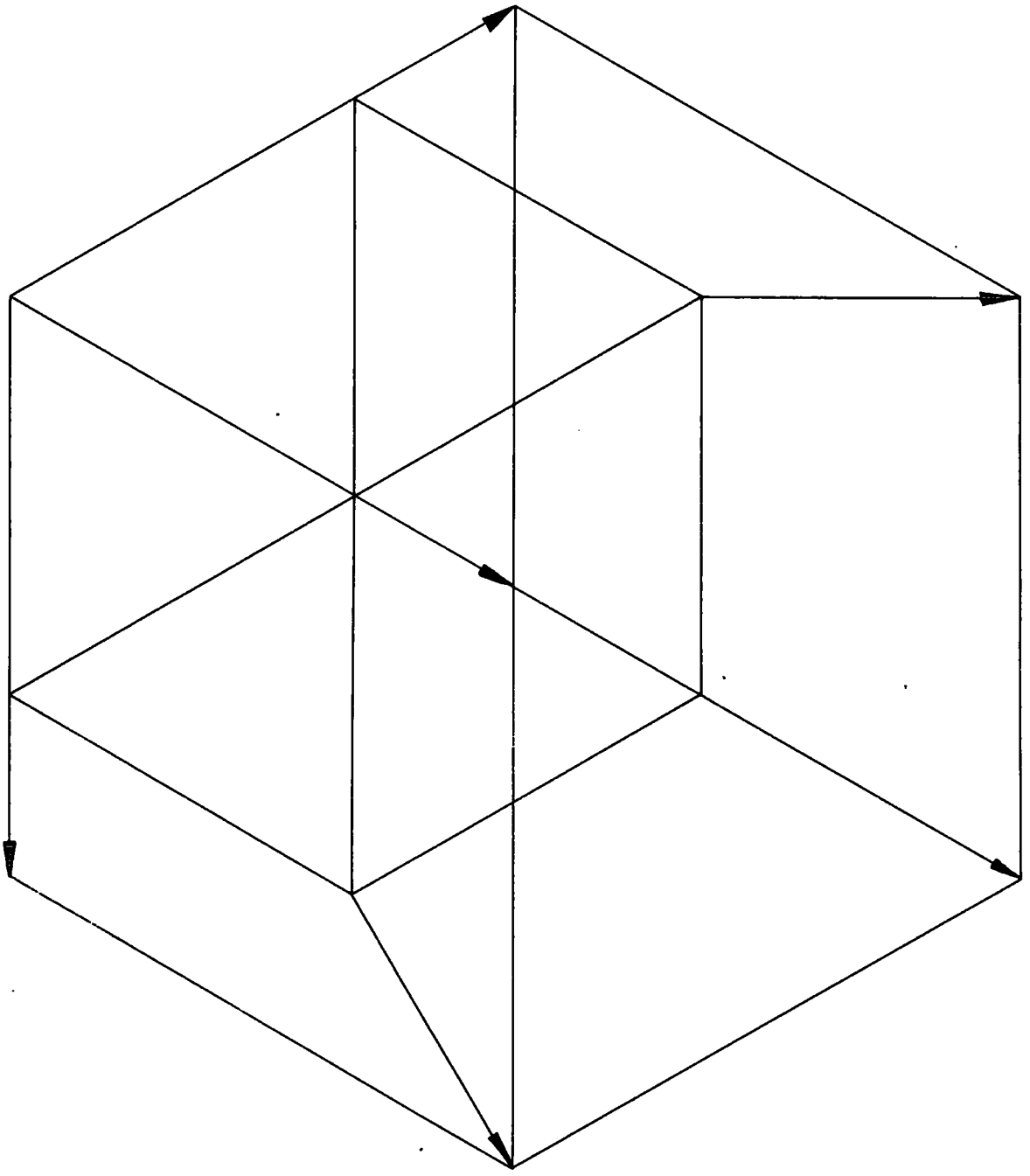

1 N VERTICAL LOAD AT CENTROID OF EACH FACE
SCALES
STRUCTURE 3:50
DISPLACEMENTS 50000:1

FIG.73 HEXAGONAL DOME

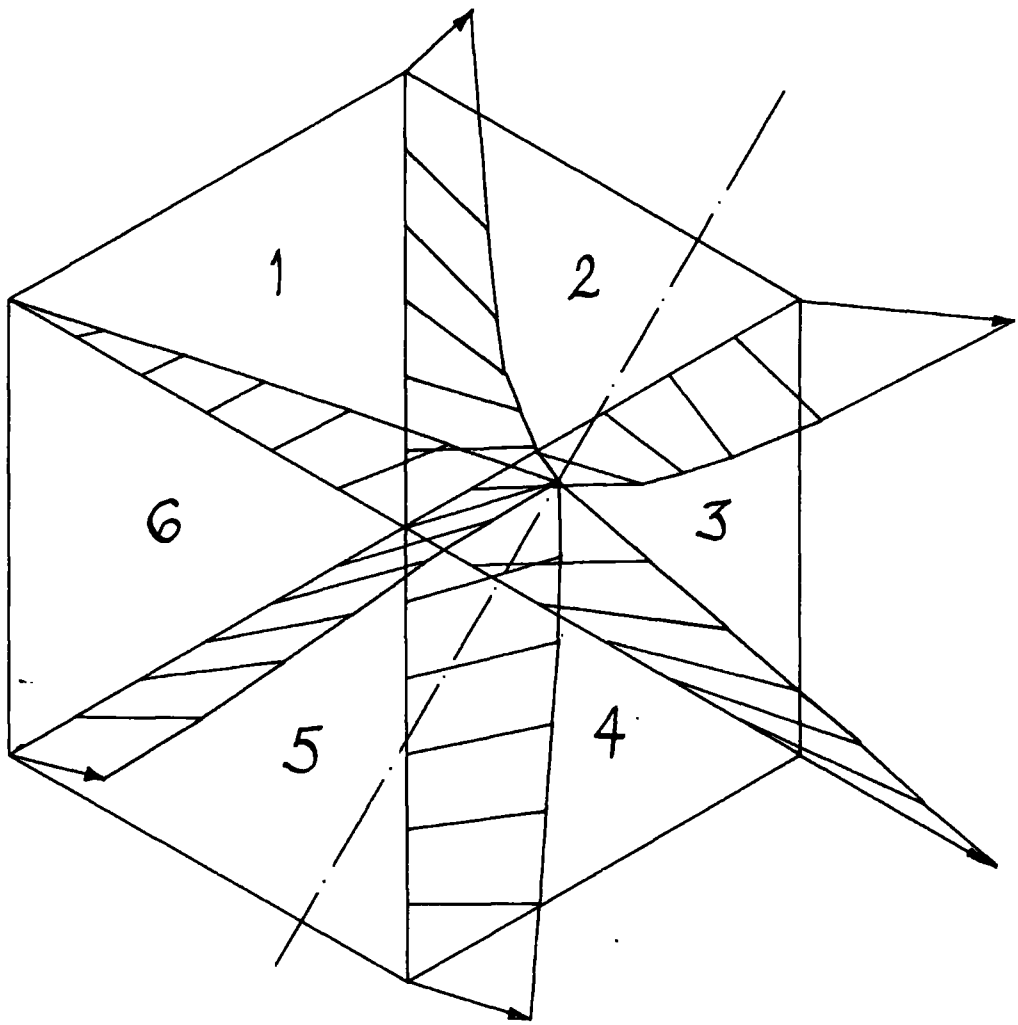

HORIZONTAL DISPLACEMENTS
1 N VERTICAL LOAD AT CENTROID OF FACE 2
SCALES
DISPLACEMENTS $1 : 10^5$
STRUCTURE $3 : 50$

FIG. 74 HEXAGONAL DOME

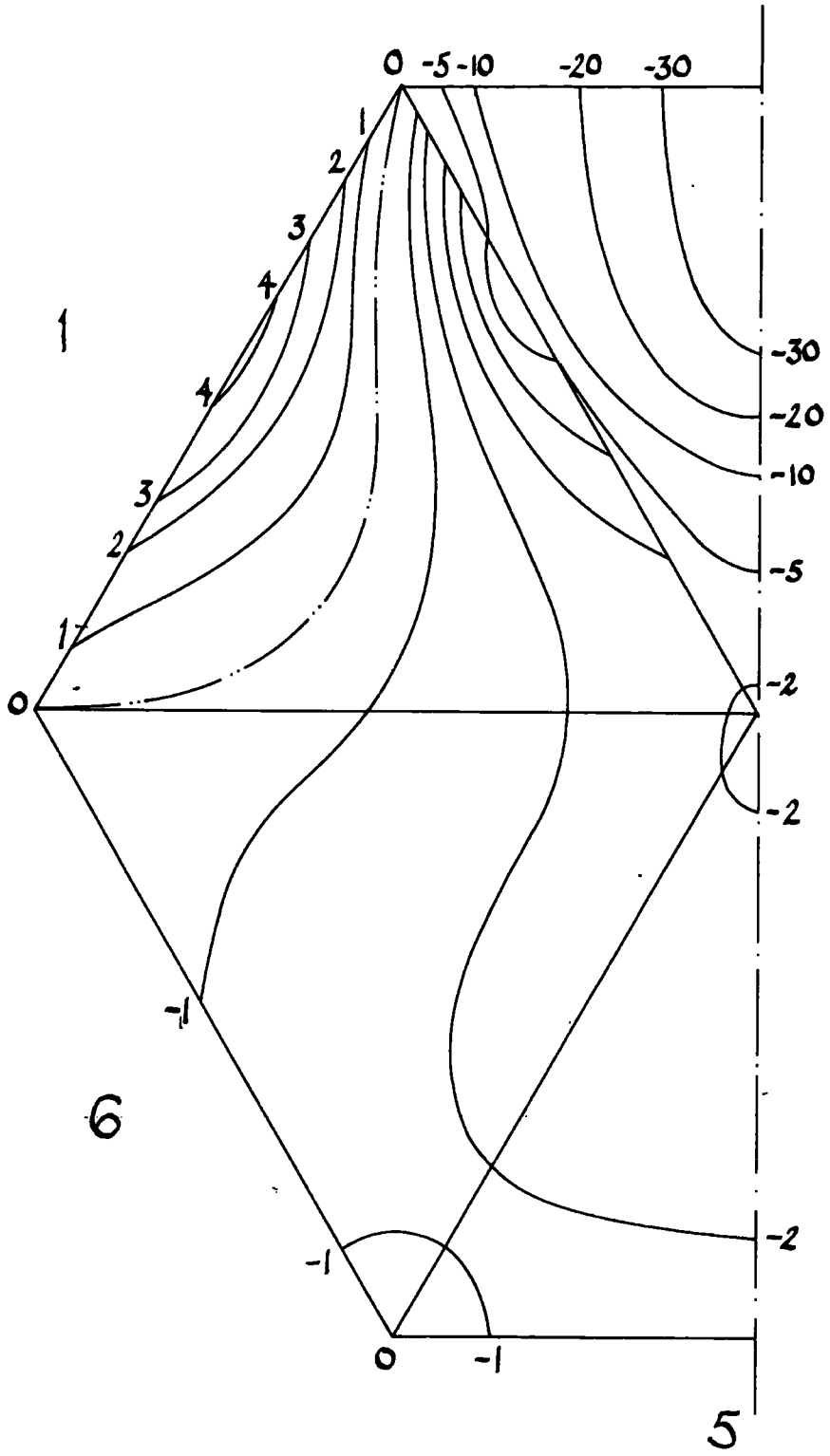

SCALE 1 : 10

NORMAL DISPLACEMENTS ($m \times 10^{-6}$)

FIG.75 HEXAGONAL DOME

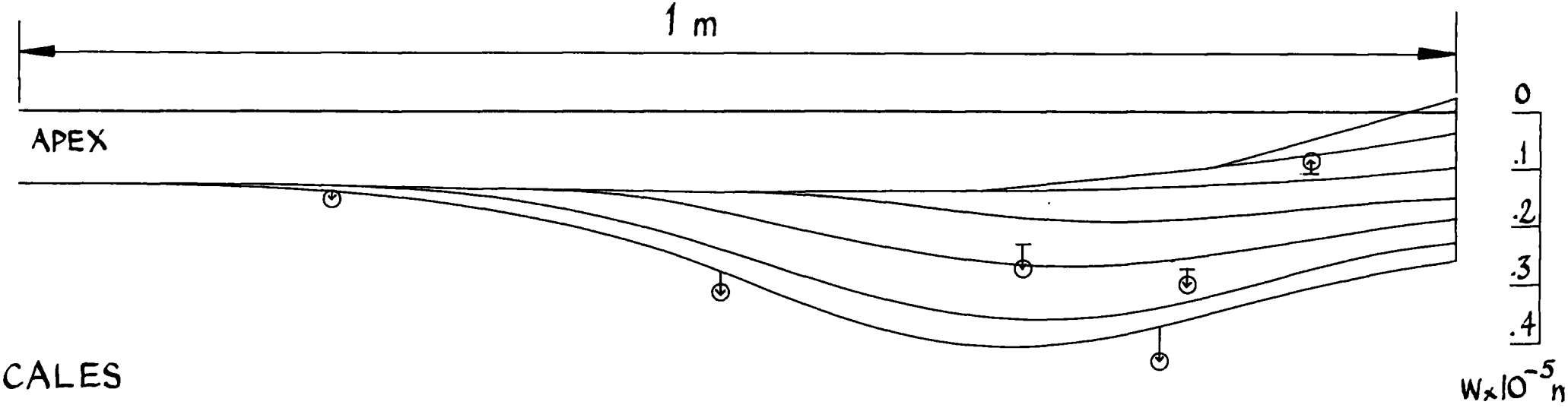

SCALES
STRUCTURE 1 : 4
DISPLACEMENTS 10^4 : 1

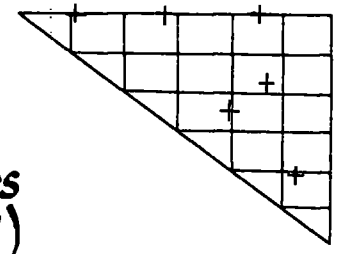

+ dial gauges
(see Fig. 41)

EXPERIMENT
FINITE ELEMENTS

1N VERTICAL LOAD AT ALL FACE CENTROIDS

FIG. 76 HEXAGONAL DOME, ALL FACES LOADED

NORMAL DISPLACEMENTS OF 1 FACE

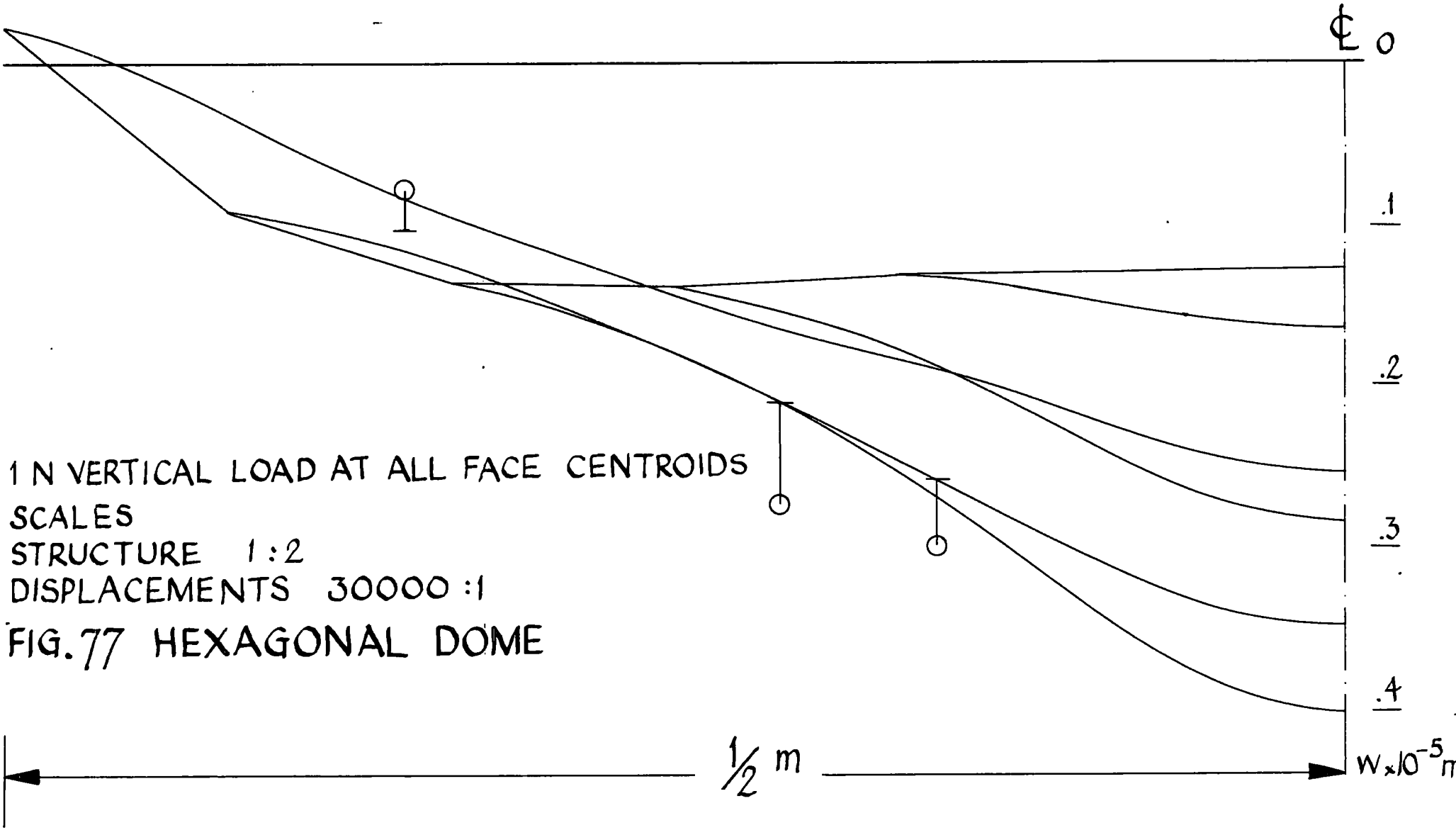

FIG. 77 HEXAGONAL DOME

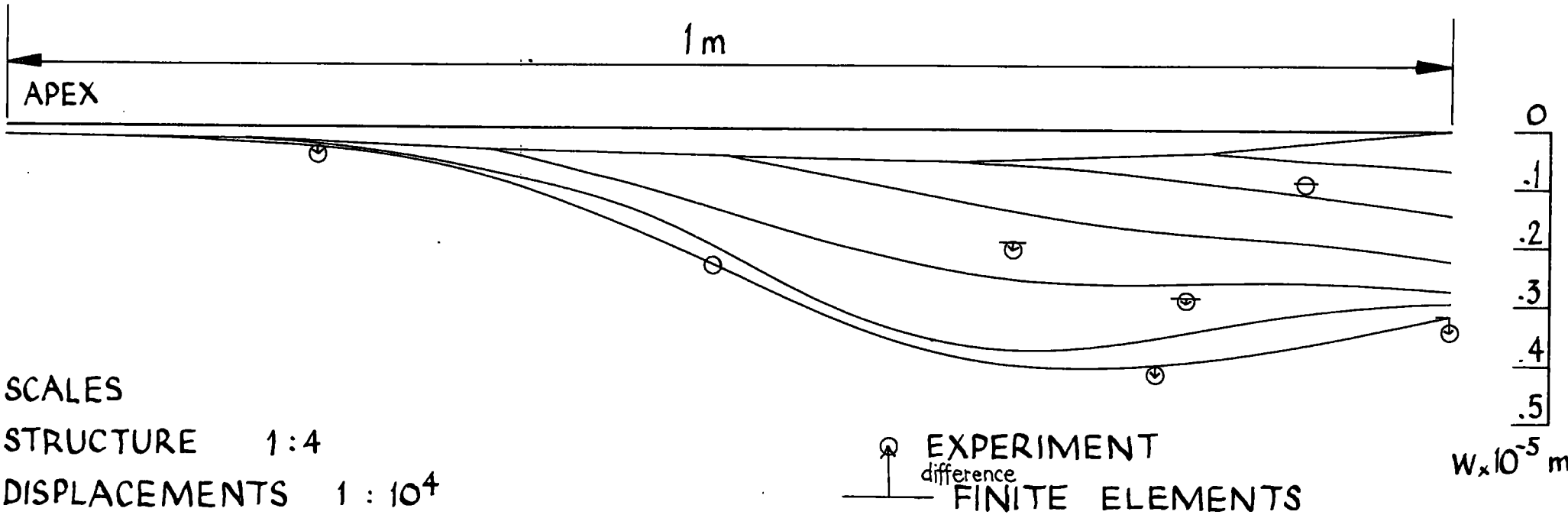

SCALES

STRUCTURE 1 : 4

DISPLACEMENTS 1 : 10^4

NORMAL DISPLACEMENTS OF LOADED FACE

FIG. 78 HEXAGONAL DOME , 1 FACE LOADED

VERTICAL LOAD OF 1 N AT CENTROID OF FACE 2

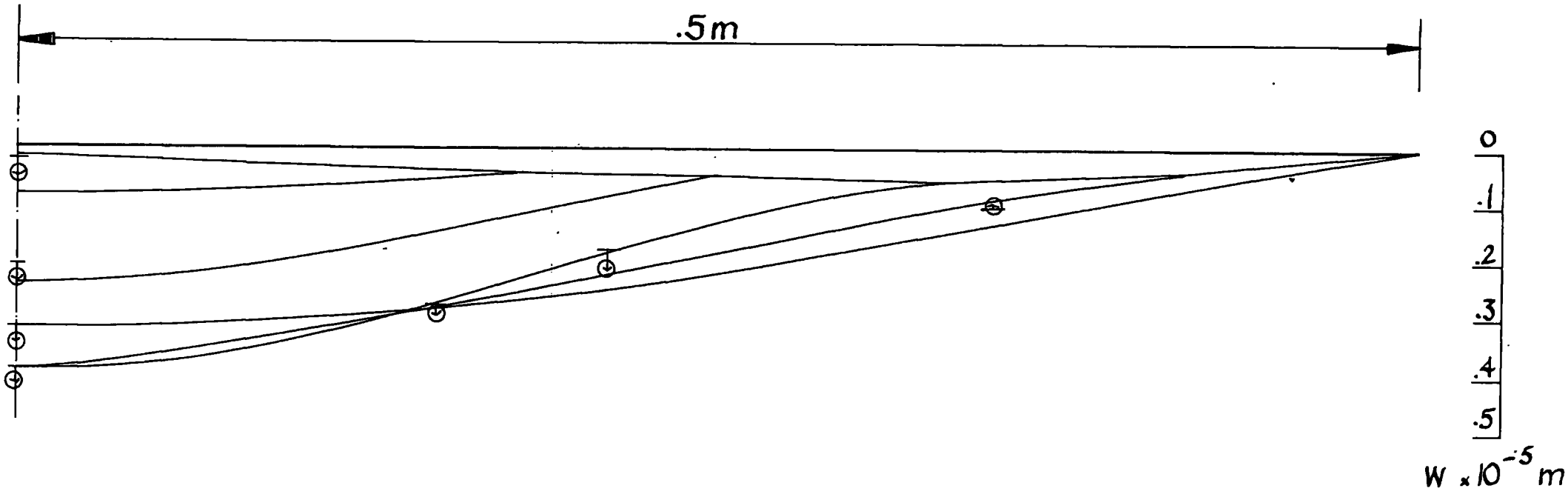

SCALES

STRUCTURE 1 : 2

DISPLACEMENTS 1 : 10^4

NORMAL DISPLACEMENTS OF LOADED FACE

FINITE ELEMENTS

difference EXPERIMENT

FIG. 79 HEXAGONAL DOME, 1 FACE LOADED

VERTICAL LOAD OF 1 N AT CENTROID OF FACE 2

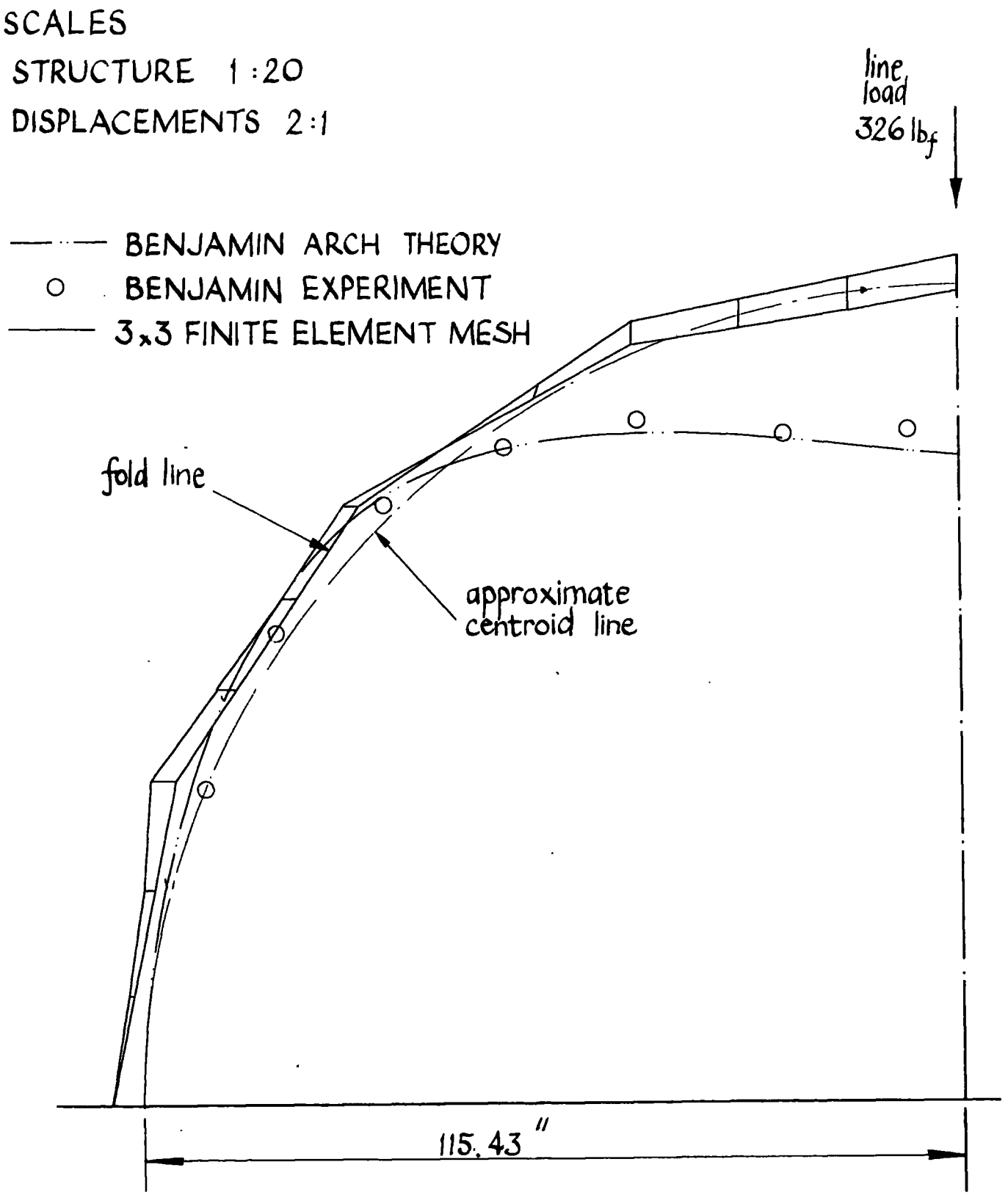

FIG. 80 BENJAMIN BARREL VAULT

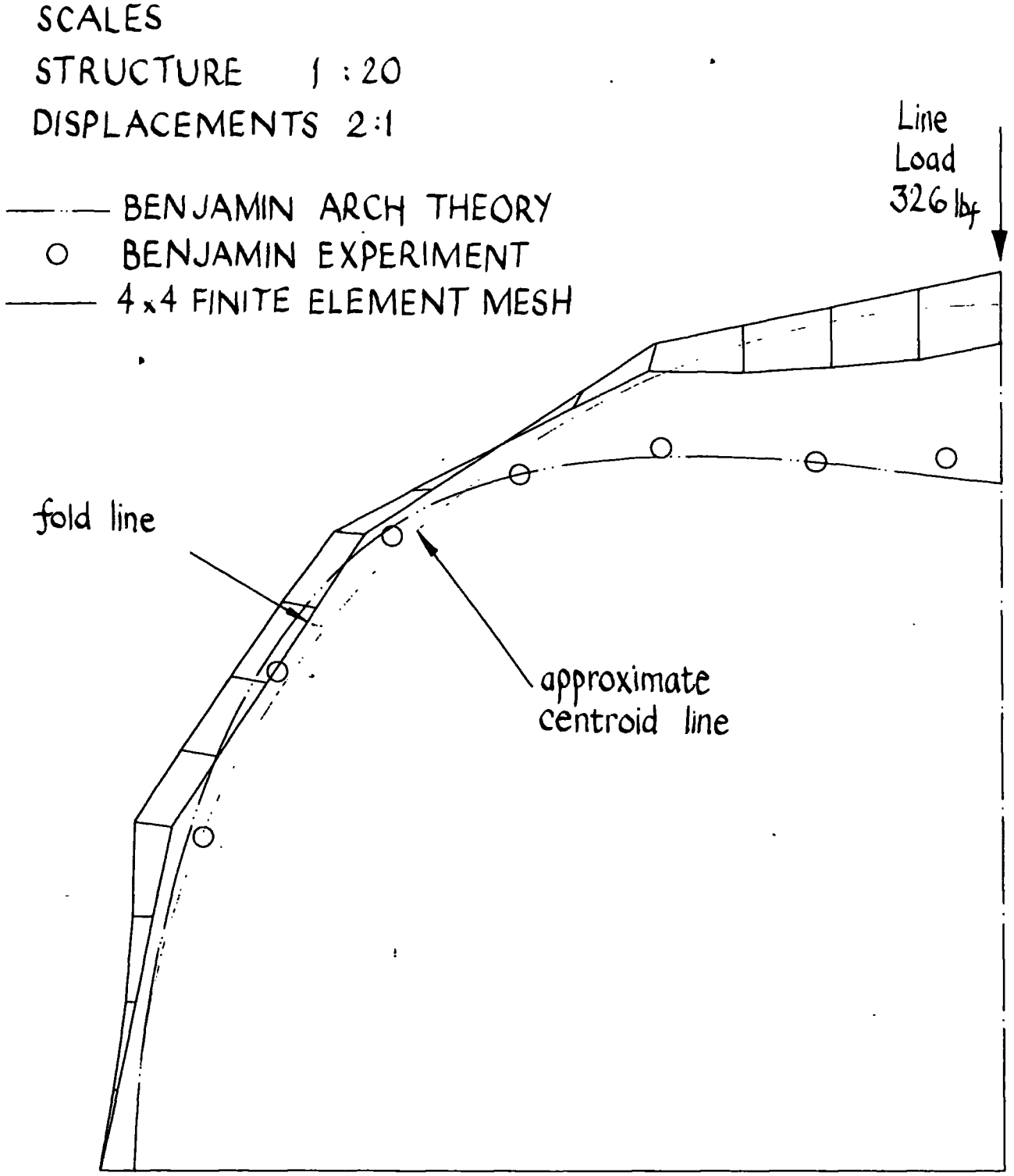

FIG. 81 BENJAMIN BARREL VAULT

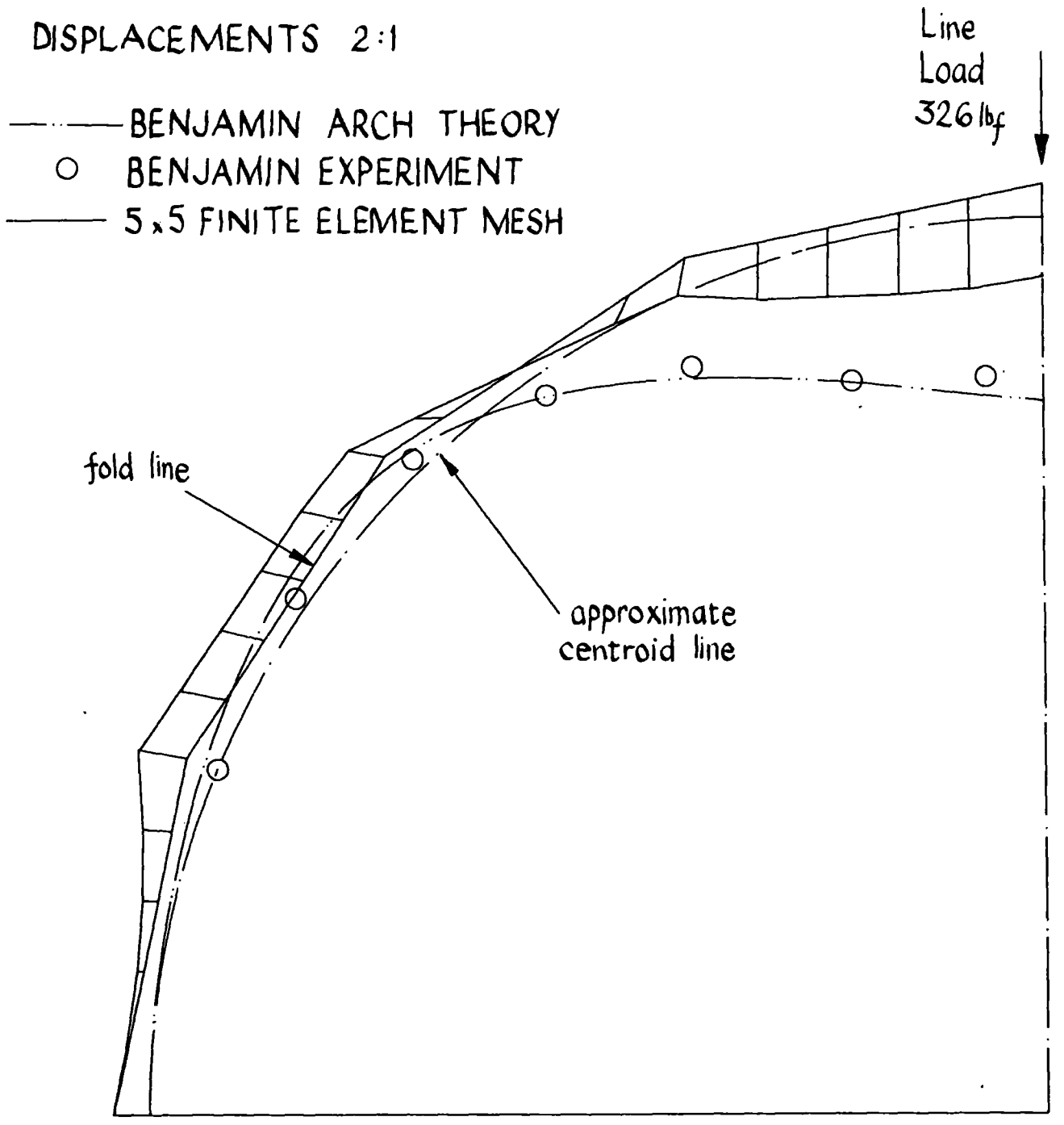

FIG. 82 BENJAMIN BARREL VAULT

SCALES

STRUCTURE 1:20

DISPLACEMENTS 2:1

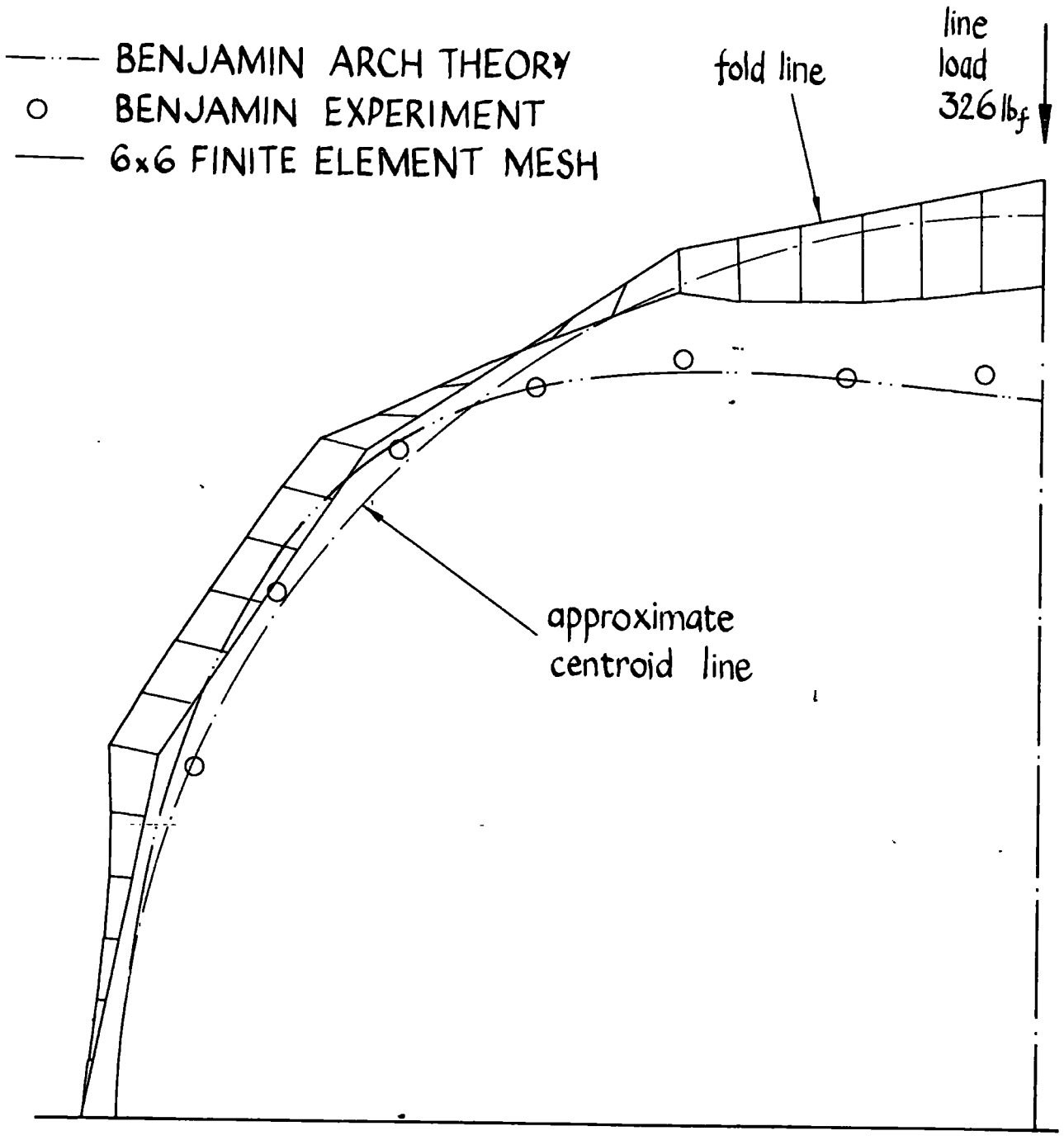

FIG. 83 BENJAMIN BARREL VAULT

SCALES

STRUCTURE 1 : 20

DISPLACEMENTS 2 : 1

—·—·— BENJAMIN ARCH THEORY

○ BENJAMIN EXPERIMENT

——— 8 x 8 FINITE ELEMENT MESH

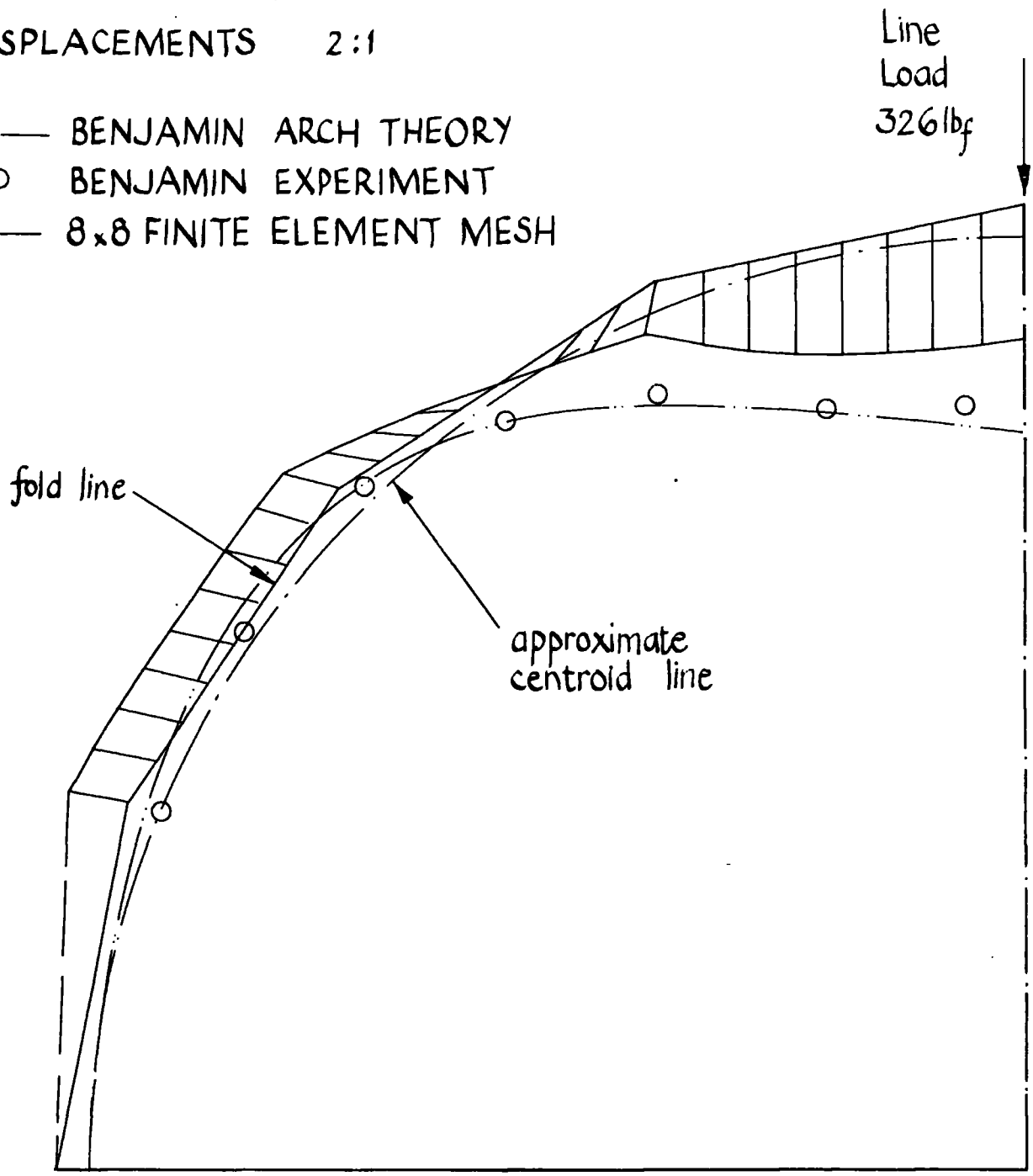

FIG. 84 BENJAMIN BARREL VAULT

SCALES

STRUCTURE 1 : 20

DISPLACEMENTS 2 : 1

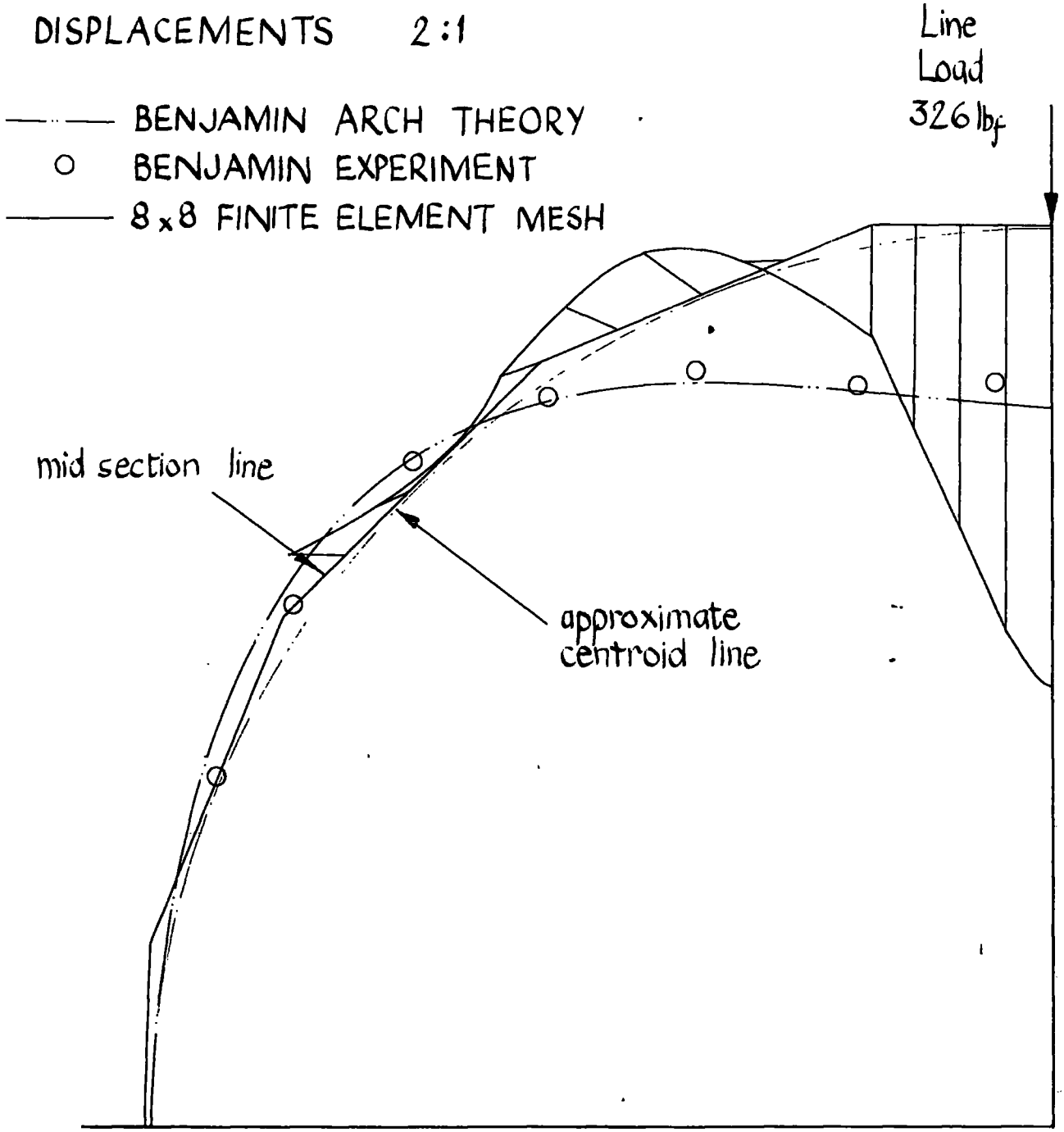

FIG. 85 BENJAMIN BARREL VAULT

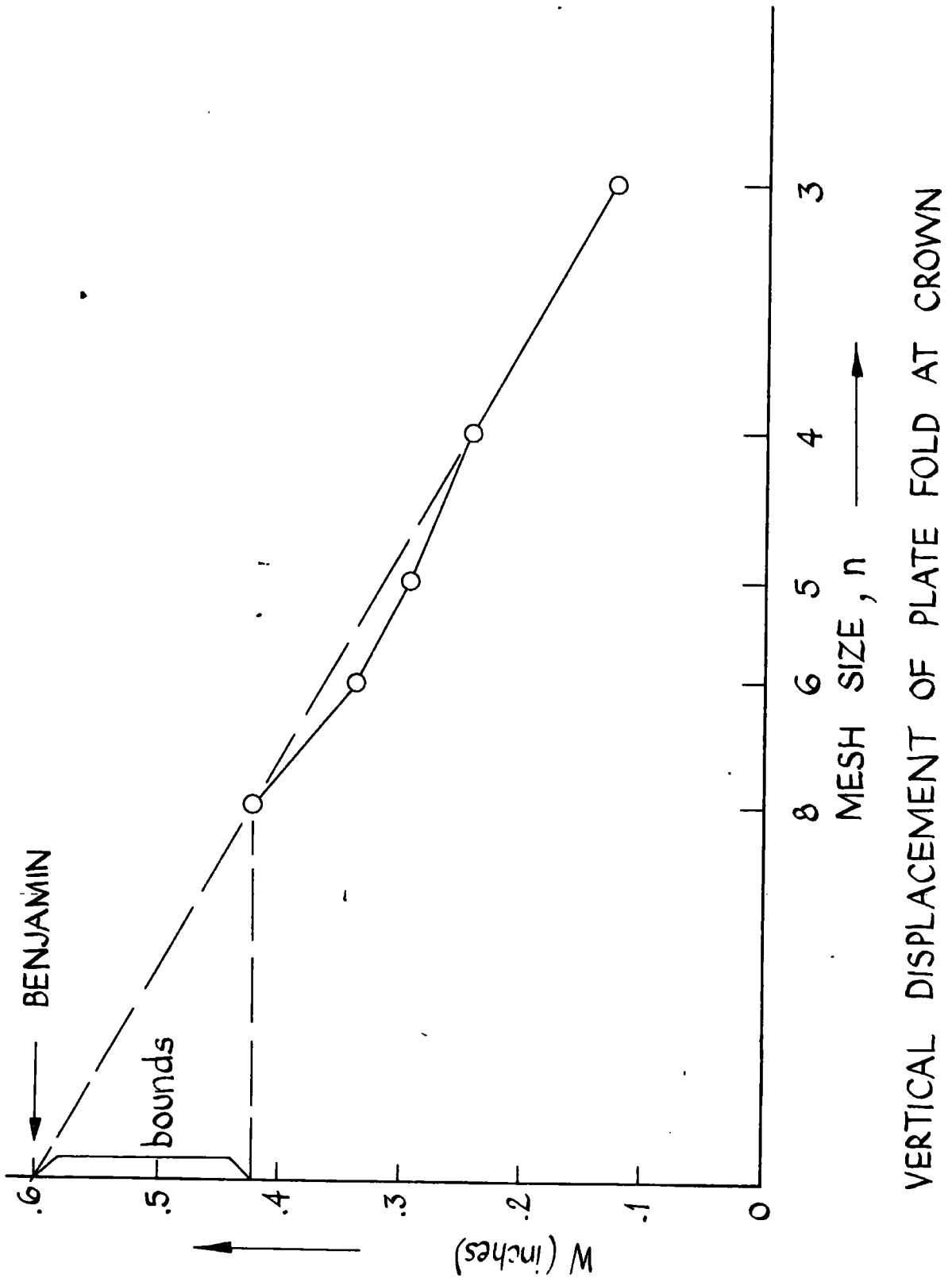

CENTRAL VERTICAL LINE LOAD OF 326 lb_f
CONVERGENCE OF CENTRE DISPLACEMENT

FIG. 86 BENJAMIN BARREL VAULT

SCALES
STRUCTURE 1 : 10
DISPLACEMENTS $5 \times 10^5 : 1$

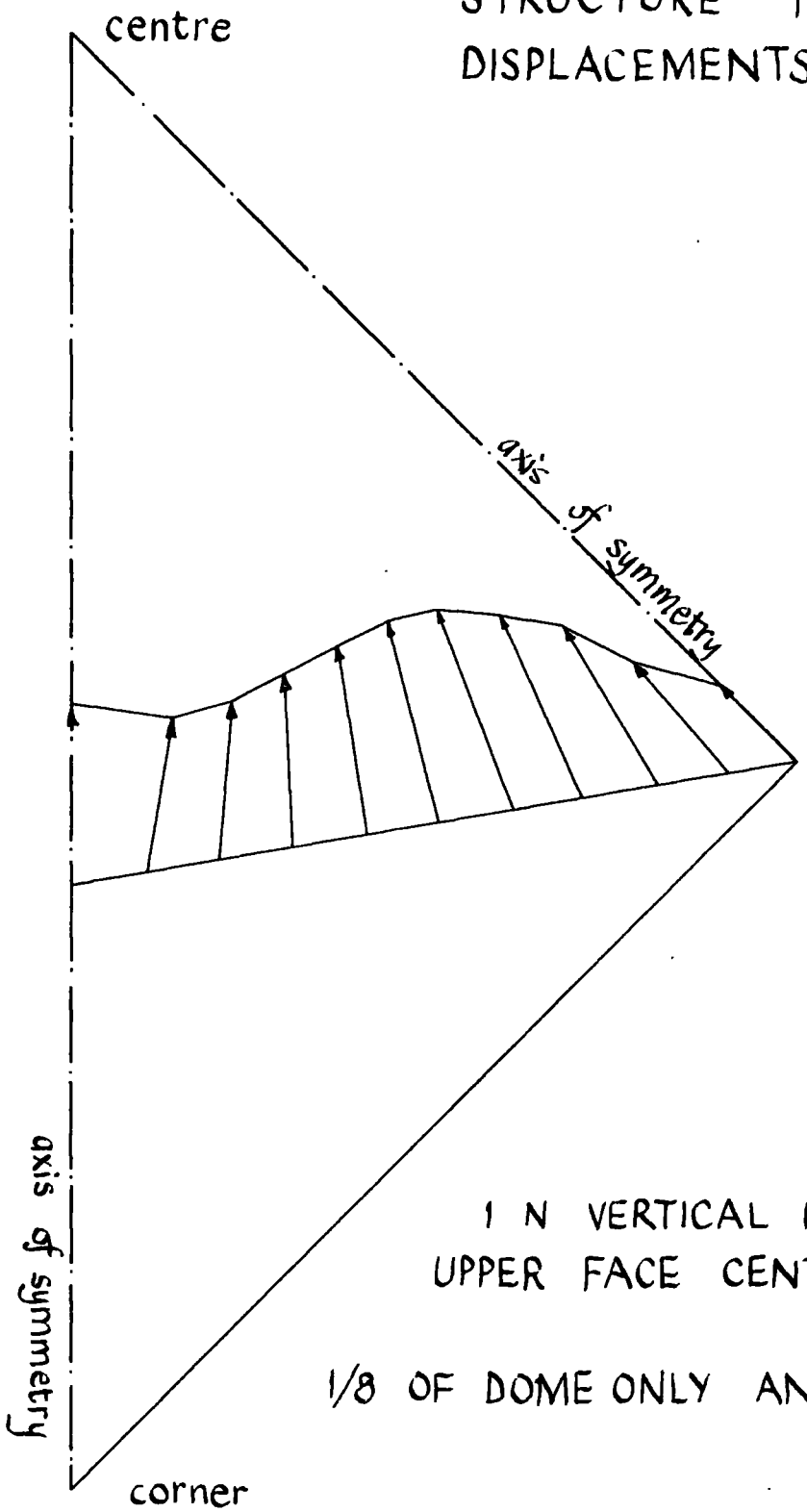

1 N VERTICAL LOAD AT
UPPER FACE CENTROID

1/8 OF DOME ONLY ANALYSED

HORIZONTAL DISPLACEMENTS

FIG. 87 16 FACED DOME

FIG. 88 16 FACED DOME

1 N VERTICAL LOAD AT INNER FACE CENTROID

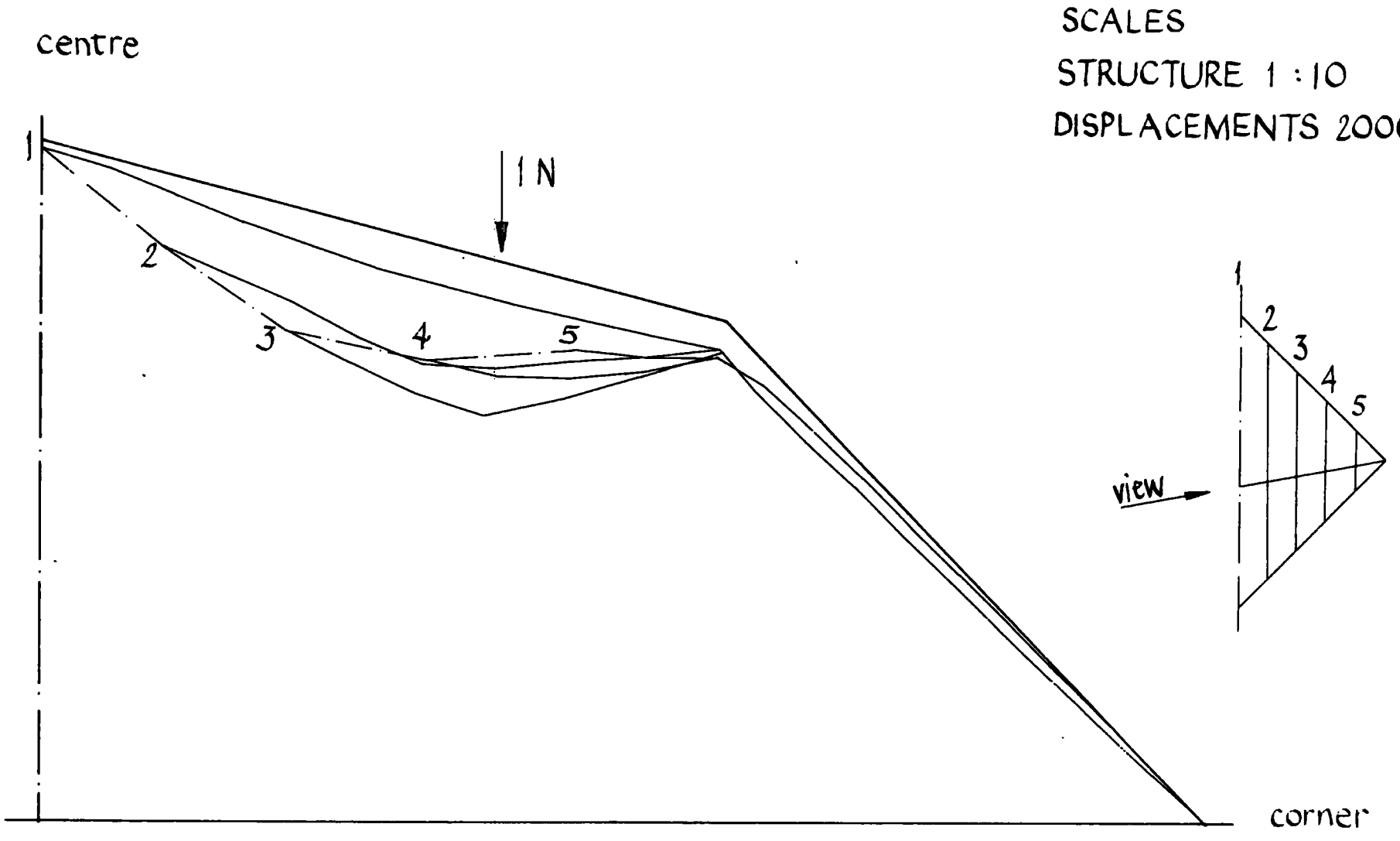

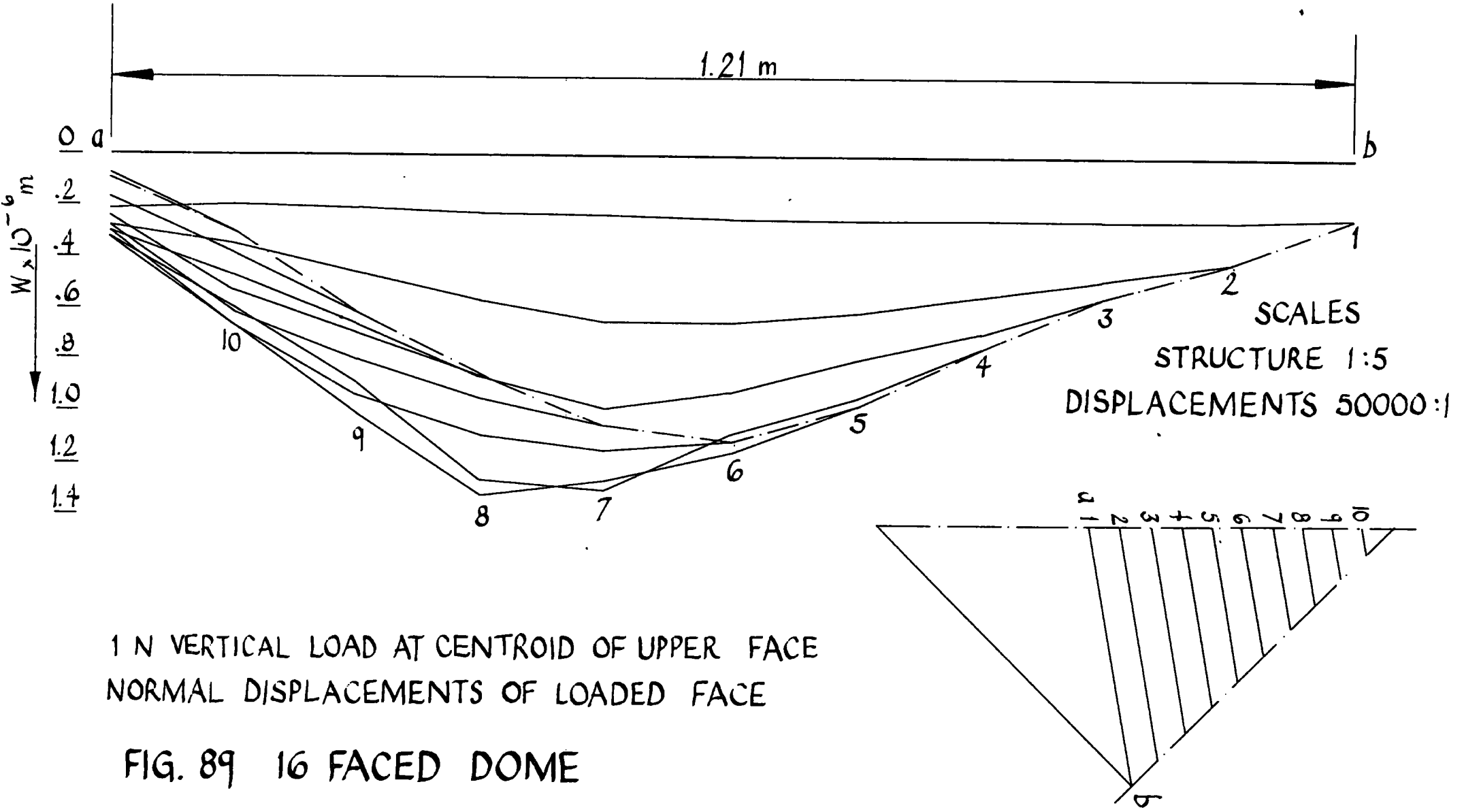

1 N VERTICAL LOAD AT CENTROID OF UPPER FACE
NORMAL DISPLACEMENTS OF LOADED FACE

FIG. 89 16 FACED DOME

Notation

Suffices, a^{ij} or $a^{\alpha\beta}$ usually indicate tensor components.

A bar $\bar{a}$ indicates a vector.

Square brackets $[A]$ denote a rectangular matrix, and curly brackets $\{A\}$ denote a column matrix.

Symbol	Meaning	Section
a	determinant of surface tensor	2.2
a^{ij}	surface tensor	2.2
$\bar{a}_3$	constant normal vector	2.2
a	plate and or rectangular element dimension	2.4,4,App.I.
$[A]$	triangular element component matrix (Fig 3)	2.5
b	plate and, or rectangular element dimension	2.4,4,App.I.
$[B]$	triangular element component matrix (Fig 3)	2.5
c	core thickness	2,3,4,Apps.
c^{ij}_{rs}	cartesian elasticity tensor	2.3,App.II, III.
$[C]$	triangular element component matrix (Fig 3)	2.5
c_i	polynomial coefficients	2.4
d_i	polynomial coefficients	2.4
$D^{\alpha\beta\lambda\mu}$	stress resultant displacement relations in curvilinear coordinates	2
$[D]$	"elasticity" matrix cartesian strain tensor	2.4, App.I.
e^{rs}	cartesian strain tensor	2.3,App.III
$[E]$	triangular element, internal continuity matrix	2.5
f	face thickness	2,3,4, Apps.
$F^{\alpha\beta\lambda\mu}$	curvilinear elasticity tensor	2.3
$\{F_i\}$	nodal forces	5
$[F]$	triangular element, condensation matrix for centre node	2.5
f^i_j	coefficients used for local transormations, triangular element	2.5
$\bar{g}_i$	base vectors	2.2
g^{ij}	metric tensor, contravariant components	2.2
g	determinant of metric tensor	2.2
$[G]$	triangular element, part of internal continuity matrix	2.5

Symbol	Meaning	Section
h	half plate thickness	2.2
h_{ij}	local transformation coefficients, triangular element	2.5
$[H]$	nodal displacements - polynomial coefficients matrix	2.4,2.5
$[I]$	unit matrix	2.5
$[K],[K']$	stiffness matrix	2,3,App.I, III
$[K_i]$	rectangular element component matrices	App. I
$[K_{ij}]$	stiffness sub matrices	5
$[l],[L]$	rectangular element transformation matrices	App. I
l_i	distances from vertices to centroid, triangular element	2.5
$m^{\alpha\beta}$	contravariant stress couple components	2,4
$\bar{m}_\alpha$	stress couple	2.2
$\bar{M}_\alpha$	stress couple	2.2
$M^{\alpha\beta}$	contravariant stress couple components	2.2
$[M]$	triangular element, upper half of condensation matrix	2.5
$n^{\alpha\beta}$	contravariant stress resultant components	2,4
$\bar{n}_\alpha$	stress resultant	2.2
$\bar{N}_\alpha$	stress resultant	2.2
$N^{\alpha\beta}$	contravariant stress resultant components	2.2
$[N]$	triangular element condensation matrix	2.5
p_i	coordinate function	3.2
$[p]$	set of triangular element nodal displacements	2.5
$[P]$	triangular element transformation matrix	2.5
q_i	coordinate function	3.2
q^α	shearing forde components	2.2,2.3,3.1,4
Q^α	shearing force components	2.2
$[Q]$	"strain"-polynomial matrix	2.4,App. I
$\{q\}$	set of element nodal displacements	2.5
$[Q_i]$	stress submatrices	5
r_i	coordinate function	3.2
$\bar{r}$	position vector	2.2
$\bar{R}$	position vector	2.2
$\{r\}$	set of triangular element nodal displacements	2.5
$[R]$	strain-displacement matrix	2,3, App. III

Symbol	Meaning	Section
s_j^i	polynomial coefficients	2.5
S^{ar}	shearing force-displacement relations	2.3,2.5,4,App. I.
$\bar{t}$	stress vector	2.2
$\bar{T}_i$	force vector	2.2
t_{ij}	cartesian stress tensor	2.3
u_j^i	polynomial coefficients	2.5
u_{ij}	local transformation coefficients for triangular element	2.5
$\bar{u}$	unit normal vector to middle line in plate	2.2
u_α	covariant components of $\bar{u}$	2.2
v_j^i	polynomial coefficients	2.5
v_α	covariant curvilinear displacement components	2,3,4,5
w	displacement normal to plate	2,4,5
$[W],[W_x],[W_y]$	triangular element curvature matrices	2.5
x_i	coordinates (variably rectangular cartesian, and oblique)	2.3
α, α'	angles in triangular element	2.5
α_i	polynomial coefficients	2.4
$[\alpha]$	polynomial coefficient matrix	2.4
β, β'	angles in triangular element	2.5
γ, γ'	angles in triangular element	2.5
$c\gamma_\alpha$	covariant shear deformation	2.3
γ_α	components	2,4,5
$\{\delta\}_e$	element nodal displacements	2.4, App. III.
Δ	area of triangle	
$\{\varepsilon\}$	"strain" matrix	2.4
$\varepsilon_{\alpha\beta}$	covariant curvilinear strain tensor	2.3
ζ_i	polynomial coefficients	3.2
η_i	polynomial coefficients	3.2
θ_i	curvilinear coordinates	2.2,2.3
θ	slopes	2.5
$[\sigma]$	stress matrix	2,5
$\tau^{\alpha\beta}$	covariant stress tensor	2.2,2.3
φ	slopes	2.5
Φ	function of c and f	2.3

References

These are arranged to be largely alphabetical. Joint authors are put in alphabetical order. The first four references are to extensive bibliographies.

1. Toupin, R.A. and Truesdell, C.
"The Classical Field Theories"
Handbuch der Physik, Volume III/1,
Springer Verlag, 1960.
Without doubt the best bibliography in mechanics.

2. Plantema, F.J. "Sandwich Construction"
Wiley, 1967.
Bibliography on Sandwich Construction.

3. Benjamin, B.S. "Structural Design with Plastics"
Van Nostrand, 1969.
Bibliography on sandwich structures and plastics.

4. Przemieniecki, J.S. "Theory of Matrix Structural Analysis"
McGraw Hill, 1968.
Bibliography on finite elements and matrix methods.

5. Abel, J.F. and Popov, E.P. "Static and dynamic finite element analysis of sandwich structures". Proceedings of the Second Conference on Matrix Methods in Structural Mechanics, Wright Patterson Air Force Base, Dayton, Ohio, 1968, AFFDL-TR-68-150.

6. Ahmad, A., Irons, B.M. and Zienkiewicz, O.C. "Analysis of Thick and Thin Shell Structures by Curved Finite Elements". International Journal for Numerical Methods in Engineering, Vol. 2. pages 419 to 451, (1970).

7. Alwan, A.M. "Large deflection of sandwich plates with orthotropic cores". J.A.I.A.A., 2, 10, October 1964, pages 1820 to 1822.

8. Anderson, Boyd, G., Birnbaum, H. and Whitney, C.S. "Reinforced Concrete Folded Plate Construction". Journal of the Structural Division, Proceedings of the American Society of Civil Engineers, October 1959, ST8. pages 15-43.

9. American Society for Testing and Materials". Shear test in Flatwise Plane of Flat Sandwich Construction or Sandwich cores" ASTM C-273.

10. Argyris, J.H. "Impact of the digital computer on engineering sciences". Aeronautical Journal, Vol. 74, number 209, January 1970, pages 13 - 41.

11. Ball, G.W., Doherty, D.J. and Walker, M.G. "The physical properties of rigid urethane foam sandwich panels". Plastics in Building Structures, Proceedings of a Conference held in London, 1965, Pergamon 1966.

12. Bacon, M.D. and Bert, C.W. "Unsymmetric Free Vibrations of Orthotropic Sandwich Shells of Revolution". J.A.I.A.A., March 1967, page 413.

13. Bamford, R.M. and Melosh, R.J. "Efficient Solution of Load-deflexion equations" Journal of the Structural Division, Proceedings of the American Society of Civil Engineers, April 1969, ST4, pages 661 to 676.

14. Basu, A.K. and Dawson, J.M. "Orthotropic Sandwich Plates". Proceedings of the Institution of Civil Engineers, 1970, Supplementary Volume (iv), Paper 7275S.

15. Batdorf, S.B. and Libove, Charles, "A General Small-Deflection Theory for Flat Sandwich Plates". N.A.C.A. Report No. 899, 1948.

16. Baylor, J.L. and Wempner, G.A. "A theory of Sandwich Shells". Developments in Mechanics, Vol. 2. Part 2, Proceedings of the Eighth Midwestern Mechanics Conference, Pergamon, 1965.

17. Beisinger, Z.E. and Key, S.W. "The Analysis of Thin Shells with transverse shear strains by the finite element method". Proceedings of the Second Conference on Matrix Methods in Structural Mechanics, Wright Patterson Air Force Base, Dayton, Ohio, 1968, AFFDL-TR-68-150.

18. Benjamin, B.S. "The transverse behaviour of the external unit of prismatic folded plate structures in plastics". Proceedings of the International Conference on Space Structures, University of Surrey, 1966, Paper K6.

19. Benjamin, B.S. "An account of some experimental work on a prototype folded plate barrel vault of plastics sandwich construction". Proceedings of the International Conference on Space Structures, University of Surrey, 1966, Paper K5.

20. Benjamin, B.S. and Makowski, Z.S. "The analysis of folded plate structures in plastics". Plastics in Building Structures, Proceedings of a Conference held in London, 1965, Pergamon 1966.

21. Benning, C.J. "Plastic foams: the physics and chemistry of product performance and process technology". Volumes I and II. Wiley Interscience. 1969.

22. British Plastics Federation "Cellular Plastics" SfB Kn 6, February 1968.

23. Carley, T.G. and Langhaar, H.L. "Transverse shearing stress in rectangular plates" Proceedings of the American Society of Civil Engineers, 1968, 94, ST1 (February), pages 137 - 151.

24. Chapman, J.C. and Williams, D.G. "Effect of shear deformation on uniformly loaded rectangular orthotropic plates" Proceedings of Institution of Civil Engineers, Supplementary Volume, 1969, Paper 7236 S.

25. Cheung, Y.K. and Zienkiewicz, O.C. "The finite element method in structural and continuum mechanics" McGraw Hill 1967.

26. Cliff, E.M. and Vincent, T.L. "Maximum-Minimum Sufficiency and Lagrange Multipliers" J.A.I.A.A., Vol. 8. No. 1, January 1970, pages 171 - 173.

27. Clough, R.W. "The finite element in structural mechanics", Chapter 7 of Stress Analysis, edited by O.C. Zienkiewicz and G.S. Holister, Wiley, 1965.

28. Clough, R.W. and Wilson, E.L. "Stress Analysis of a Gravity Dam by the Finite Element method" R.I.L.E.M. Bulletin, Vol. 19, June 1963, pages 45 to 54.

29. Clough, R.W. and Felippe, C.A. "A refined quadrilateral element for analysis of plate bending" Proceedings of the Second Conference on Matrix Methods in Structural Mechanics, Wright Patterson Air Force Base, Dayton, Ohio, 1968, AFFDL-TR-68-150.

30. Coxeter, H.S.M. "Regular Polytopes" Methuen.

31. de Veubeke, B. Fraejis "A conforming finite element for plate bending". International Journal of Solids and Structures, 1968, Vol. 4. pages 95 to 108.

32. Donnell, L.H., Drucker, D.C., Goodier, J.N. and Reissner, E. Comments on Reference 68. Journal of Applied Mechanics, Vol. 13, 1946, pages A249-A252.

33. Dunne, P.C. "Complete Polynomial Displacement Fields for Finite Element Method" Technical Note, The Aeronautical Journal of the Royal Aeronautical Society, Vol. 72, March 1968, pages 245-246.

34. Elliott, D.J. "Structural Properties of Flat Sandwich Panels" M.Sc. Thesis, University of Durham, 1970.

35. Enderby, L.J. and White, D.J. "Finite Element analysis of a multipiece piston" Journal of Strain Analysis, Vol. 4. No. 1, 1969.

36. Ergatoudis, J., Irons, B.M., and Zienkiewicz, O.C., Comments on reference 33. The Aeronautical Journal of the Royal Aeronautical Society, Vol. 72, pages 709 - 711, August 1968.

37. Evans, H.R. and Rockey, K.C. "A finite element solution for folded plate structures" International Conference on Space Structures, University of Surrey, 1966, Paper B2.

38. Faddeeva, F.N. "Computational Methods of Linear Algebra", Dover, New York, 1959.

40. Fairbairn, W. "An Account of the Construction of the Britannia and Conway Tubular Bridges", London 1849.

41. Flugge, W. "Stresses in Shells", Springer-Verlag Berlin 1960.

42. Graham, D.L. and O'Dell, W.W. "Structural behaviour of sandwich panels with foamed plastics core" Plastics in Building Structures, Proceedings of a Conference held in London, 1965, Pergamon 1966.

43. Green, A.E., and Zerna, W. "Theoretical Elasticity" Oxford, At the Clarendon Press, 1954.

44. Green, A.E., "On Reissner's Theory of Bending of Elastic Plates" Quarterly of Applied Mathematics, Vol. 7., No. 2. (1949), pages 223 - 228.

45. Gunturkun, S., Kuo Tai Yen and Pohle, F.V. "Deflections of a simply supported rectangular sandwich plate subjected to transverse loads" N.A.C.A. TN 2581 (1951).

46. Hellinger, E. "Die Allgemeinen Ansatze der Mechanik der Kontinua" Encyklopadie der Mathematischen Wissenschaften, Edited by Klein and Muller, Leipzig, 1914, Bd.IV,4., pages 600 - 694.

47. Hencky, H. "Uber die Berucksichtigung der Schubverzerrung in ebenen Platten" Ing. Archiv. XVI Band, 1947, pages 72 - 76.

48. Herrmann, L.R. "A Bending Analysis for Plates". Proceedings of the Conference on Matrix Methods in Structural Mechanics, Wright Patterson Air Force Base, Dayton, Ohio, 1965.

49. Hughes, B. and Wajda, R.L. "Plastics sandwich panels with various foamed core materials, and their behaviour under load" Plastics in Building Structures, Proceedings of a Conference held in London, 1965, Pergamon 1966.

50. I.C.I. "Plastic Materials Guide".

51. Irons, B.M. "Lagrange Multiplier Techniques in Structural Analysis" J.A.I.A.A., 3, 6, 1172, (1965).

52. Irons, B.M. "Roundoff Criteria in direct stiffness solutions" J.A.I.A.A., 6, 7, pages 1308 - 1312, (1968).

53. Irons, B.M. "A Frontal Solution Program for Finite Element Analysis" International Journal for Numerical Methods in Engineering, Vol. 2. No. 1. January 1970, pages 5 to 32.

54. Irons, B.M. "Computer Program Report No. 27:Mark VI Front Assembly and Solution for Finite Element Scheme"University of Wales, Swansea, Civil Engineering Department.

55. Kirchhoff, G. "Uber das Gleichgewicht und die Bewegung einer elastischen Scheibe" Zeitung fur reine und angewandete Mathematic, Vol. 40, 1850.

56. Lanczos, C. "The Variational Principles of Mechanics"University of Toronto Press, Toronto, 1949.

57. Lockwood Taylor, J. "Strength of Sandwich Panels" Proceedings of the VII International Congress of Applied Mechanics, 1948, 1, pages 187 - 199.

58. Love, A.E.H. "A Mathematical Theory of Elasticity". Cambridge University Press.

59. Mahon, D.S. "Plastics sandwich panels as cladding and wall elements". Plastics in Building Construction, Proceedings of a Conference at the University of Surrey, 1964, Blackie 1966, pages 23 - 31.

60. Makowski, Z.S. "The structural applications of plastics". Plastics in Building Construction, Proceedings of a Conference at the University of Surrey, 1964. Blackie 1966, pages 49 - 78.

61. Mayers, J. and Stein, M. "A Small Deflection Theory for Curved Sandwich Plates" N.A.C.A. 1008, Washington, D.C. 1951.

62. Monforton, G.R. and Schmit, L.A. "Finite element analysis of sandwich plates and cylindrical shells with laminated faces". Proceedings of the Second Conference on Matrix Methods in Structural Mechanics, Wright Patterson Air Force Base, Dayton, Ohio, 1968, AFFDL-TR-68-150.

63. Parme, A.L.L. "Direct solution of folded plate concrete roofs". Bulletin of the International Association for Shell Structures, No. 6.

64. Poisson, S.D. "Memoire sur l'equilibre et le mouvement des corps elastiques". Academie des Sciences, Paris, Memoires, 1829, Tome VII, pages 357 - 570.

65. Raville, M.E. "Deflexions and stresses in a uniformly loaded, simply supported, rectangular sandwich plate". F.P.L. Report 1847, December 1955, Reprinted September 1962.

66. Reiss, M. "Cantilevered and continuous folded plates" International Conference on Space Structures, University of Surrey, 1966. Paper B3.

67. Reissner, E. "On the Theory of Bending of Elastic Plates" Journal of Mathematical Physics, Volume 23, (1944), pages 184 - 191.

68. Reissner, E. "The Effect of Transverse Shear Deformation on the Bending of Elastic Plates" Journal of Applied Mechanics, Volume 12, (1945), pages A68 - A77.

69. Reissner, E. "On Bending of Elastic Plates" Quarterly of Applied Mathematics, Vol. 5., (1947), pages 55 - 68.

70. Reissner, E. "Small Bending and Stretching of Sandwich Type Shells", N.A.C.A., 975, Washington D.C. 1950.

71. Reissner, E. "On a Variational Theorem in Elasticity" Journal of Mathematical Physics, 29, (1950), pages 90 - 95.

72. Reissner, E. "Finite Deflections of Sandwich Plates". Journal of the Institute of Aeronautical Sciences, Vol.15, July 1948, pages 435 - 440.

73. Sander, G. "Applications de la Methode des Elements Finis a la Flexion des Plaques" Universite de Liege, Faculte des Sciences Appliques, Collection des Publications, No.15, 1969.

74. Tait, and Thompson "Treatise on Natural Philosophy" Cambridge: at the University Press, 1895, Vol. II, page 189.

75. Timoshenko, S. and Woinowsky-Krieger, S. "Theory of Plates and Shells" McGraw Hill, 2nd edition.

76. Wempner, G.A. "Theory for Moderately Large Deflections of Thin Sandwich Shells" A.S.M.E. Journal of Applied Mechanics Vol. 32, March 1965, pages 76 - 80.

Acknowledgements

I thank the Science Research Council and Van Mildert College, Durham University for financial assistance.

I thank my supervisor, Mr. Parton, and Professor Higginson, of the Department of Engineering Science, Durham University, for help with both practical and theoretical work.

I thank Mr. Scurr and Mr. Emery and the other technicians for help with the laboratory work.

I thank Mr. Oddy, Mr. Sheehan, Mr. Lander, Mr. Young and the rest of the Durham University Computer Unit for help with programming and with running programs.

I thank the staff of Durham University Library.

I thank Mrs. Ribchester for typing my script.

Appendix I

The Component Matrices of the Rectangular Sandwich Plate Bending Element

The stiffness matrix may be written as

$$[L]^T\left\{[K_1]D_{11}''+[K_2]D_{22}^{22}+[K_3]D_{12}^{12}+[K_4]D_{22}''+[K_5]S_1'+[K_6]S_2^2\right\}[L]$$

where $$[L]=\begin{bmatrix} 1 & 0 & 0 & 0 \\ 0 & 1 & 0 & 0 \\ 0 & 0 & 1 & 0 \\ 0 & 0 & 0 & 1 \end{bmatrix}$$

and $$[l]=\begin{bmatrix} 1 & 0 & 0 & 0 & 0 \\ 0 & 2b & 0 & 0 & 0 \\ 0 & 0 & 2a & 0 & 0 \\ 0 & 0 & 0 & 2a & 0 \\ 0 & 0 & 0 & 0 & 2b \end{bmatrix}$$

Each matrix $[K_i]$, i = 1 to 6, has the following pattern of symmetrical submatrices, if the signs of the degrees of freedom 5, 8, 9, 10, 12, 17, 18, 19 are reversed.

$$\begin{bmatrix} A & B & C & D \\ B & A & D & C \\ C & D & A & B \\ D & C & B & A \end{bmatrix}$$

It is most convenient to present only A, B, C and D for each matrix.

These component matrices for $[K_i]$, i = 1 to 6 and the matrix $[Q]$ are on the following pages. The matrices $[K_5]$ and $[K_6]$ are very sparse, and are shown in condensed form.

COMPONENTS OF $[K_1]$

$$[A] = \frac{b}{240a^3}$$

240	0	120	0	0
0	0	0	0	0
120	0	80	-20	0
0	0	-20	20	0
0	0	0	0	0

$$[B] = \frac{b}{240a^3}$$

-240	0	-120	0	0
0	0	0	0	0
-120	0	-40	-20	0
0	0	-20	20	0
0	0	0	0	0

$$[C] = \frac{b}{240a^3}$$

120	0	60	0	0
0	0	0	0	0
60	0	40	-10	0
0	0	-10	10	0
0	0	0	0	0

$$[D] = \frac{b}{240a^3}$$

-120	0	-60	0	0
0	0	0	0	0
-60	0	-20	-10	0
0	0	-10	10	0
0	0	0	0	0

COMPONENTS OF $[K_2]$

$$[A] = \frac{a}{240b^3}$$

240	-120	0	0	0
-120	80	0	0	20
0	0	0	0	0
0	0	0	0	0
0	20	0	0	20

$$[B] = \frac{a}{240b^3}$$

120	-60	0	0	0
-60	40	0	0	10
0	0	0	0	0
0	0	0	0	0
0	10	0	0	10

$$[C] = \frac{a}{240b^3}$$

-240	120	0	0	0
120	-40	0	0	20
0	0	0	0	0
0	0	0	0	0
0	20	0	0	20

$$[D] = \frac{a}{240b^3}$$

-120	60	0	0	0
60	-20	0	0	10
0	0	0	0	0
0	0	0	0	0
0	10	0	0	10

COMPONENTS OF $[K_3]$

$$[A] = \frac{1}{240ab}$$

336	-24	24	60	60
-24	32	0	0	10
24	0	32	-10	0
60	0	-10	20	15
60	10	0	15	20

$$[B] = \frac{1}{240ab}$$

-336	24	-24	-60	-60
24	-32	0	0	-10
-24	0	8	-10	0
-60	0	-10	-10	-15
-60	-10	0	-15	-20

$$[C] = \frac{1}{240ab}$$

-336	24	-24	-60	-60
24	8	0	0	10
-24	0	-32	10	0
-60	0	10	-20	-15
-60	10	0	-15	-10

$$[D] = \frac{1}{240ab}$$

336	-24	24	60	60
-24	-8	0	0	-10
24	0	-8	10	0
60	0	10	10	15
60	-10	0	15	10

COMPONENTS OF $[K_4]$

$$[A] = \frac{1}{240ab}$$

120	-60	60	-30	-30
-60	0	-60	30	0
60	-60	0	0	-30
-30	30	0	0	15
-30	0	-30	15	0

$$[B] = \frac{1}{240ab}$$

-120	60	0	-30	30
60	0	0	30	0
0	0	0	0	0
-30	30	0	0	15
30	0	0	15	0

$$[C] = \frac{1}{240ab}$$

-120	0	-60	30	-30
0	0	0	0	0
-60	0	0	0	-30
30	0	0	0	15
-30	0	-30	15	0

$$[D] = \frac{1}{240ab}$$

120	0	0	30	30
0	0	0	0	0
0	0	0	0	0
30	0	0	0	15
30	0	0	15	0

COMPONENTS OF $[K_5]$

b / 36a	4	9	14	19	
	4	-2	2	-1	4
	-2	4	-1	2	9
	2	-1	4	-2	14
	-1	2	-2	4	19

COMPONENTS OF $[K_6]$

a / 36b	5	10	15	20	
	4	2	-2	-1	5
	2	4	-1	-2	10
	-2	-1	4	2	15
	-1	-2	2	4	20

			2			$6x_1$	$2x_2$			$6x_1x_2$			-1		$-x_2$				
					2			$2x_1$	$6x_2$		$6x_1x_2$							-1	$-x_1$
				2			$4x_1$	$4x_2$		$6x_1^2$	$6x_2^2$			-1	$-x_1$		-1		$-x_2$
												1	x_1	x_2	x_1x_2				
																1	x_1	x_2	x_1x_2

[Q], RECTANGULAR ELEMENT

Appendix II

Properties of Materials and Plates

The behaviour of face materials, in the load ranges in which they were tested, was linear. It was also time independent. The wood materials were completely linear up to failure. So the assigning of elastic properties to these materials is justified.

The core materials were both foams. The properties of foam materials in bulk, are determined not only by the real properties of the material but also by the geometry and modes of formation of the foam.(21). The precise nature of the interaction of the material properties and geometry in bulk behaviour is complex. However for the purpose of our tests the foam materials were considered as ordinary materials. They responded well to this assumption which is accepted practice (9, 21). The behaviour of the core materials was time dependent. They tended to creep under load, typically showing a 10% increase in displacement after being loaded for 24 hours. Because all tests on materials, plates, beams and domes were completed in short periods (less than 80 minutes) this effect has been entirely ignored. The high recoveries of deformation ($>$ 95%) also justify this step. For short times the behaviour of the two core materials was linearly elastic.

Elastic Constants of Materials

These are given in rectangular cartesian coordinates.

1. The face materials

Because of the assumptions made in the theory only the following elastic coefficients are relevant:

$$C^{11}_{11},\ C^{22}_{22},\ C^{22}_{11},\ C^{12}_{12},\ C^{11}_{12},\ C^{22}_{12}$$

The most general material considered was orthotropic, so that the last two terms were always zero.

2. <u>The core materials</u>

The relevant elastic coefficients are:

$$C_{23}^{23} \qquad C_{13}^{13} \qquad C_{13}^{23}$$

The last term will always be zero for orthotropic materials, and for isotropic materials $C_{23}^{23} = C_{13}^{13}$.

THE TENSOMETER CAN ONLY APPLY TENSIONS

THE SPAN IS VARIABLE (<.6m)

4 POINT BENDING

THE 3 POINT BENDING POSITION IS SIMILAR

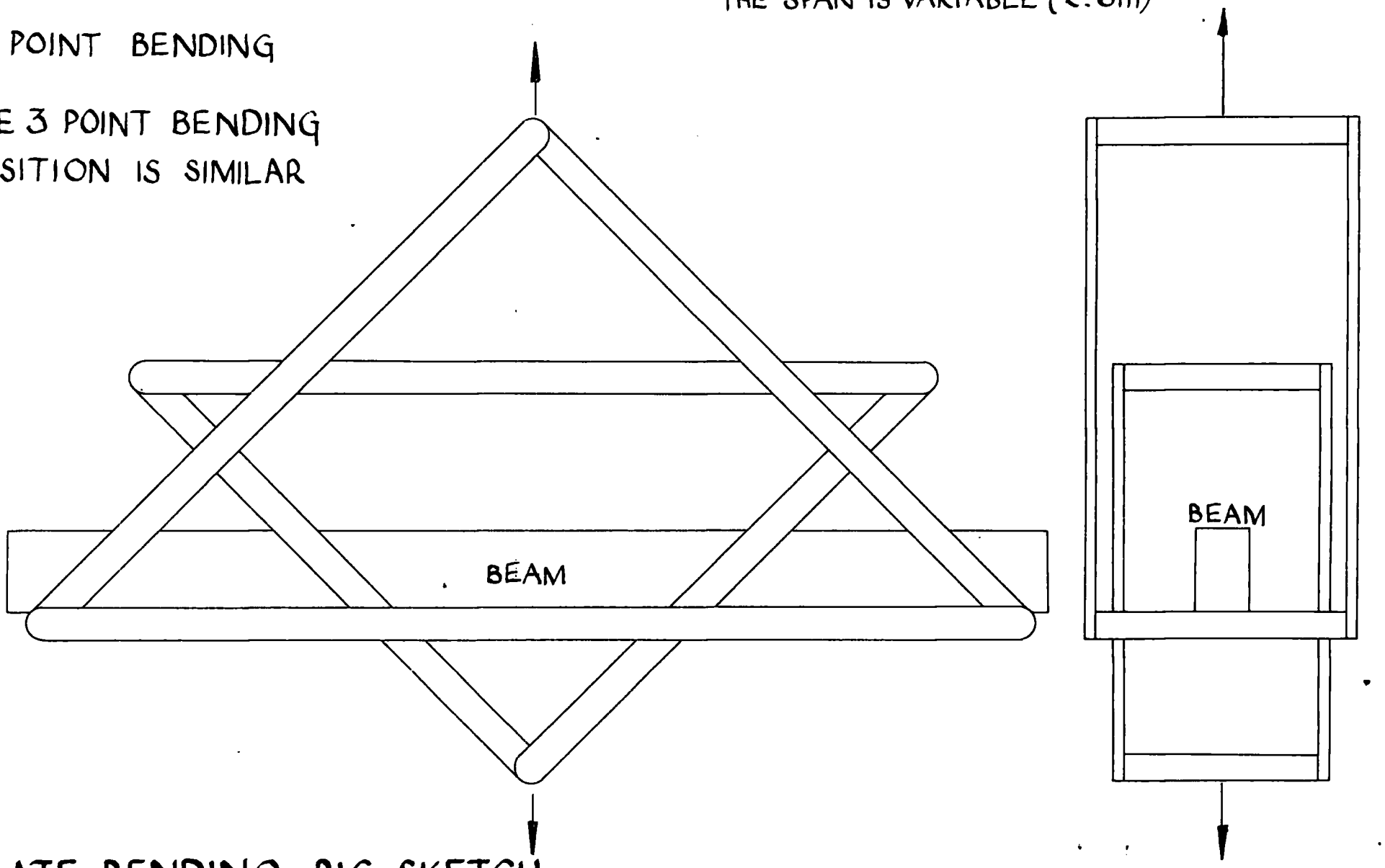

PLATE BENDING RIG SKETCH

CURVATURE MEASUREMENT

curvature $= 8d/L^2$

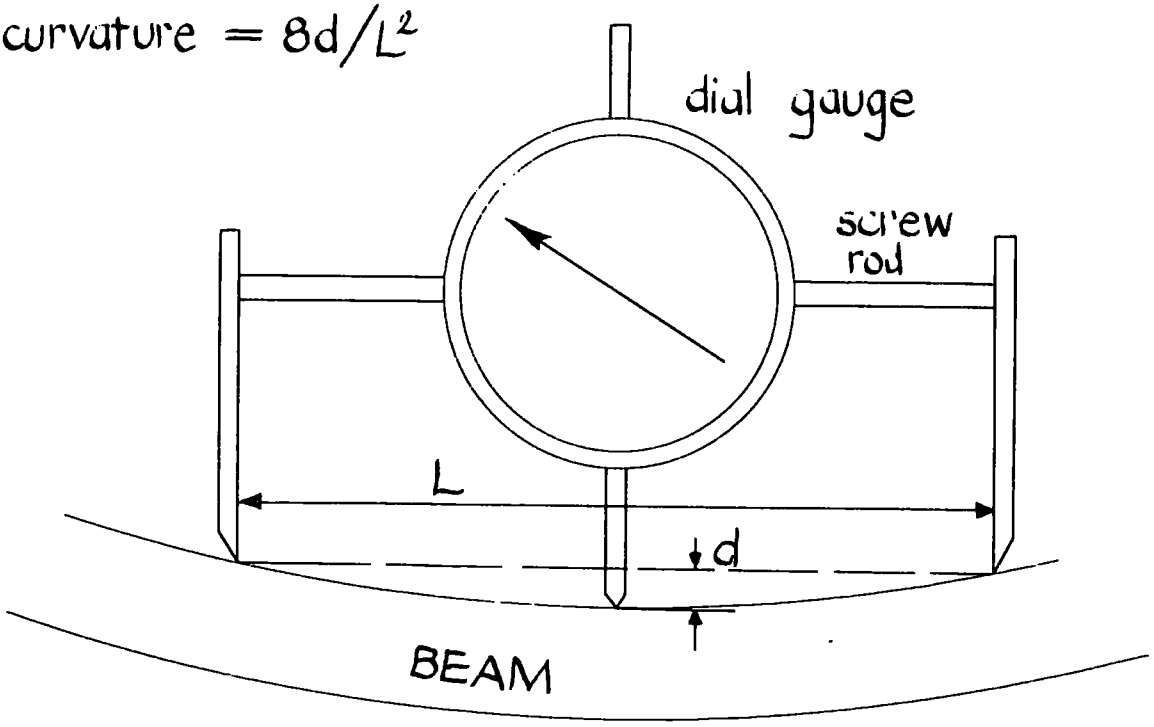

1 ELASTIC PROPERTIES OF MATERIALS

No	Name or description of material	face or core	ortho-or iso-tropic	thickness (nominal)	thickness, measured, mean (m)
1	plywood (marine, birch)	F	O	1/16"	.00166
2	aluminium	F	I	—	.000486
3	fibre glass	F	I	—	varied
4	hardboard (I.C.I.)	F	I	3/16"	.00408
5	hardboard	F	I	3/16"	.0034
6	expanded polyurethane	C	I	1"	.026
7		C	I	3/4"	.019
8		C	I	1/2"	.0125
9	(as 6, bonded to hardboard)	C	I	1"	.026
10	expanded polyvinylchloride	C	I	1/2"	.011

elastic properties c^{ij}_{pq} N/m²					
c^{11}_{11}	c^{22}_{22}	c^{11}_{22}	c^{12}_{12}	c^{23}_{23}	c^{13}_{13}
1.2 to 1.4 × 10^{10}	.78 to .91 × 10^{10}	.32 to .38 × 10^{10}	.55 × 10^{10}	—	—
.68 × 10^{11}	.68 × 10^{11}	.20 × 10^{11}	.48 × 10^{11}	—	—
.56 × 10^{10}	.56 × 10^{10}				
.42 × 10^{10}	.42 × 10^{10}				
				.2 × 10^{7} .2 × 10^{7} .2 × 10^{7} .2 × 10^{7}	.2 × 10^{7} .2 × 10^{7} .2 × 10^{7} .2 × 10^{7}
				.1 × 10^{8}	.1 × 10^{8}

2 ELASTIC PROPERTIES OF PLATES

No.	description	materials	bonding agent	total thickness (m)	c/f
1	plywood and expanded polyurethane	1 & 6	mouldrite resin UF232	.031	15.66
2	plywood and expanded polyurethane	1 & 7	mouldrite resin UF 232	.023	11.44
3	plywood and expanded polyurethane	1 & 8	mouldrite resin UF 232	.016	7.5
4	fibre glass and expanded polyvinyl chloride	3 & 10	cast	.0228	–
5	fibreglass and expanded polyvinyl chloride	3 & 10	cast	.0179	–
6	fibreglass and expanded polyvinyl chloride	3 & 10	cast	.0124	–
7	aluminium and expanded polyvinyl chloride	2 & 10	cast	.013	22.63
8	hardboard and expanded polyurethane	4 & 9	cast	.058	15.29
9	hardboard and expanded polyurethane	4 & 5 & 9	cast and mouldrite resin UF 232	.032	7.03

Nm D_{11}^{11}	D_{22}^{22}	D_{11}^{22}	D_{12}^{12}	N/m $S_1^1 = S_2^2$	N/m E_{11}^{11}	E_{22}^{22}	E_{22}^{11}	E_{12}^{12}
9700.	6800.	2600.	7100.	59000.	$.46 \times 10^8$	$.30 \times 10^8$	$.13 \times 10^8$	$.37 \times 10^8$
5400.	3800.	1500.	3900.	45000.	$.46 \times 10^8$	$.30 \times 10^8$	$.13 \times 10^8$	$.37 \times 10^8$
2540	1800.	690.	1900.	32000.	$(1.4375 \cdot 10^{11})$ $.46 \times 10^8$	$0.9375 \cdot 10^{10}$ $.30 \times 10^8$	$0.4062_{\cdot 10^{10}}$ $.13 \times 10^8$	$1.15625_{\cdot 10^{10}}$ $.37 \times 10^8$
$.29 \times 10^4$	$.29 \times 10^4$	$.86 \times 10^3$	$.20 \times 10^4$	2.5×10^5				
$.15 \times 10^4$	$.15 \times 10^4$	$.46 \times 10^3$	$.11 \times 10^4$	$.18 \times 10^6$				
$.59 \times 10^3$	$.59 \times 10^3$	$.18 \times 10^3$	$.41 \times 10^3$	1.0×10^5				
$.29 \times 10^4$	$.29 \times 10^4$	$.72 \times 10^3$	$.17 \times 10^4$	$.37 \times 10^6$	$.66 \times 10^8$	$.66 \times 10^8$	$.19 \times 10^8$	$.47 \times 10^8$
$.26 \times 10^5$	$.26 \times 10^5$	$.79 \times 10^4$	$.92 \times 10^4$	1.4×10^5				
$.57 \times 10^4$	$.57 \times 10^4$	$.17 \times 10^4$	$.4 \times 10^4$	$.99 \times 10^5$	$.41 \times 10^8$	$.41 \times 10^8$	$.12 \times 10^8$	$.29 \times 10^8$

Appendix III

Variational Statements

The theorems about elastic bodies which have been used for finite elements are widely available (1, 4, 25, 56, 71, 73). A summary of the necessary proofs is given here.

A complete solution to the problem of an elastic body under load must satisfy the requirements of equilibrium, the material stress-strain relations, compatibility, and boundary conditions. The strain-displacement relations must also be satisfied, explicitly or implicitly.

We consider a linearly elastic body, R, with a surface S, divided into S_v on which displacements are prescribed, and S_τ on which tractions are prescribed. We consider only small deformations, and for clarity rectangular cartesian coordinates. Associated with the body are a compatible displacement field, and a load field. Through the stress-strain relations corresponding stress and strain energy fields may be generated. The potential energy of the body, expressed in terms of load and displacement fields is varied with respect to the displacement field, and this variation is set equal to zero. It is asserted that this is formally equivalent to the satisfaction of equilibrium over the body and those parts of its boundaries where displacements are not prescribed.

We prove first a more general result, due to de Veubeke, and quoted for two dimensions, by Sander (73). The equations are as follows.

1. equilibrium $$t_{ij} + F_i = 0 \qquad \text{(A.III.1)}$$

2. stress-strain relations $$t_{ij} = c^{ij}_{rs}\, e_{rs} \qquad \text{(A.III.2)}$$

3. on S, either $$v_i = \hat{v}_i \qquad \text{(A.III.3)}$$

   or $$p_i = \hat{p}_i \qquad \text{(A.III.4)}$$

where a tilde indicates a fixed parameter, and

$$P_i = n_j t_{ij}$$

($\bar{n}$ is the unit outward normal vector to S).

The strain energy density, $W(e)$, defines the stress-strain relations.

$$W = \frac{1}{2} c_{rs}^{ij} e_{ij} e_{rs} \qquad \text{(A.III.5)}$$

$$\frac{\partial W(e)}{\partial e_{ij}} = c_{rs}^{ij} e_{rs} = t_{ij} \qquad \text{(A.III.6)}$$

The quantities U, P and D are now defined.

$$U = \iiint_R W(e)\, d\tau \qquad \text{(A.III.7)}$$

$$P = -\iiint_R \hat{F}_i v_i\, d\tau - \int_{S_\tau} \hat{p}_i v_i\, dS \qquad \text{(A.III.8)}$$

$$D = \iiint_R t_{ij}\left[\frac{1}{2}(v_{i,j} + v_{j,i}) - e_{ij}\right] d\tau + \int_{S_v} p_i(\hat{v}_i + v_i)\, dS \qquad \text{(A.III.9)}$$

Now consider the variation

$$\delta[U + P + D] \qquad \text{(A.III.10)}$$

δe_{ij} yields $$\iiint_R \left(\frac{\partial W}{\partial e_{ij}} - t_{ij}\right) d\tau \qquad \text{(A.III.11)}$$

δt_{ij} yields:

$$\iiint_R \left[\frac{1}{2}\left(v_{i,j}+v_{j,i}\right)-e_{ij}\right]d\tau+\int_{S_v}\eta_j\left(\hat{v}_i-v_i\right)dS \qquad \text{(A.III.12)}$$

δv_i yields (via Green's theorem):

$$\iiint_R\left(-t_{ij,j}-\hat{F}_i\right)d\tau+\int_{S_v}\left(t_{ij}\eta_j-p_i\right)dS+\int_{S_\tau}\left(p_i-\hat{p}_i\right)dS \qquad \text{(A.III.13)}$$

If the variations are equated to zero, then the equations (A.III.1 to A.III.4) are satisfied over the domain of the body. Also the strain-displacement relations

$$e_{ij} = \frac{1}{2}\left(v_{i,j}+v_{j,i}\right) \qquad \text{(A.III.14)}$$

are satisfied. If the requirements of (A.III.14), (A.III.2) and (A.III.3) are satisfied a priori, then $\mathcal{D}$ becomes identically zero. The equilibrium equations, and the remaining boundary conditions are imposed by equating the variation of $U + P$ (the potential energy), with respect to the displacement field, v_i , to zero. This is the variational statement used in displacement finite elements. We now apply this principle to finite elements. The matrix equations quoted earlier relating stresses to strain and nodal displacements (3.2.4., 2.4.8) are used again.

$$\{\sigma\} = [D]\{\varepsilon\} \qquad \text{(A.III.15)}$$

$$\{\varepsilon\} = [R]\{\delta\} \qquad \text{(A.III.16)}$$

The body force density and surface tractions are expressed in matrix form as $\{F\}$ and $\{p\}$.

We can write W , in matrix form (from A.III.5) as

$$W = \frac{1}{2} \{\varepsilon\}^T [D] \{\varepsilon\} \quad , \qquad \text{(A.III.17)}$$

and so

$$U = \frac{1}{2} \iiint_R \{\varepsilon\}^T [D] \{\varepsilon\} \, d\tau \qquad \text{(A.III.18)}$$

From (A.III.16)

$$U = \frac{1}{2} \iiint_R \{\delta\}^T [R]^T [D] [R] \{\delta\} \, d\tau \qquad \text{(A.III.19)}$$

Now in matrix form

$$P = - \iiint_R \{\delta\}^T \{F\} \, d\tau - \int_{S_\tau} \{\delta\}^T \{p\} \, dS \qquad \text{(A.III.20)}$$

If $\delta [U+P] = 0$ (varied with respect to the displacements), then

$$\frac{\partial [U+P]}{\partial \delta} = 0 \qquad \text{(A.III.21)}$$

This gives

$$\left(\iiint_R [R]^T [D] [R] \, d\tau \right) \{\delta\} - \iiint_R \{F\} \, d\tau - \int_{S_\tau} \{p\} \, dS \qquad \text{(A.III.22)}$$

This applies equally to the entire body, or to any element. The stiffness matrix $[k]$, is

$$[k] = \iiint_R [R]^T [D] [R] \, d\tau \qquad \text{(A.III.23)}$$

and the loading can be written as a column matrix $\{f\}$, where

$$\{f\} = \iiint_R \{F\} \, d\tau - \int_{S_\tau} \{p\} \, dS \qquad \text{(A.III.24)}$$

APPENDIX IV

Program Listings

1. Rectangular element.

2. Triangular element.

```
      IMPLICIT REAL*8 (A-D,F-H,O-Z)
      INTEGER ENI
      DIMENSION PARAM(4,8),AMAT(5,5),BMAT(5,5),CMAT(5,5),DMAT(5,5),
     2C(20,20),ST(13000),U(500)  ,NF(200),NB(200,5),BV(200,5),
     3 NODE(200,4),BARON(20)
      DIMENSION   CA(20),FORCE(20)
      COMMON / ONE / NBW,MAT
      COMMON / TWO / NPOINT,NELEM,NBOUND,NF,NFREE,NODE,NB
      COMMON / THREE / C,ST,U,A,B,BV,STIFXX,STIFYY,STIFXY,STIFTT,SHEARX,
     1 SHEARY,AMAT,BMAT,CMAT,DMAT,BARON,PARAM
C
C              P E T E R                    B E T T E S S
C
C          C I V I L          E N G I N E E R I N G          S E C T I O N
C
C           DEPARTMENT       OF        ENGINEERING          SCIENCE
C
C       U N I V E R S I T Y           O F           D U R H A M
C*****************************************************************************
C   S A N D W I C H   P L A T E  E L E M E N T      N U M B E R    1
C*****************************************************************************
      READ(5,1111) NPLATE
 1111 FORMAT(I10)
      DO 411 IJIJ = 1,NPLATE
      WRITE(6,1122)          IJIJ
 1122 FORMAT(1X,//15H PLATE NUMBER     ,I10)
      CALL INPUT
C   CALCULATE  MATRIX SIZE AND BANDWIDTH
      MAT = 0
      NBW = 0
      DO 410 JJ=1,NELEM
      DO 410 I=1,4
      LATE=NODE(JJ,I)
      IF(LATE.GT.MAT) MAT=LATE
      DO 410 J=1,4
      LOOT=NODE(JJ,I) - NODE(JJ,J)
      IF(LOOT.GT.NBW) NBW=LOOT
  410 CONTINUE
      NBW=NBW * NFREE + NFREE
      MAT = NFREE * MAT
```

```
C   INITIALISE  OVERALL STIFFNESS  MATRIX
      DO 50 I= 1,13000
C     ASSEMBLY
   50 ST(I) = 0.0
      CALL STIFF
      DO 110 LK=1,NELEM
      DO 111 JOIN1=1,4
      DO 111 JOIN2=1,4
      MAMMA = NFREE*(NODE(LK,JOIN2)-1)
      MACACO=NFREE*(NODE(LK,JOIN1)-1)
      MACE = NFREE * ( JOIN1 - 1)
      MACAW = NFREE * ( JOIN2 - 1)
      DO 111 LYING=1,NFREE
      DO 111 LYDIAN=1,NFREE
      MACH = MAMMA + LYDIAN
      MACHAN=MACACO + LYING
      MACLE = MACAW + LYDIAN
      MACRON = MACE + LYING
      IF(MACH.GT.MACHAN) GO TO 111
      MENT=ENT(MACH,MACHAN)
      ST(MENT)=ST(MENT)+C(MACLE,MACRON)
  111 CONTINUE
  110 CONTINUE
C   APPLY  BOUNDARY  CONDITIONS
      DO 120 I=1,NBOUND
      MITRE = NF(I) - 1
      DO 121 J=1,NFREE
      IF(NB(I,J).NE.0) GO TO 121
      MOTOR=NFREE * MITRE + J
      NZ = MOTOR-NBW+1
      IF(NZ.LE.0) NZ=1
      DO 400 IJ=NZ,MOTOR
      MENT=ENT(IJ,MOTOR)
  400 ST(MENT)=0.0
      NZ=MOTOR + NBW - 1
      IF(NZ.GT.MAT) NZ=MAT
      DO 401 IJ=MOTOR,NZ
      MENT=ENT(MOTOR,IJ)
  401 ST(MENT)=0.0
      MENT = ENT(MOTOR,MOTOR)
```

```
      ST(MENT) =1.0
      U(MOTOR) = BV(I,J)
  121 CONTINUE
  120 CONTINUE
      CALL CHOLS
C     OUTPUT   DISPLACEMENTS
      MATE = MAT/5
      WRITE(6,1002)
 1002 FORMAT(1X,44H        SOLUTIONS      FOR      DISPLACEMENTS       )
      DO 10 II = 1,MATE
      NOT = 5*II
      NOTE = NOT - 4
      WRITE(6,1000) ( II ,(U(KK),KK=NOTE,NOT))
 1000 FORMAT(1X,I10,5E14.7)
   10 CONTINUE
      CALL STRESS
C     CALCULATE  STRESSES
      DO 14 LL = 1,NELEM
      DO 15 I = 1,4
      JJ = NODE(LL,I)
      CA(5*I-4)  = U(5*JJ-4)
      CA(5*I-3)  = U(5*JJ-3)
      CA(5*I-2)  = U(5*JJ-2)
      CA(5*I-1)  = U(5*JJ-1)
      CA(5*I)    = U(5*JJ)
   15 CONTINUE
      DO 16 I = 1,20
      FORCE(I) = 0.0
      DO 16 L = 1,20
      FORCE(I) = FORCE(I)  + C(I,L)*CA(L)
   16 CONTINUE
C     OUTPUT   STRESSES
      WRITE(6,1013)   LL
 1013 FORMAT(1X,19H  ELEMENT NUMBER   : ,I10)
      WRITE(6,1014)  LL,(FORCE(I),I=1,20)
 1014 FORMAT(3X,I10,8X,' I ',5(F12.6,4X)
     1    /  21X,' J ',5(F12.6,4X)
     2    /  21X,' K ',5(F12.6,4X)
     3    /  21X,' L ',5(F12.6,4X)                    )
   14 CONTINUE
```

```
111 CONTINUE
      STOP
      END
      SUBROUTINE INPUT
      IMPLICIT REAL*8 (A-D,F-H,O-Z)
      INTEGER ENT
      DIMENSION PARAM(4,8),AMAT(5,5),BMAT(5,5),CMAT(5,5),DMAT(5,5),
     2C(20,20),ST(13000),U(500) ,NF(200),NB(200,5),BV(200,5),
     3 NODE(200,4),BARON(20)
      DIMENSION AUK(2)
      COMMON / ONE / NBW,MAT
      COMMON / TWO / NPOINT,NELEM,NBOUND,NF,NFREE,NODE,NB
      COMMON / THREE / C,ST,U,A,B,BV,STIFXX,STIFYY,STIFXY,STIFTT,SHEARX,
     1 SHEARY,AMAT,BMAT,CMAT,DMAT,BARON,PARAM
      DATA AUK / 'UDL','PTS'/
C
C         INPUT    DATA
C
C        GENERAL  DATA
      READ(5,1122) NPOINT,NELEM,NBOUND,NFREE,NSIDE
 1122 FORMAT(6I5)
      WRITE(6,6791) NPOINT,NELEM,NBOUND,NFREE ,NSIDE
      CRUM = NSIDE
      A = 1.0/(CRUM * 2.0)
      A = A * 0.5
      READ(5,2000) ASPECT
      WRITE(6,2001) ASPECT
 2000 FORMAT(1X,F10.5)
 2001 FORMAT(1X,'   ASPECT  RATIO  ',F10.5//)
      B = A
      B = B * ASPECT
 6791 FORMAT(1X,'*****************************************************
     1*************************************************'//
     350H NUMBER OF NODES                                    ,I10,/,
     450H NUMBER OF ELEMENTS                                 ,I10,/,
     550H NUMBER OF B. C. S                                  ,I10,/,
     550H NUMBER OF D.OF F. AT EACH NODE                     ,I10,/
     6 '   NSIDE  = ',20X,I10//)
C       STIFFNESSES
      READ(5,1006)  STIFXX,STIFYY,STIFXY,STIFTT,SHEARX,SHEARY
```

```
      WRITE(6,1006) STIFXX,STIFYY,STIFXY,STIFTT,SHEARX,SHEARY
 1006 FORMAT(1X,6E12.5)
C      ELEMENT    NUMBERING
      DO   11=I,NELEM
      WRITE(6,1003) I
 1003 FORMAT(16H ELEMENT NUMBER ,I10)
      READ(5,1002)(NODE(I,J),J=1,4)
      WRITE(6,1002) (NODE(I,J) ,J=1,4)
 1002 FORMAT(4I10)
    1 CONTINUE
C     BOUNDARY    CONDITIONS
      DO   2 I = 1,NBOUND
      READ (5,1004) NF(I),(NB(I,J),J=1,5),(BV(I,J),J=1,5)
      WRITE(6,1004) NF(I),(NB(I,J),J=1,5),(BV(I,J),J=1,5)
 1004 FORMAT(1X,I5,5I2,5F10.5)
    2 CONTINUE
      DO 55 I = 1,500
   55 U(I) = 0.0
C     LOADING  TYPE
      READ(5,1000) TYPE
      IF(TYPE.EQ.AUK(1) ) GO TO 3
      IF(TYPE.EQ.AUK(2)) GO TO 4
      WRITE(6,1007) TYPE
 1007 FORMAT(/'   ERROR  IN  THE  LOADING '/40X,A3/)
 1000 FORMAT(1X,A3)
C    UNIFORM    LOADING
    3 READ(5,2000) Q
      DO 56 I = 1,20
   56 BARON(I) = 0.0
      MAT = NPOINT * NFREE
      DO 51 J = 1,4
      BARON(5*J-4) = 1.0/4.0
      BARON(5*J-3) = B/12.0
   51 BARON(5*J-2) = A/12.0
      BARON(2) = -BARON(2)
      BARON(7) = - BARON(7)
      BARON(8) = -BARON(8)
      BARON(18) = -BARON(18)
      DO 50 I = 1,NELEM
      DO 52 J = 1,4
```

```
      KK = NODE(I,J)
      U(5*KK-4) = U(5*KK-4)    + BARON(5*J-4)
      U(5*KK-3) = U(5*KK-3)    + BARON(5*J-3)
      U(5*KK-2) = U(5*KK-2)    + BARON(5*J-2)
   52 CONTINUE
   50 CONTINUE
      DO 53 I = 1,MAT
   53 U(I) = U(I) * 4.0 *A*B*0
      RETURN
C        POINT   LOADING
    4 READ(5,1002) NLOAD
      WRITE(6,1009) NLOAD
 1009 FORMAT(/'   NUMBER   OF   POINT   LOADS ',I10/)
      DO 5 I = 1,NLOAD
      READ(5,1008) IMP,APPLE
      WRITE(6,1010) IMP,APPLE
      U(IMP) = APPLE
 1010 FORMAT(1X,'   D.  OF  F.  ',I10,'   LOAD   ',F10.5)
 1008 FORMAT(I5,F10.5)
    5 CONTINUE
      RETURN
      END
      SUBROUTINE CHOLS
      IMPLICIT REAL*8 (A-D,F-H,O-Z)
      INTEGER ENT
      DIMENSION  PARAM(4,8),AMAT(5,5),BMAT(5,5),CMAT(5,5),DMAT(5,5),
     2C(20,20),ST(13000),U(500)  ,NF(200),NB(200,5),BV(200,5),
     3 NODE(200,4),BARON(20)
      COMMON / ONE / NBW,MAT
      COMMON / TWO / NPOINT,NELEM,NBOUND,NF,NFREE,NODE,NB
      COMMON / THREE / C,ST,U,A,B,BV,STIFXX,STIFYY,STIFXY,STIFTT,SHEARX,
     1 SHEARY,AMAT,BMAT,CMAT,DMAT,BARON,PARAM
C
C     SOLUTION OF   OVERALL EQUILIBRIUM   EQUATIONS,  BY   CHOLESKI   METHOD
C     FOR   SYMMETRICAL   MATRICES
C
      WRITE(6,1002)       NBW,MAT
 1002 FORMAT(1X,12H BANDWIDTH  , I10/16H SIZE OF MATRIX ,I10)
      MENT = ENT(1,1)
C     ST(MENT) = SQRT(ST(MENT))
```

```
      ST(MENT) =DSQRT(ST(MENT))
      DO 99 J = 2,NBW
      MENT = ENT(1,J)
      MONT = ENT(1,1)
      ST(MENT) = ST(MENT)/ST(MONT)
   99 CONTINUE
      DO  1  I =  2,MAT
      NEWT = I + NBW -1
      IF(NEWT.GT.MAT)  NEWT = MAT
      DO 1 J = I,NEWT
      SUM = 0.0
      IF(I.EQ.J)  GO  TO  2
      NZ = J - NBW+1
      IF(NZ.LE.0)  NZ  = 1
      NULL = I - 1
      IF(NZ.GT.NULL)  GO TO 20
      DO 3 M = NZ,NULL
      MENT = ENT(M,I)
      MONT = ENT(M,J)
    3 SUM = SUM + ST(MENT)*ST(MONT)
   20 MENT = ENT (I,J)
      MONT = ENT(I,I)
      ST(MENT)=(ST(MENT) - SUM)/ST(MONT)
      GO TO 1
    2 NZ = I - NBW    + 1
      IF(I.LE.NBW)  NZ = 1
      NULL = I-1
      DO 4 M = NZ,NULL
      MENT = ENT(M,J)
    4 SUM = SUM +  (ST(MENT) **2)
      MENT = ENT(I,J)
C     ST(MENT)= SQRT(ST(MENT) - SUM)
      ST(MENT)=DSQRT(ST(MENT) - SUM)
    1 CONTINUE
      MENT = ENT(1,1)
      U(1) = U(1)/ST(MENT)
      DO 5  N = 2,MAT
      SUM = 0.0
      NZ = N - NBW    +1
      IF(NZ.LE.0)  NZ = 1
```

```
      NODDY = N-1
      DO 6  J = NZ,NODDY
      MENT = ENT(J,N)
    6 SUM = SUM + ST(MENT)* U(J)
      MENT = ENT(N,N)
    5 U(N) = (U(N) - SUM)/ST(MENT)
      MENT = ENT(MAT,MAT)
      U(MAT)=U(MAT)/ST(MENT)
      DO 7     N = 2,MAT
      I = MAT- N +1
      NZ = I +  NBW   -  1
      IF(NZ.GE.MAT) NZ = MAT
      SUM = 0.0
      IMP = I + 1
      DO 8 J = IMP,NZ
      MENT = ENT(I,J)
    8 SUM = SUM + ST(MENT)*U(J)
      MENT = ENT(I,I)
    7 U(I) = (U(I) - SUM)/ST(MENT)
      RETURN
      END
      INTEGER FUNCTION ENT(I,J)
      COMMON / ONE / NBW,MAT
C
C    INTEGER   FUNCTION  FOR  LOCATING  ELEMENT   IN  ROW I  AND
C   COLUMN  J  OF  OVERALL  STIFFNESS   MATRIX,  IN   SINGLY   DIMENSIONED
C     ARRAY, ST
C
      ENT  =  J - I + 1 + (I-1)*NBW
      RETURN
      END
      SUBROUTINE STIFF
      IMPLICIT REAL*8 (A-D,F-H,O-Z)
      INTEGER ENT
      DIMENSION  PARAM(4,8),AMAT(5,5),BMAT(5,5),CMAT(5,5),DMAT(5,5),
     2C(20,20),ST(13000),U(500)  ,NF(200),NB(200,5),BV(200,5),
     3 NODE(200,4),BARON(20)
      COMMON / ONE / NBW,MAT
      COMMON / TWO / NPOINT,NELEM,NBOUND,NF,NFREE,NODE,NB
      COMMON / THREE / C,ST,U,A,B,BV,STIFXX,STIFYY,STIFXY,STIFTT,SHEARX,
```

```
     1 SHEARY,AMAT,BMAT,CMAT,DMAT,BARON,PARAM
C
C      FORMATION   OF   ELEMENT    STIFFNESS   MATRIX
C
    70 AB240 = 240. * A*B
       PSQ =(A*A)/(B*B)
       DO 20 I = 1,5
       DO 20 J = 1,5
       AMAT(I,J) = 0.0
       BMAT(I,J) = 0.0
       CMAT(I,J) = 0.0
    20 DMAT(I,J) = 0.0
       DO 21 I = 1,4
       DO 21 J = 1,8
    21 PARAM(I,J)   = 0.0
       DO 22  I = 1,20
       DO 22  J = 1,20
    22 C(I,J) = 0.0
       CARROT = SHEARX*B/(9.0*A)
       SPROUT = SHEARY* A  /(9.0* B)
       DO 1 I = 1,2
       PARAM(I,1) = 240.
       PARAM(I,2) = 120.
       PARAM(I,3) = 80.
       PARAM(I,4) = 60.
       PARAM(I,5) = 40.
       PARAM(I,6) = 20.
     1 PARAM(I,7) = 10.
       PARAM(3,4) = 15.
       PARAM(3,3) = 30.
       PARAM(3,2) = 60.
       PARAM(3,1) = 120.
       PARAM(4,8) = 8.
       PARAM(4,7) = 10.
       PARAM(4,6) = 15.
       PARAM(4,5) = 20.
       PARAM(4,4) = 24.
       PARAM(4,3) = 32.
       PARAM(4,2) = 60.
       PARAM(4,1) = 336.
```

```
      DO 2 I = 1,8
      PARAM(1,I) = ((STIFXX*PARAM(1,I))/AB240)/PSQ
      PARAM(2,I) = (STIFYY*PARAM(2,I) / AB240) *  PSQ
      PARAM(3,I) = STIFXY*PARAM(3,I) / AB240
      PARAM(4,I) = STIFTT * PARAM(4,I) / AB240
    2 CONTINUE
      AMAT(1,1) = -PARAM(1,2)-PARAM(2,2)+PARAM(3,1)+PARAM(4,1)
      AMAT(1,2) = + PARAM(2,4) - PARAM(4,4)
      AMAT(1,3) = -PARAM(1,4) + PARAM(4,4)
      AMAT(1,4) = PARAM(3,3) + PARAM(4,2)
      AMAT(1,5) = AMAT(1,4)
      AMAT(2,2) = - PARAM(2,6) - PARAM(4,8)
      AMAT(2,3) =    0.0
      AMAT(2,4) =   0.0
      AMAT(2,5) = PARAM(2,7)  - PARAM(4,7)
      AMAT(3,3)= - PARAM(1,6) - PARAM(4,8)
      AMAT(3,4) = - PARAM(1,7) + PARAM(4,7)
      AMAT(3,5) = 0.0
      AMAT(4,4) = PARAM(1,7) + PARAM(4,7) - CARROT/ 4.0
      AMAT(4,5) = PARAM(3,4) + PARAM(4,6)
      AMAT(5,5) =  PARAM(2,7) + PARAM(4,7) - SPROUT / 4.0
      BMAT(1,1) = PARAM(1,2)-PARAM(2,1) -PARAM(3,1) - PARAM(4,1)
      BMAT(1,2) = PARAM(2,2) + PARAM(4,4)
      BMAT(1,3) = PARAM(1,4) - PARAM(3,2) - PARAM(4,4)
      BMAT(1,4)= PARAM(3,3) - PARAM(4,2)
      BMAT(1,5) = - PARAM(3,3) - PARAM(4,2)
      BMAT(2,2) = - PARAM(2,5) + PARAM(4,8)
      BMAT(2,3) = 0.0
      BMAT(2,4) = 0.0
      BMAT(2,5) = PARAM(2,6) + PARAM(4,7)
      BMAT(3,3)=  PARAM(1,5) - PARAM(4,3)
      BMAT(3,4) =-PARAM(1,7) + PARAM(4,7)
      BMAT(3,5) = - PARAM(3,3)
      BMAT(4,4) = + PARAM(1,7) - PARAM(4,5) + CARROT / 2.0
      BMAT(4,5) = PARAM(3,4) - PARAM(4,6)
      BMAT(5,5)= PARAM(2,6) - PARAM(4,7) - SPROUT  / 2.0
      CMAT(1,1) = -PARAM(1,1)+PARAM(2,2) -PARAM(3,1) - PARAM(4,1)
      CMAT(1,2)= -PARAM(2,4) + PARAM(3,2) + PARAM(4,4)
      CMAT(1,3) = -PARAM(1,2)-PARAM(4,4)
      CMAT(1,4) = -PARAM(3,3) - PARAM(4,2)
```

```
      CMAT(1,5) = + PARAM(3,3) - PARAM(4,2)
      CMAT(2,2) = PARAM(2,5) -PARAM(4,3)
      CMAT(2,3) = 0.0
      CMAT(2,4) = PARAM(3,3)
      CMAT(2,5) = PARAM(2,7) - PARAM(4,7)
      CMAT(3,3) = - PARAM(1,5) + PARAM(4,8)
      CMAT(3,4) = -PARAM(1,6)-PARAM(4,7)
      CMAT(3,5) = 0.0
      CMAT(4,4) = PARAM(1,6) - PARAM(4,7) - CARROT / 2.0
      CMAT(4,5) = PARAM(3,4) - PARAM(4,6)
      CMAT(5,5) = PARAM(2,7) - PARAM(4,5) + SPROUT  / 2.0
      DMAT(1,1) = PARAM(1,1) + PARAM(2,1)+PARAM(3,1)+PARAM(4,1)
      DMAT(1,2) = -PARAM(2,2) -PARAM(3,2) - PARAM(4,4)
      DMAT(1,3) = PARAM(1,2) + PARAM(3,2) + PARAM(4,4)
      DMAT(1,4) = -PARAM(3,3) + PARAM(4,2)
      DMAT(1,5) = -PARAM(3,3) + PARAM(4,2)
      DMAT(2,2) = PARAM(2,3) + PARAM(4,3)
      DMAT(2,3) = - PARAM(3,2)
      DMAT(2,4) = PARAM(3,3)
      DMAT(2,5) = PARAM(2,6) + PARAM(4,7)
      DMAT(3,3) = PARAM(1,3) + PARAM(4,3)
      DMAT(3,4) = -PARAM(1,6) -PARAM(4,7)
      DMAT(3,5) = -PARAM(3,3)
      DMAT(4,4) = PARAM(1,6) + PARAM(4,5) + CARROT
      DMAT(4,5) =   PARAM(3,4) + PARAM(4,6)
      DMAT(5,5) = PARAM(2,6) + PARAM(4,5) + SPROUT
      DO 3 I = 1,5
      DO 3 J = 1,5
      AMAT(J,I) = AMAT(I,J)
      BMAT(J,I) = BMAT(I,J)
      CMAT(J,I) = CMAT(I,J)
      DMAT(J,I) = DMAT(I,J)
    3 CONTINUE
 1000 FORMAT(1X,5F12.6)
      DO 5 I = 1,5
      DO 5 J = 1,5
      C(I,J) = DMAT(I,J)
      C(I+5,J+5)        = DMAT(I,J)
      C(I+10,J+10)      =  DMAT(I,J)
      C(I+15,J+15)      =  DMAT(I,J)
```

```
      C(I+15,J)          =    AMAT(I,J)
      C(I+10,J+5)        =    AMAT(I,J)
      C(I+5,J+10)         =    AMAT(I,J)
      C(I,J+15)          =   AMAT(I,J)
      C(I+5,J)       =       CMAT(I,J)
      C(I,J+5)       =       CMAT(I,J)
      C(I+15,J+10)  =    CMAT(I,J)
      C(I+10,J+15) =    CMAT(I,J)
      C(I+10,J)     = BMAT(I,J)
      C(I+15,J+5)   =            BMAT(I,J)
      C(I,J+10)     =          BMAT(I,J)
    5 C(I+5,J+15) = BMAT(I,J)
      DO 6   I = 2,17,5
      DO 6 J = 1,20
      C(I,J)= C(I,J)* 2.0*B
    6 C(I+2,J)= C(I+2,J)*(2.0*A)
      DO 7 I = 2,17,5
      DO 7 J = 1,20
      C(J,I)  = C(J,I) * 2.0 * B
    7 C(J,I+2) = C(J,I+2)*(          2.0 * A )
      DO 8 I = 3,18,5
      DO 8 J = 1,20
      C(I,J) = C(I,J) * 2.0 * A
    8 C(I+2,J)= C(I+2,J)*(2.0*B          )
      DO 9 I = 3,18,5
      DO 9 J = 1,20
      C(J,I) = C(J,I) * 2.0 * A
    9 C(J,I+2) = C(J,I+2)*(2.0*B              )
      DO 10 I = 1,20
      C(I,8) = -C(I,8)
      C(I,9)= -C(I,9)
      C(I,12)=   -C(I,12)
      C(I,5) = - C(I,5)
      C(I,1) =-C(I,10)
      DO 11 J = 17,19
   11 C(I,J)= -C(I,J)
   10 CONTINUE
      DO 12 I = 1,20
      C(8,I) = -C(8,I)
      C(9,I) = -C(9,I)
```

```
      C(12,I)=  -C(12,I)
      C(5,I) = - C(5,I)
      C(10,I) = - C(10,I)
      DO 13 J = 17,19
   13 C(J,I) = - C(J,I)
   12 CONTINUE
      WRITE(6,1001)
 1001 FORMAT(//'  ELEMENT   STIFFNESS   MATRIX'///)
      WRITE(6,1002) ((C(I,J),J=1,10),I=1,20)
      WRITE(6,1002) ((C(I,J),J=10,20),I=1,20)
 1002 FORMAT(1X,10F12.6)
      RETURN
      END
      SUBROUTINE STRESS
      IMPLICIT REAL*8 (A-D,F-H,O-Z)
      DIMENSION PARAM(4,8),AMAT(5,5),BMAT(5,5),CMAT(5,5),DMAT(5,5),
     2C(20,20),ST(13000),U(500)  ,NF(200),NB(200,5),BV(200,5),
     3 NODE(200,4),BARON(20)
      COMMON / ONE / NBW,MAT
      COMMON / TWO / NPOINT,NELEM,NBOUND,NF,NFREE,NODE,NB
      COMMON / THREE / C,ST,U,A,B,BV,STIFXX,STIFYY,STIFXY,STIFTT,SHEARX,
     1 SHEARY,AMAT,BMAT,CMAT,DMAT,BARON,PARAM
C
C   FORMATION   OF   ELEMENT   STRESS   MATRIX
C
      DO 1 I = 1,20
      DO 1 J = 1,20
    1 C(I,J) = 0.0
      P =  A/B
      C(1,1) =  -6.0 *STIFXX/P  - 6.0*STIFXY * P
      C(1,2) = 8.0 * A * STIFXY
      C(1,3)= -8.0 * B * STIFXX
      C(1,4) = 2.0 * STIFXX * B
      C(1,5)= -2.0 * A * STIFXY
      C(1,6) =  6.0 * STIFXX/P
      C(1,8) = -4.0 * B * STIFXX
      C(1,9) = -2.0 * B * STIFXX
      C(1,11) = 6.0 * P * STIFXY
      C(1,12) = 4.0 * A * STIFXY
      C(1,15) =  2.0 * A * STIFXY
```

```
C
      C(2,1)  = -6.0 * P * STIFYY - 6.0* STIFXY/P
      C(2,2) = 8.0 * A * STIFYY
      C(2,3)  = -8.0 * B * STIFXY
      C(2,4)  =  2.0 * B * STIFXY
      C(2,5)  = -2.0 * A * STIFYY
      C(2,6)  =  6.0 * STIFXY/P
      C(2,8)  = -4.0 * B * STIFXY
      C(2,9) =  -2.0 * B * STIFXY
      C(2,11) =  6.0 * P * STIFYY
      C(2,12) = 4.0 * A * STIFYY
      C(2,15) =  2.0 * A * STIFYY
C
      C(3,1)  =  -2.0 * STIFTT
      C(3,2) = 4.0 * B * STIFTT
      C(3,3)  =  -4.0 * A * STIFTT
      C(3,4)  =   2.0 * A * STIFTT
      C(3,5)  =  -2.0 * B * STIFTT
      C(3,6)  =   2.0 * STIFTT
      C(3,7)  = - C(3,2)
      C(3,10) = - C(3,5)
      C(3,11) = - C(3,1)
      C(3,13) = - C(3,3)
      C(3,14) = - C(3,4)
      C(3,16) =   C(3,1)
C
      C(4,4)  =  4.0 * A*B * SHEARX
C
      C(5,5)  = -4.0 * A*B * SHEARY
C
      AB4  = 4.0 * A * B
      DO 2 I =1,5
      DO 2 J =1,20
    2 C(I,J) =  C(I,J)/AB4
      DO 3 I = 1,5
      C(I,15) =   -C(I,15)
      C(I,8)  =  - C(I,8)
      C(I,9)  =  - C(I,9)
      C(I,20) =   -C(I,20)
      C(I,12)=  - C(I,12)
```

```
      C(I,17) =  -C(I,17)
      C(I,18) =  -C(I,18)
    3 C(I,19) =  -C(I,19)
      DO 5 I =1,5
      DO 5 J = 1,5
      C(I+5,J+5) = C(I,J)
      C(I+10,J+10) = C(I,J)
      C(I+15,J+15) = C(I,J)
      C(I+5,J)  = C(I,J+5)
      C(I+10,J+15) = C(I,J+5)
      C(I+15,J+10) = C(I,J+5)
      C(I+5,J+15)  = C(I,J+10)
      C(I+10,J)    = C(I,J+10)
      C(I+15,J+5)  = C(I,J+10)
      C(I+5,J+10)  = C(I,J+15)
      C(I+10,J+5)  = C(I,J+15)
      C(I+15,J)    = C(I,J+15)
    5 CONTINUE
      DO 6 I =1,20
      C(I,8) =  -C(I,8)
      C(I,9) = -C(I,9)
      C(I,15) =  -C(I,15)
      C(I,20) =  -C(I,20)
      C(I,12) = - C(I,12)
      C(I,17) = - C(I,17)
      C(I,18) = - C(I,18)
    6 C(I,19) = - C(I,19)
       DO 77 J =1,20
      C(8,J) = -C(8,J)
   77 C(13,J) = -C(13,J)
 7777 FORMAT(1X,10F10.3)
      RETURN
      END
```

```
      SUBROUTINE STIFF
      IMPLICIT REAL*8 (A-H,O-Z)
      DIMENSION STIF(10),
     2IB(16),DAHLIA(16,16),DAIL(16,16), DAISY(16,16),ELAST(6,6),
     3FRODO(2,2),ROGER(6,6),RUM(20),       AARD(3),AARON(3),ABAFF(23,20)
     4,ABASH(3,3),ABASE(3,3),ABACUS(3,12),AAAAA(3),BOAT(2,3),HOLL(2,3),
     5ABLAUT(20,20),ABBEY(3),ABLAZE(3),TWIT(2,2),ABJURE(6),BERRY(2),
     6 DAA(6,16),STIGMA(23,23),TRAN(2,2),TUM(20) ,IND(28)
      DIMENSION ID(6)
      DIMENSION ELAST1(6,6), TAISY(6,16),TEMD(36)
      DIMENSION A(3),B(3),C(3),STR(3,6),ELA(3,3),X1(2,3),BALF(6,6),
     1 TEMP(3,6)
      DIMENSION SAURON(8,8)
      DIMENSION XDASH(3,3),DIRCOS(3,3)
      DIMENSION SPY(28,28)
       DIMENSION W21(4,24),W22(4,4),LU(6),MU(6)
      DIMENSION SPYL(784),W21L(96),W22L(16),GROAN(36,24),Q2(36,4)
      DIMENSION BLUNT(2,24,24),BLINT(2,27,24)
      COMMON /FIVE/ IB
      COMMON /SIX/ ID
      COMMON / STI / X(3,20),YOUNG(12),STUCK(36,36),STICK(36,36),
     1 FORCE(36),INFO(20)
      EQUIVALENCE (SPY(1,1),SPYL(1)),(W21(1,1),W21L(1)),
     1 (W22(1,1),W22L(1))
      EQUIVALENCE (STICK(1,25),Q2(1,1))
      DATA IND/3,4,5,10,11,12,17,18,19,22,23,24,6,7,13,14,20,21,
     1 27,28,1,2,8,9,15,16,25,26 /
C*****************************************************************************
C
C       TRIANGULAR FLEXURAL    FINITE  ELEMENT  FOR   SANDWICH    PLATES
C
C                     P E T E R                B E T T E S S
C
C              DEPARTMENT        OF        ENGINEERING       SCIENCE
C
C          U N I V E R S I T Y          O F        D U R H A M
C
C                              MAY      1971
C*****************************************************************************
C
```

```
C     ARITHMETIC  FUNCTION  STATEMENTS
      SIN(AX) = DSIN(AX)
      COS(AX) = DCOS(AX)
      SQRT(AX) = DSQRT(AX)
      ABS(AX) = DABS(AX)
C    INITIALISE  ARRAYS
      DO 46 I = 1,8
      DO 46 J = 1,8
   46 SAURON(I,J) = 0.0
      DO 1 I = 1,23
      DO 1 J = 1,23
    1 STIGMA(I,J) = 0.0
      DO 80 I = 1,36
      FORCE(I) = 0.0
      DO 80 J = 1,36
   80 STICK(I,J) = 0.0
      DO 583 I = 1,3
      DO 583 J = 1,3
  583 XDASH(I,J) = X(J,I)
C    OBTAIN   TRANSFORMATION MATRIX, LOCAL TO GLOBAL COORDINATES
      CALL DIRECT(XDASH,DIRCOS)
C    CALCULATE  COORDINATES IN LOCAL SYSTEM
      DO 584 I = 1,3
      DO 584 J = 1,3
      SUM = 0.0
      DO 586 K = 1,3
  586 SUM = SUM + DIRCOS(K,I) * XDASH(J,K)
  584 X(I,J) = SUM
C     OPTIONAL   DIAGNOSTIC   WRITES
      IF(INFO(11).EQ.999) WRITE(6,1004)((X(I,J),J=1,3),I=1,3)
 1004 FORMAT(1X,3D15.6)
      IF(INFO(11).EQ.999) WRITE(6,1004)((DIRCOS(I,J),J=1,3),I=1,3)
C     FIND   CENTROID
      DO 500 I = 1,2
  500 X(I,4) = (X(I,1)+X(I,2)+X(I,3))/3.0
C  OPTIONAL JUMP IF THE STIFFNESS MATRIX HAS BEEN FOUND PREVIOUSLY
      KLOCK = INFO(12)
      IF(KLOCK.EQ.1.OR.KLOCK.EQ.2) GO TO 400
C    FIND DISTANCES, CENTROID TO VERTICES
      DO 4 I = 1,3
```

```
      4 AARD(I) = SQRT((X(1,I)-X(1,4))**2 + (X(2,I)-X(2,4))**2)
        DO 501 I = 1,10
    501 STIF(I) = YOUNG(I)
        COD = YOUNG(11)
        DAB = YOUNG(12)
C    CALCULATES THE ANGLES  ALPHA,ALPHADASHED,BETA,BETADASHED,GAMMA,GAMMADASHED
        DO 5 I = 1,3
        J= I+1
        IF(J.GT.3) J =1
        ABAYA = X(2,J)-X(2,I)
        ABBOT = X(1,J)-X(1,I)
        ABET = X(2,I)-X(2,4)
        ABIET = X(1,I) -X(1,4)
        AARON(I) =  WCBTAN(ABIET,ABET)
      5 ABBEY(I) =  WCBTAN(ABBOT,ABAYA)
C
        ALPHA  = AARON(2) - AARON(1)
        BETA   = AARON(3) - AARON(2)
        GAMMA  = AARON(1) - AARON(3)
        IF(ALPHA.LT.0.0) ALPHA = ALPHA +6.2831853
        IF(BETA.LT.0.0)  BETA  = BETA  +6.2831853
        IF(GAMMA.LT.0.0) GAMMA = GAMMA +6.2831853
C
C FORM THE  20 * 23 CONDENSATION  MATRIX ABAFF
C
        DO 6 I = 1,20
        DO 6 J = 1,23
      6 ABAFF(J,I) = 0.0
        DO 7 I = 1,20
        J=I + 3
      7 ABAFF(J,I) = 1.0
C
C  ABACUS IS A  3 * 12  TEMPORARY  MATRIX
C
C  ABASH IS A TEMPORARY  3 * 3 MATRIX
C  ABASE IS A TEMPORARY  3 * 3 MATRIX
C
        ABATE  =  SIN(ALPHA)/SIN(ALPHA +BETA)
        ABEAM  =  SIN(ALPHA)/SIN(BETA)
        ABAFT  =  SIN(BETA)/SIN(ALPHA + BETA)
```

```
      ABASH(1,1) =  -1.0/AARD(2) +ABAFT/AARD(1)+ABATE/AARD(3)
      ABASH(1,2) = -3.0/(AARD(1)*AARD(2))+3.0*ABATE/(AARD(3)*AARD(1))
     1 + 3.0 * ABAFT/(AARD(1)**2)
      ABASH(1,3) = 0.0
      ABASH(2,1) = 1.0/(ABEAM*AARD(2))- ABAFT/AARD(3) -
     1 ABAFT/(ABEAM* AARD(1))
      ABASH(2,2) =  -3.0/(AARD(2)*AARD(3))+ 3.0*ABATE/(AARD(3)*AARD(3))
     2 + 3.0*ABAFT/(AARD(1) * AARD(3))
      ABASH(2,3) =  -1.0/(ABATE*AARD(2))+1.0/AARD(3)+ 1.0/(AARD(1)
     1 *ABEAM )
      ABASH(3,1) = 0.0
      ABASH(3,2) =  -3.0/(AARD(1)*AARD(2)) + 3.0/(AARD(2)*AARD(2)*ABAFT)
     1 -3.0 * ABEAM/(AARD(2)*AARD(3))
      ABASH(3,3) =  -1.0/AARD(1) + 1.0/(ABAFT*AARD(2))-ABEAM/AARD(3)
      ABOUT  =  0.0
      ABOUT  = ABASH(1,1)* ABASH(2,2) * ABASH(3,3)
      ABOUT  = ABOUT - ABASH(1,1)* ABASH(2,3) * ABASH(3,2)
      ABOUT  = ABOUT - ABASH(2,1)* ABASH(1,2) * ABASH(3,3)
      ABASE(1,1) =  ABASH(2,2)*ABASH(3,3) -ABASH(3,2) *ABASH(2,3)
      ABASE(1,2) =  -ABASH(1,2) * ABASH(3,3)
      ABASE(1,3) =  ABASH(1,2) * ABASH(2,3)
      ABASE(2,1) = -ABASH(2,1) * ABASH(3,3)
      ABASE(2,2) =  ABASH(1,1) * ABASH(3,3)
      ABASE(2,3) =  -ABASH(1,1)* ABASH(2,3)
      ABASE(3,1) =  ABASH(2,1) * ABASH(3,2)
      ABASE(3,2) =  -ABASH(1,1) * ABASH(3,2)
      ABASE(3,3) = ABASH(1,1)* ABASH(2,2) -ABASH(2,1)*ABASH(1,2)
      DO 8 I = 1,3
      DO 8 J = 1,3
    8 ABASE(I,J)  = ABASE(I,J)/ABOUT
      DO 9 I = 1,12
      DO 9 J = 1,3
    9 ABACUS(J,I) = 0.0
      ABACUS(1,1) = -3.0/(AARD(1)*AARD(2))+3.0*ABAFT/(AARD(1)*AARD(1))
      ABACUS(1,2) = 0.5/AARD(2) -1.5 * ABAFT/AARD(1)
      ABACUS(1,3) =-0.5/AARD(1)
      ABACUS(1,5) =-0.5/AARD(2)
      ABACUS(1,7) = 3.0 *ABATE/(AARD(3) *AARD(1))
      ABACUS(1,8) = 0.5*ABAFT/AARD(1)  + ABATE/AARD(3)
      ABACUS(1,9) = - 0.5/AARD(1)
```

```
      ABACUS(1,10) =  2.0/AARD(2)
      ABACUS(1,12) = -2.0 *ABATE /AARD(1)
      ABACUS(2,2)  = -0.5 *ABAFT/(ABEAM *AARD(1))
      ABACUS(2,3)  =  0.5/(ABEAM * AARD(1))
      ABACUS(2,4)  = - 3.0 /(AARD(2) * AARD(3))
      ABACUS(2,5)  =  1.0 /(ABEAM *AARD(2))
      ABACUS(2,6)  =  0.5 /AARD(3) - 1.0/(AARD(2)*ABATE)
      ABACUS(2,7)  =  3.0 *ABATE/(AARD(3)*AARD(3))+ 3.0*ABAFT/(AARD(3)*
     2 AARD(1))
      ABACUS(2,8)  = 2.0* ABAFT/AARD(3) + 0.5*ABAFT/(ABEAM*AARD(1))
      ABACUS(2,9)  =-1.5/AARD(3) - 0.5/(AARD(1)*ABEAM)
      ABACUS(2,11) =   2.0 /AARD(3)
      ABACUS(2,12) = - ABAFT * 2.0 /AARD(1)
      ABACUS(3,1) = -3.0/(AARD(1)* AARD(2))
      ABACUS(3,2) =  0.5/AARD(2)
      ABACUS(3,3) = -1.0/AARD(1)
      ABACUS(3,4) = 3.0/(AARD(2)*AARD(2)*ABAFT)-3.0*ABEAM/(AARD(2)*
     2 AARD(3))
      ABACUS(3,5) =  0.5/AARD(2)
      ABACUS(3,6) = - 2.0/(AARD(2)*ABAFT) + 0.5*ABEAM/AARD(3)
      ABACUS(3,9) = - 0.5 * ABEAM /AARD(3)
      ABACUS(3,10) =  2.0 /AARD(2)
      ABACUS(3,11) =  2.0 *ABEAM /AARD(3)
C
C NOW  POST MULTIPLY ABASE BY ABACUS AND STORE IN ABACUS AGAIN
C
      DO 10 J = 1,12
      DO 11 I = 1,3
      AAAAA(I) =  0.0
      DO 11 K = 1,3
   11 AAAAA(I) =  AAAAA(I) + ABACUS(K,J) * ABASE(I,K)
      DO 12 I = 1,3
   12 ABACUS(I,J)  =  AAAAA(I)
   10 CONTINUE
      DO 13  J = 1,12
      ABAFF(2,J)  = ABACUS(1,J)
      ABAFF(1,J)  = ABACUS(2,J)
   13 ABAFF(3,J)  = ABACUS(3,J)
C
C THIS COMPLETES THE FORMULATION OF THE CONDENSATION MATRIX ABAFF
```

```
C
C
C FORMATION OF THE 20*20 TRANSFORMATION MATRIX,ABLAUT
C
C THE LENGTHS OF THE EXTERNAL SIDES ARE ABJURE(I),I=1 TO 3
C
      DO 14 I = 1,3
      J = I + 1
      IF(J.GT.3) J= 1
   14 ABJURE(I) = SQRT((X(2,J)-X(2,I))**2+(X(1,J)-X(1,I))**2)
      DO 15 I = 1,20
      DO 15 J = 1,20
   15 ABLAUT(I,J) = 0.0
      TWIT(1,1) = (X(2,1)-X(2,4))/AARD(1)
      TWIT(1,2) = (X(1,1)-X(1,4))/AARD(1)
      TWIT(2,1) = (X(2,2)-X(2,4))/AARD(2)
      TWIT(2,2) = (X(1,2)-X(1,4))/AARD(2)
      DO 16 I = 1,7,3
      ABLAUT(I,I) = 1.0
      ABLAUT(I+1,I+1)  = TWIT(1,1)
      ABLAUT(I+1,I+2)  = TWIT(1,2)
      ABLAUT(I+2,I+1)  = TWIT(2,1)
      ABLAUT(I+2,I+2)  = TWIT(2,2)
   16 CONTINUE
      DO 17 J = 1,3
      BOAT(1,J) = AARON(1)- ABBEY(J)
   17 BOAT(2,J) =  AARON(2) - ABBEY(J)
      DO 18 I = 1,2
      DO 18 J = 1,3
   18 IF(BOAT(I,J).LT.0.0) BOAT(I,J) = BOAT(I,J) + 6.2831853
      DO 19 J = 1,3
      HOLL(1,J)  = SIN(BOAT(2,J))/SIN(BOAT(2,J)- BOAT(1,J))
   19 HOLL(2,J)  = SIN(BOAT(1,J))/SIN(BOAT(1,J)- BOAT(2,J))
      DO 20 I = 1,3
      AARON(I) = AARON(I) + 3.141592
      IF(AARON(I).GT.6.2831853) AARON(I) = AARON(I)-6.2831853
      ABLAZE(I) = AARON(I) - ABBEY(I)
      IF(AARON(I).LT.ABBEY(I)) ABLAZE(I)=ABLAZE(I) + 6.2831853
   20 CONTINUE
C
```

```
      ABLAUT(10,1) = 1.5 * COS(ABLAZE(1))/ABJURE(1)
      ABLAUT(10,4) = - ABLAUT(10,1)
      ABLAUT(10,3) = (COS(ABLAZE(1))/4.0) *(TWIT(1,2)*HOLL(1,1)
     2 +  TWIT(2,2) * HOLL(2,1))
      ABLAUT(10,6) = ABLAUT(10,3)
      ABLAUT(10,2) = (COS(ABLAZE(1))/4.0) *(TWIT(1,1)*HOLL(1,1)
     2  +  TWIT(2,1) * HOLL(2,1))
      ABLAUT(10,5)  =  ABLAUT(10,2)
      ABLAUT(11,4) = 1.5* COS(ABLAZE(2))/ABJURE(2)
      ABLAUT(11,7) =  -ABLAUT(11,4)
      ABLAUT(11,6) = (COS(ABLAZE(2))/4.0) * (TWIT(1,2) * HOLL(1,2)
     2  + TWIT(2,2) * HOLL(2,2)  )
      ABLAUT(11,9) =  ABLAUT(11,6)
      ABLAUT(11,5) = (COS(ABLAZE(2))/4.0)*(TWIT(1,1)* HOLL(1,2)
     2  + TWIT(2,1) * HOLL(2,2)  )
      ABLAUT(11,8) = ABLAUT(11,5)
      ABLAUT(12,7) = 1.5 * COS(ABLAZE(3))/ABJURE(3)
      ABLAUT(12,1) = - ABLAUT(12,7)
      ABLAUT(12,9) =(COS(ABLAZE(3))/4.0) * (TWIT(1,2)* HOLL(1,3)
     2   +TWIT(2,2)  * HOLL(2,3)  )
      ABLAUT(12,3)   = ABLAUT(12,9)
      ABLAUT(12,8) = (COS(ABLAZE(3))/4.0) *(TWIT(1,1)* HOLL(1,3)
     2 + TWIT(2,1) * HOLL(2,3) )
      ABLAUT(12,2) = ABLAUT(12,8)
      ABLAUT(10,10) =  SIN(ABLAZE(1))
      ABLAUT(11,11) =  SIN(ABLAZE(2))
      ABLAUT(12,12) =  SIN(ABLAZE(3))
 1221 FORMAT(1X,20F5.3)
      DO 76 I = 13,19,2
      ABLAUT(I,I)      =  TWIT(1,1)
      ABLAUT(I,I+1) = TWIT(1,2)
      ABLAUT(I+1,I) = TWIT(2,1)
      ABLAUT(I+1,I+1) = TWIT(2,2)
   76 CONTINUE
      DO 21 MMM = 1,3
      LMS = 0
C
C THE TRANSFORMATION OF THE ELASTICITY MATRIX IN THE CORE OF THE
C        STIFFNESS MATRIX
C
```

```
      NNN = MMM +1
      IF(NNN.GT.3) NNN = NNN -3
      ANGLE = WCBTAN(COD,DAB)
      BERRY(1) = AARON(MMM) - ANGLE
      BERRY(2) = AARON(NNN) - ANGLE
      DO 766 I = 1,2
  766 IF(BERRY(I).LT.0.0) BERRY(I) = BERRY(I) +6.28318530
      BRRY = SIN(BERRY(1)- BERRY(2))
      FRODO(1,1)  =  -SIN(BERRY(2))/ BRRY
      FRODO(1,2)  =  SIN(BERRY(1))/BRRY
      FRODO(2,1)  =  COS(BERRY(2))/BRRY
      FRODO(2,2)  = -COS(BERRY(1))/BRRY
      DO 768 I =1,6
      DO 768 J =1,6
  768 ROGER(I,J)  = 0.0
      ROGER(1,1) = FRODO(1,1) * FRODO(1,1)
      ROGER(1,2) = FRODO(1,1) * FRODO(1,2)
      ROGER(1,3) = FRODO(1,2) * FRODO(1,1)
      ROGER(1,4) = FRODO(1,2) * FRODO(1,2)
      ROGER(2,1) = FRODO(1,1) * FRODO(2,1)
      ROGER(2,2) = FRODO(1,1) *FRODO(2,2)
      ROGER(2,3) = FRODO(1,2) * FRODO(2,1)
      ROGER(2,4) = FRODO(1,2) * FRODO(2,2)
      ROGER(3,1) = FRODO(2,1) * FRODO(1,1)
      ROGER(3,2) = FRODO(2,1) * FRODO(1,2)
      ROGER(3,3) = FRODO(2,2) * FRODO(1,1)
      ROGER(3,4) = FRODO(2,2) * FRODO(1,2)
      ROGER(4,1) = FRODO(2,1) * FRODO(2,1)
      ROGER(4,2) = FRODO(2,1) * FRODO(2,2)
      ROGER(4,3) = FRODO(2,2) * FRODO(2,1)
      ROGER(4,4) = FRODO(2,2) * FRODO(2,2)
      ROGER(5,5) = FRODO(1,1)
      ROGER(5,6) = FRODO(1,2)
      ROGER(6,5) = FRODO(2,1)
      ROGER(6,6) = FRODO(2,2)
      DO 770 I = 1,6
      DO 770 J = 1,6
  770 ELAST(I,J) = 0.0
      ELAST(1,1) = STIF(1)
      ELAST(1,4) = STIF(2)
```

```
      ELAST(2,2) = STIF(4)
      ELAST(3,3) = STIF(4)
      ELAST(4,4) = STIF(3)
      ELAST(4,1) = STIF(2)
      ELAST(5,5) = STIF(5)
      ELAST(6,6) = STIF(6)
      DO 771 I = 1,6
      DO 772 J = 1,6
      RUM(J)=0.0
      DO 772 K=1,6
  772 RUM(J)=  RUM(J) + ELAST(I,K)* ROGER(K,J)
      DO 771 J= 1,6
  771 ELAST(I,J) =  RUM(J)
      DO 70 I = 1,6
      DO 70 J = 1,6
   70 ELAST1(I,J) = ELAST(I,J)
      DO 773 J= 1,6
      DO 774 I= 1,6
      RUM(I) =0.0
      DO 774 K = 1,6
  774 RUM(I) = RUM(I) + ELAST(K,J)*ROGER(K,I)
      DO 773 I = 1,6
  773 ELAST(I,J) = RUM(I)
       DO 778 I = 1,6
      DO 778 J = 1,6
  778 ELAST(I,J) = -ELAST(I,J) * BRRY
C
C     FORMATION OF MATRICES  A, B , C
C                DAHLIA     =  A         (6 * 16)
C                DAIL       =  B         (6 * 16)
C                DAISY      =  C         (6 * 16)
C
C    LENGTHS OF  TRIANGLE SIDES  AARD(I)
C
      I = MMM
      J = NNN
      CYN = AARD(J)* AARD(J)* AARD(I)
      CYO = AARD(I)* AARD(I)* AARD(J)
      CYP = AARD(I)* AARD(I)* AARD(I)
      CYQ = AARD(J)* AARD(J)* AARD(J)
```

```
      DO 22 K = 1,16
      DO 22 L = 1,16
      DAHLIA(K,L) = 0.0
      DAIL  (K,L) = 0.0
   22 DAISY (K,L) = 0.0
C
      DAHLIA(1,2)  = - CYN
      DAHLIA(1,5) = CYN
      DAHLIA(1,11) =  CYN
      DAHLIA(1,12) = -CYN
      DAHLIA(2,3)  = -CYN
      DAHLIA(2,6)  =  CYN
      DAHLIA(2,11) = CYO / 2.0
      DAHLIA(3,11) = CYO / 2.0
      DAHLIA(2,13) = - CYO /2.0
       DAHLIA(3,13) = -CYO / 2.0
      DAHLIA(3,3)  = -CYN
      DAHLIA(3,6)  =  CYN
      DAHLIA(3,14) =  CYN / 2.0
      DAHLIA(2,14) = CYN / 2.0
      DAHLIA(3,15) = -CYN / 2.0
      DAHLIA(2,15) = -CYN / 2.0
      DAHLIA(4,2)  =  CYP
      DAHLIA(4,3)  =  -2.0*CYO
      DAHLIA(4,4)  =  -6.0 * AARD(I)* AARD(I)
      DAHLIA(4,5)  =    CYP
      DAHLIA(4,6) =  - 2.0 *  CYO
      DAHLIA(4,7)  =   6.0 * AARD(I)* AARD(I)
      DAHLIA(4,9)  = - 2.0 * CYO
      DAHLIA(4,10) =  4.0 * CYP
      DAHLIA(4,14) =   CYO
      DAHLIA(4,16) =  -  CYO
C
      DAHLIA(5,11) = AARD(I)*AARD(I)*AARD(J)*AARD(J)/2.0
      DAHLIA(5,12) = DAHLIA(5,11)
      DAHLIA(6,14) = DAHLIA(5,11)
      DAHLIA(6,15) = DAHLIA(5,11)
C
C
      DAIL(1,2) =  - 2.0 * CYN
```

```
      DAIL(1,3) =  CYQ
      DAIL(1,5) =  -  CYN
      DAIL(1,6) = -CYQ
      DAIL(1,8) =  - CYN
      DAIL(1,10) = 4.C* CYN
      DAIL(1,11) =  CYN
      DAIL(1,12) = -CYN
      DAIL(2,2)  = -CYO
      DAIL(2,8)  =  CYO
      DAIL(2,11) = CYO / 2.0
      DAIL(3,11) = CYO/2.C
      DAIL(2,13) = -CYO/2.0
      DAIL(3,13) = -CYO/2.0
      DAIL(3,2)  = -CYO
      DAIL(3,8)  = +CYO
      DAIL(3,14) = CYN / 2.0
      DAIL(2,14) =  CYN / 2.0
      DAIL(3,15) = -CYN / 2.0
      DAIL(2,15) = -CYN /2.0
      DAIL(4,3) = -CYO
      DAIL(4,9) = CYO
      DAIL(4,14) = CYO
      DAIL(4,16) = -CYO
      DAIL(5,11) = DAHLIA(5,11)
      DAIL(5,13) = DAHLIA(5,11)
      DAIL(6,14) = DAHLIA(5,11)
      DAIL(6,16) = DAHLIA(5,11)
C
C
      DAISY(1,1) = 6.0 *AARD(J)*AARD(J)
      DAISY(1,2) = CYN
      DAISY(1,3) = CYQ
      DAISY(1,4) = -DAISY(1,1)
      DAISY(1,5) =  2.0 * CYN
      DAISY(1,6) =  - CYQ
      DAISY(1,8) = - CYN
      DAISY(1,10) =  4.0 * CYN
      DAISY(1,11) = CYN
      DAISY(1,12) = - CYN
C
```

```
      DAISY(2,1)  = 6.0 *AARD(I)*AARD(J)
      DAISY(2,2)  = CYO
      DAISY(2,3)  = CYN
      DAISY(2,4)  = -6.0* AARD(I)* AARD(J)
      DAISY(2,5)  = CYO
      DAISY(2,6)  =  -CYN
      DAISY(2,10) =  4.0 * CYO
      DAISY(2,11) = CYO / 2.0
      DAISY(3,11) = CYO / 2.0
      DAISY(2,13) = - CYO / 2.0
      DAISY(3,13) = -CYO / 2.0
      DAISY(3,1)  =  6.0 * AARD(I) * AARD(J)
      DAISY(3,2)  =  CYO
      DAISY(3,3)  =  CYN
      DAISY(3,4)  = - 6.0 * AARD(I) * AARD(J)
      DAISY(3,5)  =  CYO
      DAISY(3,6)  =  -CYN
      DAISY(3,10) =  4.0 * CYO
      DAISY(3,14) = CYN / 2.0
      DAISY(2,14) = CYN / 2.0
      DAISY(3,15) = -CYN / 2.0
      DAISY(2,15) = -CYN / 2.0
      DAISY(4,1)  =  6.0 *_AARD(I)* AARD(I)
      DAISY(4,2)  =  CYP
      DAISY(4,3)  =  CYO
      DAISY(4,4)  =  - DAISY(4,1)
      DAISY(4,5) =   CYP
      DAISY(4,6)  =  -2.0 * CYO
      DAISY(4,9)  =  CYO
      DAISY(4,10) = 4.0 * CYP
      DAISY(4,14) =  CYO
      DAISY(4,16) = - CYO
C
      DAISY(5,12) = DAHLIA(5,11)
      DAISY(5,13) = DAHLIA(5,11)
      DAISY(6,15) = DAHLIA(5,11)
      DAISY(6,16) = DAHLIA(5,11)
C
      CALL TIMES(ELAST1,DAISY,TAISY,6,6,16,16,6,16,6,16,6,0)
C
```

```
C  THE MATRICES A,B AND C ARE USED TO PRE- AND POST- MULTIPLY THE
C ELASTICITY MATRIX (ELAST). THE SUM OF THESE PRODUCTS GIVES THE SUB-
C ELEMENT STIFFNESS MATRIX IN OBLIQUE COORDINATES.  IT IS THEN TRANSFORMED
C ACCORDING TO WHICH TRIANGLE IS BEING DEALT WITH, AND ASSIGNED TO THE CORRECT
C LOCATIONS IN STIGMA(23,23)
      LL = MMM
      NN = NNN
      CALL TIMES(ELAST,DAISY,DAA,6,6,16,16,6,16,6,16,6,0)
      CALL TIMES(DAISY,DAA,DAISY,16,16,6,16,16,16,16,16,6,1)
      CALL TIMES(ELAST,DAIL,DAA,6,6,16,16,6,16,6,16,6,0)
       CALL TIMES(DAIL,DAA,DAIL,16,16,6,16,16,16,16,16,6,1)
      CALL TIMES(ELAST,DAHLIA,DAA,6,6,16,16,6,16,6,16,6,0)
      CALL TIMES(DAHLIA,DAA,DAHLIA,16,16,6,16,16,16,16,16,6,1)
      DO 24 I = 1,16
      DO 24 J = 1,16
   24 DAISY(I,J) = DAISY(I,J) + DAIL(I,J) + DAHLIA(I,J)
      ZUT = 6.0*AARD(NN)*AARD(NN)*AARD(NN)*AARD(LL)*AARD(LL)*AARD(LL)
       ZUT = 1.0/ZUT
      DO 25 I = 1,16
      DO 25 J = 1,16
   25 DAISY(I,J) = DAISY(I,J) * ZUT
      ZUT = AARD(NN)*AARD(NN)*AARD(LL)*AARD(LL)
      ZUT = 1.0 / ZUT
      DO 109 I = 1,6
      DO 109  J = 1,16
  109 TAISY(I,J) = TAISY(I,J) * ZUT
      GO TO(26,27,28),LL
C    TRAN IS THE LOCAL TRANSFORMATION MATRIX
C    TRIANGLE I GO TO 26
C   TRIANGLE II
   27 TRAN(1,1) = 0.0
      TRAN(1,2) = 1.0
      TRAN(2,1) = -SIN(BETA)/SIN(ALPHA)
      TRAN(2,2) = SIN(ALPHA+BETA) /SIN(ALPHA)
      GO TO 29
C  TRIANGLE  III
   28 TRAN(1,1) = SIN(ALPHA+GAMMA) /SIN(ALPHA)
      TRAN(1,2) = -SIN(GAMMA) /SIN(ALPHA)
      TRAN(2,1) = 1.0
      TRAN(2,2) = 0.0
```

```
C    POST  AND PRE MULTIPLICATION
   29 DO 30 J = 2,8,3
      DO 31 K = 1,16
      RUM(K) = DAISY(K,J) *TRAN(1,1) + DAISY(K,J+1)*TRAN(2,1)
      TUM(K) = DAISY(K,J)*TRAN(1,2) + DAISY(K,J+1)*TRAN(2,2)
   31 CONTINUE
      DO 30 K = 1,16
      DAISY(K,J) = RUM(K)
      DAISY(K,J+1) = TUM(K)
   30 CONTINUE
      DO 90 J = 2,8,3
      DO 91 K = 1,6
      RUM(K) = TAISY(K,J) *TRAN(1,1) + TAISY(K,J+1)*TRAN(2,1)
      TUM(K) = TAISY(K,J)*TRAN(1,2) + TAISY(K,J+1)*TRAN(2,2)
   91 CONTINUE
      DO 90 K = 1,6
      TAISY(K,J) = RUM(K)
      TAISY(K,J+1) = TUM(K)
   90 CONTINUE
      DO 92 J = 11,13
      DO 93 K = 1,6
      TUM(K) = TAISY(K,J)*TRAN(1,2)+TAISY(K,J+3)*TRAN(2,2)
      RUM(K) = TAISY(K,J)*TRAN(1,1) + TAISY(K,J+3)*TRAN(2,1)
   93 CONTINUE
      DO 92 K = 1,6
      TAISY(K,J) = RUM(K)
      TAISY(K,J+3) = TUM(K)
   92 CONTINUE
      DO 32 J = 11,13
      DO 33 K = 1,16
      TUM(K) = DAISY(K,J)*TRAN(1,2) + DAISY(K,J+3)*TRAN(2,2)
      RUM(K) = DAISY(K,J) *TRAN(1,1) + DAISY(K,J+3)*TRAN(2,1)
   33 CONTINUE
      DO 32 K = 1,16
      DAISY(K,J) = RUM(K)
      DAISY(K,J+3) = TUM(K)
   32 CONTINUE
      DO 34 K = 2,8,3
      DO 35 J = 1,16
      RUM(J) = DAISY(K,J)*TRAN(1,1) + DAISY(K+1,J)*TRAN(2,1)
```

```
      TUM(J) = DAISY(K,J)*TRAN(1,2) + DAISY(K+1,J)*TRAN(2,2)
   35 CONTINUE
      DO 36 J = 1,16
      DAISY(K,J) = RUM(J)
      DAISY(K+1,J) = TUM(J)
   36 CONTINUE
   34 CONTINUE
      DO 37 K = 11,13
      DO 38 J = 1,16
      RUM(J) = DAISY(K,J)*TRAN(1,1) + DAISY(K+3,J)*TRAN(2,1)
      TUM(J) = DAISY(K,J)*TRAN(1,2) + DAISY(K+3,J)*TRAN(2,2)
   38 CONTINUE
      DO 37 J = 1,16
      DAISY(K,J) = RUM(J)
      DAISY(K+3,J) = TUM(J)
   37 CONTINUE
   26 CALL IBO(LL)
C    ADDITION  OF  SUB-ELEMENT  STIFFNESS  MATRICES, TO FORM  ELEMENT
C   STIFFNESS  MATRIX
      DO 39 I = 1,16
      DO 39 J = 1,16
      KK = IB(I)
      MM = IB(J)
      STIGMA(KK,MM) = STIGMA(KK,MM) + DAISY(I,J)
   39 CONTINUE
      ICY = (LL-1)*9
      DO 71 I = 1,6
      DO 71 J = 1,16
      JJ = IB(J)
   71 STICK(ICY+I,JJ) = DAISY(I,J)
C    FORMATION  OF  PLANE   STRESS  ELEMENT  STIFFNESS  MATRIX
      DO 73 I = 1,2
       X1(I,1) = X(I,4)
      X1(I,2) = X(I,LL)
   73 X1(I,3) = X(I,NN)
      DET = 0.0
      DO 74 II = 1,3
      IJ = II + 1
      IM = II + 2
      IF(IJ.GT.3) IJ = IJ - 3
```

```
      IF(IM.GT.3) IM = IM - 3
      A(II) = X1(1,IJ)*X1(2,IM)-X1(1,IM)*X1(2,IJ)
      DET = DET + A(II)
      B(II) = X1(2,IJ)  - X1(2,IM)
      C(II) = X1(1,IM) - X1(1,IJ)
   74 CONTINUE
      DO 75 I = 1,3
      DO 75 J = 1,6
   75 STR(I,J) = 0.0
      DO 81 I = 1,3
      IJ = (I-1)*2 + 1
      STR(1,IJ) = B(I)
      STR(2,IJ+1) = C(I)
      STR(3,IJ) = C(I)
      STR(3,IJ+1) = B(I)
   81 CONTINUE
      DO 77 I = 1,3
      DO 77 J = 1,3
   77 ELA(I,J) = 0.0
      ELA(1,1) = YOUNG(7)
      ELA(1,2) = YOUNG(8)
      ELA(2,1) = ELA(1,2)
      ELA(2,2) = YOUNG(9)
      ELA(3,3) = YOUNG(10)
      CALL TIMES(ELA,STR,TEMP,3,3,3,6,3,6,3,6,3,0)
      CALL IDO(MMM)
      DO 82 I = 1,3
      DO 82 J = 1,6
      JJ = ID(J)
      NICK = ICY + I +6
      NOCK = JJ + 23
      STICK(NICK,NOCK) = TEMP(I,J)/DET
   82 CONTINUE
      CALL TIMES(STR,TEMP,BALF,3,6,3,6,6,6,6,6,3,1)
      DO 79 I = 1,6
      DO 79 J = 1,6
   79 BALF(I,J) = BALF(I,J) / (DET*2.0)
      CALL IDO(MMM)
       DO 45 J = 1,6
      DO 45 K = 1,6
```

```
      NU = ID(J)
      NO = ID(K)
      SAURON(NU,NO) = SAURON(NU,NO) + BALF(K,J)
   45 CONTINUE
   21 CONTINUE
C    CONDENSATION, TO ELIMINATE 3 DEGREES OF FREEDOM AT CENTROIDAL NODE
C   FOLLOWED  BY  TRANSFORM  TO  GLOBAL COORDINATES
      CALL TIMES(STIGMA,ABAFF,STIGMA,23,23,23,20,23,23,23,20,23,0)
      CALL TIMES(ABAFF,STIGMA,STIGMA,23,20,23,23,23,23,20,20,23,1)
      CALL TIMES(STIGMA,ABLAUT,STIGMA,23,23,20,20,23,23,20,20,20,0)
      CALL TIMES(ABLAUT,STIGMA,STIGMA,20,20,23,23,23,23,20,20,20,1)
      CALL TIMES(STICK,ABAFF,STICK,36,36,23,20,36,36,36,20,23,0)
      CALL TIMES(STICK,ABLAUT,STICK,36,36,20,20,36,36,36,20,20,0)
      DO 85 I = 1,36
      DO 85 J = 1,8
      JJ = J + 20
      JJJ = J + 23
   85 STICK(I,JJ) = STICK(I,JJJ)
      DO 66 I = 1,28
      DO 66 J = 1,28
   66 STUCK(I,J) = 0.0
      DO 64 I = 1,20
      II = IND(I)
      DO 64 J = 1,20
      JJ = IND(J)
   64 STUCK(II,JJ) = STIGMA(I,J)
      DO 65 I = 1,8
      II = IND(I+20)
      DO 65 J = 1,8
      JJ = IND(J+20)
   65 STUCK(II,JJ) = SAURON(I,J)
      DO 83 I = 1,36
      DO 84 J = 1,28
   84 TEMO(J) = STICK(I,J)
      DO 83 J = 1,28
      JJ = IND(J)
   83 STICK(I,JJ) = TEMO(J)
C    ELIMINATION  OF  REMAINING 4 DEGREES OF  FREEDOM  AT  CENTROID
C     BY   STATIC   CONDENSATION
      DO 101  I = 1,28
```

```
      DO 101  J = 1,28
  101 SPY(I,J)  =  STUCK(I,J)
      CALL DXCPY(SPYL,W21L,25,1,4,24,28,28,0)
      CALL DXCPY(SPYL,W22L,25,25,4,4,28,28,0)
      CALL DMINV(W22L,4,DET,LU,MU)
      CALL TIMES(W22,W21,STUCK,4,4,4,24,36,36,4,24,4,0)
      CALL TIMES(Q2,STUCK,GROAN,36,4,36,36,36,24,36,24,4,0)
      DO 106 I = 1,36
      DO 106 J = 1,24
  106 STICK(I,J) = STICK(I,J) - GROAN(I,J)
      CALL TIMES(W21,STUCK,STUCK,4,24,36,36,36,36,24,24,4,1)
      DO 102 I = 1,24
      DO 102 J = 1,24
  102 STUCK(I,J) =  SPY(I,J) -  STUCK(I,J)
C   CHANGE  SIGNS OF  DW/DY  D. OF F.S    ( OX =  - DW/DY)
C
      DO 103 I =1,3
      K  = (I-1) * 7 + 4
      K1 = K + 2
      DO 103  J = 1,24
      STUCK(K,J) = -STUCK(K,J)
      STUCK(J,K) = -STUCK(J,K)
      STUCK(K1,J) = -STUCK(K1,J)
      STUCK(J,K1) = - STUCK(J,K1)
      STICK(J,K) = - STICK(J,K)
      STICK(J,K1)= -STICK(J,K1)
  103 CONTINUE
C
C   CHANGE  D. OF  F.  TO  TOTAL  ROTATIONS
C
      DO  48 I = 1,24
      DO  47 J = 1,24
   47 SPY(I,J) = 0.0
   48 SPY(I,I) = 1.0
      DO 49 I = 1,3
      K = (I-1)*7
      SPY(K+5,K+7) =  1.0
   49 SPY(K+4,K+6) =   1.0
C
C   NOW  CHANGE  MIDSIDE  NODES
```

```
C
      DO  50 I = 1,3
      KI = (I-1) * 7
      J    = I+1
      IF(J.GT.3)  J= J-3
      KJ = (J-1) * 7
      ANG  =  ABBEY(I)
      I21  = I+21
      SPY(I21,KI+6) =  COS(ANG)/2.0
      SPY(I21,KI+7) =  SIN(ANG)/2.0
      SPY(I21,KJ+6) =  COS(ANG)/2.0
      SPY(I21,KJ+7) =  SIN(ANG)/2.0
   50 CONTINUE
      CALL TIMES(STUCK,SPY,STUCK,36,36,28,28,36,36,24,24,24,0)
      CALL TIMES(STICK,SPY,STICK,36,36,28,28,36,36,36,24,24,0)
      CALL TIMES(SPY,STUCK,STUCK,28,28,36,36,36,36,24,24,24,1)
C
C  STUCK NOW HOLDS STIFFNESS MATRIX  WITH  TOTAL ROTATIONS AS D.OF F.
C
C   OPTIONAL  RETRIEVAL OF PAST STIFFNESS  MATRICES,OR STORAGE OF  PRESENT ONE
      IF(KLOCK.EQ.0) GO TO 405
      KLOCK= KLOCK-10
      DO 401 I=1,24
      DO 401 J = 1,24
  401 BLUNT(KLOCK,I,J) = STUCK(I,J)
      DO 402 I = 1,27
      DO 402 J = 1,24
  402 BLINT(KLOCK,I,J) = STICK(I,J)
      GO TO 405
  400 DO 403 I = 1,24
      DO 403 J = 1,24
  403 STUCK(I,J) = BLUNT(KLOCK,I,J)
      DO 404 I = 1,27
      DO 404 J = 1,24
  404 STICK(I,J) = BLINT(KLOCK,I,J)
  405 CONTINUE
C   OPTIONAL  LOCAL  TRANSFORMATIONS
C   FOR USE AT PLATE  INTERSECTIONS
      IF(INFO(1).EQ.0) GO TO 53
      KINK  =  INFO(1)
```

```
      DO  51  I =  1,KINK
      K  =  (I-1)*3 + 2
      L = INFO(K)
      DO 56 IT = 1,24
      DO 57 IS = 1,24
   57 SPY(IT,IS) = 0.0
   56 SPY(IT,IT) = 1.0
      KK = (L-1) * 7
      DO 58 II = 1,3
      DO 58 JJ = 1,3
      SPY(KK+II,KK+JJ) = DIRCOS(JJ,II)
   58 CONTINUE
      K1 = INFO(K+1)
      K2 = INFO(K+2)
C  K1 AND K2 ARE THE NUMBERS OF THE ENDS OF THE EDGE BEING TRANSFORMED.
C THEY ALSO DEFINE ITS DIRECTION.
C    K2 IS FURTHER OUT
C    K1 IS FURTHER IN.
      IF(K1.EQ.0) GO TO 52
      AA = X(2,K2) - X(2,K1)
      AB = X(1,K2) -X(1,K1)
      ANG = WCBTAN(AB,AA)
      SPY(KK+4,KK+4) =  COS(ANG)
      SPY(KK+4,KK+5) = -SIN(ANG)
      SPY(KK+5,KK+4) =  SIN(ANG)
      SPY(KK+5,KK+5) =  COS(ANG)
      SPY(KK+6,KK+6) =  COS(ANG)
      SPY(KK+6,KK+7) = -SIN(ANG)
      SPY(KK+7,KK+6) =  SIN(ANG)
      SPY(KK+7,KK+7) =  COS(ANG)
      CALL TIMES(STUCK,SPY,STUCK,36,36,28,28,36,36,24,24,24,0)
      CALL TIMES(STICK,SPY,STICK,36,36,28,28,36,36,36,24,24,0)
      CALL TIMES(SPY,STUCK,STUCK,28,28,36,36,36,36,24,24,24,1)
      KUK = KK+6
      CALL CNDNS(KUK)
      STUCK(KUK,KUK) = 1.0
      GO TO 51
   52 CALL CNDNS(KK+6)
      CALL CNDNS(KK+7)
      STUCK(KK+7,KK+7) = 1.0
```

```
      DO  54  II = 1,3
      DO  54  JJ = 1,3
   54 SPY(KK+II+3,KK+JJ+3) = DIRCOS(JJ,II)
      CALL TIMES(STUCK,SPY,STUCK,36,36,28,28,36,36,24,24,24,0)
      CALL TIMES(STICK,SPY,STICK,36,36,28,28,36,36,36,24,24,0)
      CALL TIMES(SPY,STUCK,STUCK,28,28,36,36,36,36,24,24,24,1)
   51 CONTINUE
   53 CONTINUE
C    OPTIONAL  DIAGNOSTIC  WRITE  OUT
      IF(INFO(11).EQ.999) WRITE(6,1003)((STUCK(I,J),J=1,24),I=1,24)
 1003 FORMAT(3X,7D14.5/3X,7D14.5/3X,7D14.5/10X,3D14.5)
      RETURN
      END
       SUBROUTINE IBO(KKKKK)
      DIMENSION IB(16)
      COMMON /FIVE/ IB
C    SUB ELEMENT  LOCATION SUBROUTINE, (BENDING)
      IB(1) = 1
      IB(2) = 2
      IB(3) = 3
      IB(11) = 22
      IB(14) = 23
      GO TO (1,2,3),KKKKK
    1 DO 5 I = 4,9
    5 IB(I) = I
      IB(10) = 13
      IB(12) = 16
      IB(15) = 17
      IB(13) = 18
      IB(16) = 19
      RETURN
    2 DO 6 I = 4,9
    6 IB(I) = I +3
      IB(10) = 14
      IB(12) = 18
       IB(15) = 19
      IB(13) = 20
      IB(16) = 21
      RETURN
    3 DO 7 I = 4,6
```

```
    7 IB(I) = I +6
      DO 8 I = 7,9
    8 IB(I) = I-3
      IB(10) = 15
        IB(12) = 20
      IB(15) = 21
      IB(13) = 16
      IB(16) = 17
      RETURN
      END
      SUBROUTINE IDO(KKKKK)
      COMMON /SIX/ ID
      DIMENSION ID(6)
C     SUB ELEMENT  LOCATION SUBROUTINE, (PLANE STRESS)
      ID(1) = 7
      ID(2) = 8
      GO TO (1,2,3),KKKKK
    1 ID(3) = 1
      ID(4) = 2
      ID(5) = 3
      ID(6) = 4
      RETURN
    2 ID(3) = 3
      ID(4) = 4
      ID(5) = 5
      ID(6) = 6
      RETURN
    3 ID(3) = 5
      ID(4) = 6
      ID(5) = 1
      ID(6) = 2
      RETURN
      END
      DOUBLE PRECISION FUNCTION WCBTAN(X,Y)
      IMPLICIT REAL*8 (A-H,O-Z)
C   WCBTAN IS THE WHOLE CIRCLE BEARING OF THE POINT (X,Y), IN RADIANS
C   WITH THE BEARING OF (1,0) TAKEN AS ZERO. (MEASURED ANTI CLOCKWISE)
      ATAN(AX) = DATAN(AX)
      IF(X.EQ.0.0) GO TO 4
      IF(X.LT.0.0) GO TO 1
```

```
      IF(Y.LT.0.0) GO TO 2
      WCBTAN = ATAN(Y/X)
      RETURN
    1 WCBTAN = ATAN(Y/X) + 3.1415926
      RETURN
    2 WCBTAN = ATAN(Y/X) + 6.2831852
      RETURN
    4 IF(Y.GT.0.0) GO TO 5
      WCBTAN = 4.7123889
      RETURN
    5 WCBTAN = 1.5707963
      RETURN
      END
      SUBROUTINE DIRECT(X,DIRCOS)
      IMPLICIT REAL*8 (A-H,O-Z)
      DIMENSION X(3,3),DIRCOS(3,3)
      SQRT(AX) = DSQRT(AX)
C
C   FORMS MATRIX TRANSFORMATION FROM GLOBAL TO LOCAL CO-ORDINATES
C
C    (GLOBAL) = (DIRCOS)*(LOCAL)
C
      DO 1 I = 1,3
      DO 1 J = 1,3
    1 DIRCOS(I,J) = 0.0
      AA = (X(2,2)-X(1,2))*(X(3,3)-X(1,3))
     1   - ((X(3,2)-X(1,2))*(X(2,3)-X(1,3)))
      AB = -((X(2,1)-X(1,1))*(X(3,3)-X(1,3)))
     1   +(X(3,1)-X(1,1)) * (X(2,3)-X(1,3))
      AC =   (X(2,1)-X(1,1)) *(X(3,2)-X(1,2))
     1   -((X(3,1)-X(1,1))*(X(2,2)-X(1,2)))
      IF((AA.GT.-.1E-12.AND.AA.LT.0.1E-12).AND.(AB.GT.-.1E-12.AND.AB.
     1   LT.0.1E-12)) GO TO 2
      AD = SQRT(AA*AA + AB*AB +AC*AC)
      AE = SQRT(AA*AA + AB*AB)
       DIRCOS(1,3) = AA/AD
      DIRCOS(2,3) = AB/AD
      DIRCOS(3,3) = AC/AD
      DIRCOS(1,1) = -AB/AE
      DIRCOS(2,1) = AA/AE
```

```
      DIRCOS(1,2) =-AA * AC /(AE*AD)
      DIRCOS(2,2) =-AB*AC /(AE*AD)
      DIRCOS(3,2) = (AA*AA + AB*AB) /(AE*AD)
       RETURN
    2 DO 3 I = 1,3
    3 DIRCOS(I,I) = 1.0
      RETURN
      END
      SUBROUTINE CNDNS(K)
      IMPLICIT REAL*8 (A-H,O-Z)
      DIMENSION B(36)
      COMMON /STI/X(3,20),YOUNG(12),STUCK(36,36),STICK(36,36),
     1 FORCE(36),INFO(20)
C     CONDENSES OUT K TH. DEGREE OF  FREEDOM
      A = 1.0 / STUCK(K,K)
      DO 4 I = 1,24
    4 B(I) = STUCK(K,I)
      DO 1 I=1,24
      DO 1 J=1,24
    1 STUCK(I,J) = STUCK(I,J) - B(I)*B(J)*A
      DO 2 I = 1,36
      D = STICK(I,K)
      DO 2 J = 1,24
    2 STICK(I,J) = STICK(I,J) - B(J)*A*D
      D = FORCE(K)
      DO 3 I = 1,24
    3 FORCE(I) = FORCE(I) - B(I)*D*A
      RETURN
      END
```